Experimental study of volume change and shear strength behaviour of statically compacted collapsible soil

Suhad Abdulsattar Almahbobi

Geoenvironmental Research Centre

School of Engineering

Cardiff University

Thesis submitted in candidature for the degree of Doctor of Philosophy at Cardiff University

October 2018

DECLARATION

This work has not been submitted in substance for any other degree or award at this or any other university or place of learning, nor is being submitted concurrently in candidature for any degree or other award.

Signed (Suhad Almahbobi) Date

STATEMENT 1

This thesis is being submitted in partial fulfilment of the requirements for the degree of Doctor of Philosophy (PhD).

Signed (Suhad Almahbobi) Date

STATEMENT 2

This thesis is the result of my own independent work/investigation, except where otherwise stated, and the thesis has not been edited by a third party beyond what is permitted by Cardiff University's Policy on the Use of Third Party Editors by Research Degree Students. Other sources are acknowledged by explicit references. The views expressed are my own.

Signed (Suhad Almahbobi) Date

STATEMENT 3

I hereby give consent for my thesis, if accepted, to be available online in the University's Open Access repository and for inter-library loan, and for the title and summary to be made available to outside organisations.

Signed (Suhad Almahbobi) Date

STATEMENT 4

I hereby give consent for my thesis, if accepted, to be available online in the University's Open Access repository and for inter-library loans **after expiry of a bar on access previously approved by the Academic Standards & Quality Committee.**

Signed …… (Suhad Almahbobi) Date

Acknowledgements

In the Name of Allah, the All-Merciful, the All-Compassionate.

The praise is due to Allah, the All-Powerful, the All-Knowing, the All-Wise and the Compassionate for giving me the strength, health, patience and perseverance to complete this work in its best.

To my supervisor's Dr Snehasis Tripathy and Dr Peter Cleall, I wish to express my heartfelt gratitude and appreciation for all the support, guidance, patience and time that they have given me this great opportunity in making this thesis a reality. My special thanks also extended to all academic staff especially Dr Michael Harbottle for his annual reviews of my research.

I am extremely grateful to the technical staff at ENGIN, in particular, Steff, Harry Paul, Richard, Ian, Garry, Carl, Gareth, and Jeff. I am thankful not only for their endless assistance but also for their friendship and encouragement for everything they did and do. May the words cannot reveal my deep gratitude to them. I would also like to thank the staff of ENGIN Research Office, Chris, Aderyn, Jeanette, Ffion and Sandra for their constant help, support and encouragement.

Many thanks to all my friends in GRC; Osama, Hassanien, Khabeer, Sahar, Yahya and Maram for providing a very enjoyable and motivating environment. My deepest love and gratitude go to my best friends in Iraq; Fatima, Nada, Hawera and Huda.

To my beloved mother and father who was always so patient and understanding, it would not have been possible without their prayers and motivational words. To my wonderful brothers, sisters, and their families for all their love, support, and encouragement. Extraordinary thanks and love to my best friend and husband; Duraid and my kids, Ali and Ahmed, I am entirely thankful for having you in my life and for all the acceptance, backing, and inspiration that you gave me, and the sacrifices that you made during the challenging period of my study.

I would like to especially thank the Embassy of the Republic of Iraq / Cultural attaché for financial support during my study. My gratitude is also extended to all to my supervisors during my Master study Professor Al-Shakarchi, Professor Hussain and Professor Fattah for teaching me the principles of engineering and support me to complete my PhD study in the UK.

Abstract

Collapsible soils present significant geotechnical and structural engineering challenges. These soils are known to withstand relatively high stresses at unsaturated state. Upon exposure to a saturation front at a constant surcharge, the volume change of such soils usually occurs within a short time period. It has been shown that the magnitudes of collapse strain and the shear strength depend upon the applied stress and suction. This thesis presents an experimental study of the effects of confining stress and suction on volume change and shear strength behaviour of a collapsible soil.

Laboratory tests were carried out on statically compacted soil specimens. A mixture of M400 silt (40%), Leighton Buzzard sand (40%) and 20% Speswhite kaolin was considered for preparing the soil. The percentages of various particle-size fractions in the soil are similar to that is found in naturally occurring aeolian soil deposits. A series of single and double oedometer tests have been carried out to investigate the effects of different compaction parameters, such as initial water content, initial dry unit weight, compaction pressure and overburden pressure on the collapse strain. Wetting tests under isotropic stress conditions and consolidated drained triaxial shearing tests were carried out to study the impact of confining stress (100, 250 and 400 kPa) on the volume change and shear strength of the statically compacted soil specimens at several suction during the wetting process. The suction – degree of saturation relationship at high suctions from chilled-mirror dew-point tests and the test results from the wetting tests (based on the water volume and total volume changes) enabled establishing the SWCCs. The relationship between suction and suction stress (i.e., suction stress characteristic curve, SSCC) was established from the wetting water retention data at various applied confining stresses and suctions. Similarly, the SSCC was established based on the shear strength test data.

The results indicated that the impact of confining stress on the volumetric strain and wetting SWCCs of the soil was distinct. The SWCCs in terms of water content were affected the applied confining stress; however, the differences in the SWCCs in terms of the degree of saturation were found to be insignificant. As the soil underwent the wetting process (a decrease in soil suction), the friction angle ($\emptyset'$) decreased slightly, the cohesion value decreased non-linearly, and the angle $\emptyset^b$ (angle indicating the rate of change in shear strength relative to changes in matric suction) increased to attain a maximum value at saturation. The impact of applied confining stress on the suction stress characteristic curve (SSCC) was found to be insignificant. The SSCCs based on the water retention behaviour and from the triaxial shear strength tests were found to be very similar emphasizing that a strong linkage exists between water absorption and shear strength of unsaturated collapsible soils.

Table of Contents

List of Figures

List of Tables

List of Symbols

AEV	Air entry value
AExV	Air expulsion value
ASTM	American Society for Testing and Materials
a	Fredlund & Xing fitting parameter related to the inflection point on the SWCC
α	van Genuchten fitting parameter related to the inverse of air-entry value
β	Contact angle of the air–water interface
CD	Consolidated drained
CP	Collapse potential
CSL	Critical-state line in the deviatoric stress–effective mean stress plan
c'	Effective cohesion
c	Cohesion intercept
DPT	High-accuracy differential pressure transducer
d'	Intercept of the failure envelope corresponding to the saturated condition in ($p - u_a$) - q space
E	Energy
e	Void ratio during wetting stages under isotropic stress
$\boldsymbol{e_0}$	Iinitial void ratio
$\boldsymbol{e_i}$	Void ratio at as-compacted water content during oedometer test
$\boldsymbol{e_f}$	Void ratio at saturation during oedometer test
$\boldsymbol{\varepsilon_a}$	Axial strain
$\boldsymbol{\varepsilon_c}$	Vertical strain
$\boldsymbol{\varepsilon_v}$	Volumetric strain
f	Subscript refers to the state of failure
G_s	Specific gravity
Δh	Change in specimen height
$\boldsymbol{h_1}$	Specimen height immediately before wetting
k	Saturated hydraulic conductivity

LL	Liquid limit
M	Slope of the failure envelopes in ($p - u_a$) - q space
m	Fitting parameter related to the residual water content or residual degree of saturation
n	Pore-size parameter
P	Mean total stress, $p = (\sigma_1 + 2\sigma_3)/3$
p'	Mean effective stress, $p' = (\sigma_1 + 2\sigma_3)/3 - u_a - \sigma^s$
PL	Plastic limit
P_m	Meniscus stress
P_b	Bulk stress
q	Deviator stress
R^2	Correlation coefficient
$\boldsymbol{r_s}$	radius of the tube in the physical capillary model
s	Matric suction, $s = (u_a - u_w)$
S_r	Degree of saturation
S_e	Effective degree of saturation
S_{res}	Residual degree of saturation
SL	Shrinkage limit
SSCC	Suction stress characteristic curve
SWCC	Soil-water characteristic curve
T_s	Surface tension of the air–water interface
τ	Shear stress
τ_f	Shear stress at failure
USCS	Unified Soil Classification System
ΔV	Change in the total volume of the specimen
V_0	Initial total volume of the specimen
v	Specific volume (v=1+e)
v_w	Specific water volume (v_w=1+ wGs)

WP4C	Chilled-mirror dew-point potentiometer test
w	Gravimetric water content
w_s	Saturated gravimetric water content
χ	Effective stress parameter
u_a	Pore air pressure
u_w	Pore water pressure
$\emptyset'$	Angle of internal friction associated with the net normal stress
$\emptyset^b$	Angle of shearing resistance with respect to matric suction
σ	Total stress
σ'	Effective stress
σ^s	Suction stress
σ_1	Major normal principle stress
σ_3	Minor normal principle stress or confining/cell pressure
$(\sigma - u_w)$	Effective normal stress
$(\sigma_3 - u_w)$	Effective Confining stress
$(\sigma - u_a)$	Net normal stress
$(\sigma_3 - u_a)$	Net confining stress
$(u_a - u_w)_f$	Matric suction in the specimens at failure conditions
$(u_a - u_w)_b$	Air- expulsion value (AExV)
$(u_a - u_w)_{res}$	Suction at residual conditions

CHAPTER 1

Introduction

1.1 Background and motivations

Collapsible soils are known to withstand relatively high stresses at unsaturated state. During wetting at constant stress, the collapse usually occurs within a short time period (Barden et al. 1973; Lawton et al. 1992; Pereira and Fredlund 2000; Houston et al. 2001a; Khalili et al. 2004). In general, collapsible soils are moisture-sensitive and considered as one of the problematic and widely distributed soils in the world especially in arid or semi-arid regions (Knight and Dehlen 1963). Structures founded on collapsible soils require special considerations for their design. Soil collapse is responsible for the failure of earth dams, slope failure and failure of building a foundation (Lawton et al. 1992; Rollins and Kim 2010; Rabbi et al. 2014a; Li et al. 2016). Therefore, understanding the collapse phenomenon is helpful for ensuring satisfactory performance of any important structure on such soils (Tadepalli et al. 1992; Rabbi et al. 2014a).

Collapsible soils are typically silt and sand size with a small amount of clay (Tadepalli and Fredlund 1991; Houston et al. 2001b). The meta-stable structure of collapsible soils is associated with the cementation provided by the fine-grained soil fractions at the inter-particle contacts of coarse fractions in the soils (Barden et al. 1973; Murray and Sivakumar 2010). With an increase in the water content or a decrease in soil suction, the cementation at the inter-particle contacts weakens. The collapse of the open pore structure in collapsible soils is due primarily to a decrease in the shear strength at interparticle level (Barden et al. 1973; Lawton et al. 1992; Rabbi and Cameron 2014; Almahbobi et al. 2018).

Soils are usually compacted and used in many civil engineering applications (Fredlund and Rahardjo 1993a). Compacted soil at dry of optimum may produce a form of structure that leads the soil to collapse due to wetting (Pereira and Fredlund 2000; Li et al. 2016). A majority of compacted soils can exhibit collapse upon wetting if the applied

stress is sufficiently high (Tadepalli and Fredlund 1991; Lawton et al. 1992; Houston et al. 2001a; Sun et al. 2004).

Several factors that have a significant influence on the amount of collapse include soil type, yield stress, prewetting water content, and dry unit weight (Lim and Miller 2004). The effects of these factors on the volume change behaviour of collapsible soils have been studied extensively in the past (Jennings and Knight 1957; Matyas and Radhakrishna 1968; Dudley 1970; Escario and Saez 1973; Reginatto and Ferrero 1973; Booth 1975; Mitchell 1976; El Sohby and Rabbaa 1984; Maswoswe 1985; Drnevich et al. 1988; Feda 1988; Lawton et al. 1989; Basma and Tuncer 1992; Lawton et al. 1992; Alwail et al. 1994; Rogers 1995; Pereira and Fredlund 2000; Rao and Revanasiddappa 2000; Alawaji 2001; Houston et al. 2001a; Miller et al. 2001; Ng and Chiu 2001; Lim and Miller 2004; Cui et al. 2004; Jotisankasa 2005; Jefferson and Ahmad 2007; El Howayek et al. 2011; Rabbi et al. 2014a; Rabbi et al. 2014b; Li et al. 2016). Numerous researchers have reported that at the same dry density and overburden pressure, the amount of collapse increases as the initial water content decrease. Also, the collapse strain decreases with increasing initial dry unit weight for specimens compacted at a constant water content.

Several researchers have found that collapse strain during wetting is a maximum at some critical value of applied vertical stress (Booth 1976; Witsman and Lovell 1979; Lawton 1989; Lawton et al. 1992) or applied confining stress (Sun et al. 2004; Sun et al. 2007), beyond which the collapse potential decreases with increasing the applied stress. This value of applied stress (yield stress) approximately equal to the compactive prestress (the apparent pre-consolidation pressure induced in the soil by the application and removal of mechanical energy during compaction). However, study the effects of yield stress which result from statically compacted two specimen sizes (oedometer and triaxial specimens) on the magnitude of collapse strain during conventional oedometer tests, and wetting process under isotropic stress conditions have not been investigated yet.

It is generally recognized that suction is one of the key factors governing the behaviour of unsaturated soil and it is one of the important stress-state variables that cause changes in the strength and volume change characteristics of this soil (Sivakumar 1993; Fredlund et al. 1996; Wheeler et al. 2003; Fredlund et al. 2012). The relationship between soil suction and water content (or degree of saturation or volumetric water content) is

termed as soil-water characteristic curve (SWCC) and it is a crucial tool to predict and interpret the behaviour and response of unsaturated soils including volume change and shear strength (Fredlund and Rahardjo 1993b; Vanapalli et al. 1996; Khalili et al. 2004; Yang et al. 2004; Lu and Likos 2004, 2006). Many studies have been conducted to study the factors that affect the SWCC such as soil type and fabric, the initial water content, density of soil, method of compaction, the process of establishing the SWCC (i.e., drying or wetting paths) (Vanapalli et al. 1999; Yang et al. 2004; Gao and Sun 2017). The effect of the normal or the confining stress on the SWCC has been studied in the past by several researchers (Fredlund and Rahardjo 1993a; Kato and Kawal 2000; Ng and Pang 2000; Lee et al. 2005; Oh and Lu 2014). However, limited researches have investigated the influences of an increase in the confining stress on the wetting SWCCs of statically compacted collapsible soils.

The effects of a decrease in matric suction on the volume change and shear strength of collapsible soils can be studied by carrying out unsaturated triaxial tests (Lu and Likos 2004; Fredlund et al. 2012). Since the amount of water present and the magnitude of the suction control the volume change and shear strength of unsaturated soils, studies covering the step-wise suction reduction and its impact on the volume change and shear strength are expected to provide a thorough understanding of the macroscopic behaviour of collapsible soils (Bishop 1962; Bishop and Wesley 1975; Fredlund et al. 1978; Yong and Townsend 1980; Ho and Fredlund 1982; Gan et al. 1988; Fredlund and Rahardjo 1993; Rassam and Williams 1999; Lu and Likos 2004; Ng and Menzies 2007; Houston et al. 2008; Murray and Sivakumar 2010; Fredlund et al. 2012). However, detailed studies of the effects of step-wise suction reduction on the volume change and shear strength of compacted collapsible soils under isotropic conditions and for higher stress levels are very limited.

Shear strength behaviour of unsaturated soils could be described by different failure criteria (Bishop 1959; Fredlund et al. 1978; Fredlund et al. 1995; Vanapalli et al. 1996; Khalili and Khabbaz 1998; Rassam and Cook 2002; Tombolato and Tarantino 2005; Sheng et al. 2011). Currently, there are three approaches for evaluating the shear strength of unsaturated soils. Initially, the single effective stress state variable (Bishop 1959; Bishop and Donald 1961a), the two independent stress variables, net stress and suction, approach proposed by Fredlund and Morgenstern (1977), and more recent approach shifted towards a new choice of stress variables, which take into account the contributions

of both suction and degree of saturation to the effective stress, similar to the Bishop (1959) approach namely the suction stress concept introduced by Lu and Likos (2006). Many challenging difficulties in experimental determination and theoretical development of the Bishop's effective stress parameter could be avoided by adopting effective stress concept using suction stress approach (Lu et al. 2010). The macroscopic engineering behaviour of unsaturated soils can be described using the suction stress concept which has been proposed to more efficiently express and evaluate the influence of suction on the effective stress and shear strength of unsaturated soils (Lu and Likos 2004, 2006).

Lu et al. (2010) showed that suction stress either could be measured from tensile strength tests, can be calculated based on the shear strength tests, or used theoretical considerations to establish it (Baille et al. 2014). Based on the SWCC of the soil, the suction stress characteristic curve (SSCC) (i.e., the relationship between suction stress and degree of saturation or water content or suction) can be determined. Studies in the past have provided some key validations of suction stress approach based on the shear strength and volume change behaviour of soils (Lu et al. 2010; Kim et al. 2010; Oh et al. 2013; Oh and Lu 2014; Baille et al. 2014; Pourzargar et al. 2014; Haeri et al. 2014). These studies have provided some significant step forward to consider effective stress as the sum of net stress and suction stress. However, at the research planning stage, an initial review of the literature revealed that detailed studies of the SSCCs of collapsible soils derived from both shear strength and volumetric variables under isotropic conditions and for a large range of suction and higher stress levels are very limited. Therefore, the main contribution of this study is: To explore the validity of the true effective stress and SSCC concepts of Lu et al. (2010) for collapsible soils.

Soil collapse forms a major hazard in large parts of Iraq which covers about 20 to 30% of total Iraq's area (Al-Saoudi et al. 2013). Failure of different structures (e.g. schools, roads, water tanks and other infrastructure) constructed on the collapsible soils in various regions in Iraq have been noticed and have an adverse effect on living and even lives (Schanz and Karim 2018). That adverse effect has been a challenge for the engineer due to the increased construction activity. For example, such a problem causes serious danger in Al- Mosul dam foundation (largest dam located northern Iraq) which is built on highly collapsible soil (Schanz and Karim 2018). The seepage through the soil under foundation causes leaching and dissolution to the gypsum which brought the dam to the danger imminent of collapse, which could kill hundreds of thousands of people.

Therefore, understanding of the mechanical behaviour of this type of soil based on advances and breakthroughs in soil science research knowledge is thus required, which could introduce a safe and cost-effective solution to this engineering problem.

1.2 Study objectives

The main objectives of this study were:

i. To study the effect of compaction water content and compaction mould size on the static compaction characteristics and to study the difference between static compaction curves using two specimens mould sizes and dynamic compaction curve of collapsible soil.
ii. To study the effects of compaction conditions (initial water content, initial dry unit weight and yield stress) on the one-dimensional volume change behaviour of the statically compacted soil.
iii. To study the impact of confining stress and suction on the volumetric strain and SWCCs of the statically compacted collapsible soil during the wetting process.
iv. To study the impact of confining stress and suction on the shear strength behaviour and parameters of the statically compacted collapsible soil during the wetting process and compare the SSCCs based on the shear strength tests and the SWCCs of collapsible soils.
v. To study the validity of the unsaturated effective stress principle of the statically compacted collapsible soil during the wetting process.

1.3 Scope and limitations of the study

Detailed experimental studies concerning the effect of thermal and thermo-hydraulic gradients on the volume change, water retention characteristics and stress-strain behavior of compacted collapsible soil and the effect of hydraulic hysteresis are beyond the scope of this research due to the limited time of research.

Further, this research does not take into account any chemical bonding that may occur in naturally occurring collapsible soils which may affect the microstructural organization and behavior of these soils to wetting collapse in-situ.

1.4 Thesis overview

A brief description of each chapter is presented below.

CHAPTER 1 presents the background and motivation, objectives of this research, scope and limitations and the outline of the thesis.

CHAPTER 2 presents a review of literature pertaining to the studies undertaken. The chapter presents general information about the behaviour of unsaturated collapsible soils and focuses on some topics such as collapse mechanisms and laboratory test techniques that have been used to quantify the collapse potential. The review of the characteristics of SWCC is also presented. The volume change and shear strength behaviour of unsaturated soil have been highlighted through a review of the state-of-the-art studies. The effective stress and suction stress concepts are discussed.

CHAPTER 3 describes the properties of the soil used in this investigation, the details of the equipment used along with the working principles and descriptions of the various components of the equipment. The procedures adopted for preparing soil specimens for various tests are presented. The test procedures adopted for various tests are also described.

CHAPTER 4 presents the experimental results of the static compaction tests of the selected soil at several values of energy and pressure for oedometer and triaxial mould. The results of static compaction with those of the Proctor compaction tests is compared. Also, some factors influencing the collapse strain are investigated by analyzing single and double oedometer test results.

CHAPTER 5 presents the effects of confining stress on the volumetric strain of the identical statically compacted specimens during the wetting process. The water retention curves for a large range of suction are established from wetting tests (based on the water volume and total volume changes) and from chilled-mirror dew-point potentiometer tests. The best-fit models such as van Genuchten (1980) and Fredlund and Xing (1994) were applied, and the effects of confining stresses on the SWCCs and the fitting parameters are also presented in this chapter.

CHAPTER 6 presents the results of saturated and unsaturated triaxial shearing tests under drained conditions of the identical statically compacted collapsible specimens at several suction and confining stresses. The characteristics of the shear strength and the volume change are investigated. Further, the impact of suction reduction on the shear strength parameters are studied in detail.

CHAPTER 7 presents the SSCCs that were established based on the SWCCs and the shear strength test results for a large range of suction and higher stress levels during the wetting process. The impact of confining stress on the SSCCs is studied. The uniqueness of the SSCCs determined from both shear strength, and SWCCs is examined. The validity of the effective stress principle based on both the suction stress approach and the Bishop's effective stress approach under varying stress state conditions is investigated.

CHAPTER 8 presents the overall conclusions of the study and discuss possible future work.

CHAPTER 2

Literature review

2.1 Introduction

The literature review on the topics related to this research is presented in this chapter. A brief review of the collapse behaviour of unsaturated soils is given first. Subsequently, static compaction, the concept of suction, soil-water characteristics (SWCC), volume change and shear strength in unsaturated soils are presented in the following sections. The effective stress and suction stress concepts are reviewed in the last section.

2.2 Origin of collapsible soils

Collapsible soils can be found in arid and semi-arid regions where evaporation rates exceed rainfall (Houston et al. 2001b; Li et al. 2016). Naturally occurring collapsible soils are typically formed from debris flow such as wind-blown sediments (e.g. loess), cemented high salt content metastable soils (e.g. gypsums deposits), and residual tropical soil. Collapsible soils can be formed artificially through poor compaction control or where compaction is dry of optimum (Ng and Menzies 2007; Caicedo et al. 2013).

The most extensive deposited of collapsible soils are aeolian or wind-deposited sands and silts (Ng and Menzies 2007). These deposits consist of materials transported by the wind which form dunes, loess, loessial type deposits, and large volcanic dust deposits (Maswoswe 1985). The natural structure of these soils may contain clay cement binders. Loess is a classical metastable collapsible soil covers approximately 10% of the Earth's land mass (Jefferson and Ahmad 2007). According to Barden et al. (1973), loess soils can be defined as silt-sized particles ranging between 20-60 mm with clays, carbonates and capillary water acting as bonding materials at particle junctions. Some layers of loess are characterised by significant calcareous content, higher porosity and

low plasticity (Cui et al. 2004; Delage et al. 2005). These features lead to a metastable structure that is strengthened by suction when the soil is partially saturated. Subsequent soil saturation may thus induce a loss of stability of the structure with relatively large volumetric deformations due to the collapse of the open structure of the soil.

In addition to naturally deposited collapsible soils, engineered compacted fills may exhibit volume moisture sensitivity if compaction specifications and quality control are not appropriate. Compacted fills may exhibit moisture sensitivity depending on the soil type, compactive effort, compaction water content and stress level at the time of wetting (Houston 1995). Compaction to low density dry of optimum produces the greatest susceptibility to densification upon wetting, but almost any compacted soil can exhibit collapse if the applied pressure is sufficiently high (Houston et al. 2001b).

2.3 Mechanism of collapse in soils

There are three main bonding mechanisms present in collapsible soils (Jennings and Knight 1957; Barden et al. 1973; Popescu 1986; Feda 1988; Jefferson and Ahmad 2007), namely: (i) capillary or matric suction forces (Figure 2.1a); (ii) clay and silt particles at coarser particle contacts (Figure 2.1b–d); (iii) cementing agents, such as iron oxide, calcium carbonate, etc., (Figure 2.1e).

In cemented soils, collapse typically involves the destruction of all three bonding types. In contrast, in uncemented dry soils, collapse simply occurs if the capillary forces are destroyed. Although the bond strength derived from cementing and suction among soil grains can be characterised in similar ways, however, on wetting the suction will reduce and disappear, whereas chemical bonding is likely to be less affected by a change in suction. In addition, salt and clay bonds that occur at particle contacts will tend to be removed or weakened after wetting and hence collapse occurs. Furthermore, the collapse of an uncemented dry collapsible soil is due to the loss in the normal stress between soil particles leading to shear failure as a result of a reduction of capillary (matric suction) forces from wetting (Fredlund and Gan 1994). Rogers (1995) concluded that the particle shape and the particle attraction, whether by cementation, chemical or physical attraction or negative pore water pressures, are two important factors affecting the collapse mechanism.

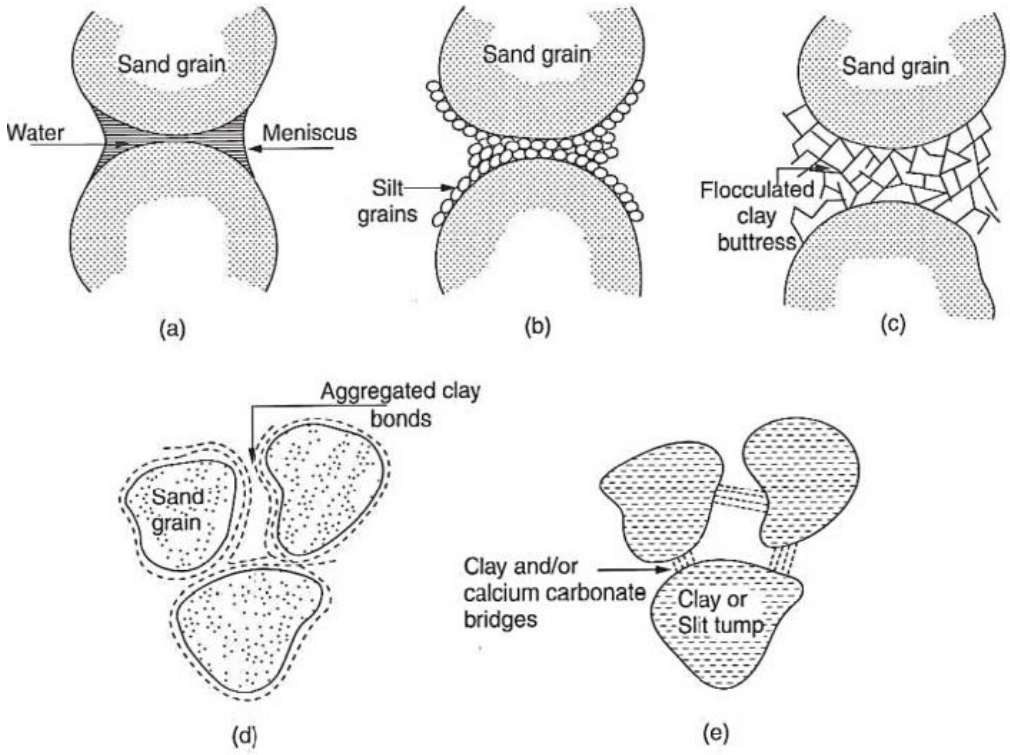

Figure 2.1 Typical bonding arrangement formed in collapsible soils (after Popescu 1986)

Observations regarding the behaviour of compacted collapsing soils during the wetting process have been made by Pereira and Fredlund (2000), they found that:

i. Phase 1 (Pre-collapse): High matric suction generates a metastable structure that suffers small volumetric deformations in response to relatively large decreases in matric suction occur. No particle slippage occurs, and structure remains intact.
ii. Phase 2 (Collapse): Intermediate matric suction and a significant volumetric deformation in response to reductions in matric suction occur, altering the structure through bond breakage.
iii. Phase 3 (Post-collapse): Saturation is approached and no additional volumetric deformations as it responds to further reductions in suction occur.

2.4 Factors influence the collapse strain

Collapse occurs because the soil has certain inherent properties. Typical features that are found with most collapsible soils have been reported in the literature (Barden et

al. 1973; Lawton et al. 1989; Lawton et al. 1992; Assallay et al. 1997; Pereira and Fredlund 2000; Rao and Revanasiddappa 2000; Lim and Miller 2004; Burland et al. 2012):

i. Collapsing soils mostly consist of primary mineral particles ranging from sand size or silt-size to clay-size. The particle size and shape are the factors that control the way in which the soil is laid down in an open packing structure and can maintain this loose structure.

ii. An open, partially saturated fabric of a high void ratio and low dry density. This property makes the soil easily undergo re-arrangement and structural collapse.

iii. A high enough net total stress that will cause the structure to be metastable.

iv. A soil with inherent low interparticle bond strength.

v. A sufficiently large soil suction or other bonding or cementing agent is available to stabilize the intergranular contacts, so the addition of water to the soil, which causes the bonding or cementing agent to be reduced and the interaggregate or intergranular contacts to fail in shear, resulting in a reduction in total volume of the soil mass.

vi. They are a geologically young or recently altered deposit (derives from the likelihood that collapse would have occurred via natural processes).

It is clear that the magnitude of collapse depends on many factors and some of the factors are more important than others depending on the type of soil (Lawton et al. 1992; Tadepalli et al. 1992; Cerato et al. 2009; Rabbi and Cameron 2014). Several researchers studied the effect of initial water content, dry density and overburden pressure on the magnitude of collapse (Barden et al. 1973; El Sohby and Rabbaa 1984; Lawton 1989; Fredlund and Gan 1994; Alawaji 2001; Lim and Miller 2004).

The state of moisture of soil when dealing with the collapse behaviour of compacted soils divided into dry and wet of optimum (Lawton et al. 1989). Numerous researchers have reported that any soil compacted at dry of the optimum condition typically exhibits collapse behaviour upon wetting, while soils compacted at wet of

optimum condition show less collapsibility (Barden et al. 1973; Lawton et al. 1989; Lawton et al. 1992; Tadepalli and Fredlund 1991). Barden et al. (1973) have suggested that collapse did not occur for samples compacted wet of optimum. However, tests carried out by Booth (1976) showed that there still is a tendency for a little collapse for samples compacted wet of Proctor optimum. Lawton et al. (1989) found that the collapse could be reduced by compacting the clayey sand soil at water contents on the wet side of optimums for impact compaction. Also, they noted that with the same dry density and overburden pressure, the amount of collapse increases continually as the initial water content decrease. This concept was also proposed by El Sohby and Rabbaa (1984), Basma and Tuncer (1992) and Fredlund and Gan (1994).

Booth (1975) investigated the effect of the initial dry density on the collapse of compacted soil. He stated that the magnitude of collapse at any specific value of water content has a maximum value which occurs at a lower initial dry density. According to El Sohby and Rabbaa (1984) and Lawton et al. (1989) test results, the initial dry density is the most important factor in determining the magnitude of collapse when the soil is compacted very dry of the line of optimum. However, close the line of optimum, the collapse potential is controlled by the degree of saturation rather than by the initial dry density. It was concluded that the susceptibility of soil to collapse inversely proportional to the initial dry density. Fredlund and Gan (1994) laboratory test results show that collapse potential decreases linearly with increasing initial dry unit weight for specimens statically compacted at a constant water content. Alawaji (2001) indicated that the rate of collapse settlement decreases with increased dry unit weight and this behaviour may be explained by the specimens' permeability. The effect of dry density ratio (is the ratio of initial dry density to the maximum dry density of the soil) on the collapse behaviour of silty glacial sand was investigated by Rabbi and Cameron (2014), Rabbi et al. (2014a) and Rabbi et al. (2014b). They were found that the dry density ratio is thought to be one of the key parameters that control the collapse behaviour of soil. The Collapse Potential (CP) of soil decreases as the dry density ratio increases. This can be explained as follows; as the dry density ratio increases the void space reduces, and therefore the soil becomes less susceptible to collapse. However, these results appear to be contradicted by data presented by Reginatto and Ferrero (1973) who presented results from laboratory oedometer collapse tests on loess soil. It was found that, contrary to common belief, dry density is not the main factor affects the collapse of soils they used, and some of the most

stable soils have the lowest densities. They have proposed that the number of dissolved salts and other chemical constituents in the pore fluid were more important than initial unit weight in contributing to collapse.

The effect of applied stress at wetting on the magnitude of collapse was also investigated by Booth (1975), Witsman and Lovell (1979), El Sohby and Rabbaa (1984), Drnevich et al. (1988), Basma and Tuncer (1992), Lawton et al. (1989, 1992), Lim and Miller (2004), Sun et al. 2007, Rabbi and Cameron (2014), Rabbi et al. (2014a) and Rabbi et al. (2014b). Their studies have concluded that:

i. The applied stress at wetting has a significant effect on the behaviour of soil.
ii. Collapse potential increases with increasing wetting pressure up to a certain point (yield stress), after which collapse potential remains the same or decreases with further increase in wetting pressure depending on the dry density ratio, soil fabric and fines fraction in the soil (Booth 1975; Witsman and Lovell 1979; Lawton et al. 1989; Sun et al. 2007).
iii. Collapse upon wetting is a direct consequence of a shift in the pre-consolidation pressure or the yield stress of the collapsible soil with suction (Loret and Khalili 2000; Khalili et al. 2004).

There are many other important factors affecting the collapse of soils. Dudley (1970) reported that the amount and rate of collapse appear to be affected by the type and quantity of clay minerals in the soil. Lawton et al. (1992) indicated that the highest collapse potential tends to exhibit when tested compacted soils containing between 10% and 40% clay particles. Alwail et al. (1994) investigated the effect of fines content on the magnitude of collapse in sand-silt-clay mixtures. Based on their results, it was noted that an increase in collapse index with increasing clay-size fraction and clay-to-silt ratio based on double-oedometer tests on sand-silt-clay combinations compacted at 90% relative compaction and a moisture content 3% below the optimum water content. The increase of collapse index with increasing clay-size fraction is attributed to the higher matric suction developed with a greater clay-size fraction. Jefferson and Ahmad (2007) noted that the maximum collapse is observed for clay contents of 25%. Basma and Tuncer (1992) have found that well-graded soils (different grain sizes) were more susceptible to collapse than poorly sorted mixtures of granular soils.

Table 2.1 presents the compositions of some collapsible soil mixtures with initial conditions and collapse strain based on previous studies. It was noted in this table that the collapse occurs in soil mixtures have different grain sizes, a low clay-size fraction (less than 35%) and low values of dry unit weight and water content.

The collapse potential was found to be directly related to the matric suction of compacted soil. The soil structure was shown to be more rigid (or less compressible) at high matric suctions. Radhakrishna and Matyas (1968) performed two series of tests on a collapsible soil. The results indicated that the compressibility of the soil is a function of matric suction. Escario and Saez (1973) conducted three series of tests on a Madrid clayey sand using a modified oedometer apparatus. It was reported that there was a reduction in total volume as a result of a matric suction decrease and that the volume change became most significant at relatively low suction values. Maswoswe (1985) carried out suction-controlled tests on collapsible clay soil. It was shown that the occurrence of the collapse was not due to overall shear failure but quite likely due to a reduction in matric suction. Fredlund and Gan (1994) conducted laboratory tests on the collapsible soil. They observed that the collapse of dry collapsible soil is due to the loss in the normal stress between soil particles leading to shear failure as a result of a reduction of matric suction from wetting. Similar behaviour was observed by Rao and Revanasiddappa (2000). It was found that the collapse potential decreases with decreasing initial matric suction of compacted specimens, and it generally increased with decreasing relative compaction.

Table 2.1 The compositions and initial conditions of some collapsible soils based on previous studies

Reference	Silt (%)	Clay (%)	Sand (%)	Dry unit weight (kN/m^3)	Water content (%)	Vertical stress (kPa)	Collapse strain (%)
Jotisankasa (2005)	52	26	22	15.30	10.2	200	3.4
Rao and Revanasiddappa (2000)	26	32	42	15.40	10.6	400	15
Pereira and Fredlund (2000)	35	13	52	14.75	10.5	200	7.2
Medero et al. (2009)	32.4	13	54.6	15.79	16.0	200	6.5
El Howayek et al. (2011)	72.5	13.5	14	15.40	21	200	11.4
Tadepalli et al. (1992)	32	6	62	14.52	12.8	55	18.6
Habibagahi and Mokhberi (1998)	66	25	9	14.80	12	400	5.7
Haeri et al. (2014)	70	20	10	15.07	7.12	200	7.12

Rabbi and Cameron (2014), Rabbi et al. (2014a) and Rabbi et al. (2014b) stated that an increase of collapse potential was observed with a decrease of the degree of saturation. These studies also investigated the role of matric suction on the collapse behaviour. A decrease in collapse potential was found with a decrease in initial matric suction. Soils with lower clay fines gave lower matric suction value even at the same initial water content and subsequently were able to settle less on wetting.

Lawton (1986) have found that the method of compaction (impact, kneading, or static) has a relatively minor influence on the wetting-induced collapse and the magnitude

of maximum collapse is the greatest for static compaction and the lowest for kneading method.

A study conducted by Basma and Tuncer (1992) involved a multiple regression analysis on results of 138 single-oedometer tests. The tests were conducted on eight natural soils prepared at relatively low dry unit weights and moisture contents. The majority of the samples were compacted at relative compaction of 80% and moisture contents of 10–13% dry of the OMC. They have found that factors that had the most impact on the magnitude of collapse were initial water content, dry unit weight, stress at wetting. From the results of Garakani et al. (2015) study, it is concluded that any increase in the magnitude of mechanical stresses (confining net stress or shear stress) or degree of saturation (wetting process) results in an increase in the magnitude of collapse.

2.5 Identification of collapse potential and test methods

Standard oedometer or modified triaxial equipment are typically conducted to employ collapse tests. In both types of laboratory tests and after equilibrium conditions under the applied stresses are reached, the soil specimen is provided with free access to water. In standard oedometer tests, the sample is submerged; in triaxial tests, water is commonly introduced from the bottom of the sample under a small positive head. Two loading-wetting sequences have been used in the laboratory to study collapse. The more frequently used method consists of incrementally loading the as-compacted soil to reach the desired vertical stress, allowing the sample to come to equilibrium under the applied stresses, at the end of this loading the specimen is wetting with water and left for a given time interval (Drnevich et al. 1988; ASTM D5333-03 2012). This wetting-after-loading method has been used in both one-dimensional analyses using oedometers (known as the single-oedometer collapse test) and three-dimensional analyses using the triaxial equipment (Lawton et al. 1992). The single oedometer test is simple and fast (Lim and Miller 2004).

A second load-wetting sequence is known as the double-oedometer procedure (Jennings and Knight 1957). In this method, two identical samples are prepared and tested individually in oedometer device. One specimen is initially inundated with water under a small seating load and allowed to swell then loaded in a standard incremental fashion. The other specimen is tested at the as-compacted water-content using standard

incremental loading procedure. The vertical strain difference between the as-compacted and inundated test results at a given stress level is assumed to be the collapse potential. The major advantage of the double-oedometer tests is that a large amount of data that can be obtained from a single test as this procedure allows a determination of collapsibility under any level of stress within the range tested.

Although the sequence of loading and wetting is different between the single and double-oedometer methods, many researchers found that the two methods generally agree in the collapse value (Booth 1976; Justo et al. 1984; Lawton et al. 1989; Lim and Miller 2004). However, there have been several studies reporting that there is generally a poor agreement between single and double oedometer test results such as Drnevich et al. (1988).

Based on the oedometer-collapse tests, the collapse potential can be assessed and used to indicate the problem severity of collapse. Table 2.2 provides details presented by Jennings and Knight (1975) and ASTM D5333-03 (2012), showing a slight difference between the two references in the collapse potential range corresponding to problem severity.

Table 2.2 The severity of the collapse potential

ASTM D5333-03 (2012)		Jennings and Knight (1975)	
CP (%)	Severity of problem	CP (%)	Degree of collapse
0 - 1	No problem	0	None
1 -5	Moderate trouble	0.1-2.0	Slight
5 - 10	Trouble	2.1-6.0	Moderate
10 -20	Severe trouble	6.1-10.0	Moderately severe
> 20	Very severe trouble	> 10:0	Severe

Since this laboratory testing is expensive and a time-consuming process, several researchers have introduced empirical equations to determine the collapse potential (CP) (Basma and Tuncer 1992; Zorlu and Kasapoglu 2009; Rabbi and Cameron 2014).

2.6 Static compaction of soils

Compaction is a method of mechanical stabilization of soil which consists of densification by reduction of air voids without changing water content (Monroy 2005). Compaction generally increases the strength of soil, reduces its compressibility and permeability. The main variables that control the compaction of a given soil are water content (Cui and Delage 1996), type of compaction and compactive effort (Zhemchuzhnikov et al. 2016). The state of soil after compaction has generally been assumed to be the initial state of the soil in constitutive modelling. In the other word, when the compaction properties of a soil are known, it is possible to prepare samples in the laboratory representative of the material to be used for the determination of its engineering characteristics such as volume change and shear strength (Tarantino and De Col 2008).

Laboratory compaction tests can provide a set of curves showing the relationship between water content and dry density for different energy levels, from which the values of water content corresponding to maximum dry density can be obtained. As compaction energy increases, maximum dry density becomes higher and optimum water content decreases (Fredlund and Rahardjo 1993a).

The volume of the soil decreases continually when its statically compacted, as the load is applied to the whole area of the sample by using a hydraulic pump concept (Turnbull 1950). Once water content approaches saturation, and no more air can be expelled, either consolidation starts, water is drained from the soil, or, if there is no way for water to drain, pore pressure begins to grow at an equal rate as the applied load, for water is relatively incompressible. The parameter that in most cases is used to control static compaction is maximum stress rather than energy (Walker 2004; Lawson et al. 2011). Unlike in the Proctor test, where the energy transmitted to the soil is constant, the energy in static compaction test, can be calculated by integration of the force-displacement curve, for a constant maximum pressure or strain. Static compaction curve

plotted for constant maximum pressure, and a dynamic one, which is plotted for equal energy input cannot be compared directly.

Static compaction test can be performed at a constant rate of stress or constant rate of strain using either maximum force or maximum displacement as the limiting condition. High compaction speed can cause a rapid increase in pore pressure especially in fine-grained soils (Reddy and Jagadish 1993). Table 2.3 shows some of the displacement rates have been adopted in the static compaction tests from previous studies.

Turnbull (1950), Olivier and Mesbah (1986) and Doris et al. (2011) obtained static compaction curves are similar to the Proctor compaction curves in shape. and the energy contribution to the soil varies with the amount of water content. Reddy and Jagadish (1993) performed static compaction of a silty clay at a constant rate of strain of 1.25 mm/min. In their study, the static compaction tests were carried out on three different block sizes. Five different quantities of moist soil were used. For each water content, force-displacement curves were obtained, and energy density was calculated. Compaction curves were plotted for different energy inputs and compared with the results of the Proctor test. The shape of static compaction curves was different from the dynamic one as they presented no wet side of optimum. Similar static compaction curves were obtained by Mesbah et al. (1999) and Tarantino and De Col (2008). Reddy and Jagadish (1993) also reported that the increase in surface area of a compacted specimen with respect to its volume lead to a greater loss of energy due to boundary friction.

Table 2.3 Displacement rates in the static compaction tests based on literature

Reference	Soil types	Displacement rate (mm/min)
Rahardjo et al. (2004)	Sandy clay (CL) Sand (%) =34.0 Silt (%) =24.0 Clay (%) =42.0	1.5
Jotisankasa (2005)	70% silt, 20% Kaolin, and 10% clay	1.5
Ng and Menzies (2007)	Expansive soil Sand (%) = 7 Silt (%) = 44 Clay (%) = 49	0.3
Estabragh and Javadi (2008, 2014)	Silt with low plasticity (ML) Sand (%) = 5 Silt (%) = 90 Clay (%) = 5	1.5
Hoyos et al. (2011)	Silty sand (SM) Sand (%) = 55 Silt (%) = 37 Clay (%) = 8	1
Romero (1999)	Clay powder	0.5
Reddy and Jagadish (1993)	Loose soil Sand (%) = 48.8 Silt (%) = 22.4 Clay (%) = 28.8	1.25
Cui and Delage (1996)	Aeolian silt	0.15
Hoyos et al. (2010)	Silty sand	1.25
Saad et al. (2012)	Sand (%) = 53.3 Silt (%) = 37.5 Clay (%) = 9.2	2.54
Vogler et al. (2007)	Silty clay	0.6
Sharma (1998)	Bentonite/kaolin mixture	1.5
Estabragh and Javadi (2008)	Sand (%) = 5 Silt (%) = 90 Clay (%) = 5	1.5

The effect of friction between compaction mould and the soil was mentioned by a number of researchers (Walker 2004; Olivier and Mesbah 1986; Reddy and Jagadish 1993; Zhemchuzhnikov et al. 2016), yet there are no quantitative results available.

Whitman et al. (1960) found that static compaction methods gave substantial density variations within specimens, with a height to diameter ratio of unity.

Gau and Olson (1971) compared dynamic, static, and kneading compaction and concluded that the static method gave the most uniform specimens. This finding is consistent with the study by Booth (1976), which showed that the greatest uniformity is achieved by static compaction in one thin layer.

2.7 Unsaturated soil mechanics framework for collapsible soil

In general, soil mechanics can be divided into two parts namely: saturated and unsaturated soil mechanics. The main difference between saturated and unsaturated soil mechanics is the consideration of air phase when studying the mechanical behaviour of soils. Soils near the ground surface are usually in a moist condition and therefore will be subjected to negative pore-water pressure (Fredlund and Rahardjo 1993a). Problems associated with unsaturated soil cannot be solved using classical saturated soil mechanics as the behaviour of unsaturated soil can differ greatly from that of saturated soils. Thus, understanding the engineering behaviour of unsaturated soil is important.

Over the past decades, published research has attempted to explain the collapse phenomenon using theories of unsaturated soil mechanics. Barden et al. (1973) explained that the phenomenon of collapse which underlies all soil mechanics theory was apparently a conflict of the principle of effective stress, as wetting cause increase in pore pressures. As a result, decrease the effective stress and hence is expected to cause swell rather than settlement. However, more detailed consideration of the mechanism indicated that local shear failure between soil grains cause collapse, and hence is appropriate with the principle of effective stress.

The principles of unsaturated soils mechanics provide a reasonable framework for the characterization of collapsible soils (Knodel 1992; Fredlund and Gan 1994). The applied stress and the suction are the two separate components of effective stress that could explain the collapse process in unsaturated soils (Fredlund and Gan 1994). These two components develop intergranular stress by different mechanisms; thus, the applied stress develops shear stresses and hence potential instability at intergranular contacts, while the suction is strictly normal stress and hence increases the stability at intergranular

contacts (Bishop and Blight 1963). The suction in a soil profile can vary widely, whereas the net stress state may remain entirely constant.

2.7.1 Concept of suction

Soil suction is a major factor affecting the behaviour of unsaturated soils and is made up of two components, namely matric suction and osmotic suction. The sum of the two components is called total suction (Fredlund and Rahardjo 1993a; Fredlund et al. 2012). Matric suction is associated with the capillary phenomena arising from the surface tension of water whereas osmotic suction is a difference in salt concentrations in the pore water in the system being analysed, and the surrounding water, and is written in terms of pressure (Fredlund and Rahardjo 1993a).

It is well known that most engineering problems involving unsaturated soils are caused by environmental changes (e.g., rainfall or evaporation) which result in a change in pore- water pressures and are therefore directly linked to the matric suction (Fredlund and Rahardjo 1993a; Murray and Sivakumar 2010). Water infiltration into an unsaturated collapsible soil primarily involves a change in matric suction (Because an increase in water content is unlikely to lead to a significant change in the osmotic suction). Matric suction is one of the principal stress variables can be used to define the constitutive behaviour of collapsing soils. In engineering practice, the matric suction (s) is defined as the excess of pore air pressure (u_a) over pore water pressure (u_w) as expressed by:

$$s = (u_a - u_w) \tag{2.1}$$

In unsaturated soils, matric suction is controlled by a capillary effect and adsorption of water (Fredlund and Rahardjo 1993a). The study of capillary phenomena is directly related to the surface tension of water. The surface tension is caused by the unbalanced intermolecular forces acting on molecules at the air-water interface, which is known as the contractile skin. The contractile skin under the influence of surface tension behaves like a stretched elastic curved membrane (see Figure 2.2). In unsaturated soils, pores with small radii act as capillary tubes and cause the soil water to rise above the water table. The smaller the tube radius, the greater the curvature, and the higher the

capillary rise. The water pressure inside the capillary tube is less than the air pressure, which is generally atmospheric. In the capillary tube, the pressure difference between pore air and pore water pressure can be calculated by using the Young-Laplace equation:

$$u_a - u_w = \frac{2T_s cos\beta}{r_s} \tag{2.2}$$

where T_s refers to the surface tension of the air–water interface (contractile skin), β the contact angle of the air–water interface with the wall of the capillary tube, and r_s is the radius of the tube.

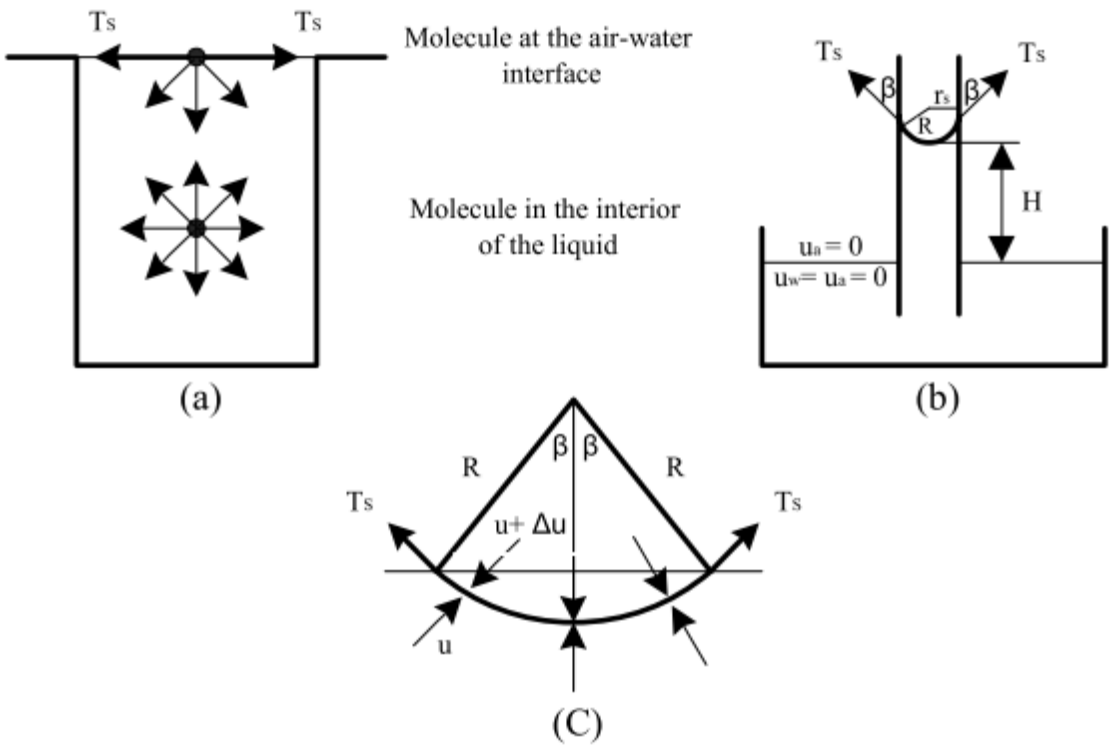

Figure 2.2 Physical capillary model (from Fredlund and Rahardjo 1993)

The surface adsorption is principally relevant to clay minerals and occurs as a result of the clay particles' negatively charged surfaces (Mitchell 1976). In this situation, water molecules will be strongly attracted and adsorbed onto the clay particles due to their electrical polarity. This adsorbed water forms a hydration envelope that covers the whole

surface area of the particles, as shown in Figure 2.3a. This is an important phenomenon, as the mechanical behaviour of clayey soils is significantly influenced by the degree of hydration of its clay particles. The positively charged cations in the soil solution and polar water molecules attracted to the clay surface form an electrical double layer. The double layer refers to two parallel layers of charge surrounding the clay particles, as shown schematically in Figure 2.3b. According to Hillel et al. (1998), in reality, capillary and adsorbed water cannot be considered separately. It was therefore concluded that the value of the measured matric suction, especially if the soil contains a significant amount of clay minerals, denotes the total effect resulting from capillary and adsorption together. As noted by Hillel et al. (1998), for low values of matric suction (0-100 kPa), the amount of pore water retained within the soil matrix will depend primarily on capillary effects. With increasing matric suction, however, the dominant effect controlling the amount of water within the soil matrix will increasingly become adsorption, with capillarity reducing in importance.

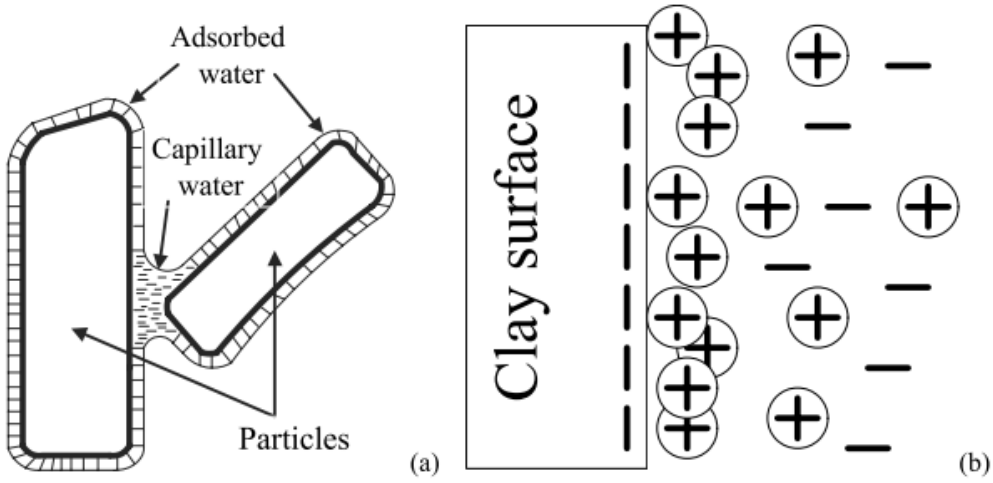

Figure 2.3 (a) Water in unsaturated soil, subjected to capillary and adsorption (after Hillel, 1998) (b) Diffuse Double Layer

There are numerous descriptions of the effect of suction on the mechanical behaviour of unsaturated soils. Karube and Kato (1994) proposed the concept of 'Meniscus water' and 'Bulk water' from a microscopic point of view (see Figure 2.4). The bulk water is the pore water which occupies the pore volume between soil particles, and meniscus water exists at the contact point between soil particles. The proportion of bulk

water in the soil water increases with the degree of saturation. On the contrary, the proportion of meniscus water increases with the decrease of the degree of saturation. Thus, the proportions of bulk water and meniscus water would be affected by matric suction. The meniscus water increases the intergranular adhesive force acting perpendicularly on the contact plane between soil particles, and it causes an increase in the stiffness of the soil skeleton. On the other hand, the bulk water induces not only an increase in the stiffness of soil skeleton but also a decrease of the volume of the soil mass due to slippage between soil particles at contact points. Karube et al. (1996) defined the stress components caused by the influence of meniscus water and bulk water as the meniscus stress (P_m) and the bulk stress (P_b), respectively. The summation of two stress components is equal to suction stress (σ^s). Thus, it could be said that the net stress is induced by the external load, but the suction stress develops from the effect of suction and influences the mechanical behaviour of unsaturated soil. The relationship between the suction stress, the meniscus stress and the bulk stress are expressed as follows:

$$\sigma^s = P_m + P_b \tag{2.3}$$

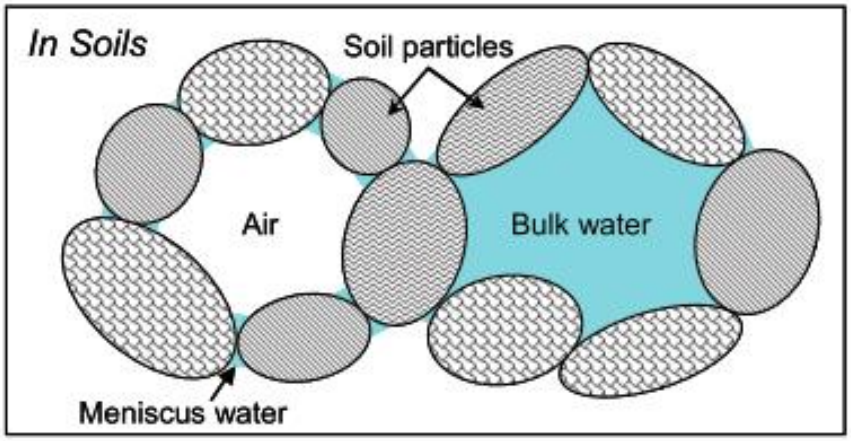

Figure 2.4 Concept of meniscus water and bulk water (after Karube et al. (1996)).

Wheeler and Karube (1996) who have considered that the water menisci at the particle contact points result in an additional interparticle force. This additional normal force improves the stability of unsaturated soil. The water menisci can be considered to

act as bonds holding the soil particles together. The soil's resistance to compression and swelling increases due to the presence of this interparticle bonding. The removal of the interparticle bonds between particles by wetting the soil may result in particle slippage and collapse of the structure.

2.7.1.1 Overview of suction measurement

Attempts to measure and control the suction have thus been central to the laboratory testing of unsaturated soils (Fredlund and Rahardjo 1993a). The accurate measurement of soil suction is thus vital to understanding the behaviour of unsaturated soils. However, magnitudes of suction can vary enormously (between 0 and 1000000 kPa) (Fredlund and Rahardjo 1993b; Fredlund et al. 2012). There is no unique technique or device which covers the entire range of suction measurements of unsaturated soils. Therefore, in order to measure a wide range of suction, a combination of two or more techniques may be used (Fredlund and Rahardjo 1993b; Fredlund et al. 2012).

The different methods can be broadly divided into direct and indirect techniques. The direct approach measures the equilibrium of a soil water system without involving any external medium, while the indirect approach involves the use of an external medium that achieves moisture equilibrium with the soil (Fredlund and Rahardjo 1993b; Leong et al. 2003; Lu and Likos 2004; Agus and Schanz 2005; Tripathy et al. 2005; Rahardjo and Leong 2006; Ng and Menzies 2007; Bulut and Leong 2008; Delage et al. 2008; Tarantino 2009; Tripathy et al. 2016).

2.7.1.1.1 Chilled-mirror dew-point technique

In geotechnical engineering, the chilled-mirror dew-point technique has been used for measuring total suction of soils (Leong et al. 2003; Agus and Schanz 2005; Campbell et al. 2007; Tripathy and Rees 2013; Tripathy et al. 2016). The working principle of the chilled-mirror potentiameter device is based on the thermodynamic relationship between relative humidity, temperature and total suction. The device computes the total suction based on the equilibrium of the liquid phase of the water in a soil specimen with the vapour phase of the water in the air space above the sample in a sealed chamber. Due to the rapid suction increase with decreasing relative humidity at low suctions, the dew point potentiometer is considered accurate for suction measurements of above 1000 kPa (Lu

and Likos 2004). The main advantages of chilled-mirror hygrometer for soil suction measurement are its simplicity and speed (Fredlund et al. 2012).

2.7.1.2 Suction control

Various methods have been adopted for controlling matric in a soil specimen during unsaturated soil experiments. The axis translation technique is one of the most common techniques for imposing suction. A brief review of the axis translation method is given here.

2.7.1.2.1 Axis-translation technique

The axis-translation technique (Hilf 1956) was primarily developed in order to overcome the problem of cavitation (Cavitation is the term that describes the process of phase translation from the liquid phase to vapour phase along a path of decreasing pressure) at low negative water pressures. The basic principle of this technique is to elevate the pore water pressure and pore air pressure by the same amount so that the matric suction remains constant. In this technique, both pore water pressure and pore air pressure are controlled and measured independently. Axis-translation is accomplished by separating air and water phases in the soil through a saturated high air-entry porous material, usually a ceramic disk. The saturated high air-entry ceramic disk allows water passage but prevents the flow of free air when the applied matric suction does not exceed the air-entry value of the ceramic disk (Fredlund et al. 2012).

Fredlund (1989) used this technique for the measurement of matric suction in a soil sample. As shown in Figure 2.5, when the soil specimen, with initial negative pore water pressure, is placed on top of the saturated high air-entry disk, draws water through the porous disk. This causes the pressure transducer to commence registering a negative value. The test is performed by applying air pressure in the chamber until there is no further tendency for flow in or out of the soil sample through the high air entry disk. In this way, the water pressure in the measuring system becomes a positive value, and the problem of cavitation is prevented. Controlling of matric suction using this technique is limited by the air entry value of the ceramic disk used.

The axis-translation technique is commonly used in the laboratory testing of unsaturated soils because it is relatively easy to convert existing equipment for saturated

soil testing by simply adding a high air entry filter and an air pressure source. This technique has been applied successfully for measurement of SWCC, unsaturated shear strength and volume change testing by many researchers with equipment including oedometers, direct shear and triaxial apparatus (e.g., Bishop and Donald 1961; Fredlund and Morgenstern 1977; Fredlund et al. 1978; Escario and Sáez 1986; Gan et al. 1988; Wheeler and Sivakumar 1995; Vanapalli et al. 1996; Fredlund et al. 1996; Khalili and Khabbaz 1998; Rassam and Williams 1999; Rassam and Cook 2002; Leong et al. 2004; Sun et al. 2007; Goh et al. 2010; Ng et al. 2017).

One of the main limitations related to the axis translation technique involves the air and water phases to be continuous in order to characterize actual suction within the soil sample. Good contact between the soil specimen and the saturated ceramic disk should be established throughout the experiment to ensure the continuity between the water phase in the soil specimen tested and that in the pores of the ceramic disk used (Bishop and Donald 1961a; Fredlund et al. 1978; Sivakumar 1993; Fredlund and Rahardjo 1993a; Murray and Sivakumar 2010; Fredlund et al. 2012).

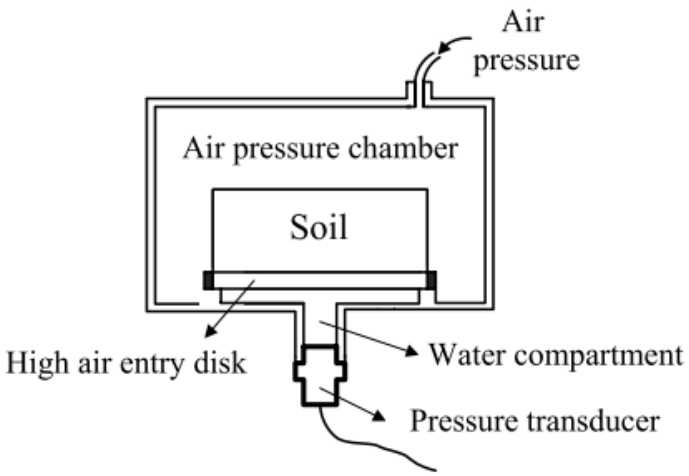

Figure 2.5 Schematic diagram of the axis translation device used by Fredlund (1989) for measuring matric suction

2.7.2 Stress state variables

The mechanical behaviour of soil (i.e., the volume change and shear strength behaviour) can be described in terms of the state of stress in the soil. The state of stress in soil consists of certain combinations of stress variables (Fredlund and Rahardjo

1993a). Up to now, there are many approaches for describing stress state variables for unsaturated soil which are important for constitutive models and for analysing the mechanical behaviours of unsaturated soil. Brief introductions of popular approaches are presented as follows:

2.7.2.1 Single effective stress

The principle of effective stress is regarded as one of the most fundamental concepts, which plays a central role in saturated soil mechanics (Fredlund and Rahardjo 1993b). For saturated soil, Terzaghi (1936) defined effective stress quantity as "that part of the total stress which produces measurable effects such as compaction or an increase of the shearing resistance". The effective stress is the stress state variable which is independent of soil properties. The effective stress (σ') is defined as the excess of the total applied stress (σ) over the pore water pressure (u_w) (Lu and Likos 2004) as follows:

$$\sigma' = \sigma - u_w \tag{2.4}$$

The success of the principle of effective stress in describing the mechanical behaviour of saturated soils led researchers to search for an equivalent single effective stress for unsaturated soils. Bishop (1959), among many others, proposed a form of effective stress under unsaturated conditions. It explicitly modified the pore water pressure in Terzaghi's effective stress by a factor of χ, which varies between 0 and 1. The equation is commonly referred to as Bishop's effective stress equation for unsaturated soils which is incorporate both pore air pressure (u_a) and pore water pressure (u_w):

$$\sigma' = (\sigma - u_a) + \chi(u_a - u_w) \tag{2.5}$$

where χ is an effective stress parameter related to the degree of saturation (S_r) with zero corresponding to completely dry soil and unity corresponding to fully saturated soil and $(\sigma - u_a)$ is the net stress.

Later, Jennings and Burland (1962) showed that during inundation at constant applied stress, samples of silt reduce in volume, even when the effective stress decreases. A decrease in effective stress should induce an increase in void ratio, which is contrary to the experimental observation. Another example of difficulties in using the single effective stress approach for describing unsaturated soils behaviour is the influence of suction on the interparticle forces. As stated by Jennings and Burland (1962) and many subsequent authors such as Burland (1965) and Wheeler and Karube (1996), matric suction and externally applied stresses have a qualitatively different effect on the stability of the soil structure and, therefore, it is not possible to model the soil response in a realistic manner with a single stress variable. In addition, the χ parameter appears to be difficult to evaluate and seems to have different magnitudes for different problems and different magnitudes for different types of soil (Bishop and Blight 1963; Burland 1965; Lu and Likos 2006). Morgenstern (1979) found that the χ parameter, when determined for the volume change process, has a different value from that determined for shear strength. Another theoretical difficulty is that Equation 2.5 predicts zero effective stress for any soil in a dry state under no external stress. However, many soils, such as clays, under dry conditions, can have effective stresses of the order of several hundred kPa (Lu and Likos 2006; Lu et al. 2010). For these reasons, the general applicability of this effective stress approach for unsaturated soil mechanics have been limited in practice and continues to be a subject of debate (Lu and Likos 2004; Fredlund et al. 2012).

2.7.2.2 Two stress state variables

To overcome the inability of the single effective stress approach to explaining the mechanical behaviour of unsaturated soils, several researchers including Coleman (1962) and Bishop and Blight (1963) suggested that net stress and matric suction must be considered as independent stress variables with their own separate influences on stress-strain behaviour. Further work by Fredlund and Morgenstern (1977) indicated that any two of the three independent stress variables among the following: $(\sigma - u_a)$, $(\sigma - u_w)$ and $(u_a - u_w)$ may be used to describe the stress state considering the soil as a four-phase system. The most common independent stress state variables are net stress $(\sigma - u_a)$ and matric suction $(u_a - u_w)$ (Wheeler and Karube 1996). This approach was the basis for developments in constitutive modelling of unsaturated soils. Compared with the use of a single effective stress variable, the adoption of two independent stress

variables has produced more meaningful and consistent descriptions of unsaturated soil behaviour (Alonso et al. 1990), which plays a central role in the development of a class of elastoplastic models for unsaturated soil (e.g., Alonso et al. 1990; Wheeler and Sivakumar 1995). This class of models has some interesting features in consistently describing shear failure and wetting induced collapse phenomena (e.g., Alonso et al. 1990; Wheeler and Sivakumar 1995; Gallipoli et al. 2003).

While this approach provides insight into important concepts such as loading collapse and suction increase and decrease curves, it's like the single variable effective stress state approach add additional complexity by requiring additional material parameters that are often either variable or difficult to determine experimentally reflects $\emptyset^b$ the increase in shear strength with respect to matric suction (Lu et al. 2010). Using these two stress state variables, it is not possible to incorporate the influence of the degree of saturation on mechanical behaviour because the occurrence of hysteresis in the water retentive curve during drying and wetting process means that two samples of the same soil subjected to the same values of suction can be at significantly different values of degree of saturation, if one is on a drying path and the other is on a wetting path. The inter-particle forces produced by meniscus water, bulk water and air are qualitatively different (Wheeler et al. 2003). Even if net stresses, suction and void ratio are all same for two samples, these samples may show different mechanical behaviour at a different degree of saturation, which make the inter-particle forces transmitted by soil skeleton different. For these reasons, the practical applicability of the two independent stress state variable approach have been limited as well (Khalili and Khabbaz 1998; Nuth and Laloui 2008; Lu et al. 2010).

2.7.2.3 True effective stress state variable approach

To avoid the fate of Bishop's effective stress and the two-independent stress state variable approach deficiency, Lu and Likos (2006) proposed the suction stress (σ^s) concept to characterize the matric suction more effectively and clarify its influence on the effective stress and shear strength of unsaturated soil. This concept represents the state of stress for unsaturated soil using a single stress variable by expanding Terzaghi's (1943) and Bishop's effective stresses (1959) and expresses the state of stress using SWCC. The suction stress refers to the net interparticle force generated within a matrix of unsaturated soil particles due to the combined effects of the physicochemical stress induced by the

van der Waals attractions, the electrical double layer repulsion and the chemical cementation and the matric suction, which is generalized by surface tension and negative pore water pressure. The macroscopic consequence of suction stress is a force that tends to pull the soil grains toward one another. The suction stress composed of inter-particle forces can express the functions of the water content, the degree of saturation and the matric suction. Therefore, the suction stress is expressed as the characteristic function of the soil–water system. That is, the suction stress has a particular relationship with the matric suction or effective degree of saturation, and this relationship is defined as the suction stress characteristic curve (SSCC) (Lu and Likos, 2004, 2006; Lu et al. 2009, 2010; Oh et al. 2012, 2014).

2.7.3 Soil-water characteristic curve (SWCC)

The SWCC is certainly the most widely used tool in engineering practice when unsaturated soils are involved. It is linked not only to flow problems but also to shear strength and compressibility (Song 2014; Marinho 2018). SWCC is a function, which describes the relationship between suction and the corresponding state of wetness of the soil. The state of wetness can be expressed in various ways, the degree of saturation, gravimetric water content, or volumetric water content. Each form of SWCC would provide similar information to the geotechnical engineer if the soil did not undergo volume change (Fredlund et al. 2011). When a soil undergoes volume change as soil suction change, the air-entry value and residual conditions need to be determined from a plot of degree of saturation versus soil suction (Fredlund et al. 2011). The degree of saturation versus soil suction plays a crucial role in understanding and modelling the characteristics of shear strength and volume change for unsaturated soils (e.g., Fredlund and Rahardjo 1993b; Vanapalli et al. 1996; Jotisankasa 2005).

2.7.3.1 Features of SWCC

Two variables that are often identified on an SWCC are the air-entry value (AEV) and the residual state condition (Fredlund and Rahardjo 1993b; Fredlund et al. 2011). Air-entry value and/or residual state condition are often used in unsaturated soil property functions such as the unsaturated shear strength. Vanapalli et al. (1996) proposed the graphical method, which is still commonly used by researchers, for the determination of the air-entry value, residual suction and residual saturation. The air-entry value is defined

as the soil suction at which air first enters the pores of the soil (Brooks and Corey 1964; Thu et al. 2007; Fredlund et al. 2011). AEV is usually determined as the soil suction at the intersection of the horizontal line through the saturated degree of saturation and the tangent line at the inflection point of the SWCC as illustrated in Figure 2.6. This technique has been extensively used by several researchers (Vanapalli et al. 1998; Leong and Rahardjo 1997; Tekinsoy et al. 2004; Yang et al. 2004). At suction values smaller than the air-entry value, the soil remains saturated, and the stress-strain behaviour of the soil should be represented in terms of the conventional effective stress for saturated soil. Moreover, the air-entry value provides an indication of the point where the shear strength versus matric suction starts to exhibit nonlinear shear strength behaviour (Fredlund et al. 2012). The air-entry value of a soil is significantly influenced by its structure and is largely dependent on particle size for granular soils and on pore size for clayey soils (Georgiadis 2003; Fredlund and Rahardjo 1993a).

Residual state condition is generally referred to as the condition when the water phase in the soil becomes discontinuous and therefore immobile or when a large change in soil suction is required to further remove water from the soil. The importance of residual state condition for unsaturated soil property functions was recognized by various researchers (Brooks and Corey 1964; White et al. 1970; van Genuchten 1980; Luckner et al. 1989; Vanapalli et al. 1996; Thu et al. 2007; Schnellmann 2015). Most commonly, researchers used a construction method on a semi-logarithmic plot of the SWCC to identify residual state condition. For the construction method, a tangent line is drawn at the inflection point of the SWCC, and another line is approximated at high soil suction values (see Figure 2.6). Residual state condition is identified at the intersection point of the two straight lines (Rassam and Williams 1999; Goh et al. 2010; Zhai and Rahardjo 2012).

Vanapalli et al. (1996) introduced three zones, namely the boundary effect zone, transition zone and residual zone, associated with SWCC, as illustrated in Figure 2.6. These three zones are defined by their air-entry value (AEV) and residual suction. The zone where the matric suction is less than AEV is the boundary effect zone, the zone where the matric suction is greater than the residual suction is the residual zone, and the zone where the suction is between AEV and residual suction is defined as the transition zone. When soil is in the boundary effect stage, all the pores in the soil are still filled with water. The water content reduces rapidly and significantly with increasing matric suction

in the transition stage. In the residual stage, the soil pores are mainly occupied by air and water phase becomes discontinuous. A small change in the water content of the soil although a large increase in matric suction is applied in this stage.

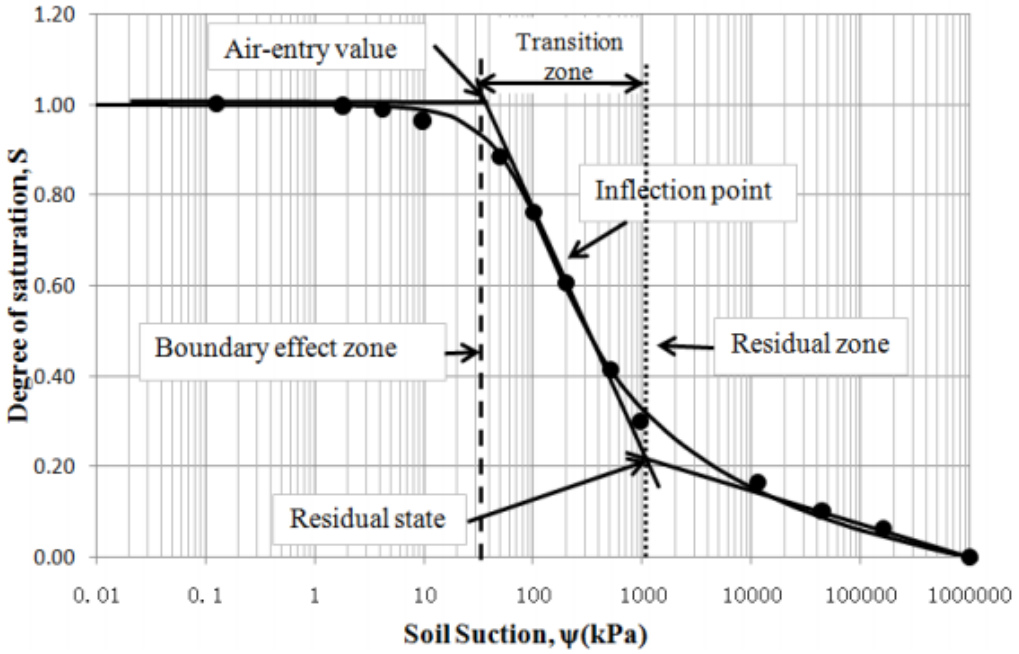

Figure 2.6 Illustration of the situ zones of desaturation defined by SWCC (after Fredlund (2006))

Soil-water characteristic curve (SWCC) can be categorized as a drying curve and a wetting curve. The drying curve is obtained by measuring the water content of a soil sample during the drying process, while the wetting curve is obtained by measuring the water content of a soil sample during the wetting process. Different starting points for drying or wetting processes result in different curves. These curves are normally called scanning curves. Phenomena associated with the different curves of the wetting and drying processes are commonly referred to as the hysteretic property of soil (Pham et al. 2005; Tarantino 2009; Gallipoli et al. 2015).

2.7.3.2 Measuring SWCC using modified triaxial apparatus

Measuring SWCC has been proven to be the most important test for a successful application of unsaturated soil mechanics in geotechnical engineering (Fredlund 2006). A number of devices have been developed for applying a wide range of soil suction values

include pressure plate extractors, hanging column, chilled mirror hydrometer. In addition, modified triaxial and odometer apparatus can also be used to obtain the SWCC of a soil (Fredlund et al. 2012).

A modified triaxial cell is a rather elaborate apparatus that can be used to measure the SWCC. The triaxial equipment needs to have a high-air-entry disk sealed onto the base pedestal used to control the water pressure and a low-air-entry material used to control the air pressure at the top of the soil specimen. There are a number of advantages associated with the use of the modified triaxial equipment (Fredlund et al. 2012). First, the triaxial apparatuses provide greater flexibility in terms of the stress path that can be followed. It is possible to apply a net confining pressure, which is similar to the in-situ condition of the soil, can be applied to the soil specimen during the SWCC test. Second, both total volume change and water volume change can be measured continuously and accurately. This is relatively important for measuring the collapsible soil specimens which experiences a significant total volume change during wetting processes.

2.7.3.3 Factors that influence the shape SWCC

The shape of the SWCC is strongly controlled by the grain-size distribution of the soil. The slope of the grain-size distribution is related to the slope of the SWCC (Yang et al. 2004; Gao and Sun 2017). A steep slope in the grain-size distribution results in a steep slope in the SWCC.

The SWCC of soils under different net confining stresses (or net normal stresses) were investigated in various studies. (Fredlund and Rahardjo 1993a; Kato and Kawal 2000; Ng and Pang 2000; Lee et al. 2005; Oh and Lu 2014). Vanapalli et al. (1996) and Ng and Pang (2000) found that under a higher applied net normal stress has a gentler SWCC slope and a higher AEV than those under a lower net normal stress. Lee et al. (2005) investigated the effect of net confining stresses on the SWCCs and revised triaxial tests were carried out on weathered granite soil. The study indicated that as the net confining pressure increases, the AEV increases linearly, the degree of saturation at the same matric suction increases and the slope of SWCC beyond AEV becomes more flatten. A series of SWCCs was determined for statically compacted nondeformable silt specimens in a triaxial cell apparatus under different net confining stresses by Thu et al. (2007). The results showed that the air-entry value increased with increasing net confining

stress. Oh and Lu (2014) examined the SWCCs of a decomposed granitic soil were made with different confining stresses under both drying and wetting conditions. The results showed that air entry suction tends to increase in the drying SWCC as the confining stress increases. In the case of the wetting curves, the air-expulsion pressure, which is largely controlled by smaller pores, is much less affected by the confining stress because the confining stress has less effect on smaller pores. Also, the data showed that the SWCC is clearly independent of the confining stresses and it can be uniquely defined in terms of the effective degree of saturation. Vanapalli et al. (1996) and Ng and Pang (2000) have found that for the same matric suction as the confining stress increases, the water content decreases. The SWCC is dependent on the applied confining stress if it is expressed in terms of the water content.

2.7.3.4 Modelling of soil-water characteristic curves

The SWCC is generally represented through empirical equations. Several equations to best-fit SWCC measurements have been proposed over the past decades (e.g., Brooks and Corey 1964; van Genuchten 1980; Fredlund and Xing 1994). These equations consist either of two or three fitting parameters. As discussed by Fredlund and Rahardjo (1993a), all of the proposed equations have one variable that bears a relationship to the air-entry value (AEV) of soil and a second variable that is related to the rate at which the soil desaturates. A third variable is used for some equations, and it allows the low matric suction range, which is near the AEV, to have a shape that is independent of the high matric suction range, which is near the residual matric suction. The use of three parameters for the SWCC provides greater flexibility for the best-fitting analysis.

Fredlund et al. (2012) stated that best-fit equations were needed because many applications of the SWCC require it to be differentiated or integrated and be continuous. Leong and Rahardjo (1997) reviewed and evaluated the popular SWCC models and found out that the van Genuchten (1980) model and the Fredlund and Xing (1994) model are the best SWCC models for a variety of soils.

van Genuchten (1980) proposed an equation using the relationship between the effective degree of saturation (S_e) and the pressure head based on the original equation of Mualem (1976). The advantages of the van Genuchten (1980) model are (Sillers et al., 2001): (*i*) it provides a wide range of flexibility in fitting SWCC data from a variety of

soil types, (*ii*) the model parameters have physical meaning, (*iii*) the effect of one soil parameter can be distinguished from the effect of the other two parameters.

Adopting the concept of pore-size distribution, Fredlund and Xing (1994) proposed another continuous best-fit equation similar to van Genuchten's (1980) equation. Fredlund and Xing (1994) assumed the form of the pore-size distribution function and derived the best-fit equation by integrating the pore-size distribution function. The advantages of the Fredlund and Xing (1994)'s model are as follows (Leong and Rahardjo 1997; Sillers et al. 2001): (*i*) it is continuous over the entire soil suction range, (*ii*) there is great flexibility for the model to fit a wide variety of datasets, (*iii)* the soil parameters are meaningful, and (*iv*) the effect of one parameter can be distinguished from the effect of the other two parameters.

2.7.4 Volume change behaviour of collapsible soil

Measuring the overall volume change is important when testing a collapsible soil specimen (Fredlund and Rahardjo 1993a). Several researchers studied the volume changes occurring in collapsible soils during the wetting process. Matyas and Radhakrishna (1968) carried out two series of tests on a collapsible soil. The results indicated that the compressibility of the soil is a function of matric suction. The soil structure was shown to be less compressible at high matric suction. Escario and Saez (1973) conducted tests on Madrid clayey sand using a modified oedometer apparatus. It was reported that there was a reduction in total volume as a result of a matric suction decrease and that the volume change became most significant at relatively low suction values. Tadepalli and Fredlund (1991) and Tadepalli et al. (1992) conducted collapse tests using an oedometer specially designed with controlled matric suction. Their results indicated a unique relationship between the change in matric suction and the total volume change during the collapse. Pereira and Fredlund (2000) and Pereira et al. (2005) conducted further investigations on the volume change behaviour of collapsible soils. They concluded that irrespective of the variation in collapses resulting from net vertical stress, the metastable soil structure seemed to show the same increases in degrees of saturation when the matric suction was reduced to zero.

Houston et al. (2001b) studied the effect of full and partial wetting processes on the volume change behaviour of typical silty collapsible soil. The results show that there

is an apparent unique relationship between the void ratio, matric suction and net stress. This relationship can be observed when collapse deformation occurs as a result of a reduction in matric suction under constant net vertical stress.

Sun et al. (2007) tested the collapse for compacted Pearl clay in a controlled-suction triaxial cell with the different initial void ratio. It was detected that the collapse deformation due to a suction reduction depends mainly upon the density and stress state under which the collapse occurs. The results observed that the occurrence of the volume change due to a suction reduction is seeming to be controlled by the changes in the degree of the saturation.

Al-badran (2011) investigated the volume change behaviour of a compacted mixture of bentonite and sand under slurry and unsaturated loose conditions by using a suction-controlled oedometer apparatus. The tests result demonstrated that wetting processes under constant net normal stress under initially loose conditions result in three different phases of collapse deformation after a reduction in suction (i.e. wetting process). He continued, by stating that the volume change is significantly influenced by the location of void ratios before the wetting process with respect to the saturated normal consolidation line (NCL) of the net vertical stress versus the void ratio relationship.

The results of Haeri et al. (2012) reported significant changes in both volume and water content during wetting. The rates of change of both water content and deformation, however, were different depending on the state of stress that was applied to the specimens. At higher levels of suction, the soil specimens experienced a fairly small increase in void ratio with matric suction decrease. At lower levels of suction, more water was absorbed by the mineral structure during wetting; as a result, these specimens experienced appreciable collapse and dramatic changes in soil volume.

2.7.4.1 Laboratory measurement of volume change (double-wall cells)

Several types of equipment were designed according to the double wall concept. Bishop and Donald (1961) first used a modified cell, for measuring volume changes of unsaturated soils. An open-top inner cylindrical container was used inside a conventional cell. The inner container was filled with mercury. Outside, the inner container was filled with water. Volume changes of the unsaturated soil specimen were measured by monitoring the vertical position of a stainless-steel ball floating on the surface of the

mercury using a cathetometer. Following Bishop and Donald's work (1961), Wheeler (1988) developed a double-wall cell in which the two cells were filled with water. Cui and Delage (1996) presented a cell similar to that presented by Bishop and Donald (1961) where coloured water rather than mercury was used as inner cell fluid. In order to avoid the absorption of air by the water and to reduce the evaporation of water, a thin layer of silicon oil was placed above the water. Sivakumar (1993) increased the stiffness of the cell by reinforcing the cells with fibreglass bands. Sivakumar et al. (2006) presented a double-wall cell with an essential difference that the inner cell was made of the high-quality glass eradicating the absorption of the water by the acrylic walls of the inner cell.

Rampino et al. (1999) developed a technique for measuring volume changes of unsaturated soils using the ideas proposed by Okochi and Tatsuoka (1984). The method was successfully used by many other researchers, including Aversa and Nicotera (2002), Ng et al. (2002) and Yin (2003). The method is based mainly on level measurements between the water inside the open-ended bottle shaped inner cell and the reference water level. The level measurements were recorded using a high-accuracy differential pressure transducer (DPT). Ng et al. (2002) used aluminium instead of acrylic materials to make the inner cell in order to prevent creep, hysteretic effects, and absorption of water. Ng et al. (2002) used paraffin to avoid evaporation of water with time. In addition, the outer and inner cells (above the reference water levels) were pressurized with air, and this can be dangerous when operating the system under high pressures.

There have been ongoing attempts to further improve measurements of total volume change of unsaturated soil specimens. One such system was developed at the Hong Kong University of Science and Technology and later manufactured by GDS Instruments (Ng and Menzies 2007). Figure 2.7 shows how a double-walled cell can be used in conjunction with an accurate differential pressure transducer to measure soil specimen volume changes. The differential pressure transducer was used to monitor the change in the level of the inner cell fluid. In the double-wall system, both the inner and outer cells are pressurized by the same pressure during the test. Theoretically, null expansion of the inner cell can be achieved. As a result, the volume change of the inner cell fluid measured during the test will be equal to the volume change of the unsaturated soil specimen tested.

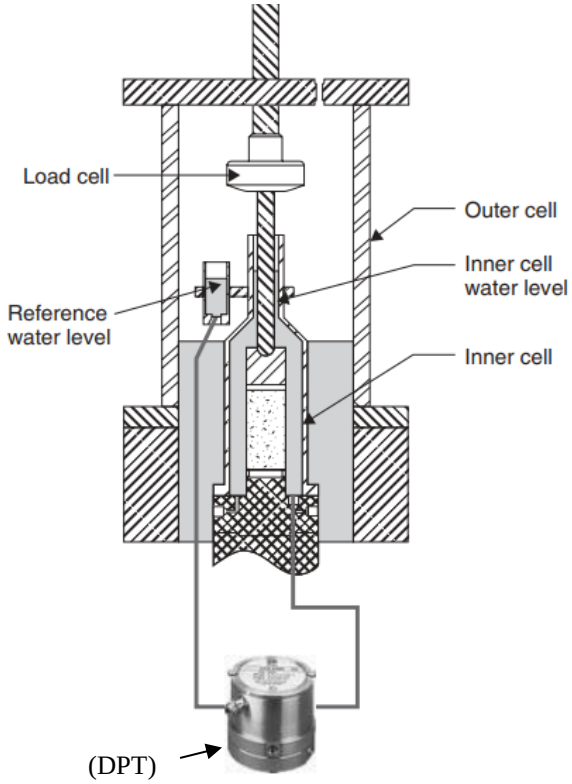

Figure 2.7 Double-walled triaxial cell (Courtesy of GDS Instruments, London.)

2.7.5 Shear strength and failure criteria

The shear strength of soil, whether saturated or unsaturated, may be defined as the maximum shear stress the soil is capable of sustaining along the failure plane under a given external and/or internal stress state (Fredlund and Rahardjo 1993a). Shear strength can be related to the stress state of the soil. There are three main approaches as described previously to evaluate the stress state in unsaturated soil; the single stress-state variable approach proposed by Bishop (1959), the two stress-state variable approach proposed by Fredlund and Morgenstern (1977), and the true effective stress concept introduced by Lu and Likos (2006). Referring to these approaches, different failure criteria and different models have been formulated to describe the shear strength behaviour of unsaturated soil (Bishop et al. 1960; Fredlund et al. 1978; Fredlund et al. 1996; Vanapalli et al. 1996; Rassam and Williams 1999; Rassam and Cook 2002; Khalili et al. 2004; Tarantino 2007; Sheng et al. 2011). The shear strength criteria relevant to the current study are reviewed in this section.

The shear strength of a saturated soil can be described using the Mohr-Coulomb failure criterion and the effective stress variable Terzaghi (1936).

$$t_f = c' + (\sigma - u_w)_f \tan\phi' \quad (2.6)$$

where τ_f is the shear stress on the failure plane at failure, c' is intercept of the "extended" Mohr-Coulomb failure envelope on the shear stress axis when the net normal stress and the matric suction at failure are equal to zero; it is also referred to as the "effective cohesion", $(\sigma - u_w)_f$ is the effective normal stress on the failure plane at failure, and $\emptyset'$ is the angle of internal friction associated with the net normal stress state variable.

In unsaturated soil, there is internal stress acting locally on soil grains that results specifically from partial saturation of the soil, and it is independent of external loading. Lu and Likos (2006) stated that this stress originates from the combined effects of negative pore-water pressure and surface tension. The effect of the internal loading on the shear strength may be captured by incorporating the matric suction into the Mohr-Coulomb failure criterion in one of the following approaches.

2.7.5.1 The extended Mohr-Coulomb criterion

Considering the two stress-state variable approaches, Fredlund et al. (1978) proposed expression for the shear strength (τ_f) of unsaturated soils (Equation 2.7) to describe the shear strength behaviour of unsaturated soil by introducing an additional parameter, $\emptyset^b$, to capture the increase in shear strength with increasing matric suction, and may be written as:

$$t_f = c' + (\sigma - u_a)_f \tan\phi' + (u_a - u_w)_f \tan\phi^b \quad (2.7)$$

where $(\sigma - u_a)_f$ is the net normal stress on the failure plane at failure, $(u_a - u_w)_f$ is the matric suction at failure, and $\emptyset^b$ is an angle indicating the rate of change in shear strength relative to changes in matric suction.

The Mohr circles for an unsaturated soil are plotted with respect to the net normal stress axis $(\sigma - u_a)$, in the same manner, as the Mohr circles are plotted for saturated soils with respect to the effective stress axis $(\sigma - u_w)$. The location of the Mohr circle

plot in the third dimension is a function of the matric suction (Figure 2.8). The surface tangent to the Mohr circles at failure is referred to as the extended Mohr-Coulomb failure envelope for unsaturated soils. The extended Mohr-Coulomb failure envelope defines the shear strength of an unsaturated soil. The intersection line between the extended Mohr-Coulomb failure envelope and the frontal plane is the failure envelope for saturated conditions. The inclination of the failure plane is defined by joining the tangent point on the Mohr circle to the pole point. The tangent point on the Mohr circle at failure represents the stress state on the failure plane at failure. The planar failure envelope that intersects the shear stress axis in Figure 2.8, giving a cohesion intercept (c). The envelope has slope angles of ϕ' and $\emptyset^{\mathrm{b}}$ with respect to $(\sigma - u_a)$ and $(u_a - u_w)$ axis, respectively. The cohesion intercept c and the slope angles ϕ' and $\emptyset^b$ are the strength parameters used to relate shear strength to the stress state variables. The failure envelope intersects the shear stress versus matric suction plane along a line of intercepts. The line of intercepts represents the increase in strength as matric suction increases.

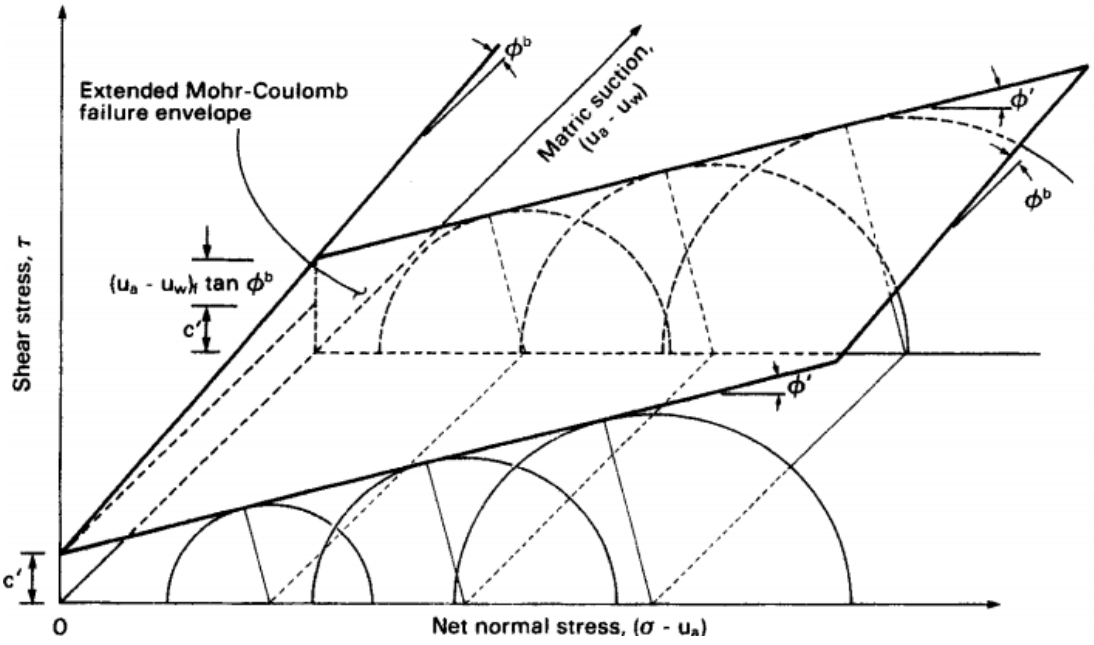

Figure 2.8 Extended Mohr-Coulomb failure surface for unsaturated soils (Fredlund and Rahardjo 1993a)

2.7.5.2 Single stress state Mohr-Coulomb criterion

As introduced in section 2.7.2.1, in the single stress state variable approach proposed by Bishop (1959), Terzaghi's effective stress was extended to join both two independent state variables, net normal stress and matric suction, by incorporating the modified effective stress equation for unsaturated soils into the classical Mohr-Coulomb failure criterion as:

$$t_f = c' + \left[(\sigma - u_a)_f + \chi(u_a - u_w)_f\right] tan\phi' \quad (2.8)$$

The effective stress parameter χ is a function to the degree of saturation or matric suction. Determination of the effective stress parameter and its dependency on the amount of water in the system is essential in order to evaluate effective stress in unsaturated soil (Lu and Likos 2004).

2.7.5.3 True effective stress failure criterion

To avoid the uncertainties and ambiguities in the theoretical formulation and experimental determination of $\emptyset^b$ and χ. Lu and Likos (2004) suggested the use of suction stress concept. Mohr-Coulomb criterion incorporating Bishops effective stress can be re-written as:

$$\tau = c' + (\sigma - u_a)\tan\phi' - \sigma^s \tan\phi' \quad (2.9)$$

An important practical implication of using the true effective stress equation is all classical soil mechanics work on limit analysis can be readily extended to unsaturated soil conditions (Lu et al. 2010). The suction stress characteristic curve (SSCC) can be used as the important index to estimate the stress state of the unsaturated soil, and the soil strength can be predicted and evaluated depending on the water contents. Literature reviews have indicated that suction stress approach has been shown to better conjugate the effective stress in describing the shear strength behaviour of unsaturated soils for the entire range of degree of saturation (Lu et al. 2010; Oh et al. 2012; Song 2014).

2.7.5.4 Unsaturated shear strength behaviour

Several researchers measured the unsaturated shear strength (i.e., Escario and Sáez 1986; Fredlund and Rahardjo 1993b; Vanapalli et al. 1996; Cui and Delage 1996; Cunningham et al. 2003; Lee et al. 2005; Jotisankasa 2005; Zhan and Ng 2006; Suits et al. 2007; Hossain and Yin 2010), and some general statements about the unsaturated shear strength behaviour have made:

i. Higher matric suctions result in higher shear strengths under the same confining pressures.

ii. Higher confining pressures result in higher shear strengths under the same matric suction.

iii. The relationship between shear strength and soil suction is nonlinear when the applied soil suctions increased beyond the air-entry value of the soil. The shear strength increases most rapidly in the low-matric-suction range. and then gradually flattens (or even decreases) at high suctions (i.e., suctions approaching residual conditions).

iv. The shear strength envelopes show that the air-entry value is near the point where shear strength starts to deviate from the effective angle of internal friction, $\emptyset'$.

2.7.5.5 Linear failure envelope with respect to net normal stress

Experimental studies show that shear strength with respect to net normal stress follows a linear relationship at constant soil suction (Fredlund et al. 2012). Some studies however indicate that for some soils, the effective friction angle increases slightly with increasing soil suction (Escario and Sáez 1986; Alawaji 2001; Cunningham et al. 2003; Lee et al. 2005; Zhan and Ng 2006; Shen et al. 2009; Wang et al. 2014; Haeri and Garakani 2016). Escario (1989) showed that the angle $\emptyset'$ is assumed to be constant with suction is approximately valid for most soils. Ng et al. (2000) also found that this is true for loosely compacted volcanic fills. Gan and Fredlund (1996) and Ng and Chiu (2003) reported that the angle of internal friction is a constant for the limited range of applied suction and suction does not appear to affect it. Wheeler and Sivakumar (1995a) have shown that $\emptyset'$ is a function of the suction by considering a wider range of suction. Vanapalli et al. (1996) stated that the effective friction angle might be considered constant for most practical

applications and for soil suction values up to 500 kPa. Toll (1990) and Toll and Ong (2003), however, found that $\emptyset'$ increases with decreasing degree of saturation based on their results from triaxial tests on lateritic gravel and residual sandy clay. On the other hand, Maatouk et al. (1995) have found that for silty soils, $\emptyset'$ decreases with increasing suction. An increase in the effective friction angle with respect to soil suction is often attributed to the higher dilation behaviour with increasing soil suction (Cunningham et al. 2003; Lee et al. 2005).

2.7.5.6 Nonlinearity of failure envelope

The slope of the shear strength envelope of unsaturated soils with suction is described by $\tan \emptyset^b$ (Fredlund et al. 1978). The shear strength envelope might be planar, that is, $\emptyset^b$ is constant, or curved, meaning that $\emptyset^b$ varies as a function of matric suction. Ho and Fredlund (1982) reported a linear increase in strength with respect to matric suction for two Hong Kong residual soils. A similar trend was observed by Rahardjo et al. (1995) for a residual clay in Singapore. Vanapalli et al. (1996) attributed this linearity to the fact that the soils tested are resistant to desaturation and, hence, can exhibit a linear shear strength behaviour over a large range of suctions. Hence, for matric suctions below the AEV, an increase in matric suction has the same effect as increasing the effective stress.

As a wider variety of soil types have been tested over a wider range of soil suctions, it has become increasingly apparent that the shear strength versus matric suction relationship should not be limited to a linear relationship (Donald 1956; Escario and Sáez 1986; Gan and Fredlund 1988; Fredlund et al. 1996; Lee et al. 2005; Melinda et al. 2004; Zhan and Ng 2006; Houston et al. 2008; Hossain and Yin 2010; Goh et al. 2010; Sheng et al. 2011; Khalili and Khabbaz 1998; Fredlund et al. 2012; Schnellmann et al. 2013).

An examination of the effect of increasing matric suction from an initially saturated condition suggests that it is reasonable for the shear strength versus matric suction relationship to be nonlinear. At low matric suctions, the soil specimen remains saturated. Under these conditions, the effect of total normal stresses on the shear strength is characterized by the friction angle $\emptyset'$. A further increase in matric suction is not as effective in increasing shear strength as is an increase in net normal stress. As a result, it

is necessary for the $\emptyset^{b}$ angle to reduce to a value lower than $\emptyset'$ when matric suction is increased beyond the air-entry value of the soil (Fredlund et al. 2012).

Jotisankasa (2005) stated that the non-linearity of the shear strength-suction relationship could be explained qualitatively by a physical argument. For suctions below the air entry value, the degree of saturation is approximately unity, and the influence of suction is equivalent to the applied stress. In this region, $\emptyset^{b}$ is equal to $\emptyset'$. However, as the soil desaturates, the wetted contact area around the soil grains decreases and the contribution of suction to the shear strength reduces, resulting in a decrease in $\emptyset^{b}$ with suction.

2.7.6 Consolidated drained (CD) triaxial test

The laboratory shear test of saturated and unsaturated soils is most commonly performed in a triaxial test. A triaxial shear strength test is performed by loading a soil specimen with increasing applied loads until a condition of failure is reached. There are several ways to perform the triaxial test, consider a consolidated drained triaxial compression test where the pore pressures in the soil specimen are allowed to drain. The soil specimen is subjected to a constant matric suction and is surrounded by a constant net confining pressure. The specimen is failed by increasing the axial stress. The difference between the major (σ_1) and minor (σ_3) normal stresses is commonly referred to as the deviator stress (q).

2.7.7 Strain rates for saturated and unsaturated CD triaxial test

The shearing process of the triaxial test is normally performed at a constant strain rate. The strain rate should be sufficiently slow to avoid non-uniformly in the pore water pressure distribution within the sample. This is true for testing both saturated and unsaturated soils (Ho and Fredlund 1982c). For the CD triaxial test, a low shearing rate is necessary in order to maintain the drained condition for both air and water phases (Lim 1995). Table 2.4 shows some rates of shearing used in unsaturated CD triaxial tests based on literature.

Table 2.4 Rate of shearing used in unsaturated CD triaxial test based on literature

Reference	Material	Shearing rate (mm/min)
Bishop and Donald (1961)	Braehead silt	0.0021
Ho and Fredlund (1982a)	Granite and rhyolite	0.001
Ho and Fredlund (1982b)	Silty sand and sandy silt	0.0014
Fredlund and Rahardjo (1993a)	Silty Sand	0.006
Maatouk et al. (1995)	Collapsible silty soil	0.0016
Wheeler and Sivakumar (1995)	Speswhite kaolin	0.0014
Rampino et al. (1999)	Silty sand	0.0013
Laloui et al. (1997)	Sandy silt	0.0015
Schnellmann et al. (2013)	Sand with silt (SW–SM)	0.0015
Gan et al. (1988)	Glacial till soil	0.0015
Adams and Wulfsohn (1997)	Sandy clay loam soil	0.014
Rahardjo et al. (1995, 2004)	Residual soil	0.0009
Goh et al. (2010, 2014)	Sand-kaolin mixtures	0.0009
Khalili et al. (2004)	CL-ML	0.003
Houston et al. (2008)	SM, CL-ML, SP, CL	0.004
Lee et al. (2005)	Silty Sand	0.006
Meilani et al. (2005)	85 % silts and 15 % clays	0.0008
Thu et al. (2006)	Coarse Kaolin	0.0009
Fazeli et al. (2009)	Silty clay	0.0067
Shao et al. (2014)	Silty clay	0.006
Tavakoli et al. (2014)	Silty clay	0.002

2.7.8 The relationship between the SWCC and the shear strength of unsaturated soils

Laboratory studies have shown that there is a relationship between the SWCC for a particular soil and the unsaturated soil properties (Fredlund and Rahardjo 1993a; Vanapalli and Fredlund 2000). The shear strength of unsaturated soil is commonly estimated from saturated soil parameters and the soil water characteristic curve (Vanapalli et al. 1996; Fredlund et al. 1996; Khalili and Khabbaz 1998; Vanapalli and Fredlund 2000; Kim and Borden 2011). Figure 2.9 summarizes the general anticipated shear strength responses that might be predicted from a variety of soils. The shear strength of all soil types appears to respond as a saturated soil as long as the matric suction is less than the air-entry value of the soil. There is curvature in the shear strength envelope once the air-entry value is exceeded (Vanapalli et al. 1996; Fredlund et al. 1996; Fredlund et al. 2012).

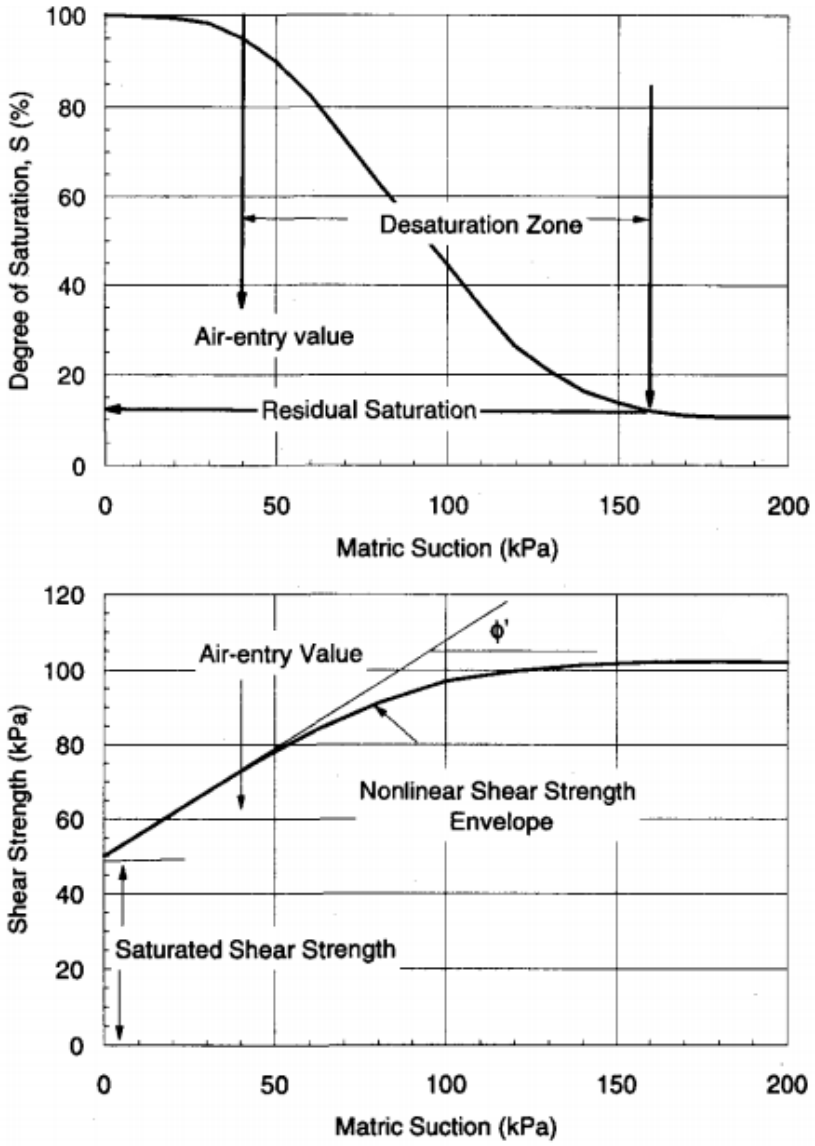

Figure 2.9 Conceptual relationship between SWCC and unsaturated shear strength envelope (after Vanapalli et al. 1996)

2.8 Suction stress based on Lu et al. (2010) study

One important aspect of effective stress in unsaturated soils is the role of the residual water content. Lu et al. (2010) provide a thermodynamic justification for including residual water content in calculations of effective stress. Residual water should be considered carefully as it plays different roles in defining the magnitude of interparticle stress in different soils. The suction stress introduced by Lu and Likos (2004, 2006) and Lu et al. (2010) unifies effective stress under both saturated and unsaturated conditions with one closed-form equation. The aim of Lu et al. (2010) study was to propose and validate a closed-form equation for effective stress in unsaturated soil in which the

contribution of matric suction, $\chi\ (u_a - u_w)$ can be defined by a sole function of matric suction or the effective degree of saturation. This closed- form equation requires only two parameters; the inverse of the air-entry pressure α, and the pore-size parameter n. These two parameters construct the SSCC and are also identical to the commonly used SWCC equation proposed by van Genuchten (1980). Theoretically, the closed- form equation for suction stress contributes to our knowledge by addressing several potentially far-reaching implications. First, it attempts to the elimination of the need for determining the Bishop's effective stress parameter (χ) and $\emptyset^b$. Effective stress can be determined simply by reducing suction stress from shear strength test results or by measuring soil water characteristic curves to identify parameters α and n. In addition, under the proposed equation, the transition from saturated to unsaturated states is continuous and smooth, ensuring mathematical consistency between Terzaghi's effective stress and the effective stress equation. Furthermore, the findings of this Lu et al. (2010) study will help to the elimination of the need for any new shear strength criterion for unsaturated soil and all classical soil mechanics work on limit analysis can be readily extended to unsaturated soil conditions. Notably, the nonzero suction stress for both silty and clayey soils at their residual saturations is one of the features in Lu et al.'s effective stress that discriminates it from Bishop's effective stress which predicts zero suction stress at the residual saturation for all soils.

The suction stress characteristic curve (SSCC) is intrinsically related to the soil water characteristic curve (SWCC). Lu et al. (2010) validated that there exists a unique relation between SWCC and SSCC; thus, both of them can be uniquely defined by the same set of material parameters. Like SWCC, SSCC can be defined by a sole function of matric suction or the effective degree of saturation. Figure 2.10 illustrates the relationship between the SWCC and SSCC. Suction stress is defined as the matric suction multiplied by the effective degree of saturation. Song et al. (2012) have found that the magnitude of suction stress for both sand and silt had a linear relationship of the same magnitude as matric suction until the matric suction equated the AEV. However, once the matric suction exceeded the AEV of soil, the SSCC exhibited a similar non-linear relationship as the SWCC with soil suction.

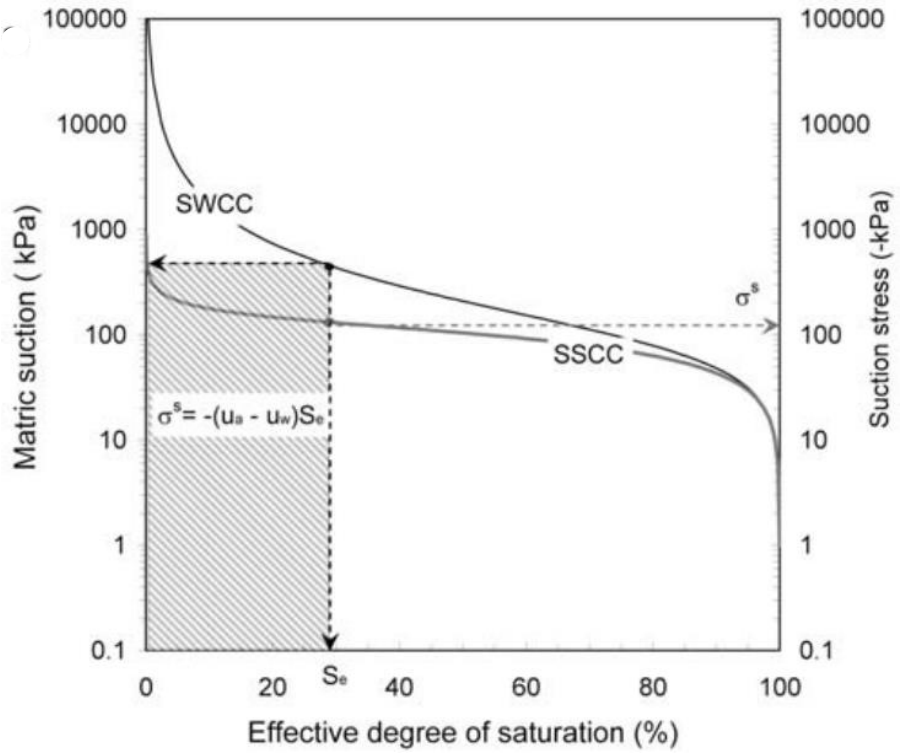

Figure 2.10 Relationship between the SWCC and SSCC (From Lu et al (2010))

2.8.1 The uniqueness of the SSCCs

The uniqueness of the SSCC determined from both shear strength, and water retention tests have been examined recently by many researchers (Lu et al. 2010; Oh et al. 2012; Oh and Lu 2014; Lu et al. 2014). These studies have demonstrated that the SSCCs of several types of soils determined from water retention tests accorded well with the SSCCs determined from shear strength tests.

Oh et al. (2012) investigated the instinct relationship between SSCC and SWCC by conducting a series of triaxial shear strength and pressure plate extractor tests for several residual soils. The results showed that the SSCC could be uniquely linked to the SWCC. To further examine the validity of the SSCC, Oh et al. (2013) provided an alternative way to obtain the SSCC by carrying out triaxial K_0 consolidation tests for decomposed granitic soils; it was found that the SSCC could be used to describe the consolidation and shear strength properties of unsaturated soils.

Oh and Lu (2014) experimentally examined the effect of confining stress (up to 200 kPa) on the SSCCs under both drying and wetting conditions through silty sand. Their

results showed that the SSCC inferred from the shear strength tests was similar to that from the SWCC measurement under the respective wetting. Such uniqueness under drying conditions is not as clear as that of the wetting branch. They also stated that SSCCs are almost independent of the confining stress.

Consolidated-drained triaxial tests were performed on silt specimens under different combinations of total suction and net normal stress by Alsherif and McCartney (2014) to evaluate the suction stress concept at high suctions. Their results were analysed to examine the applicability of predicting the SSCC using parameters from SWCC models fitted to experimental data. The SSCC predicted from the SWCC at low suctions found to overpredict the suction stress values at high suctions.

Lu et al. (2014) concluded that the SWCCs obtained from axis-translation tests were very similar or of the same order of magnitude as the SWCCs inferred from shear-strength tests on the same soils. This comparison suggests that the mathematical equation for the SWCCs is intrinsically related to the mathematical equation for the SSCCs. The analysis also showed that the SSCCs deduced from axis-translation tests were of the same order of magnitude as the SSCCs deduced from shear-strength tests, suggesting that the SWCCs and the SSCCs are consistent.

Results of triaxial shear tests on reconstituted specimens of an unsaturated natural loess soil were presented by Haeri et al. (2015). The measured shear strength data were used to define the SSCC. A comparison between the measured SSCC and those predicted using Lu et al. (2010) a closed-form equation was made. The results of their study indicated uncertainty in the uniqueness of the SSCC for loess soil.

2.8.2 The validity of the SSCC-based effective stress principle

The effective stress principle is one of the key aspects where the hydraulic properties of soils may be linked with the stress state and the mechanical properties of soils (McCartney 2018). Several researchers have explored the influence of suction stress on effective stress (Karube et al. 1997; Kato et al. 2001; Khalili et al. 2004; Lu and Likos 2006; Chae et al. 2010; Kim et al. 2010; Oh and Lu 2014; Pourzargar et al. 2014; Haeri et al. 2015).

Karube et al. (1997) examined the application of suction stress on the results obtained from the triaxial compression tests were performed on kaolin clays. It was found that the shear strengths of maximum volumetric compression point for unsaturated soil under high confining pressure condition agree with the failure line for saturated soil through the application of the suction stress as a stress component.

Kim et al. (2010) proposed suction stress-soil water retention curve method to evaluate effects of suction on the shear strength of unsaturated soils under low confining pressure and to examine the relationships between suction, shear strength behaviour, and volumetric deformation using newly developed direct shear testing equipment for compacted weathered granite soils. They have been found that the stress states at the peak shear strength point are on the same failure line for the saturated state when the suction stress is treated as a component of confining pressure. It is also noted that the estimated unsaturated shear strengths using the suction stress-soil water retention curve method agree well with the measured values from laboratory testing. Furthermore, Kim et al. (2013) reported that the unsaturated shear strength could be estimated by means of the concept of the suction stress.

Oh and Lu (2014) reported that the effective failure criterion is unique and can practically reflect the unsaturated shear strengths determined from the suction-stress based effective stresses from both the wetting and drying SSCCs. They demonstrated experimentally that the stress principle could describe the unsaturated shear strength behaviour. However, they stated that the validity of the uniqueness of the SSCC under each wetting or drying state and under a large confining stress range for other types of fine-grained soils remains to be established.

Baille et al. (2014) shed new light on using the SSCC-based effective stress representation for deformation behaviour of unsaturated soils. They experimentally confirmed that the closed form equation for the SSCC (Lu et al. 2010) could be used to describe void ratio-effective stress relationships for different clays under unsaturated oedometer conditions. Based on the results, a decrease in the suction stress caused an increase in effective stress, which in turn reduced the volume of the clays.

The validity of the SSCC-based effective stress principle representation is further demonstrated by Pourzargar et al. (2014) through triaxial shear strength tests and tensile

strength tests for kaolinite–sand mixtures. They stated that the closed form equation for the SSCC proposed by Lu et al. (2010) represent both shear strength and tensile strength behaviour for soils with non-monotonic behaviour in the SSCC.

From a detailed review of the literature presented in this chapter, it can be concluded that detailed studies of the SSCCs of collapsible soils derived from both the CD triaxial compression tests and volumetric variables during wetting process under isotropic conditions and for a large range of suction and higher stress levels are very limited. As a result, the suction stress model of Lu et al. (2010) uses the SWCC in the definition of the effective stress to predict the unsaturated shear strength of collapsible soils have not been fully investigated yet.

2.9 Concluding remarks

In this chapter, a brief review of the collapse mechanism behaviour as well as the most important parameters affecting collapse potential was presented. The laboratory collapse tests for determining the collapse strain of the soil were included. A review of the concept of suction as well as some methods for measuring and controlling soil suction was discussed. General information on the soil-water characteristic curve (SWCC) and its features and factors affecting the SWCC were covered. The impact of stress and suction on the volume change and shear strength behaviour of unsaturated soils are presented. Additionally, studies involving the uniqueness of the suction stress characteristic curves (SSCCs) determined from both shear strength and water retention tests as well as the validity of the suction stress based effective stress principle are discussed to highlight the scientific research gap.

A review of the literature highlighted some specific aspects related to volume change and shear strength behaviour of unsaturated soils. These include:

i. The specimens' initial conditions and overburden pressure have significant effects on the collapse strain.
ii. The greatest uniformity specimen is achieved by static compaction in one thin layer.
iii. The applied stress and the suction are the two separate components of effective stress that could explain the volume change and shear strength behaviour of unsaturated soils.
iv. There was a reduction in total volume occurring in collapsible soils as a result of a matric suction decrease.
v. The shear strength of unsaturated soil is commonly estimated from saturated soil parameters and the soil water characteristic curve.
vi. The suction stress characteristic curve (SSCC) of the statically compacted collapsible soil derived from both shear strength and volumetric variables under isotropic conditions and for a large range of suction and higher stress levels have not been fully investigated yet.

CHAPTER 3

Materials and methods

3.1 Introduction

This chapter describes the properties of the soil used in this investigation, the details of the equipment used along with the working principles and descriptions of the various components of the equipment. The procedures adopted for preparing soil specimens for various tests are presented. The test procedures adopted for various tests are described. The relevant information presented in this chapter are summarized at the end of this chapter.

3.2 Soil selection

As the main objective of the present research was to investigate the hydraulic and mechanical behaviour of statically compacted unsaturated collapsible soils and to interpret the collapsing phenomenon by suction stress approach, the process used for selecting the soil used in this study was as follows.

One-dimensional swell-collapse tests (ASTM D4546-14) were conducted on some selected soils during the initial phase of the investigation. The soils used were a natural loess soil collected from Pegwell Bay (Soil P), and four prepared soils consist of various predetermined percentages of Leighton Buzzard sand, M400 silt and Speswhite kaolin. The percentages of the various particle-size fractions of the prepared soils are similar to that found in many naturally occurring Aeolian deposits such as natural loess soil (Derbyshire and Mellors 1988). The percentages of sand, silt and clay in Pegwell Bay soil (Soil P) were 7.3, 84.3 and 8.4%, respectively. The values of specific gravity, liquid limit, plastic limit and plasticity index for the soil are reported in the literature as 2.69, 29.5%, 19.2 and 10.3% respectively (Derbyshire and Mellors 1988). According to the Unified Soil Classification System (USCS), the soil can be classified as clay with low plasticity (CL). Table 3.1 shows the percentages of sand, silt and clay in the four prepared

soils (A, B, C and D). The values of the specific gravity of Leighton Buzzard sand, M400 silt and Speswhite kaolin are 2.76, 2.65 and 2.61 respectively (Bennett 2014; Sibelco 2014; Singh 2007).

Table 3.1 Composition of the prepared soils

Soil name	Leighton Buzzard sand (%)	M400 silt (%)	Speswhite kaolin (%)
Soil A	30	50	20
Soil B	30	45	25
Soil C	35	45	20
Soil D	40	40	20

3.2.1 Preliminary laboratory tests

Several single oedometer tests were carried out on the selected soils by following the procedure laid out in ASTM D4546-14. Soil specimens were prepared by statically compacting soil-water mixtures directly in the oedometer ring of 100 mm diameter and 19 mm height and then transferred to the oedometer cell. The compaction conditions of the soils are shown in Table 3.2. To ensure good contact between the top porous stone and the soil specimens in the oedometer, a seating pressure of 1.5 kPa was applied before the commencement of the tests. The soil specimens were applied with an incremental loading corresponding to vertical pressures of 12.5, 25 and 50 kPa. The specimens were then inundated with distilled water at an applied vertical pressure of 50 kPa. During the tests, the dial gauge readings were recorded with an elapsed time. The vertical strain (%) was calculated from Equation 3.1 (ASTM D4546-14).

$$\text{Vertical strain, } \varepsilon_c = \frac{-100\Delta h}{h_1} \tag{3.1}$$

where Δh = change in specimen height and h_1 = specimen height immediately before wetting.

Table 3.2 Compaction conditions of the soils for one-dimensional swell-collapse tests

Soil type	Specimen no.	Water content (%)	Dry unit weight (kN/m^3)	Vertical strain (%)
Soil P	1	8.3	17.5	+1.0
Soil P	2	8.3	17	+0.9
Soil P	3	8.3	16	-0.5
Soil P	4	8.3	14.5	-3.8
Soil A	5	10.0	14	-10.6
Soil B	6	10.0	14	-11.0
Soil C	7	10.0	14	-14.0
Soil D	8	10.0	14	-16.2

+ Swell, - Collapse

3.2.2 Preliminary laboratory test results

Table 3.2 shows the vertical strains of the specimens from single oedometer tests. Figure 3.1 shows the elapsed time versus vertical strain results of the specimens. It can be seen in Table 3.2 and Figure 3.1 that the specimens of Pegwell Bay soil (Soil P) exhibited swelling at higher dry unit weights (17.5 and 17 kN/m^3) and collapsed at a dry unit weight of 16 kPa. A collapse strain of 3.8% was noted for the soil at a dry unit weight of 14.5 kPa (specimen no.4).

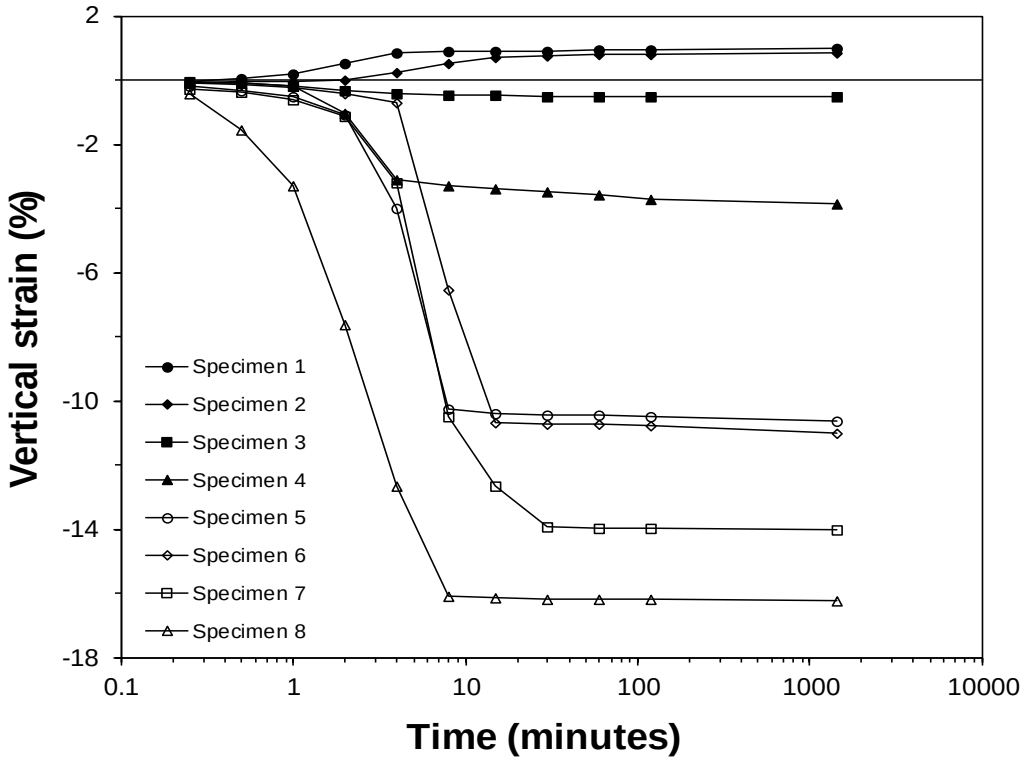

Figure 3.1 One-dimensional swell-collapse strain with elapsed time for the soils considered during the preliminary investigation

The different magnitude of collapse strains has resulted from the variation in the compaction conditions of the selected soils. The collapse strains of the prepared soils (A, B, C and D) well exceeded the collapse strains of the natural loess soil. For the compaction conditions considered, the collapse strain of soil D (specimen no.8) at an applied vertical pressure of 50 kPa was found to be the highest (16.2%), and hence soil D was chosen for all the remaining laboratory tests undertaken in this investigation. The selection of soil D was anticipated to provide meaningful test results in terms of vertical strain for various compaction conditions (water content and dry unit weight).

3.3 Properties of the selected soil

The basic properties of the selected soil (Soil D) are shown in Table 3.3. The specific gravity of the soil particles was determined using the small pycnometer method following the procedure detailed in the British Standards (BS 1377-2 1990). The specific gravity value was 2.65.

Cone penetration and rolling methods were used to determine the liquid and plastic limits of the soil following the procedures laid out in BS 1377-2 (1990). The liquid limit and plasticity index are 24% and 8%, respectively. The shrinkage limit was determined by the wax method (ASTM D4943−08) and was found to be 10.7%. The grain size distribution was determined from sieving and hydrometer tests (BS 1377-2 1990). The grading curve obtained is shown in Figure 3.2. According to the Unified Soil Classification System (USCS), the selected soil can be described as clay with low plasticity (CL).

The saturated hydraulic conductivity of the soil was estimated following the procedure detailed in the BS 1377-6 (1990) and Head (1995) and it was found to be 3.81×10^{-10} m/s. The mineralogy of the soil used in this study was determined by X-ray diffraction (XRD) method (Grim 1960; Mitchell 1976). The X-ray diffraction test result is presented in Table 3.3 and Figures 3.3. It can be seen that the predominant minerals present in the soil were quartz (86%) with a small percentage of kaolinite (14%).

Table 3.3 Properties of the selected soil

Properties	Value
Specific gravity, G_s	2.65
Standard compaction test	
Maximum dry unit weight (kN/m^3)	18.5
Optimum water content (%)	13.3
Particle size distribution	
Sand (%)	40
Silt (%)	40
Clay (%)	20
Atterberg limits	
Liquid limit, *LL* (%)	24
Plastic limit, *PL* (%)	16
Shrinkage limit, *SL* (%)	10.7
Saturated hydraulic conductivity, *k* (m/s)	3.81×10^{-10}
Mineral compositions	
Quartz (%)	86
Kaolinite (%)	14
Unified soil classification system (USCS)	CL

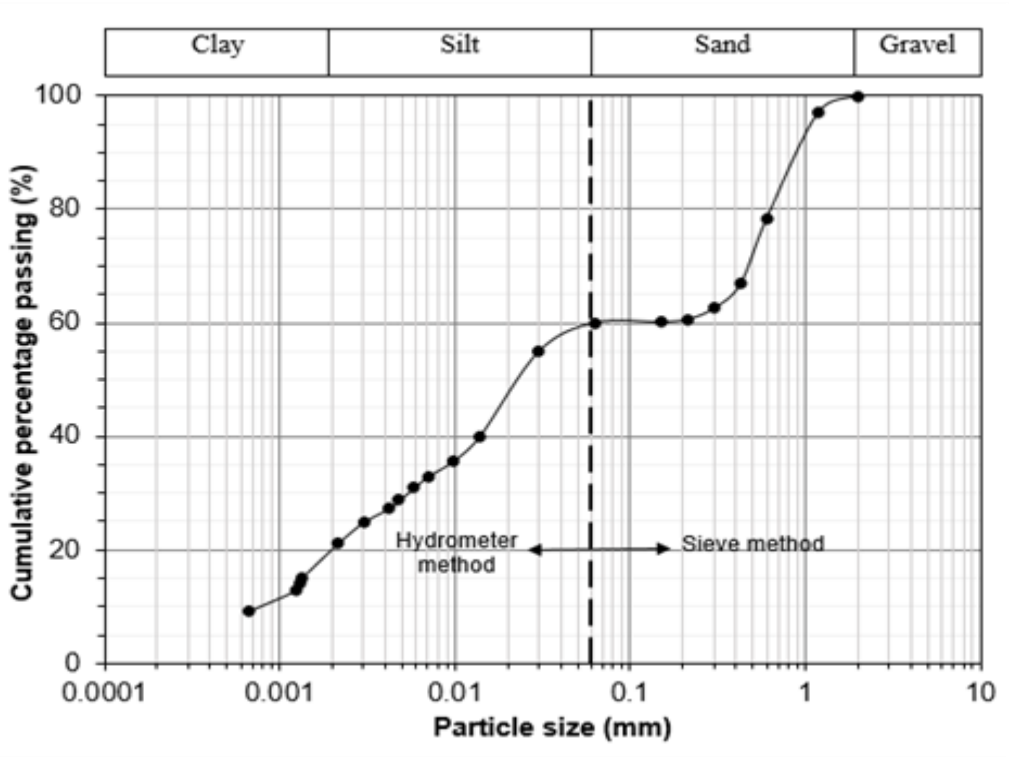

Figure 3.2 Grain size distribution of the selected soil

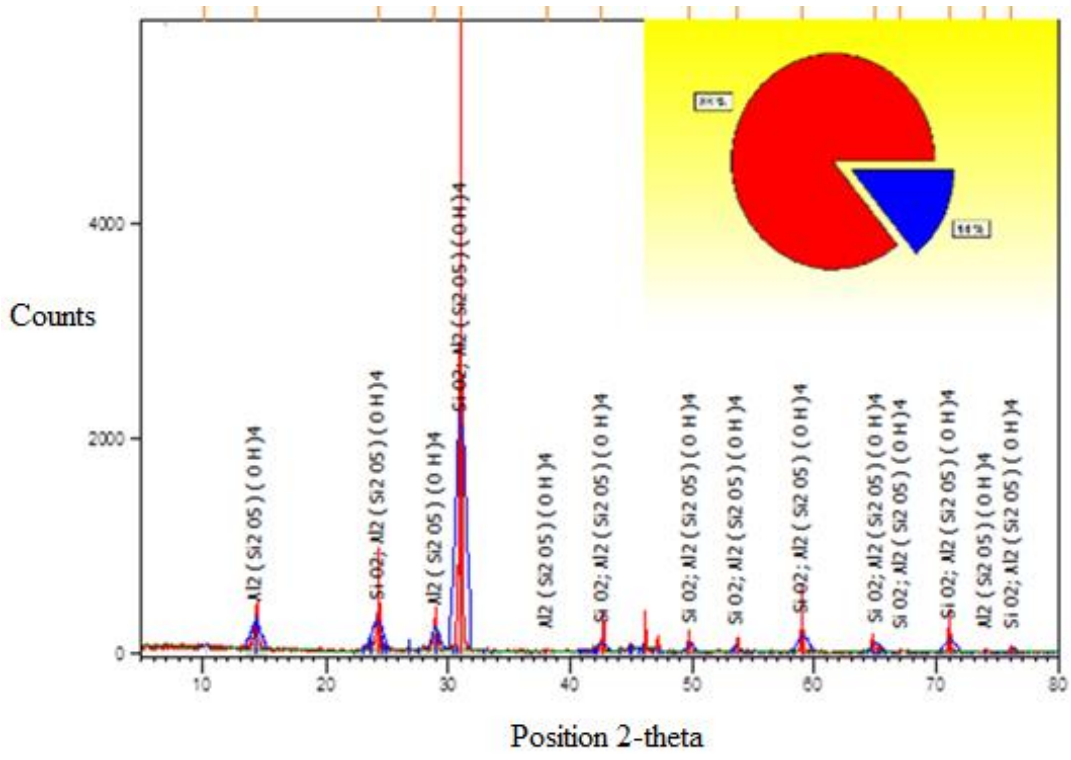

Figure 3.3 X-ray diffraction pattern of the selected soil

3.4 Compaction characteristics

Standard Proctor light compaction test was carried out by following the procedure laid out in BS 1377-4 (1990). The compaction curve of the soil is shown in Figure 3.4. The optimum water content and the maximum dry unit weight of the soil were found to be 13.3% and 18.5 kN/m^3, respectively. The optimum compaction conditions remain very close to a degree of saturation of 90%.

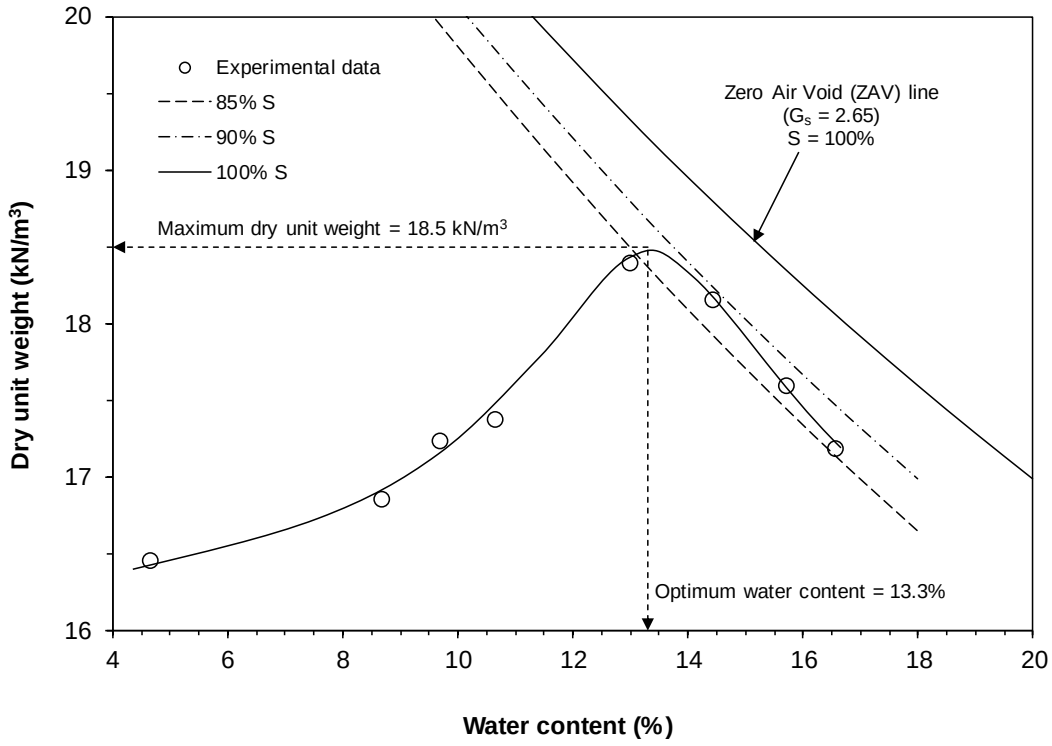

Figure 3.4 Standard Proctor compaction curve of the selected soil mixture

3.5 Experimental methods

This section describes the type of tests and discusses in detail the components of the test apparatus that have been used to carry out the laboratory tests, the procedures adopted for preparing specimens and the experimental procedures. As this research is mainly focused on volumetric collapse behaviour and shear strength and deformation characteristics under stress changes, different types of tests were performed, such as static compaction tests, compressibility behaviour of compacted specimens at different initial compaction conditions using conventional one-dimensional oedometer tests, chilled-mirror dew-point hygrometer tests, triaxial tests on saturated specimens were performed

under drained condition, and wetting-induced collapse tests followed by shearing of unsaturated soil specimens using an automated unsaturated triaxial shear strength device.

3.5.1 Preparation of the soil-water mixture

In this study, the soil mixtures were prepared by mixing 40% M400 silt, 40% Leighton Buzzard sand and 20% Speswhite kaolin. The mixtures were mixed dry, then with water by adding predetermined quantities of distilled water to the soil and mixed thoroughly on a glass plate using palette knives until uniform mixtures were formed. The prepared soil-water mixtures were placed in plastic bags and sealed properly. The sealed bags were stored in air-tight containers for one week prior to preparing soil specimens for various tests. Before preparing a specimen, the water content of the soil-water mixture was determined to ensure the targeted water content was achieved.

3.5.2 Static compaction tests

In the laboratory, soil specimens are usually prepared by statically compacting soil-water mixtures. The applied stress during the compaction process influences the volume change and shear strength behaviour of soils (Sivakumar and Wheeler 2000; Tarantino and De Col 2008). In this study, static compaction curves of the soil were established by statically compacting soil-water mixtures. The impact of specimen mould size and initial water content on the static compaction curves were studied, both in terms of applied pressure and applied energy. The equipment and procedures used for static compaction tests are similar to those used for the compaction of soil specimens for different tests.

3.5.2.1 Static compaction mould

Two types of specimen moulds were used. A mould of 99 mm in diameter was used to prepare the specimens for oedometer tests, and a mould of 50 mm in diameter was used to prepare the specimen for triaxial tests. A schematic drawing of the components of the oedometer compaction mould and their assembling are shown in Figure 3.5. The oedometer compaction mould consists of five main components; (a) a base, (b) a specimen ring, (c) a collar, (d) a locking ring and (e) a compaction piston. The specimen ring fitted into a recess in the base of the compaction mould. The collar was

placed onto the specimen ring. The locking ring was placed on the collar, securing the collar to the base of the mould. The locking ring is fastened to the base using four bolts.

The triaxial mould was specially fabricated for this research. The components of the mould and the test setup are shown in Figure 3.6. The compaction mould consists of a base, a specimen ring, a collar, and a compaction piston.

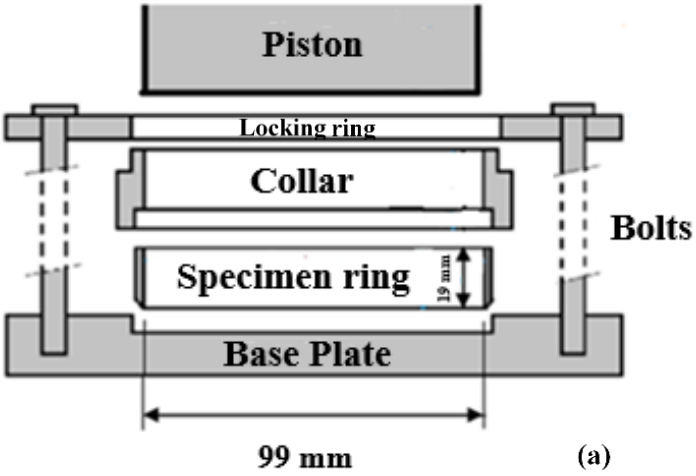

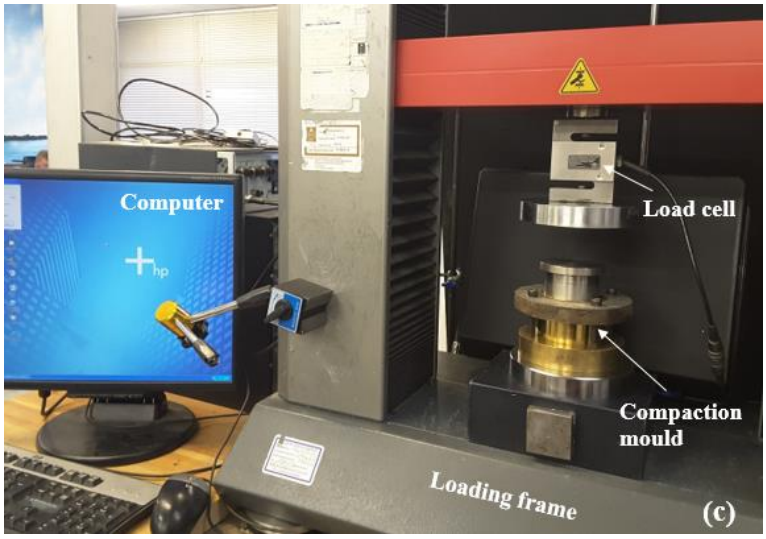

Figure 3.5 Oedometer compaction mould (a) a schematic showing various components (b) a photograph of the components and (c) a compaction setup

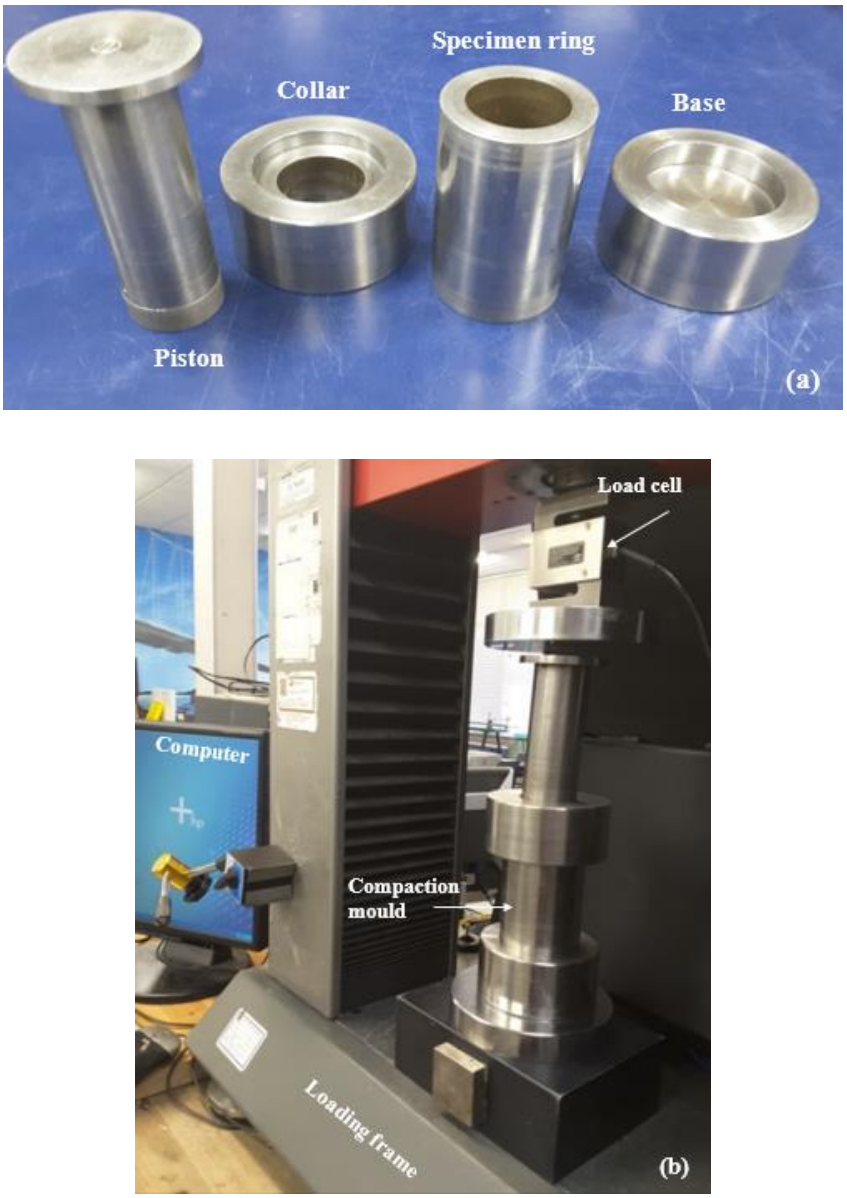

Figure 3.6 Triaxial compaction mould (a) a photograph of the components and (b) a compaction setup

3.5.2.2 Static compaction specimen preparation and testing procedure

Soil-water mixtures were prepared at six targeted water contents such as 6, 8, 10, 12, 13 and 14%. The inner surface of the specimen mould and the collar were coated with silicone grease to minimise wall friction. A soil-water mixture was made to fill the specimen mould. No stress was applied to compact the mixture during the filling process. The mass of the specimen mould along with the soil-water mixture was measured. The soil-water mixture was statically compacted using a hydraulic compression device by placing a spacer on the top of the soil specimen. A constant displacement rate of 1.25 mm/min was adopted for the static compaction process. A review of the literature (see

chapter 2, Table 2.3) suggested that this displacement rate is suitable to prevent a high excess pore-water pressure built up and to obtain a uniform density throughout the specimen (Reddy and Jagadish 1993). The vertical displacement and applied force were monitored during the compaction process. The compaction process was terminated when a predetermined height of the specimen was attained. The applied load was maintained for five minutes to minimise elastic rebound within the specimen. The top piston was given a slight twist before being pulled away from the soil to release fine particles adhering to the face. The applied compaction energy was calculated based on the displacement and applied load. The final height, water content and weight of the compacted specimen were remeasured for calculating the dry density. The results of static compaction tests are presented in Chapter 4.

3.5.3 Double and single oedometer tests

A series of conventional oedometer tests were conducted to investigate the effects of different compaction parameters, such as initial water content, initial dry unit weight, compaction pressure and overburden pressure on the collapse strain of the selected soil. Both double and single oedometer collapse tests were carried out to determine the magnitudes of collapse strain.

Numerous studies have reported that any soil compacted at dry of optimum conditions typically exhibits collapse behavior upon wetting, whereas soils compacted at wet of optimum conditions show significantly less collapse (Barden et al. 1973; Lawton et al. 1989; Tadepalli and Fredlund 1991; Lawton et al. 1992; Basma and Tuncer 1992; Fredlund and Rahardjo 1993a; Lim and Miller 2004). For both double and single oedometer collapse tests, the chosen compaction conditions of the tested specimens based on the literature (see chapter 2, Table 2.1). The results of these tests are presented in Chapter 4.

3.5.3.1 Tests procedure

The double-oedometer collapse tests were performed on pairs of identically statically compacted soil specimens. The chosen initial water contents were 6, 8, 10 and 12% and the corresponding dry unit weights were 13.65, 14.05, 14.55 and 15.14 kN/m^3, respectively. The test procedure suggested by Jennings and Knight (1957) was followed. At any given compaction conditions, two identical compacted specimens were prepared

directly within the oedometer rings by applying static compaction pressure. Both specimens were then transferred to standard consolidation loading devices. One soil specimen was loaded according to standard incremental loading procedure. A loading pressure steps of 12.5, 25, 50, 100, 200, 400, and 800 kPa were selected. Each loading increment was allowed to remain for two hours, and dial gauge readings were monitored at the following time intervals: 0, 0.25, 0.5, 1, 2, 4, 8, 15, 30, 60 and 120 minutes. A seating pressure of 1.5 kPa was applied to the second specimen. The specimen was saturated with deionised water for 24 hours. Further, the specimen was consolidated using the loading sequence of 12.5, 25, 50, 100, 200, 400, and 800 kPa. Each applied pressure was held for 24 hours. Finally, the specimen was unloaded to the token load in a stepwise process.

The difference between the equilibrium void ratios of the two specimens at each value of vertical stress is used to calculate the volumetric strain (Jennings and Knight 1957; Drnevich et al. 1988; Medero et al. 2005). The collapse potential, according to Jennings and Knight (1957) is given by:

$$\text{Collapse potential}\,(\%) = \frac{e_i - e_f}{1+e_0} \times 100 \tag{3.2}$$

where e_0 is the initial void ratio of the identical specimens, and e_i and e_f are the values of void ratio obtained from the oedometer curves at as-compacted water content and at saturation conditions respectively, under the same applied vertical stress.

Six different compaction conditions of the specimens were chosen for single oedometer tests. Compacted soil specimens were prepared at a constant water content of 10% with varying dry unit weight (14, 14.5, 15, 15.5, 16 and 17 kN/m^3). The test procedure for single oedometer tests is presented in section 3.2.1. However, in these tests, the specimens were inundated under an applied pressure of 100 kPa.

3.5.4 Suction measurements by the chilled-mirror dew-point hygrometer

The initial suction of compacted soil specimens and the water retention behaviour of the soil at high suctions (i.e., suction values greater than 500 kPa) were determined by a chilled-mirror dew-point potentiameter hygrometer (ASTM D6836-16). In this section, the details of the testing device and the test procedure are presented.

3.5.4.1 Testing device

WP4C Dewpoint PotentiaMeter produced by Decagon Devices, Inc. was used in this study. The device consists of a sealed chamber with a fan, a mirror, a photoelectric cell, and an infrared thermometer. Figure 3.7 shows the schematic and the photograph of the WP4C chilled-mirror dew-point device. The device has a special closed chamber that contains a mirror and a photodetector cell where a soil specimen can be placed. The mirror within the chamber is repeatedly cooled and heated in cycles to form, and disperse, dew on its surface. The temperature of the mirror is precisely controlled by a thermoelectric (Peltier) cooler. The photodetector cell senses the change in reflectance when condensation occurs on the mirror, whereas a thermocouple attached to the mirror records the temperature at which condensation occurs (Leong et al. 2003). The device equipped with a fan in the sealed compartment to reduce the equilibrium time between the specimen and the surrounding air. Also, a temperature controller is equipped with the device to set the temperature of the specimen at which relative humidity measurement is to be made. A temperature equilibration plate (see Figure 3.7b) which is come with the device is used to bring the temperature of the specimen cup to the set-point temperature of the device.

The device measures the relative humidity of the air space above a soil specimen and displays the equilibrium suction and temperature of the specimen at which the measurement is carried out. The calculations are performed by software within the device and displayed on an LCD panel in MPa unit along with the specimen temperature. The device is able to measure suction to an accuracy of ± 0.05 MPa from 0 to 5 MPa and an accuracy of 1% from 5 to 300 MPa (Decagon Device 2013).

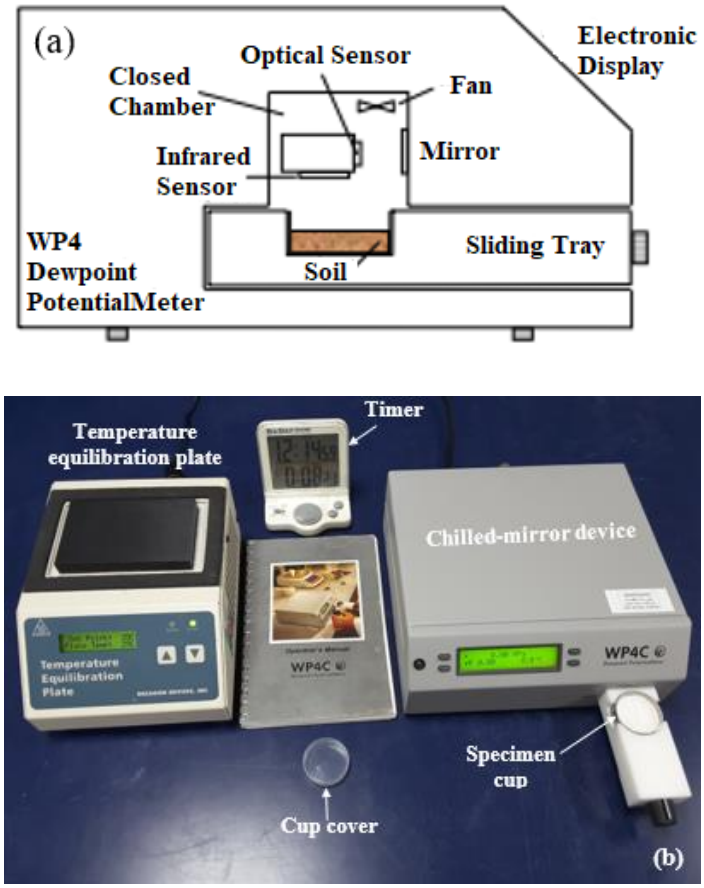

Figure 3.7 WP4C model of chilled-mirror dew point device (a) a schematic of the device (after Leong et al. 2003) and (b) a photograph of the device

3.5.4.2 Chilled-mirror dew-point hygrometer specimen preparation and testing procedure

Calibration the WP4C device with a standard 0.5 molal potassium chloride (KCl) solution provided by the manufacturer is the first step of the test procedure for measuring suction. The equilibration solution was poured into the specimen cup and placed on a temperature equilibration plate to bring the temperature of the specimen cup to the set-point temperature of the device (25 °C). The specimen cup with the salt solution was then placed in the WP4C's specimen drawer, and the drawer knob was turned to the READ position. Once the equilibrium was reached, the total suction value was then calculated and displayed on an LCD panel in MPa unit along with the specimen temperature.

For establishing the water retention behaviour at high suctions, a predefined weight of the soil mixture was statically compacted inside the specimen cup at different initial water contents and a constant dry unit weight of about 15 kN/m^3 (see Table 3.4). A

similar procedure to this used for calibration the device was carried out for total suction measurements of the soil specimens. The suction measurement time was found to vary between 10 to 40 minutes for the range of water content considered in this study. Once the total suction was measured, the water content of the soil specimen was determined by oven drying method, and this establishes one point on the SWCCs. The procedure was repeated until the total suction values corresponding to the entire range of water content were measured. The results of the chilled-mirror hygrometer test are presented in Chapter 5.

Table 3.4 Initial compaction conditions used in chilled-mirror dew-point hygrometer tests

Test no.	Initial compaction conditions	
	Water content (%)	Degree of saturation (%)
1	10.0	36.2
2	8.1	29.3
3	7.1	25.7
4	5.7	20.6
5	4.3	15.4
6	3.7	13.2
7	2.1	7.7
8	1.6	5.6
9	0.9	3.3
10	0.4	1.6

3.5.5 Saturated and unsaturated triaxial tests

The effects of confining stresses and a decrease in matric suction on the volume change and shear strength behaviour of the collapsible soil can be studied by carrying out saturated and unsaturated triaxial tests. The test results from the triaxial tests (based on volume changes and shear strength) enabled establishing water retention curves and suction stress characteristic curves. The following sections present the details of the procedure adopted for preparing specimens and the experimental program.

3.5.5.1 Specimens preparation for the triaxial tests

During the initial phase of the investigation, an attempt was made to prepare statically compacted specimens at a water content of 10% and target dry unit weight of 14 kN/m^3 (see Table 3.2). At these initial conditions, it was noted that extrusion of the specimen from compaction mould caused development cracks and segregation of soil. Therefore, it was decided to prepare soil specimens for triaxial tests at an initial water content of 10% with a dry unit weight of 15 kN/m^3. The soil-water mixture was placed in the mould shown in Figure 3.6 in one layer and compressed at a fixed displacement rate of 1.25 mm/min until a specified axial pressure equivalent to 998 kPa (correspond to static compaction curve) was reached. The final dimensions of the specimen were measured. The final weight of the specimen was measured to verify the target dry unit weight. The specimens for the triaxial tests were 100 mm high and 50 mm in diameter. The compaction conditions of the specimens for triaxial tests are shown in Table 3.5. The initial water content of the triaxial specimen was determined by oven drying method. The initial suction of the compacted soil specimen was determined by using a chilled-mirror dew-point test.

Table 3.5 The initial conditions of the triaxial specimens

Parameters	Value
Compaction water content, w (%)	10
Dry unit weight (kN/m^3)	15
Void ratio, e_0	0.732
Degree of saturation, S_r (%)	36.2
Applied compaction pressure to prepare specimen (kPa)	998
Initial suction (kPa)	563

3.5.5.2 Experimental program for the triaxial tests

Figure 3.8 shows the experimental program for the triaxial tests. In total, three series of triaxial tests were conducted in this study. The results obtained from these tests are presented in Chapter 5 and 6.

The conventional consolidated drained (CD) tests on saturated specimens at three confining stresses 100, 250 and 400 kPa were performed. The information collected from these tests as follows:

i. Elapsed time versus volume change during the consolidation stage.
ii. Axial strain ($\boldsymbol{\varepsilon_a}$) versus deviatoric stresses (q) and volumetric strain ($\boldsymbol{\varepsilon_v}$) during the shearing stage.
iii. Mohr circles and the saturated failure envelope.
iv. Effective shear strength parameters ($\boldsymbol{c'}$ and $\emptyset'$).

The test type II illustrated in Figure 3.8 is the volume change of a single specimen during step-wise suction reduction. The specimen was first subjected to confining stress of 20 kPa. The suction of the specimen was reduced to 500 kPa at this confining stress (20 kPa). Once the applied suction of 500 kPa was equilibrated (i.e., when there was no change in total and water volumes), the confining stress was increased to the predetermined value of 100 kPa. At this applied confining stress, the suction of the specimens was further reduced to 400, 300, 200, 100, 50 and 5 kPa. Each suction step

was considered to be completed when a change in the rates of total and water volume were less than 0.1 cm^3/day**.** The information collected from these tests include suction (s) versus volumetric strain (ε_v) and the void ratio (e) during the wetting stages.

The test type III illustrated in Figure 3.8 were carried out by step-wise wetting a soil specimen under predetermined confining stress followed by a consolidated drained shearing test. In total twelve identical compacted specimens were used under various magnitudes of applied matric suction, and confining stress. Each specimen was placed on the pedestal of the unsaturated triaxial device. The specimens were first subjected to confining stress of 20 kPa. The suction of the specimens was reduced to 500 kPa at this confining stress. Once the applied suction of 500 kPa was equilibrated, the confining stress was increased to a predetermined value from 100, 250, and 400 kPa. At each applied confining stress, the suction of the specimens was further reduced to 300, 100, 50, and 20 kPa. In the final stage, the shear strength test was conducted at each suction and confining stress. The information collected from these tests as follows:

i. Suction (s) versus volumetric strain ($\boldsymbol{\varepsilon_v}$), and the void ratio ($e$) during wetting stages.
ii. Axial strain ($\boldsymbol{\varepsilon_a}$) versus deviatoric stresses (q), and volumetric strain ($\boldsymbol{\varepsilon_v}$) during shearing stages.
iii. Mohr circles and the unsaturated failure envelopes.
iv. Unsaturated shear strength parameters ($\boldsymbol{c}$, $\emptyset$, and $\emptyset^{\boldsymbol{b}}$).

Triaxial tests	Test type I: Conventional CD tests on saturated soil specimens Applied confining stresses: 100, 250 and 400 kPa Number of soil specimens tested: 3 Information gathered during saturation: Volume change Information gathered during shearing: 1) q and ε_v vs. ε_a. 2) c' and $\emptyset'$.
	Test type II: Volume change of unsaturated soil specimen under isotropic stress Applied confining stresses: 100 kPa Number of soil specimens tested: 1 Suction steps: 500, 400, 300, 200, 100, 50 and 5 kPa Suction reduction mode: Step-wise suction reduction Information gathered during suction reduction: ε_v and e vs. s.
	Test type III: CD tests on unsaturated soil specimens Applied confining stresses: 100, 250 and 400 kPa Number of soil specimens tested: 12 Final suction steps: 300, 100, 50, and 20 kPa Suction reduction mode: Step-wise suction reduction. First: Suction reduction from initial suction (563 kPa) to 500 kPa at confining stress of 20 kPa. Second: Suction reduction to 300, 100, 50, and 20 kPa at confining stresses of 100, 250 and 400 kPa. Information gathered during suction reduction: 1) $\boldsymbol{\varepsilon_v}$ and e vs. s. Information gathered during shearing: 2) q and $\boldsymbol{\varepsilon_v}$ vs. $\boldsymbol{\varepsilon_a}$. 3) $\boldsymbol{c}$, $\emptyset$ and $\emptyset^{\boldsymbol{b}}$.

Figure 3.8 Experimental program of the triaxial tests

3.5.5.3 Saturated triaxial tests

The following sections describe the details of the apparatus, and the testing procedure adopted for the conventional consolidated drained tests on saturated soil specimens.

3.5.5.3.1 Conventional automated triaxial device

The apparatus used in this study was a GDS conventional automated triaxial device. A schematic of the test set up is shown in Figure 3.9.

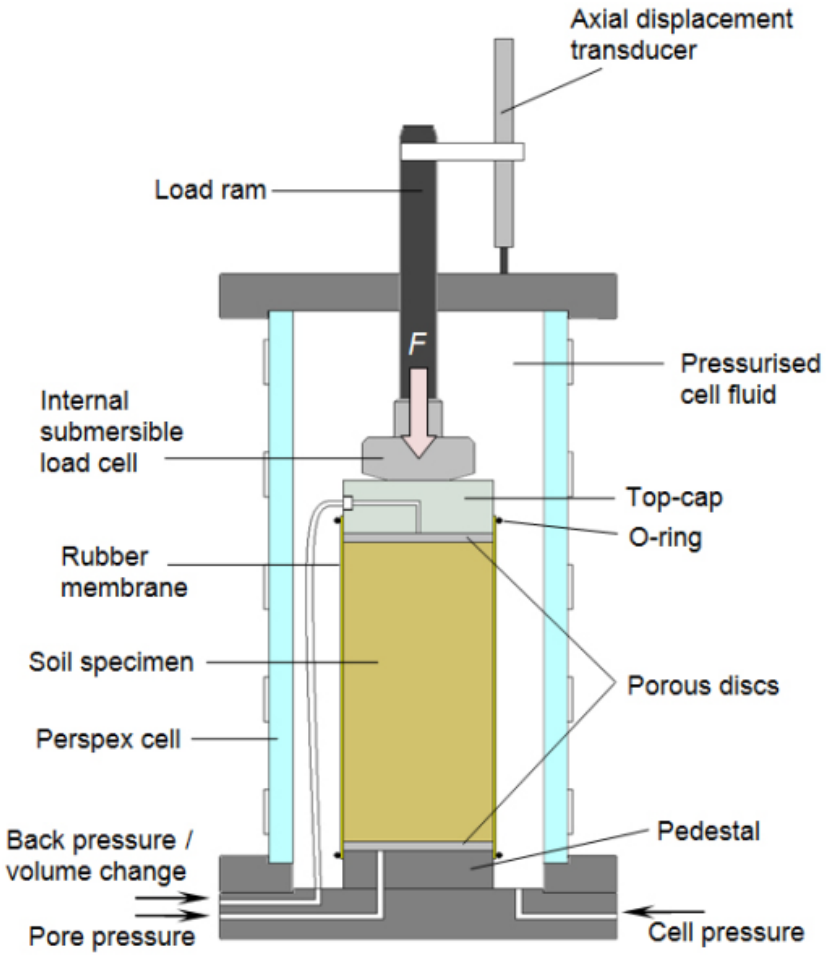

Figure 3.9 Schematic layout of the conventional triaxial device (after Rees 2013)

3.5.5.3.2 Testing procedure for the saturated triaxial tests

The triaxial test as described by geotechnical test standards (BS 1377-8 1990) typically consists of four main stages: system preparation, saturation, consolidation, and shearing. Firstly, silicon grease was applied lightly around the sides of the top cap and the

base platen. The soil specimen was then mounted in the cell with saturated porous stone. The saturated filter-paper disks of a diameter equal to that of the specimen placed between the porous disks and the specimen to avoid clogging of the porous disks. A perspex cap was subsequently positioned on top of the specimen. After ensuring that the axis of the specimen was vertical and coinciding with the axis of the loading ram, a rubber membrane was stretched over the specimen. The membrane was further sealed with two rubber O-rings at each end of the specimen (see Figure 3.10). The triaxial cell and other system components were then assembled and gradually filled with water while allowing air to escape from the top. During this stage pressure/volume controllers connected.

1- Top cap

2- Soil specimen

3- O-rings

4- Pedestal

5- Water pressure transducer

6- Load frame

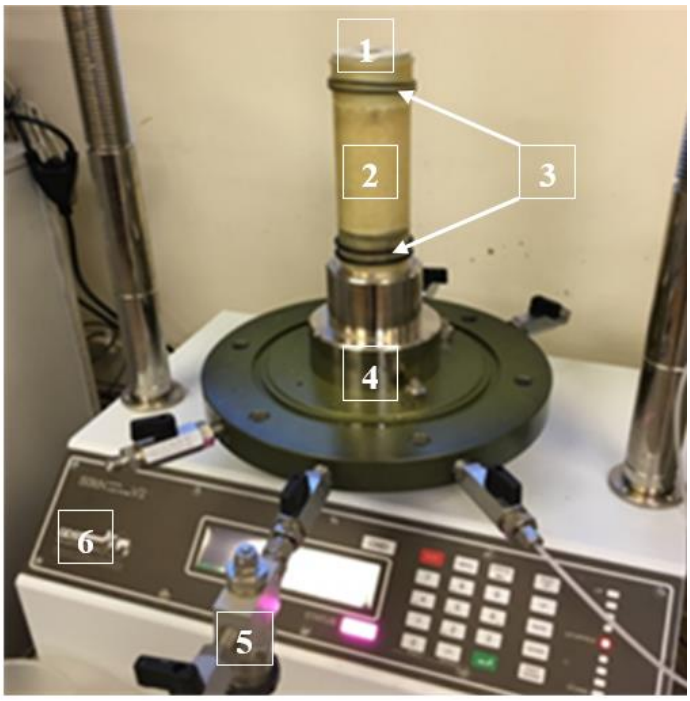

Figure 3.10 Specimen mounted on the cell

3.5.5.3.3 Back pressure saturation

During the saturation process, the GDSLab control and acquisition unit software was used to set up saturation ramp by applying a cell pressure (σ_3) and a back pressure (u_w). The saturation process is designed to ensure all voids within the test specimen are filled with water, and that the pore pressure transducer and drainage lines are properly de-aired. This may be achieved by increasing the back water pressure and cell pressure in

equal increments with a difference of 10 kPa to prevent the specimen from accidental swelling (the effective stress should not increase above the value required for shearing as this leads to specimen over-consolidation) (Rahardjo et al. 2004; Maleki and Bayat 2012). A significant period of time was required to assist the specimen in reaching full saturation. To check the degree of specimen saturation is sufficiently high before starting the consolidation stage, a short test is usually performed to determine Skempton's B-value (Equation 3.3). During this process, the drainage was closed whilst the cell pressure was raised by 50 kPa. Full saturation was assumed to have been achieved when the *B* value was greater than 0.97 as proposed by Head (1982), Khalili et al. (2004) and Viana da Fonseca et al. (2013).

$$B = \frac{\Delta u}{\Delta \sigma_3} \tag{3.3}$$

where Δu = Pore-water change after the increment of confining pressure and $\Delta \sigma_3$ = The increment of confining pressure.

3.5.5.3.4 Consolidation

After saturation had been achieved, the back water pressure was maintained constant around 300 kPa (pore pressure reached during the final saturation stage) while the cell pressure was increased to create a differential equal to the desired isotropic confining stress 100, 250 and 400 kPa. The consolidation process was monitored by recording the amount of water flow from the specimen by the digital pressure volume controller until primary consolidation was complete. Consolidation stage was continued for one overnight period after 100% primary consolidation has been achieved. The completion of consolidation was defined as once no further water volume change can be detected from the specimen, and the excess pore-water pressure had dissipated. During this stage, volume change against elapsed time relationships was determined.

3.5.5.3.5 Shearing

During the shearing stage, the specimens were sheared under the drained condition by increasing the deviatoric stress at a sufficiently slow displacement rate of 0.0015 mm/min (Gan et al. 1988). This chosen rate of axial strain was slow enough to

prevent the development of excess pore pressure during the application of the deviator stress (Head 1998). The tests were terminated at an axial strain of 25% (Fai 2001). Following the shearing process, the specimen was unloaded, and all the relevant pressures were released. Then, the soil specimen was dismantled from the pedestal. The results of the saturated triaxial tests are presented in Chapter 6.

3.5.5.4 Unsaturated triaxial tests

Suction-controlled triaxial shear strength tests were carried out on compacted specimens of prepared soil at several confining stresses, and matric suctions (see Figure 3.8). The following sections present the details of the unsaturated triaxial tests setup and procedures.

3.5.5.4.1 General layout of the unsaturated triaxial testing system

A suction controlled GDS Triaxial Automated System (HKUST-type) (GDS Instruments Ltd. UK) was used to carry out the triaxial tests on unsaturated soil specimens in this study. The photograph of the HKUST-type triaxial apparatus is illustrated in Figure 3.11. The system composes a triaxial cell (outer cell), two pressure controllers, six transducers, a digital transducer interface, an inner cell, a load frame and a computer. The general details of these main parts are:

i. The outer triaxial cell (item no.1) is a Bishop & Wesley stress-path cell (Bishop and Wesley 1975).
ii. Two GDS pressure controllers, one (item no.2) is an automatic pneumatic regulator with two channels for controlling the cell pressure in both the inner and outer cell cavities and for controlling the pore air pressure in the soil specimen, whereas the other one (item no.3) is a digital hydraulic pressure/volume controller. The pressure/volume controller is microprocessor controlled hydraulic actuators that can be used for controlling the back-water pressure as well as measuring the water volume change in the soil specimen. These two GDS controllers can be controlled independently.
iii. The six transducers are a load cell (item no.4) to measure the axial force, a linear variable differential transformer (LVDT) (item no.5) to measure the axial displacement, a wet–wet differential pressure transducer (DPT) (item no.6) (a component of the total volume change measuring system) and three other pressure transducers for monitoring the cell pressure (item no.7), the pore air pressure (item

no.8) and the pore water pressure (item no.9). All GDS transducers are supplied with a calibration certificate. The average sensitivity of the transducers is indicated in Table A-1 in appendix A.

iv. The six transducers are connected to the digital transducer interface (DTI) (item no.10) for data acquisition. A computerised control system was used to log the data from all the GDS units and control tests following predetermined stress paths. All these forms a closed-loop controlling and feedback system, which is capable of performing strain-controlled and stress-path tests in (*p*, *q*, *s*) space.

v. Inside the triaxial cell is a second cell wall (item no.11) in which the specimen is placed. This enables the cell volume change to be measured from just the inner chamber minimizing the error due to temperature and pressure changes.

vi. A triaxial load frame (item no.12) appropriate for performing constant strain rate test was used to apply axial loads to the triaxial cell piston. The load cell is attached to a loading ram inside the triaxial cell to measure the axial force applied to each specimen during shearing.

vii. The main unsaturated testing module used in this study is 4-dimensional stress path (GDS Instruments Ltd 2014). This 4-dimensional stress path enables simultaneous control of the pore air, pore water, radial stress and axial stress controllers.

3.5.5.4.2 Wet-wet differential pressure transducer (DPT)

The main difficulty of an unsaturated triaxial test is the accurately measure the specimen volume change. Referring to Figure 3.12a, the wet-wet high accuracy differential pressure transducer (DPT) was used to measure the changes in specimen volume. The basic principle of this measuring system is to measure changes in the differential pressure on both sides of the diaphragm (see Figure 3.12b) due to continuously changes in the water level inside an open-ended, bottle-shaped inner cell caused by volume change in the specimen during testing relative to the constant water level in the reference tube. Therefore, the reading of the DPT represents the specimen volume change.

Figure 3.11 Schematic layout of GDS triaxial testing system

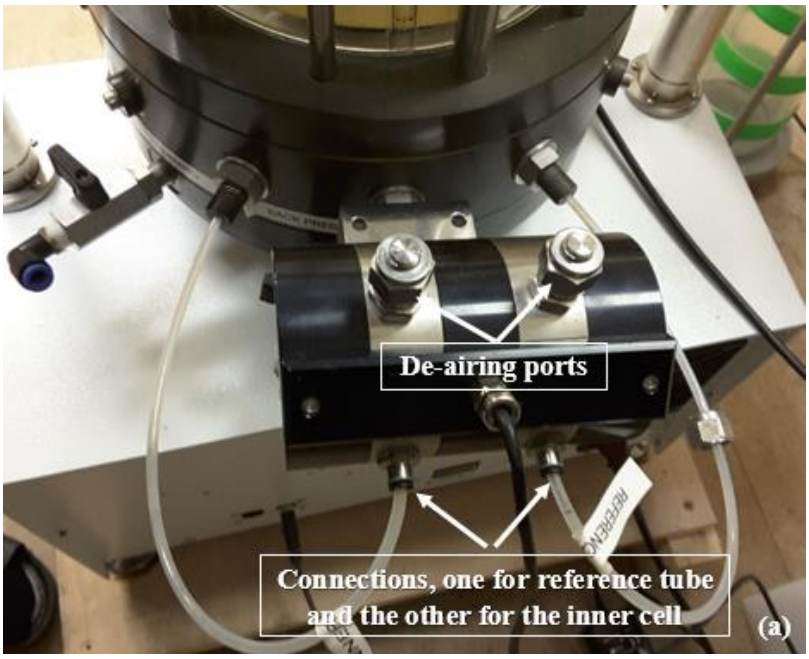

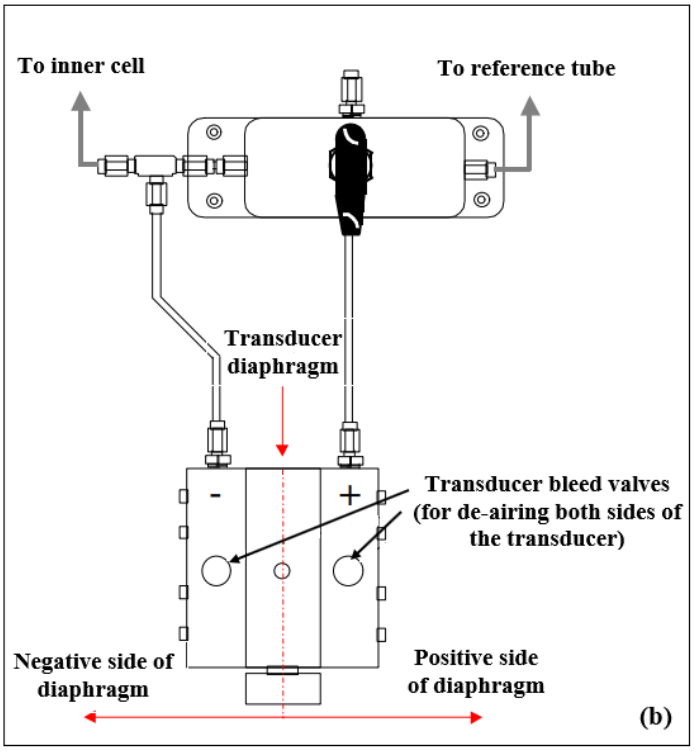

Figure 3.12 Volume change measuring system (DPT) (a) a photograph of the system and (b) a schematic layout showing various components

3.5.5.4.3 Control of matric suction

In the GDS unsaturated triaxial apparatus, axis-translation technique (Hilf 1956) was employed to control the matric suction. Pore air pressure is applied through a course low air–entry disk (5 kPa) placed on top of the soil specimen. The pore water will not go through this disk because the controlled pore water pressure is always lower than the controlled pore air pressure, and the selected disk has a low attraction for water (Liangtong 2003). The pore water pressure is controlled by a 5-bar saturated high air ceramic disk 50 mm in diameter and 6.9 mm in thickness sealed to the base pedestal of the triaxial apparatus using epoxy resin. The high air entry value ceramic disk is a very fine porous filter which allows the passage of water but prevents the flow of free air from the specimen to the water control and drainage system underneath it. Thus, matric suction is controlled as the difference between pore air pressure and pore water pressure. During unsaturated soil testing, the matric suction in each soil specimen must not exceed the air-entry value of the ceramic disk (500 kPa). Otherwise, air will enter the ceramic disk and hence causes an error in the control and measurement of pore water pressure.

3.5.5.4.4 Saturating the high air entry ceramic disk

When testing unsaturated soils, it is necessary to separate the pore-air and the pore water. This separation can be achieved by using the high air-entry porous disk. The high air-entry value ceramic disk only functions when it is saturated. Therefore, before unsaturated soil testing, the high air-entry value ceramic disk must be saturated in order to minimise the amount of air bubbles trapped inside the disk and to support a maximum air/water pressure difference equal to the air-entry value. The saturation procedure suggested by Fredlund and Rahardjo (1993) was adopted to saturate the ceramic disk in this study. First, a small positive water pressure (30 kPa) applied to the underside of the ceramic disk. This condition was maintained until water pools on the top surface of the ceramic disk. This stage has normally been completed in four hours. After that, the ceramic disk was pressurised with water in the normal direction. This saturation procedure mainly involves expelling the air in the ceramic disk with a high gradient water flow and dissolving any air bubbles left in the water by applying a high-water pressure. This was achieved by filling the triaxial cell with deaired water and applying a high air pressure (e.g., 500 kPa) inside the triaxial cell from a pneumatic controller while leaving the pore water pressure connector close. The high pressure was maintained for one hour,

during which the air left in the ceramic disk tended to be dissolved in the water. The valve connecting the pore pressure connector was then opened to the atmosphere. The air bubbles collected below the ceramic disk and the water containing the dissolved air were removed by flushing through the disk with deaired water from the cell under a high flow gradient to the atmosphere. The valve connected to the measuring system was then closed, and the pressure in the ceramic disk was built up to the pressure in the cell. The above procedure should be repeated for at least five times if the ceramic disk was newly installed. Once saturated, the cell pressure was dissipated to zero and the ceramic disk should remain covered with water until a soil specimen is ready to be placed on the disk. After each test, the high air entry ceramic disk was saturated, and it normally took twenty-four hours to accomplish the task compared to a few days for a newly mounted disk.

Prior to each new test, the measurement of saturated water permeability of ceramic disk with a constant head method was carried out to check a possible cracking happened to the disk during the previous test (any cracking will lead to a significant increase in the water permeability of the disk) or to check the saturation of the ceramic disk. The measured saturated water permeability of the ceramic disk in this study was around 1.21 x 10^{-9} m/sec.

3.5.5.4.5 Mounting the specimen

Before setting up the compacted specimen, the digital hydraulic pressure controller was flushed and then filled with fresh deaired water. The high air entry value disk was saturated, and any excess water left on it was removed with a dry tissue. Furthermore, all the water lines associated with the measurement of water volume and total volume change were flushed with fresh deaired water.

The initial dimensions and weight of the specimen were measured just before placing it on the pedestal. A rubber membrane was placed on the specimen by using a membrane stretcher. A filter paper was placed on top of the specimen to avoid fine soil particles being trapped inside the pores of the porous metal. The low air entry a coarse corundum disk and the top cap was then positioned on the top of the specimen. Subsequently, the membrane was then sealed at the top cap and the base pedestal by O-rings. The set-up of a soil specimen is shown in Figure 3.13a.

3.5.5.4.6 Mounting the inner cell

The bottle-shaped inner cell was assembled, and it was filled with deaired water to an appropriate water level within the necked part (see Figure 3.13b and Figure 3.14). The rise of water level should be made relatively slow to minimise the trapping of air bubbles inside the cell. Similarly, the reference tube was also filled with deaired water to an appropriate level (see Figure 3.14). After all the connections were fitting, all the tubes and fittings between the inner cell and the differential pressure transducer were flushed to prevent any air entrapment in the system that could affect the results. The outer cell with the loading ram was then placed in position, and it was partially filled with deaired water (see Figure 3.14). The loading ram was then contacted the specimen cap. The contact was justified by monitoring the reading from the load cell attached to the loading ram.

1- Top cap

2- Soil specimen

3- Pore air pressure connections

4- Reference tube

5- Inner cell

6- Connections to the differential pressure transducer (DPT)

7- Pedestal

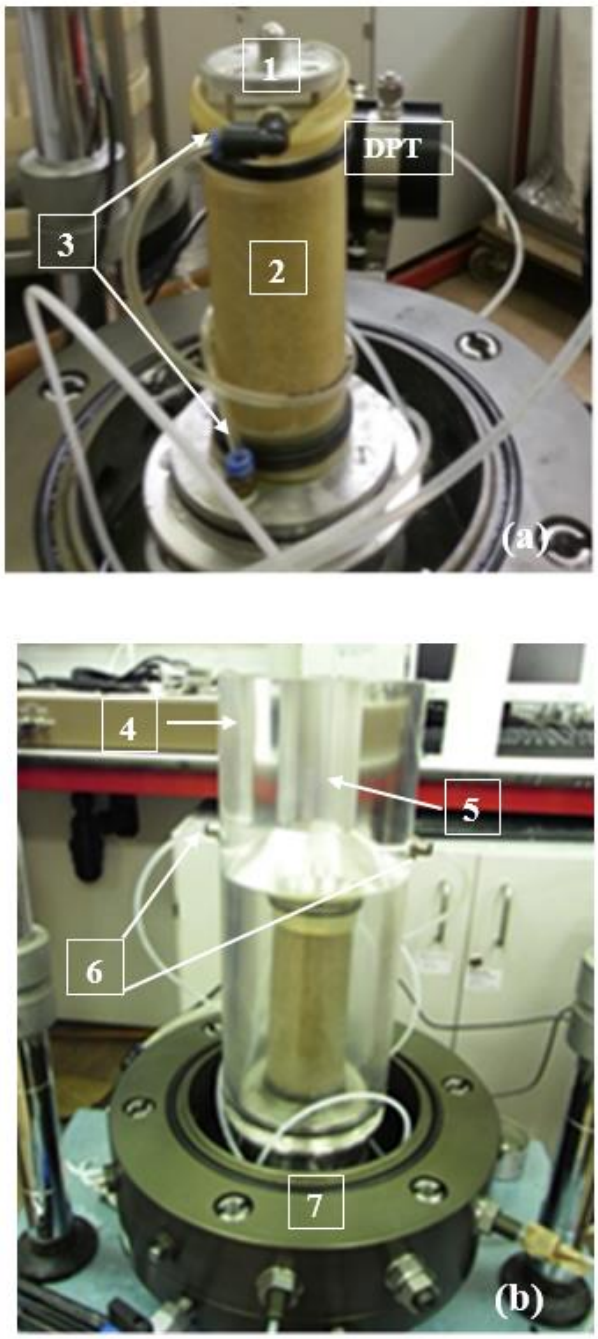

Figure 3.13 Set-up of a soil specimen (a) before place the inner cell (b) after place the inner cell

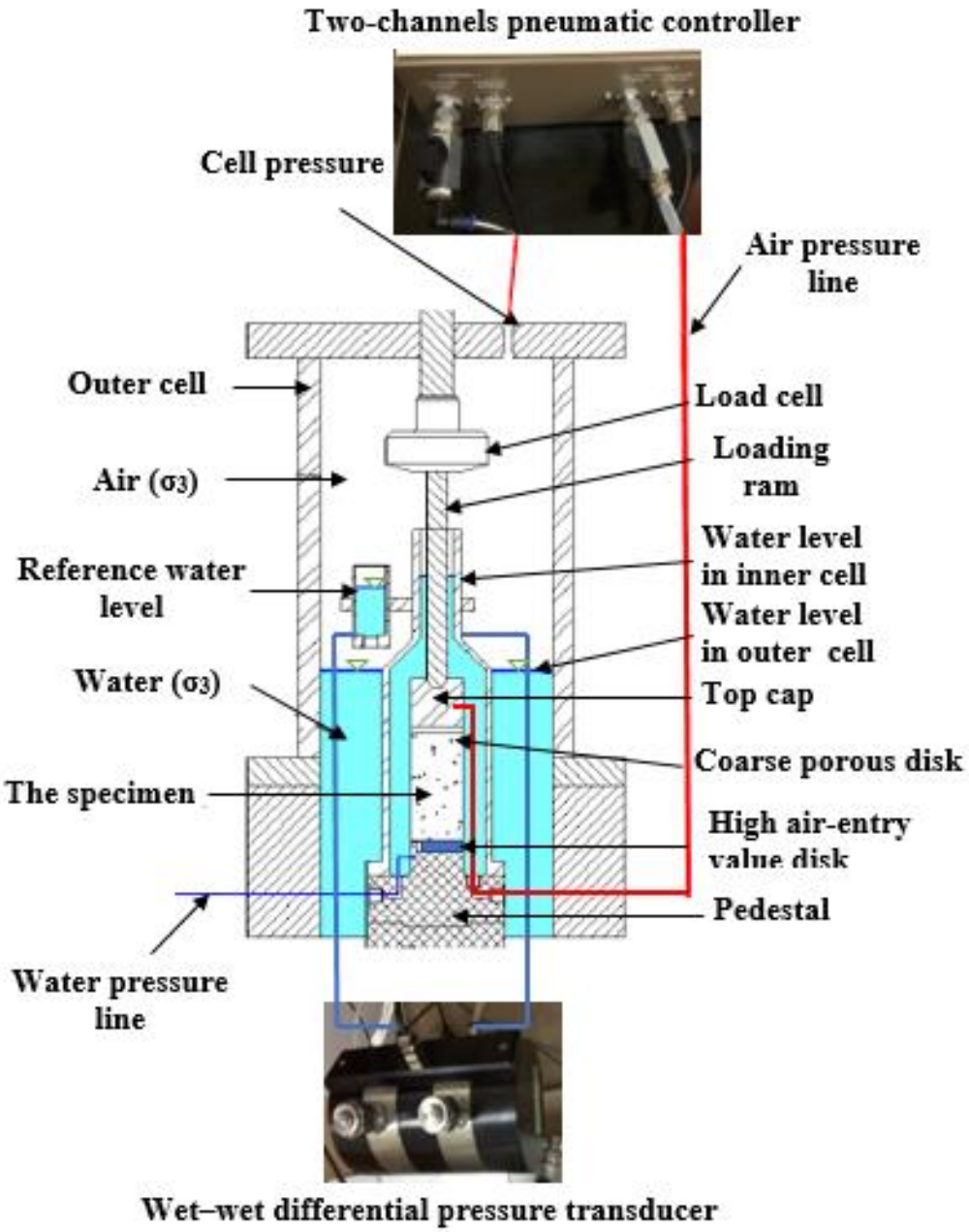

Figure 3.14 Schematic diagram of the unsaturated triaxial system

3.5.5.4.7 Test procedure

Each specimen was placed on the pedestal of the unsaturated triaxial device. The specimens were first subjected to the cell pressure (σ_3) of 20 kPa under undrained conditions. Then, the initial suction of the specimen (563 kPa) was reduced to 500 kPa at net confining stress, ($\sigma_3 - u_a$) = 20 kPa under drained condition. Once the applied suction of 500 kPa was equilibrated (i.e., when there was no change in total and water volumes), the net confining stress was increased to a predetermined value from 100, 250, and 400 kPa by increasing the cell pressure in a series of increments while maintaining constant pore-air and pore-water pressures. At each applied confining stress, the suction of the specimens was further reduced to 300, 100, 50, and 20 kPa by decreasing both air and cell pressure, whereas the pore-water pressure was maintained constant. Hence water would flow in and wet the specimen. A suction step was considered to be completed when a change in the rates of total and water volume was less than 0.1 cm^3/day (Sivakumar 1993; Wheeler and Sivakumar 1995b; Sharma 1998b; Rampino et al. 2000; Estabragh and Javadi 2008; Ng et al. 2012; Zhang et al. 2016; Ma et al. 2016).

During the shearing stage, the specimens were sheared under the drained condition by increasing the deviatoric stress at a sufficiently slow displacement rate of 0.0015 mm/min (Ho and Fredlund 1982c; Gan et al. 1988; Maatouk et al. 1995; Wheeler and Sivakumar 1995b; Laloui et al. 1997; Adams and Wulfsohn 1997; Rampino et al. 1999; Schnellmann et al. 2013) to avoid generating excess pore-water pressure in the specimen, as any excess pore-water pressure during triaxial compression testing would result in a change in matric suction (Ho and Fredlund 1982c; Sun et al. 2016). During the shearing process, the cell pressure, the pore air pressure, and the pore water pressure were held constant, and the overall and water volume changes were monitored. The shearing stage was terminated at an axial strain of 25% in all cases.

3.6 Concluding remarks

A mixture of 40% M400 silt, 40% Leighton Buzzard sand and 20% Speswhite kaolin was considered for preparing the soil used in this study. The properties of this soil, the details of the laboratory tests set up and the components, specimen preparation methods and the experimental procedures adopted to carry out various tests were presented in this chapter.

In this study, static compaction curves of the soil were established by statically compacting soil-water mixtures. A series of double and single oedometer tests were conducted to investigate the effects of initial water content, initial dry unit weight, compaction pressure on the collapse strain of the selected soil. The initial suction of the compacted soil specimens and the water retention behaviour of the soil at high suctions were determined by using a chilled-mirror dew-point potentiameter. This chapter also presents the experimental programme which has been carried out on saturated and unsaturated compacted specimens to explore the impact of net confining stress and suction on the volume change and shear strength behaviour of a collapsible soil during the wetting process.

CHAPTER 4

One-dimensional static compaction and compressibility characteristics

4.1 Introduction

Soil compaction is an essential part of earthwork during construction of civil works. The main purpose of compaction is to maximise the dry density of soils by expelling air and therefore, to achieve the desired strength, compressibility, and hydraulic conductivity of the soils used (Head 1982). Compaction water content and compactify effort are known to have a significant influence on the soil structure and pore size distribution (Turnbull 1950; Barden et al. 1969; Cui and Delage 1996; Enrique Romero 1999; Gens et al. 1995; Sivakumar and Wheeler 2000).

When the soil is compacted statically, its volume decreases continually as the load is applied gradually to the whole area of the sample (Turnbull 1950). Static compaction test at each soil has a certain amount of energy per unit volume compared to dynamic compaction which applies standard energy for all categories of soils (Romero 1999). Several laboratory research works have been aimed at understanding the effects of static compaction on various properties of soils (Turnbull 1950; Bernhard and Krynine 1952; Whitman et al. 1960; Gau and Olson 1971; Booth 1976; Olivier and Mesbah 1986; Reddy and Jagadish 1993; Mesbah et al. 1999; Romero 1999; Liangtong 2003; Walker 2004; Mitchell and Soga 2005; Tarantino and De Col 2008; Xiujuan 2008; Hafez et al. 2010; Lawson et al. 2011; Zhemchuzhnikov et al. 2016). These studies were provided with a set of curves showing the relationship between water content and dry density for different energy and pressure levels, from which the values of dry density corresponding to water content can be obtained. The general conclusion shown by several authors is that static compaction gives the most uniform specimens, and it as decided therefore to use this compaction method to prepare specimens for the determination of its engineering characteristics such as the collapse strain, SWCC and shear strength (Bernhard and

Krrynine 1952; Whitman et al. 1960; Gau and Olson 1971; Booth 1976; Reddy and Jagadish 1993; Liangtong 2003; Xiujuan 2008; Zhemchuzhnikov et al. 2016).

Several studies have reported the relevant effect of the static compaction water content on the soil structure (Turnbull 1950; Barden et al. 1969; Cui and Delage 1996). Soils compacted dry of optimum have an open structure with larger interconnected pores and tend to exhibit higher collapse during wetting than compacted samples on the wet side at the same dry density (Sivakumar and Wheeler 2000). Therefore, it is necessary to study the static compaction effects on the initial conditions established during compaction especially for the soils that suffering from a reduction in the volume (collapse) during the wetting process.

The effect of friction between compaction mould and the soil was mentioned by a number of researchers (Walker 2004; Olivier and Mesbah 1986; Reddy and Jagadish 1993; Zhemchuzhnikov et al. 2016). However, yet there are no quantitative results available related to the effects of the specimen mould size such as oedometer and triaxial mould on this amount of friction.

Numerous soil types can fall in the general category of collapsible soils, including compacted soils and natural soils such as aeolian soil deposits (loess, loessic deposits and loess-derived sediments) (Derbyshire and Mellors 1988, El Howayek et al. 2011; Li et al. 2016). Collapsible soils are under unsaturated conditions with negative pore pressure (Lawton et al. 1992; Rollins and Kim 2010; Rabbi et al. 2014a). Upon wetting, the pore pressure becomes less negative, and the water can dissolve or soften the bonds between the particles, allowing them to take a denser packing. Cases of collapse can often cause large differential settlements that reduce the serviceability of the structure and raise the frequency and cost of rehabilitation (Barden et al. 1973; Lawton et al. 1992; Pereira and Fredlund 2000; El Howayek et al. 2011).

The collapse potential is stress path dependent and is a function of applied stress, initial void ratio, initial water content, compaction pressure, suction and degree of saturation (Jotisankasa 2005). Many investigations were conducted to explore the main factors controlling the behaviour of collapse mechanisms in details (Jennings and Knight 1957; Matyas and Radhakrishna 1968; Dudley 1970; Escario and Saez 1973; Reginatto and Ferrero 1973; Booth 1975; Mitchell 1976; El Sohby and Rabbaa 1984; Maswoswe 1985; Drnevich et al. 1988; Feda 1988; Lawton et al. 1989; Basma and Tuncer 1992;

Lawton et al. 1992; Alwail et al. 1994; Rogers 1995; Pereira and Fredlund 2000; Rao and Revanasiddappa 2000; Alawaji 2001; Houston et al. 2001a; Miller et al. 2001; Ng and Chiu 2001; Lim and Miller 2004; Jotisankasa 2005; Jefferson and Ahmad 2007; El Howayek et al. 2011; Rabbi et al. 2014a; Rabbi et al. 2014b; Li et al. 2016). Witsman and Lovell (1979), Lawton et al. (1989, 1992), Maswoswe (1985) and Sun et al. (2007) stated that a maximum collapse strain occurs when the applied stress during wetting equals to the initial yielding stress (static compaction pressure) of the unsaturated collapsible soil.

The one-dimensional wetting test, which is performed using conventional consolidation equipment, represents the most frequently used laboratory collapse test for determining the collapse strain of the soil (Houston et al. 2001a). Two procedures are commonly followed in the oedometer-collapse test: double oedometer and single oedometer methods. Based on the oedometer-collapse test results, the collapse potential of the prepared soil at several initial dry unit weight, water content, compaction pressure and the overburden pressure (pressure at wetting) can be assessed and used to indicate the initial compaction conditions for the specimen used in the main tests such as wetting tests under isotropic stress conditions and triaxial shearing tests.

The objectives of this chapter were; (*i*) to study the effects of compaction water content and compaction mould size (oedometer and triaxial moulds) on the static compaction curves, both in terms of applied pressure and applied energy, and (*ii*) to investigate the effects of the compaction parameters such as initial water content, the compaction pressure which in turn affects the initial dry unit weight and the yield stress on the amount of collapse of the selected soil by using double and single oedometer collapse tests.

This chapter divided into several sections. For the static compaction tests (section 4.2), the experimental program (section 3.5.2) is recalled in section 4.2.1. The presentation of test results was included in section 4.2.2. Under test results and discussion (section 4.2.3), the experimental results involving the static compaction curves of the selected soil at several values of energy and pressure inputs for two specimens mould sizes (oedometer and triaxial moulds) are studied and compared. For the one-dimensional collapse tests performed (section 4.3), the experimental program (section 3.5.3) is recalled in section 4.3.1. Under test results and discussion (section 4.3.2), the

experimental oedometer-collapse test results and the analyses of the results are presented. The concluding remarks are presented in section 4.4.

4.2 Static compaction tests

4.2.1 Experimental program

Static compaction curves of the soil were established by statically compacting loose soil-water mixtures at six targeted water contents such as 6, 8, 10, 12, 13 and 14% (see section 3.5.2.2). Compaction of the specimens was carried out using two types of static compaction moulds and a hydraulic compression device shown in Figure 3.5 and 3.6. The displacement rate adopted during the static compaction of 1.25 mm/min. The vertical displacement and applied force were monitored during the compaction process. The compaction process was terminated when a predetermined height of the specimen was attained. As no drainage was provided during the compaction, the water content remained constant and was measured at the end of the test. The final height and weight of the compacted specimen were measured.

4.2.2 Presentation of test results

Load-displacement curves were determined directly from static compaction tests using oedometer and triaxial moulds for the considered range of compacted water content are presented in Figures 4.2a and 4.3a, respectively. The applied compaction energy during the test was calculated by integration of the area under the load-displacement curve up to the selected point at a certain water content and dry unit weight as an example below (see Figure 4.1):

i. The area of trapezoidal shape (A) was determined by: A (kN.mm) = 0.5 h (b1+b2)
ii. The energy (E) was determined by: E (kN.mm) = $A_1+A_2+A_3+A_4+\ldots$.
iii. Then, the static compaction energy per unit volume was determined.

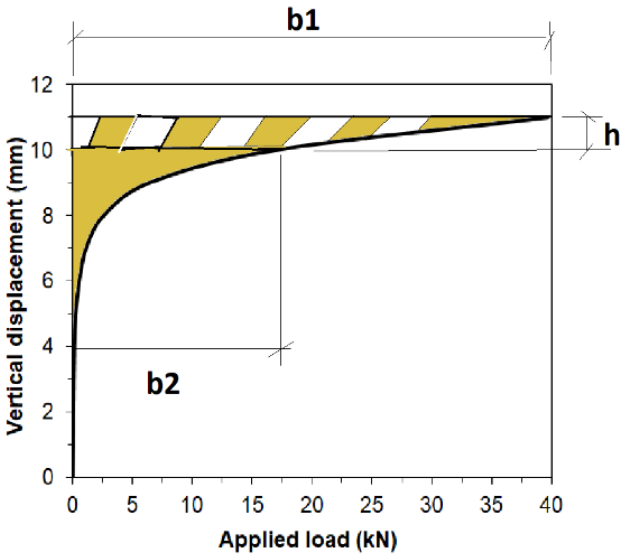

Figure 4.1 An example explains how static compaction energy was determined.

Consequently, the void ratio and hence the degree of saturation were found. As a result, a set of curves were derived (see Figures 4.2b to f and 4.3b to f).

4.2.3 Test results and discussion

4.2.3.1 Effects of the compaction water content on the static compaction characteristics

Figures 4.2b and 4.2c show the applied load and pressure versus void ratio using the oedometer compaction mould, respectively. Figures 4.3b and 4.3c show the applied load and pressure versus void ratio using the triaxial compaction moulds, respectively. It appears from the test results that the measured void ratio was found to decrease with increasing the compaction water content at constant applied load or pressure.

Figures 4.2d and 4.2e show the applied pressure and energy versus dry unit weight using the oedometer compaction mould, respectively. Figures 4.3d and 4.3e show the applied pressure and energy versus dry unit weight using the triaxial compaction moulds, respectively. It can be seen from these figures that at the same value of the compaction pressure or energy, while the compaction water content increases the dry unite weight increases. For example, it can be seen in Figures 4.2d and 4.3d that for the water content

ranging from 6 to 14% at an applied pressure of about 800 kPa, the dry unit weight varied from about 14.8 to 18.5 kN/m^2 and from about 14.3 to 16 kN/m^2, respectively.

Figures 4.2f and 4.3f show the variations of the degree of saturation with the applied pressure using the oedometer and the triaxial static compaction moulds, respectively. It is expected that for a given applied pressure, the degree of saturation increases when the compaction water content increases. For example, from Figure 4.2f it was found that over the considered range of water content 6 to 14% the degree of saturation lies between 38 and 91% for applied pressure ranging from 800 to 5000 kPa, whereas, in Figure 4.3f it was noted that in the same range of water content 6 to 14% the degree of saturation lies between 29 and 83% for applied pressure ranging from 2750 to 6500 kPa.

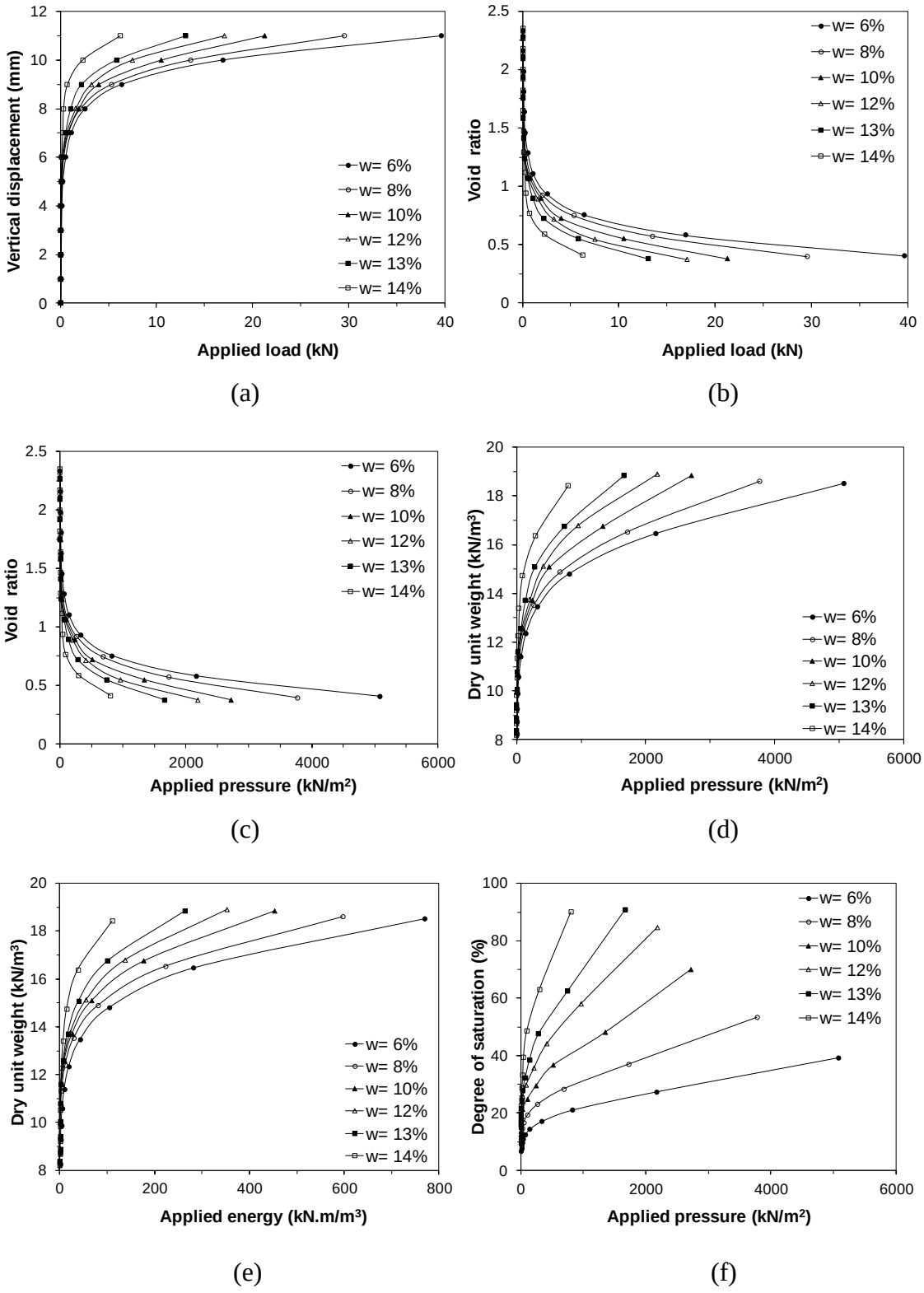

Figure 4.2 Results of static compaction tests using oedometer compaction mould

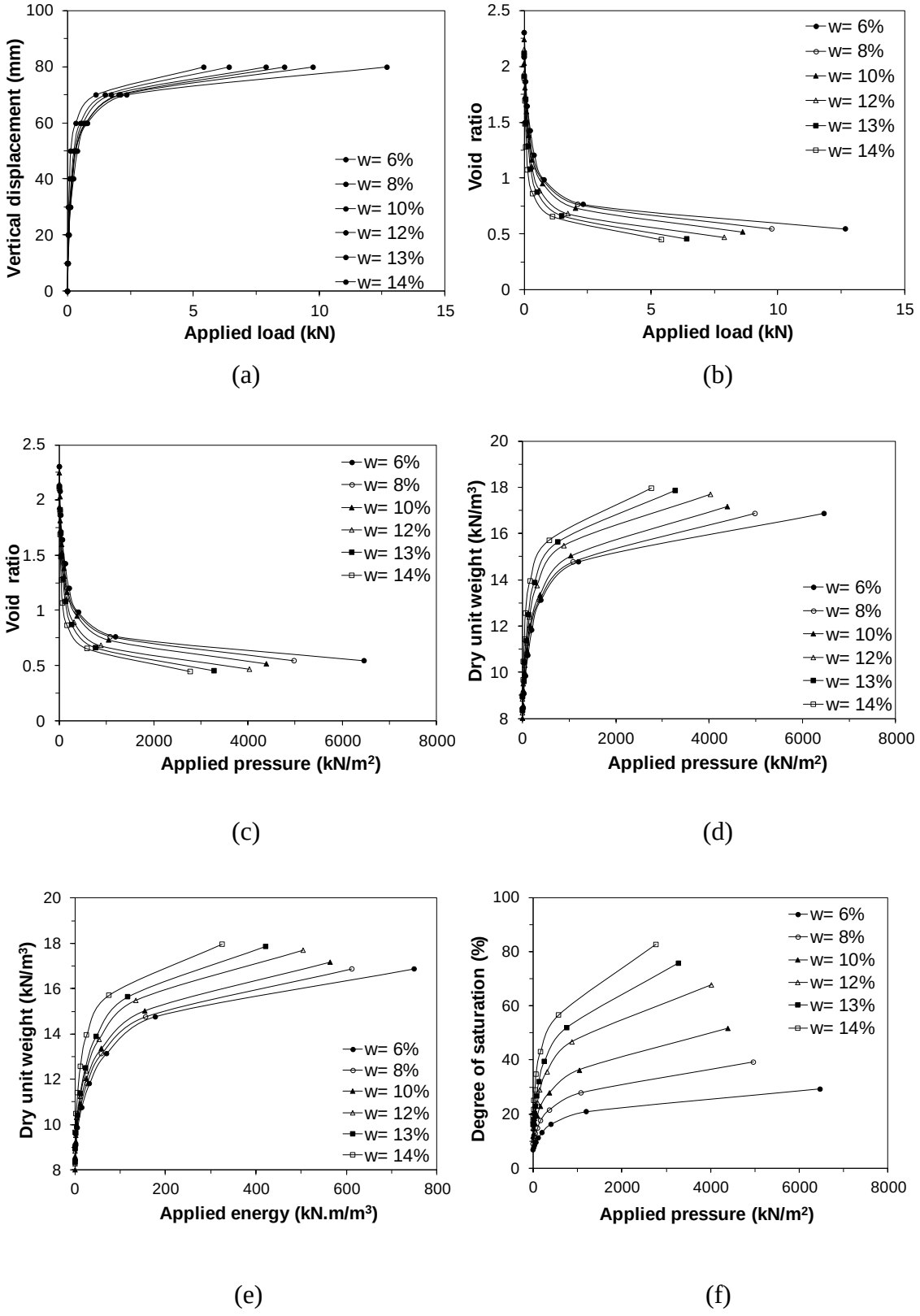

Figure 4.3 Results of static compaction tests using triaxial compaction mould

The information derived from the static compaction measurements (Figures 4.2 and 4.3) have been organised to yield curves relating dry unit weight and water content for constant energy values (see Figures 4.4a and 4.5a) and pressure input values (see Figures 4.4b and 4.5b). The Proctor compaction curve and the static compaction curve at the same Proctor curve energy were also plotted for comparison of the efficiency of static and dynamic compaction methods. The static compaction curves presented no wet side of optimum in contrast to the Proctor curve. This is probably due to when water content approaches saturation during the statically compacted process, and no more air can be expelled, either consolidation starts or, if there is no way for water to drain, pore pressure begins to grow at an equal rate as the applied load, for water is relatively incompressible. (Mitchell and Soga 2005). Reddy and Jagadish (1993) stated that the shape of static compaction curves was different from the dynamic one as they presented no wet side of optimum. However, Turnbull (1950), Olivier and Mesbah (1986), Hafez et al. (2010) and Zhemchuzhnikov et al. (2016) have found that static compaction curves are similar to the Proctor compaction curves in shape.

Figure 4.4b showed that as the compaction water content increases from 6% to 14% at each value of compaction pressure (50, 100, 200, 300, 400, 500, 600 and 800 kN/m^2), the dry unit weight increases, and the difference recorded in the dry unit weight was found to be within the range of 3 to 3.6 kN/m^3. Additionally, all the curves in Figure 4.5b indicate an upward trend with increasing compaction water content and the difference between the maximum and the minimum dry unit weight value at each value of compaction pressure (100, 200, 300, 400, 600, 800, 1000 and 1200 kN/m^2) is around 2.6 kN/m^3. Similar findings were reported by other researchers (Reddy and Jagadish 1993; Romero 1999). Mitchell and Soga (2005) stated that the compaction water content is the determinant variable of the compaction process. At low water content, water menisci are formed between soil grains which restrains their rearrangement and can cause a decrease in dry density. With the consequent increase of water content, water begins to act as a lubricant facilitating the movement of soil particles and increasing the plasticity of the clay fraction. The dry density gradually increases up to optimum water content.

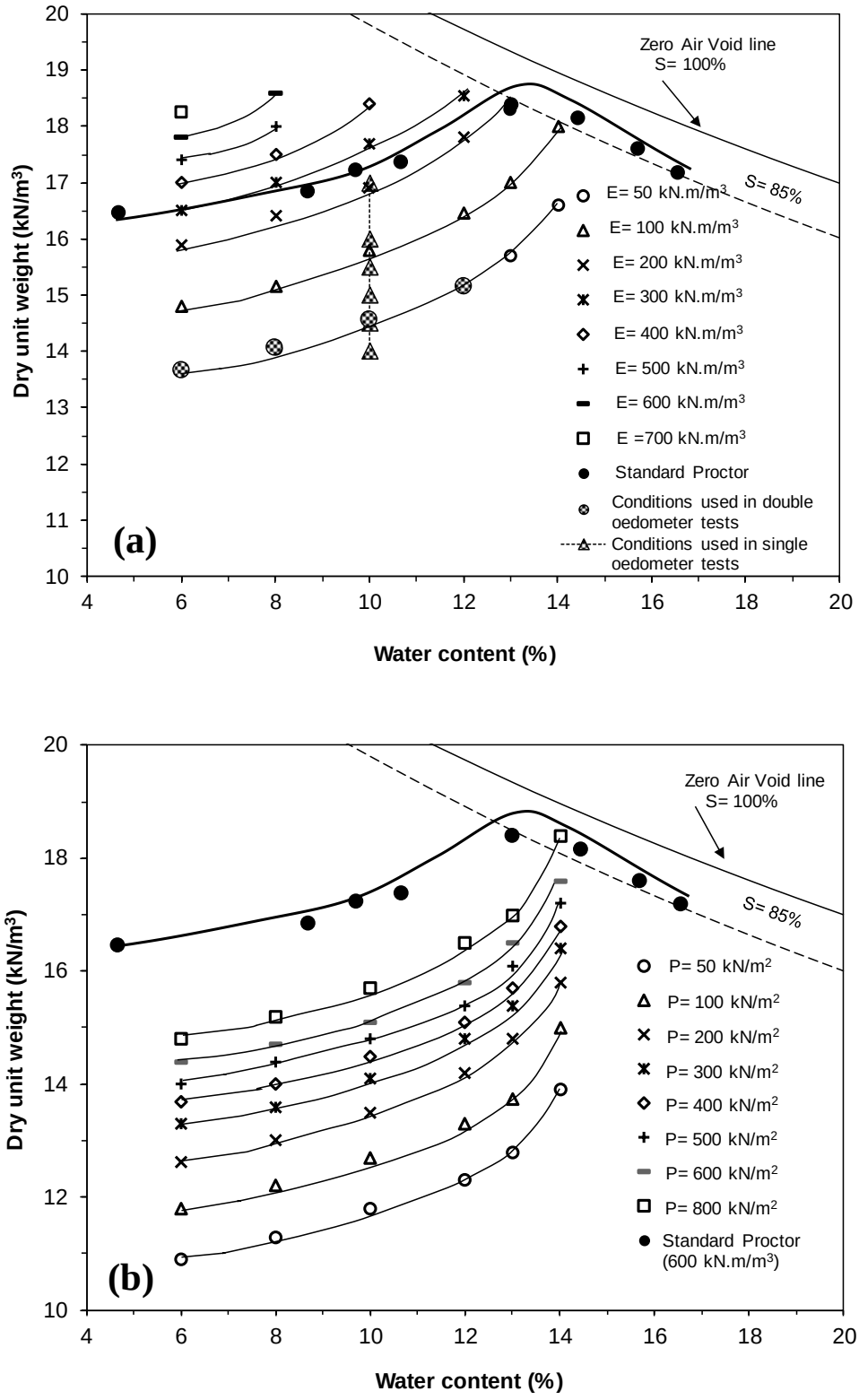

Figure 4.4 Static compaction curves using oedometer compaction mould (a) energies and dynamic compaction curves and (b) pressures and dynamic compaction curves

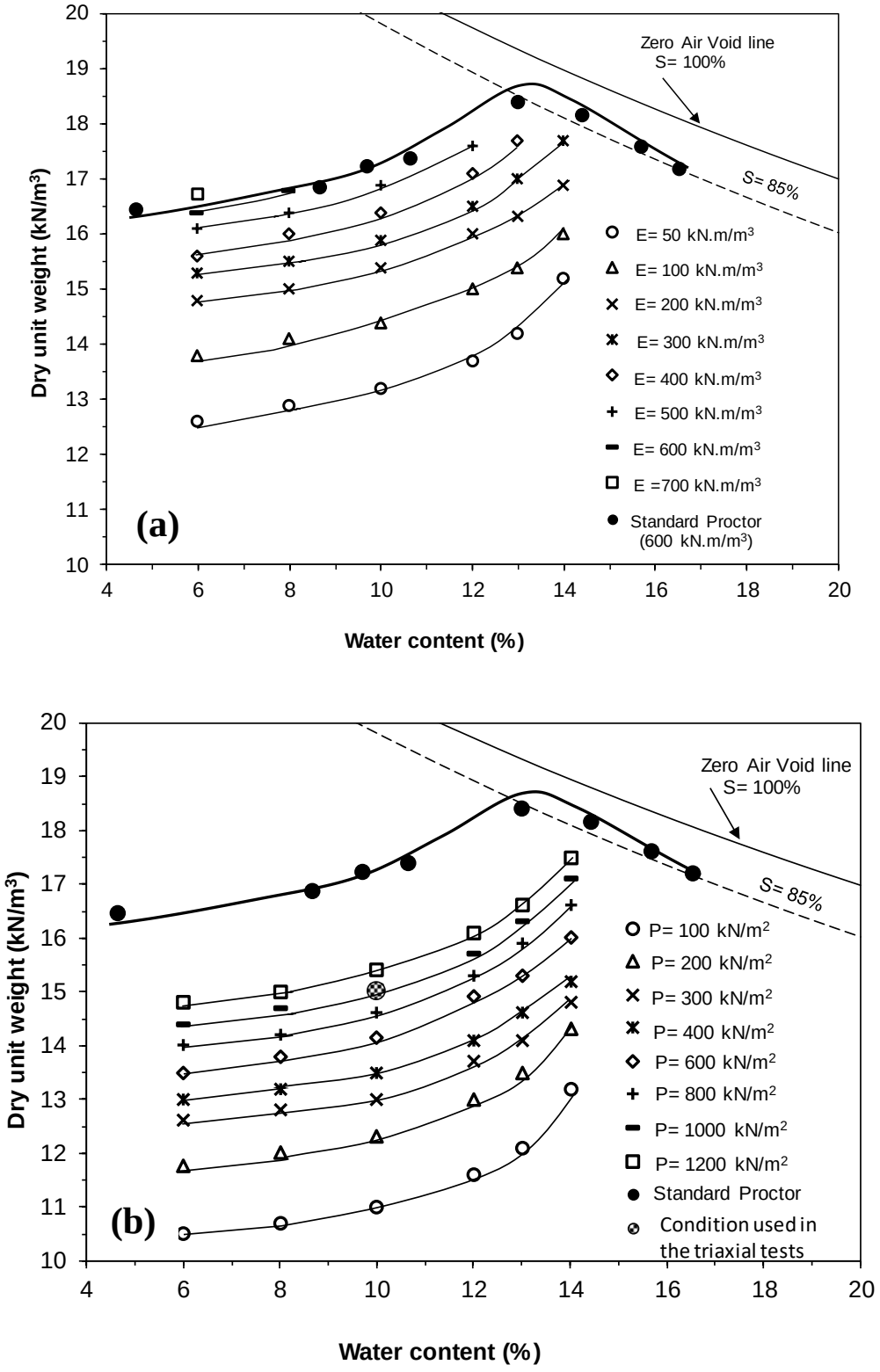

Figure 4.5 Static compaction curves using triaxial compaction mould (a) energies and dynamic compaction curves and (b) pressures and dynamic compaction curves

4.2.3.2 Effects of the mould size on the static compaction characteristics

To investigate the volume change and shear strength behaviour of the tested collapsible soil, laboratory tests were conducted on the identical specimens. These identical specimens were required in the laboratory tests such as wetting and triaxial tests to avoid the heterogeneity of the soil specimen and to ensure all results from different specimens can be related and comparable in order to establish the characteristics of the soil. Sivakumar and Wheeler (2000) and Wheeler et al. (2003) stated that the soil specimens must be homogeneous and uniform in soil composition, initial water content and initial dry density to obtain meaningful results for the accuracy of the analyses. Studies in the past have shown that the application of static pressure is effective for compacting unsaturated soil have clay partials (Hillel et al. 1998). In addition, it is easier to produce specimens with good repeatability and relatively uniform by static compaction than dynamic compaction (Bernhard and Krrynine 1952; Whitman et al. 1960; Gau and Olson 1971; Booth 1976; Reddy and Jagadish 1993; Xiujuan 2008; Zhemchuzhnikov et al. 2016). Therefore, static compaction was adopted for the preparing of the tested soil specimen in this study.

To study the effects of the compaction specimen size on the compaction pressure (yield stress), two sets of the moulds with two different inner diameters were used to prepare the specimens used in the static compaction tests. A mould of 100 mm in diameter was used to prepare the specimens for oedometer tests, and a mould of 50 mm in diameter was used to prepare the specimens for triaxial tests.

As presented in Figure 4.4a, for the same input energy per unit volume and water content value static compaction using oedometer compaction mould produces a much higher dry density than standard Proctor test. For example, at an input energy of 600 kN.m/m^3 and water content of 6 and 8%, the dry unit weight based on static compaction was found to be higher than the dry unit weight based on dynamic compaction by approximately 1.3 and 1.6 kN/m^3, respectively. This seems to indicate that the static compaction process was more energy efficient than the Proctor method when oedometer compaction mould was used. This is attributed to the higher energy losses during the impact of the falling weight in the Proctor test (Reddy and Jagadish 1993). In contrast, based on the test results in Figure 4.5a, the energy of the static compaction (600 kN.m/m^3) using triaxial compaction mould is a little less efficient than that of the standard

compaction, as the static compaction produces the relatively lower dry density as compared to dynamic compaction at the same energy and water content. This result is in agreement with those obtained by (Liangtong 2003; Walker 2004; Zhemchuzhnikov et al. 2016). A possible explanation for these results is attributed due to the ratio of specimen height to width for triaxial compaction mould was 2, whereas for the oedometer and standard Proctor moulds were about 0.2 and 1.2, respectively. Thus, during compaction tests, the friction between soil and the mould increases when the ratio of the height to the width of the compacted specimen increases.

Comparison of the effects of the mould size on the static compaction results over the considered range of compacted water content for various compaction pressure and energy are also shown in Figures 4.6 and 4.7, respectively. It appears from the test results that the two sizes of the compaction moulds used in this investigation have different effect on the dry unit weight of the soil and all soil specimens that were compacted using oedometer static compaction mould gave a higher value of the dry unit weight as compared to static compaction using the triaxial mould at the same compaction water content and compaction pressure or energy. In general, at the same compaction water content to achieve the same dry unit weight using a triaxial mould, need more than two times the value of energy which has applied using an oedeometer mould. This primarily due to the higher friction between the triaxial cylinder wall and the compaction soil caused higher energy dissipation compared to static compaction using oedometer mould.

It can be seen from Figures 4.6a to f, that a comparison of the two mould sizes results in each value of the compaction water content indicated that the smaller the value of applied pressure (100 kPa), the greater was the differences in the dry unit weight magnitudes (within the range 1.5 to 1.8 kN/m^3), whereas the smaller the difference between the dry unit weight magnitudes was shown at high applied compacted pressure (800 kPa).

Referring to Figures 4.7a to f, for each water content value, the noticeable differences in the dry unit weight magnitudes result from the two mould sizes were found to increase gradually from the minimum value (about 1.0 kN/m^3) at compaction energy of 50 $kN.m/m^3$ to highest value (nearly 2 kN/m^3) at the maximum value of energy (800, 600, 400, 300, 200 or 100 $kN.m/m^3$). Further, from the same figures (4.7a to f) for both mould sizes an increase in the dry unit weight was noted to be generally linear at a low

level of energy, with increasing the applied energy, the dry unit weight increased at the relatively lower rate.

The shapes of the increase in the dry unit weight as the applied pressure increase for both sizes of moulds at each value of compaction water content were found to be similar (see Figure 4.6a to f). Following a very similar trend (A trend line was plotted through the maximum data point) for an increase in the dry unit weight with compaction energy at each value of compaction water content were also observed in Figures 4.7a to f for both sizes of moulds.

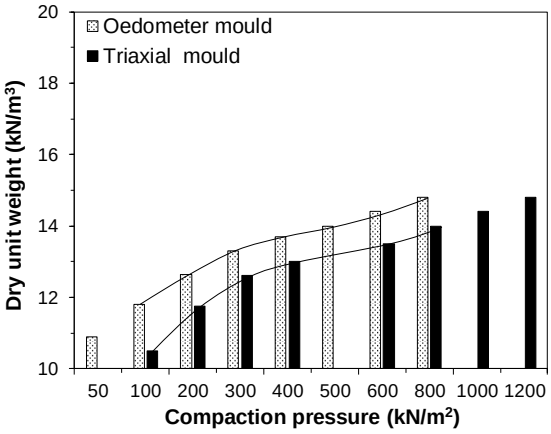

(a) 6% water content

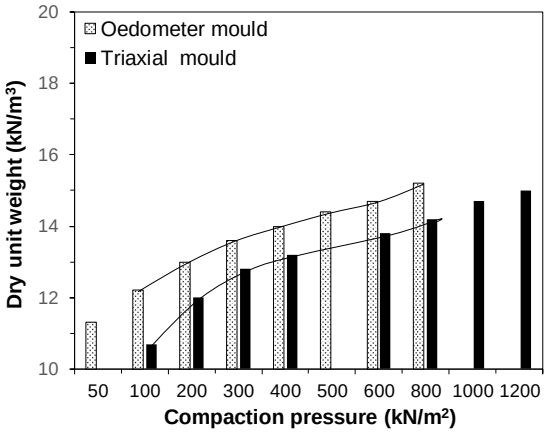

(b) 8% water content

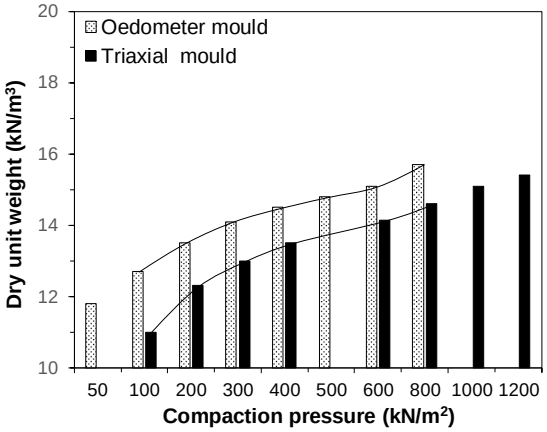

(c) 10% water content

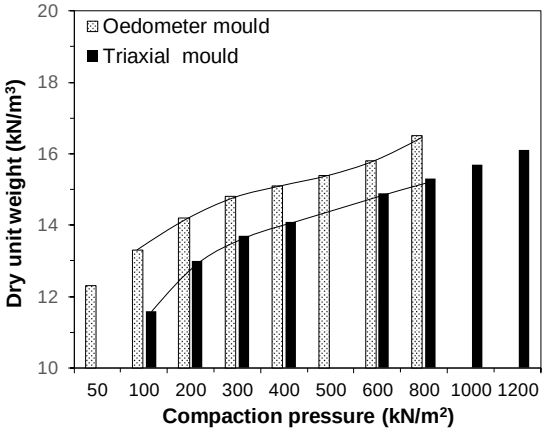

(d) 12% water content

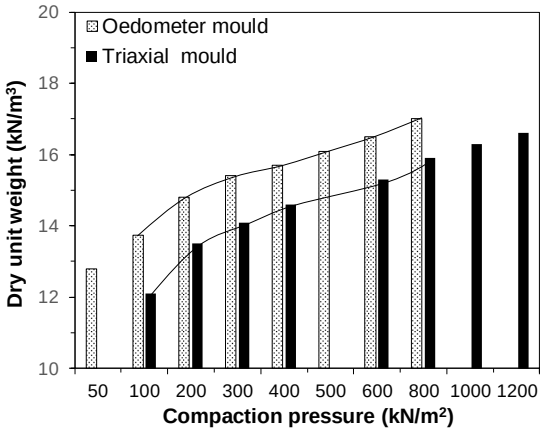

(e) 13% water content

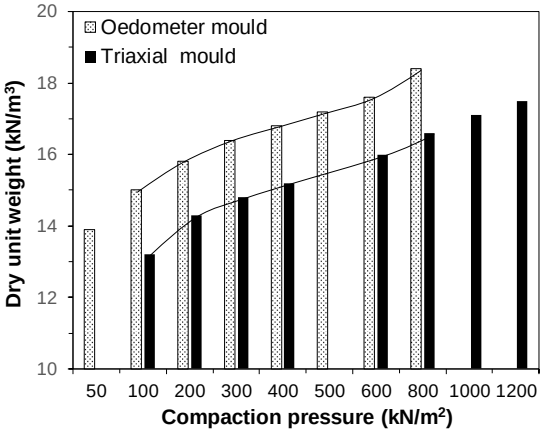

(f) 14% water content

Figure 4.6 Comparison of the effect of the mould size on the static compaction results for various compaction pressure

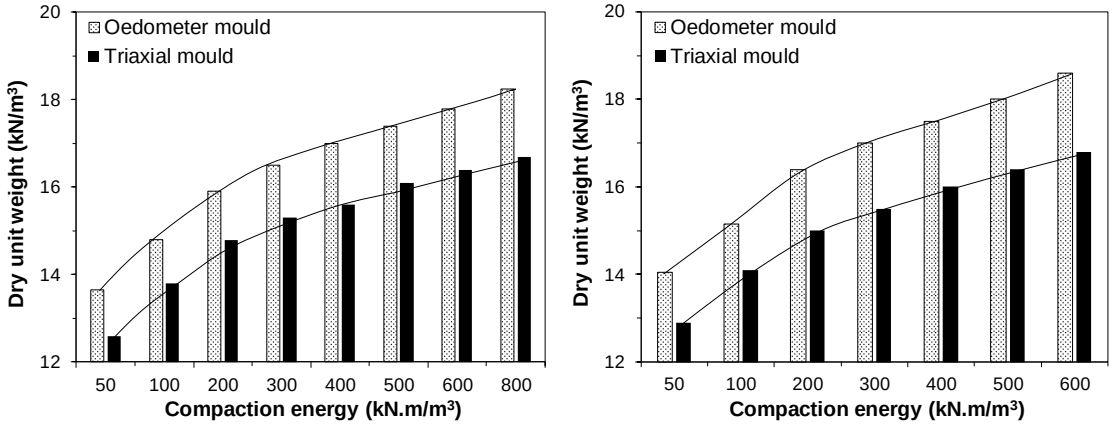

(a) 6% water content

(b) 8% water content

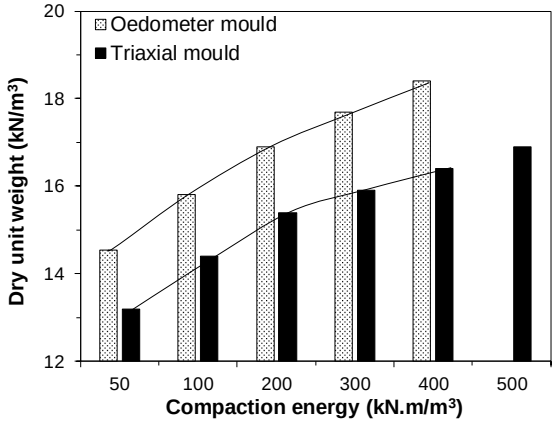

(c) 10% water content

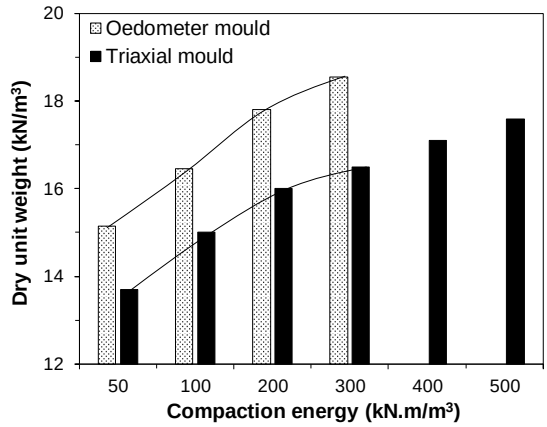

(d) 12% water content

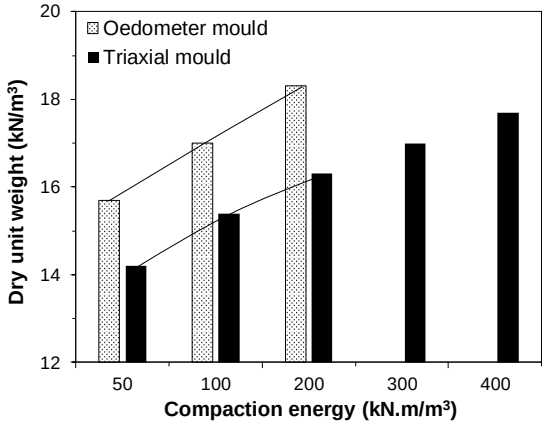

(e) 13% water content

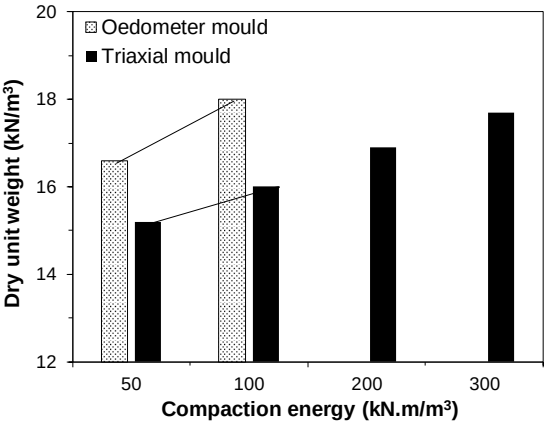

(f) 14% water content

Figure 4.7 Comparison of the effect of the mould size on the static compaction results for various compacting energy

4.3 Oedometer collapse tests

4.3.1 Experimental program

In order to study the influence of the initial conditions (compaction water content and dry unit weight) and overburden pressure on the characteristics of collapse, the double and single odometer collapse tests were performed on statically compacted specimens prepared at initial conditions selected based on the literature (see the initial conditions ranges that were included in Table 2.1).

The double odometer collapse tests were conducted using two identical specimens: one is tested at as-compacted water content, whereas the other specimen is loaded at saturation conditions. Figure 4.4a showed that at constant applied energy equal to 50 kN.m/m^3 a line passing through the desired water content of 6, 8, 10 and 12% on the dry side is necessary to produce the double odometer specimens' dry unit weight of 13.65, 14.05, 14.55 and 15.14 kN/m^3, respectively. The values of the degree of saturation for the fourth selected static compaction points are 17.6, 24.9, 33.7 and 44.3%, respectively. A loading pressure steps of 12.5, 25, 50, 100, 200, 400, and 800 kPa were selected. The difference between the equilibrium void ratios of the two specimens at each value of vertical stress was used to calculate the collapse strain.

For the single-oedometer collapse tests, a total of six tests were performed to cover a wide range of initial dry unit weights. Figure 4.4a shows a vertical line was drawn by passing through the desired water content (10%) on the dry side. The vertical line intersects three compaction curves (50, 100 and 200 kN.m/m^3) and introduces varying chosen dry unit weight (14, 14.5, 15, 15.5, 16 and 17 kN/m^3). The values of the degree of saturation for the six selected points are 50.0, 42.4, 39.1, 36.2, 33.4 and 30.9%, respectively. In single-oedometer collapse tests, the specimens were inundated under an applied pressure (overburden pressure) of 100 kPa. The deformation of the specimen induced by the addition of water was used to calculate the collapse strain.

4.3.2 Test results and discussion

4.3.2.1 Effects of the compaction conditions and yield stress on the double oedometer collapse strain

The double oedometer tests initial conditions and results are presented in Table 4.1. The relationship between the void ratio versus the vertical pressure is shown in Figure 4.8 with clear indicates that the curves of saturated specimens remained above the corresponding as-compacted compression curves under low vertical stress (less than 2.5 kPa). That occurs because a rebound effect is being experienced at the low level of stress. The percent swell was found to be less than 1%. However, as the applied stress increased, the as-compacted compression curves continued above the saturated compression curves.

Figure 4.9 presents the variations of collapse strain with the applied pressures. It is noticed from this figure that at 400 kPa un inundation vertical stress, the specimen compacted at low water content and low dry unit weight (specimen no.1) shows higher values of collapse strain (13.1%) than the specimen compacted at high water content and dry unit weight (specimen no. 4) (11.8%). From the same figure, it could be shown that the magnitude of collapse strain increased slightly with increasing inundation vertical stress lead to the maximum vertical strains occurs at a value of vertical stress (400 kPa) approximately equal to the compactive prestress (yield stress) and then decreased (see Table 4.1). Lin and Wang (1988), Lawton et al. (1991), Lawton et al. (1992) have found that the maximum collapse results in stress equal to the pressure induced in the soil by the application and removal of mechanical energy during compaction. Sun et al. (2007) stated that at stress lower than the yield stress, the soil structure remains largely unchanged and collapse increases slightly with the stress. However, the amount of collapse tends to reduce at vertical stress higher than the yield stress, due to the progressive breakage of the metastable structure of the soil skeleton under higher loads.

The test results are also presented in terms of water content versus dry unit weight and the maximum collapse strain at the yield stress (400 kPa) in Figure 4.10. It is clearly noticed that there is an inverse linear relationship between the collapse strain and both the initial water content and the dry unit weight. Such results completely corroborate the results of Lawton et al. (1992), Fredlund and Gan (1994) and Benchouk et al. (2013).

Table 4.1 Compaction conditions and collapse strain of the specimens for double-oedometer collapse tests

Specimen no.	Water content (%)	Dry unit weight (kN/m^3)	Void ratio	Degree of saturation (%)	Compaction pressure (kPa)	Applied pressures (kPa)							
						1.5	12.5	25	50	100	200	400	800
						Strain (%)							
1	6	13.65	0.91	17.6	385	+0.8	-2.1	-3.9	-6.5	-8.9	-11.4	-13.1	-11.7
2	8	14.05	0.85	24.9	410	+0.9	-1.3	-3.2	-5.6	-8.0	-10.6	-12.6	-11.2
3	10	14.50	0.79	33.4	417	+0.7	-1.6	-2.9	-5.2	-7.7	-9.9	-12.3	-10.4
4	12	15.14	0.72	44.3	413	+0.4	-0.9	-1.9	-3.9	-6.3	-9.0	-11.8	-9.1

+ Swell, - Collapse

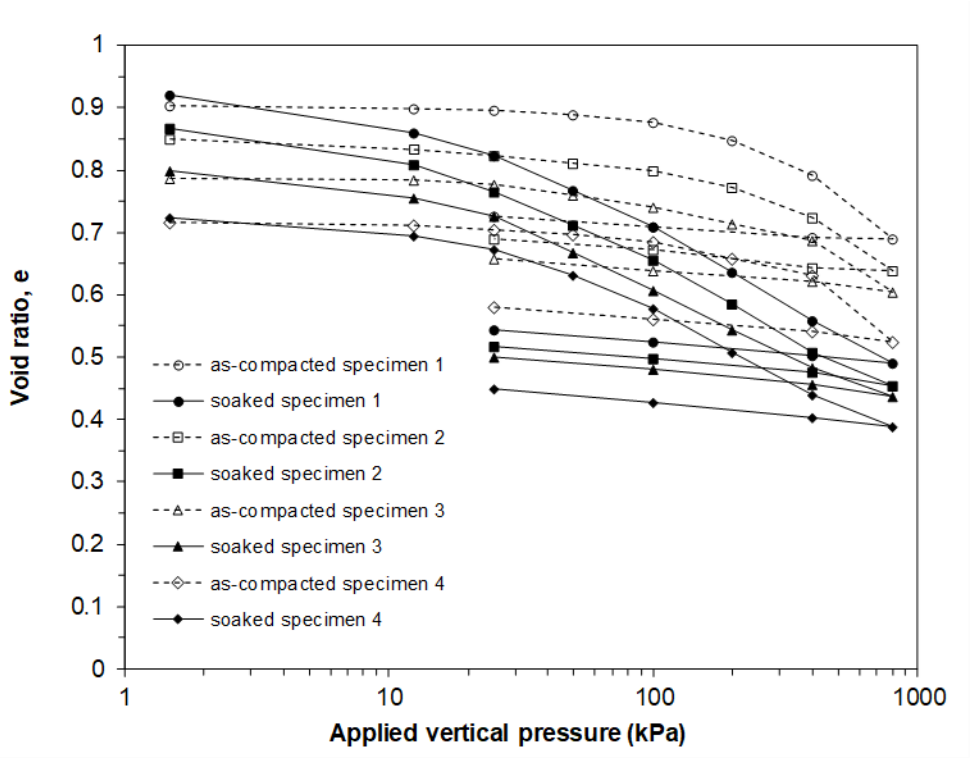

Figure 4.8 Vertical pressure versus void ratio in the double oedometer tests

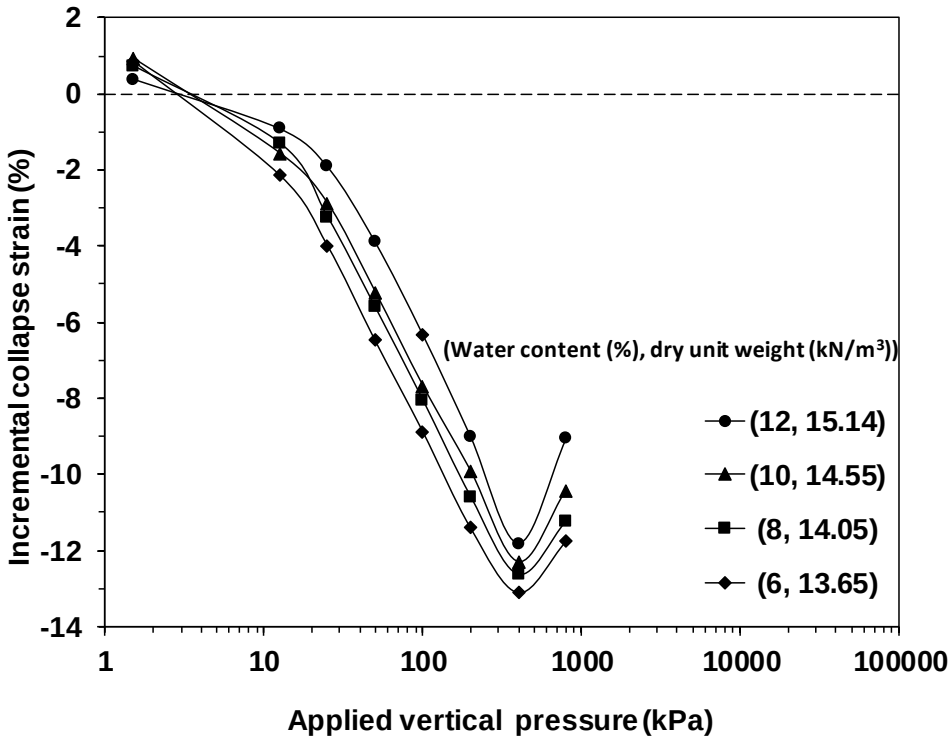

Figure 4.9 Vertical pressure versus collapse strain in the double oedometer tests

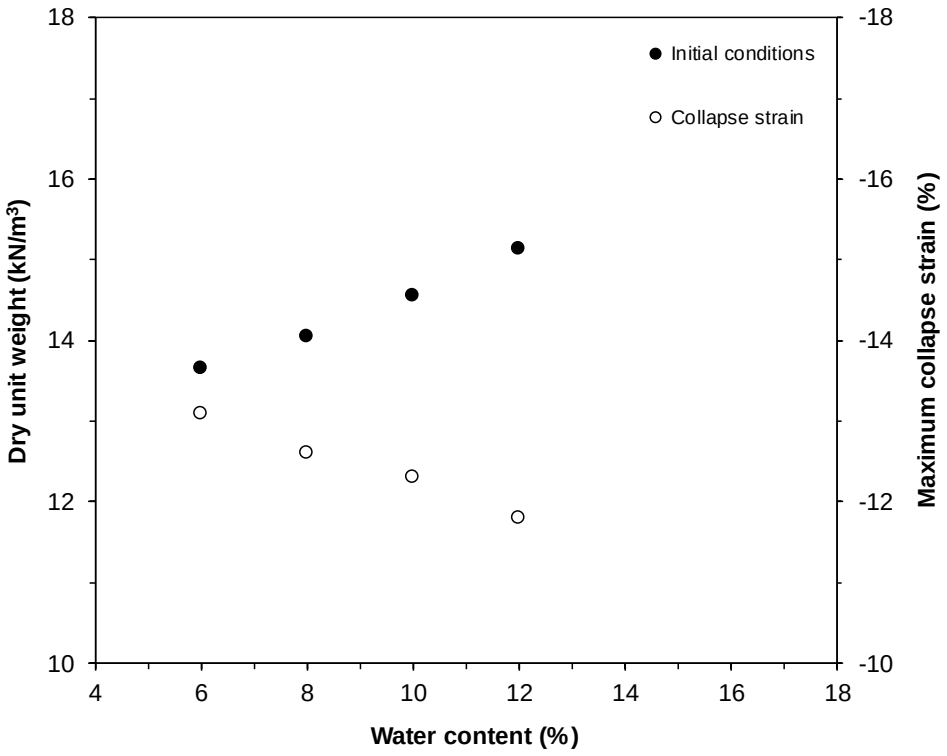

Figure 4.10 Water content versus dry unit weight and maximum collapse strain at the yield stress (400 kPa) and constant energy value (E = 50 kN. m/m^3) in the double oedometer tests

4.3.2.2 Effects of the compaction conditions on the single oedometer collapse strain

The single-oedometer collapse tests initial conditions and the collapse strain values are presented in Table 4.2. The influence of the initial dry unit weight on the amount of collapse is also presented in Figures 4.11, 4.12 and 4.13. Figure 4.11 shows the elapsed time versus collapse strain. It can be noted from this figure that the volume of the all specimens decreased significantly from the initial inundation stage to 10 minutes after inundation. Then, the volume decreased at a slower rate in the next 10-100 minutes then remained almost constant. It is important to mention that it seems that there were three distinct regions of collapse taking place. The first region occurred when the water flowed through the porous stone and entered the specimen. The second region happened when the water percolated through the specimen, which resulted in a reduction in capillary tension and a softening of the bonds. Finally, the third region resulted in some minor or negligible creep when the collapse was complete. Lawton et al. (1992) stated that collapse occurs quickly in oedometer samples inundated in the laboratory, usually

within several hours or less. From the same Figure (4.11), it can also see that, at the initial conditions of dry unit weight and water content respectively 17 kN/m^3 and 10%, the soil is liable to collapse (the recorded collapse is around 0.4%). With the same water content, and decreasing the initial dry unit weight to 16, 15.5, 15 and 14.5 kN/m^3, higher values of deformation were obtained. The highest value of the reduction in the void ratio was obtained at a unit weight of 14 kN/m^3 (13.7%).

Dry unit weight versus collapse strain was presented in Figure 4.12. The results indicate that the amount of collapse varies inversely and linearly with initial dry unit weight. It appears from all single oedometer collapse test results were included in Figure 4.13 that the initial dry unit weight has a considerable effect on the final void ratio of the specimen due to wetting at given water content and vertical stress. As the initial dry unit weight increased, means that the particles have better contact and the soil mass is more stable and therefore less collapse resulted in wetting. These relationships between the amount of collapse and the dry unit weight is in agreement with the observations made by Dudley (1970), Foss (1973), Pells et al. (1975), Popescu (1986), Lawton et al. (1989), Tadepalli and Fredlund (1991), Wheeler and Sivakumar (1995), Sivakumar and Wheeler (2000), Abbeche et al. (2007), Okonta (2012) and Thyagaraj et al. (2016).

Table 4.2 Compaction conditions and collapse strain of the specimens for single-oedometer collapse tests

Specimen no.	Water content (%)	Dry unit weight (kN/m^3)	Degree of saturation (%)	Compaction pressure (kPa)	Pressure at inundation (kPa)	Collapse strain (%)
1	10	17.0	50.0	1522	100	-0.4
2	10	16.0	42.4	992	100	-4.2
3	10	15.5	39.1	739	100	-6.1
4	10	15.0	36.2	567	100	-10.8
5	10	14.5	33.4	406	100	-12.5
6	10	14.0	30.9	305	100	-13.7

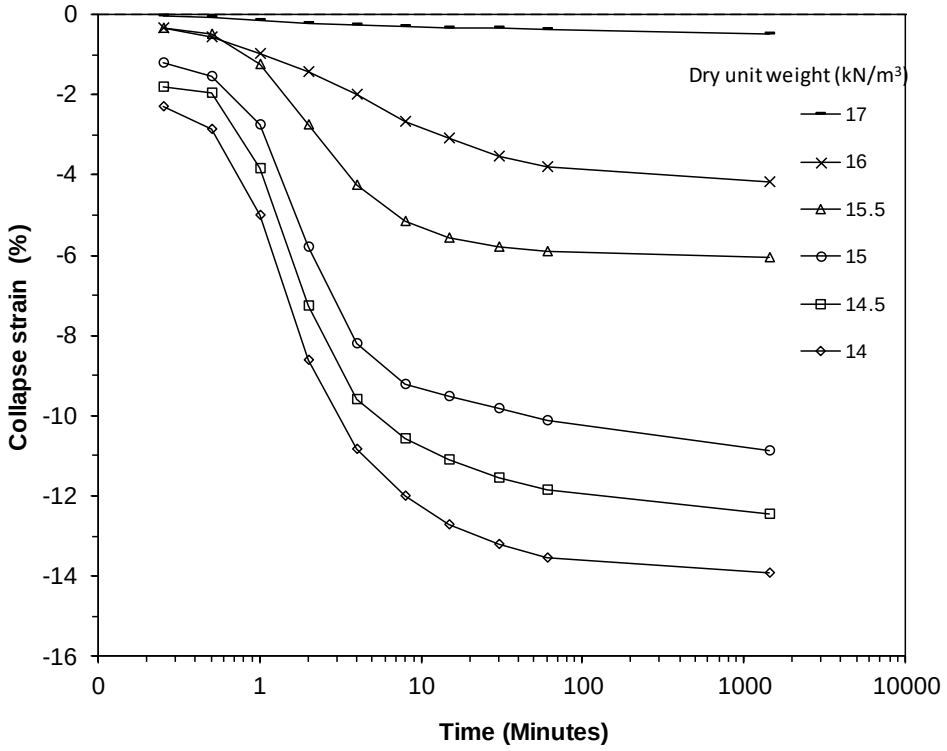

Figure 4.11 Elapsed time versus collapse strain in the single oedometer tests

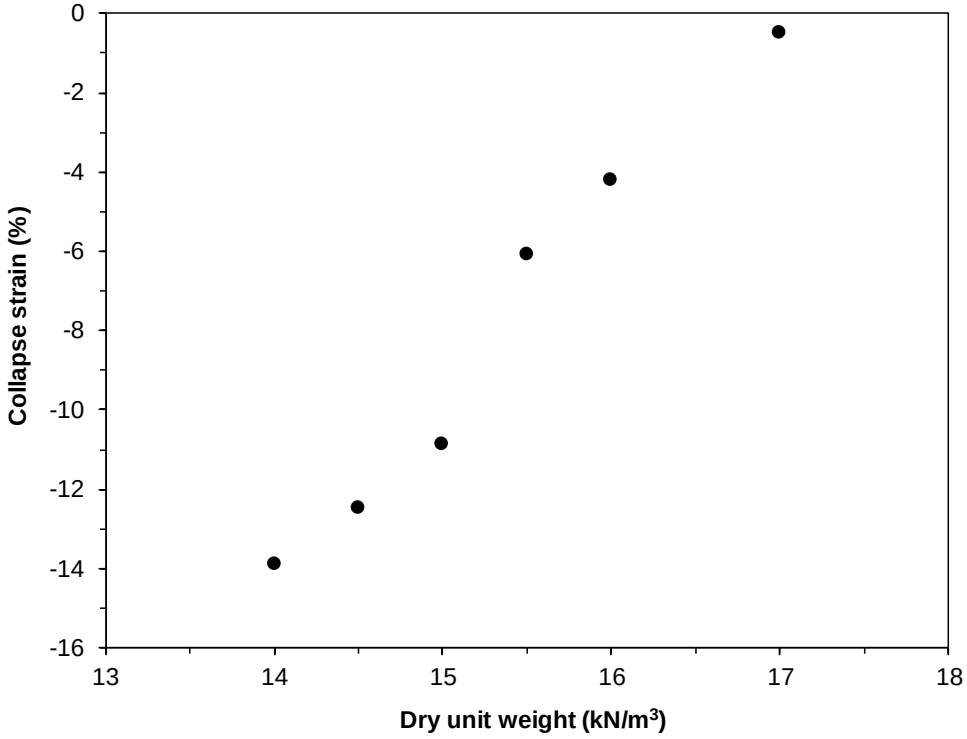

Figure 4.12 Dry unit weight versus collapse strain in the single oedometer tests

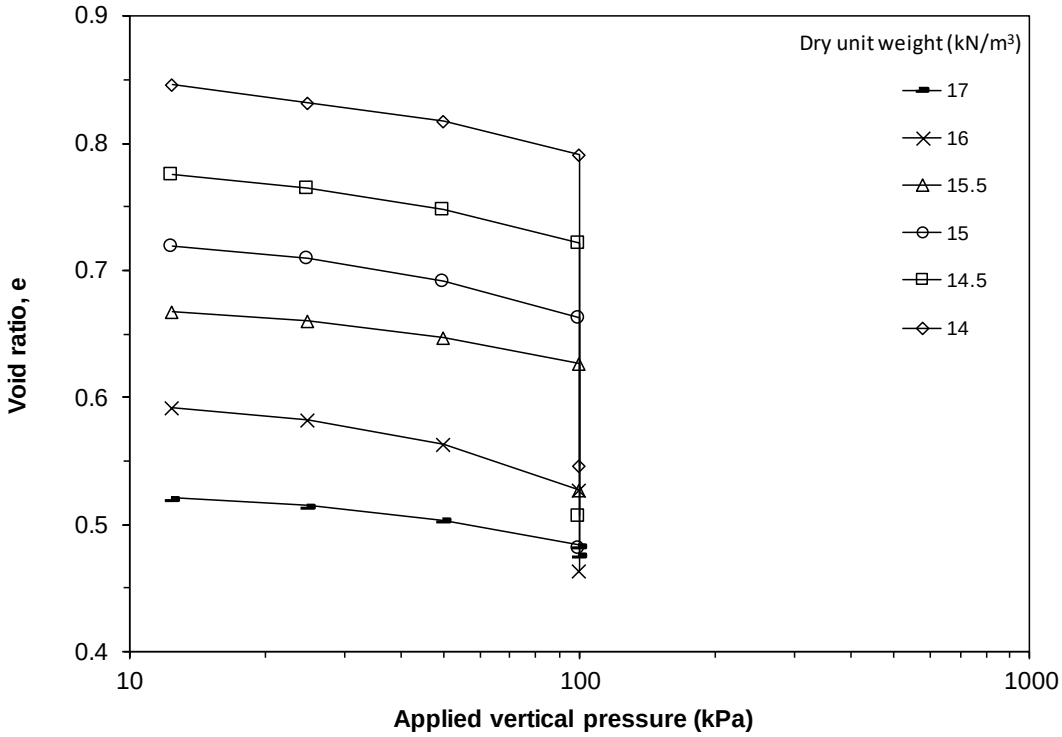

Figure 4.13 Void ratio versus applied vertical pressure in single oedometer tests

4.3.2.3 Comparison between double and single oedometer test results

Comparing the value of collapse strain that were obtained from double oedometer tests (specimens no.3) and that from single oedometer test (specimens no.5) at an initial water content of 10%, initial dry unit weight of 14.5 kN/m^3 and inundation vertical stress of 100 kPa, it can be noted that the value of collapse strain (about 8%) determined from double oedometer tests was found to be lower than the value of collapse strain (12.5%) form single oedometer test. Drnevich et al. (1988) have found that there can be significant differences in collapse potential obtained from single and double oedometer tests. They stated that the double oedometer procedure, which only measures the difference in deformation characteristics between partially and fully saturated specimens, assumes that the mechanism that produces collapse also produces this difference in deformation behaviour. This may not be similar to the case when the amount of volume change was measured when a partially saturated soil becomes submerged under constant stress. On the other hand, many researchers found that although the sequence of loading and wetting is different between the single and double oedometer methods, the two methods mostly agree in the collapse strain value (Booth 1976; Justo et al. 1984; Lawton et al. 1989; Lim and Miller 2004).

4.4 Concluding remarks

In this chapter, the impact of compaction water content and compaction mould size (oedometer and triaxial mould) on the static compaction curves of the selected soil in terms of applied pressure and applied energy were studied and compared. Additionally, the effects of the compaction parameters such as initial water content, initial dry unit weight and the overburden pressure on the amount of wetting collapse by using double and single oedometer collapse tests were studied. The following points emerged from the test results:

i. At the same value of the compaction pressure or energy, when the compaction water content increases, the dry unit weight increases. As a result, all the static compaction curves show an upward trend with increasing compaction water content. Similar findings were reported by other researchers (Booth 1976; Reddy and Jagadish 1993; Hafez et al. 2010; Doris et al. 2011; Zhemchuzhnikov et al. 2016).

ii. At the same water content and dynamic compaction energy, dynamic compaction tests produce a much lower and slightly higher dry unit weight as compared to the dry unit weight values produce from static compaction tests using oedometer and triaxial moulds, respectively.

iii. During compaction tests, the friction between soil and the mould increases when the ratio of mould height to width increases. Further, the effects of mould height to width reduces with increasing the applied compaction pressure and increase with increasing the applied compaction energy.

iv. The amount of collapse varies inversely and linearly with initial water content and dry unit weight. Similar findings have been reported by several researchers (Booth 1975; El Sohby and Rabbaa 1984; Lawton et al. 1989, 1992; Rabbi and Cameron 2014 and Rabbi et al. 2014a, b).

v. The amount of collapse strain increased with increasing the magnitude of the vertical overburden stress at which the soil was wetted up to yielding stress and then decreased, and the value of the yield stress was found to be equal to the static compaction pressure. The tests results agree well with the findings reported in the literature (Booth 1975; Witsman and Lovell 1979; Lawton et al. 1989, 1992).

CHAPTER 5

Effects of confining stress and suction on the volume change behaviour during wetting

5.1 Introduction

Measurement of suction and the associated volumetric strains of the soil are required for establishing the SWCC (Lynch et al. 2018). For collapsible soil, a decrease in suction usually results in a reduction in the volume of the soil. Therefore, measurements of water and total volume changes are extremely relevant for establishing the suction-degree of saturation SWCCs of the soil. Many properties of unsaturated soils, such as the shear strength and the volume change can be related to the amount of water present in the soil pores at any suction, which can be obtained from the SWCC (Fredlund et al. 2012).

The effects of a decrease in suction on the volume change of collapsible soil can be studied by carrying out the wetting process under isotropic stress conditions (Maatouk et al. 1995; Pereira and Fredlund 2000; Sun et al. 2007; Haeri et al. 2014; Garakani et al. 2015). The triaxial apparatuses provide greater flexibility in terms of the stress path that can be followed, and both total volume change and water volume change can be measured continuously and accurately. This is relatively important for measuring the collapsible soil specimens which experiences a significant total volume change due to changes in stress and suction (Fredlund and Rahardjo 1993; Pereira and Fredlund 2000).

Lu et al. (2010) stated that the best-fit equations were needed because many applications of the SWCC (such as SSCC) require it to be continuous for a wide range of suctions (i.e., 0 kPa to 1000000 kPa). Pereira and Fredlund (2000) stated that the best-fit modelling is essential for predicting the volume change behaviour of the compacted metastable-structured soils during the wetting-induced collapse. Leong and Rahardjo (1997) reviewed and evaluated the popular SWCC models and found out that the van

Genuchten (1980) and the Fredlund and Xing (1994) are the best SWCC models for a variety of soils.

The objectives of this chapter were; (*i*) to study the impact of confining stress and suction on the volumetric strain of the statically compacted specimens during the wetting process and (*ii*) to study the impact of confining stress on the wetting SWCCs and SWCCs best-fit model parameters of the soil studied.

This chapter is presented in several sections. The experimental program is recalled in section 5.2 (Test types II and III; section 3.5.5.2). Under test results and discussion (section 5.3), the experimental results involving the volume change of the statically compacted specimens was determined at several suctions and net confining stresses during the wetting processes are presented. The best-fit models such as van Genuchten (1980) and Fredlund and Xing (1994) are applied, and the effects of confining stresses on the wetting SWCCs and best-fit parameters are presented. The concluding remarks are presented in section 5.4.

5.2 Experimental program

The wetting tests under isotropic stress conditions were carried out on statically compacted soil specimens of the prepared soil at an initial water content of 10% and a dry unit weight of 15 kN/m^3 (see Table 3.5 in chapter 3 and Figure 4.5b in chapter 4). The diameter and the height of the specimens were 50 and 100 mm, respectively. Compaction of the specimens was carried out using a triaxial static compaction mould and a hydraulic compression device shown in Figure 3.6. The main components of the unsaturated triaxial device (HKUST-type) were used to carry out the tests are presented in section 3.5.5.4.1.

As shown in Figure 3.8 in chapter 3, there are two types of wetting tests under isotropic stress conditions were carried out (Test types II and III; section 3.5.5.2). Test type II was carried out to examine the volume change of a single specimen during step-wise suction reduction at applied confining stress of 100 kPa. Table 5.1 presents the details of the various stresses considered during wetting of the single specimen (tests type II). The states of the single specimen after wetting (The water content, the void ratio and the degree of saturation) were also included in this table. These results will be discussed in section 5.3.3 and 5.3.4.

In the test type III, in total twelve identical compacted specimens namely 1-12 were used. At each applied confining stress (100, 250, and 400 kPa), the suction of the specimens was reduced to 300, 100, 50, and 20 kPa. Table 5.2 presents the details of the various stresses considered during wetting of the multiple specimens (tests type III). The states of the twelve specimens after wetting (The water content, the void ratio and the degree of saturation) were also included in this table. These results will be discussed in section 5.3.3 and 5.3.4. Figure 5.1 shows the stress and suction paths for the wetting tests (Test type III).

The initial suction of the compacted soil specimens used for wetting tests under isotropic stress conditions and the water retention behaviour of the soil at high suctions were determined by a chilled-mirror dew-point potentiameter tests. For establishing the water retention behaviour at suctions greater than 500 kPa, specimens were prepared by static compaction method at different initial water contents and a constant dry unit weight of about 15 kN/m^3.

Table 5.1 Details of various stresses considered during wetting and state of the single specimen after wetting (tests type II)

Step no.	σ_3 (kPa)	u_a (kPa)	u_w (kPa)	$(\sigma_3 - u_a)$ (kPa)	$(u_a - u_w)$ (kPa)	w (%)	e	S_r (%)
1	650	550	50	100	500	10.3	0.712	38.5
2	550	450	50	100	400	10.6	0.705	39.8
3	450	350	50	100	300	11.0	0.699	41.6
4	350	250	50	100	200	11.5	0.684	44.6
5	250	150	50	100	100	13.6	0.650	55.4
6	200	100	50	100	50	17.4	0.590	78.2
7	155	55	50	100	5	19.6	0.530	98.1

Table 5.2 Details of various stresses considered during wetting and states of the twelve specimens after wetting (tests type III)

Specimen no.	σ_3 (kPa)	u_a (kPa)	u_w (kPa)	$(\sigma_3 - u_a)$ (kPa)	$(u_a - u_w)$ (kPa)	w (%)	e	S_r (%)
1	400	300	0	100	300	10.8	0.702	40.7
2	200	100	0	100	100	12.9	0.668	51.1
3	150	50	0	100	50	17.9	0.628	75.5
4	120	20	0	100	20	19.6	0.589	88.1
5	550	300	0	250	300	10.5	0.661	42.2
6	350	100	0	250	100	12.7	0.617	54.5
7	300	50	0	250	50	16.3	0.584	74.2
8	270	20	0	250	20	17.5	0.545	85.1
9	700	300	0	400	300	10.3	0.626	43.6
10	500	100	0	400	100	12.5	0.578	57.4
11	450	50	0	400	50	15.2	0.530	75.9
12	420	20	0	400	20	16.1	0.470	90.6

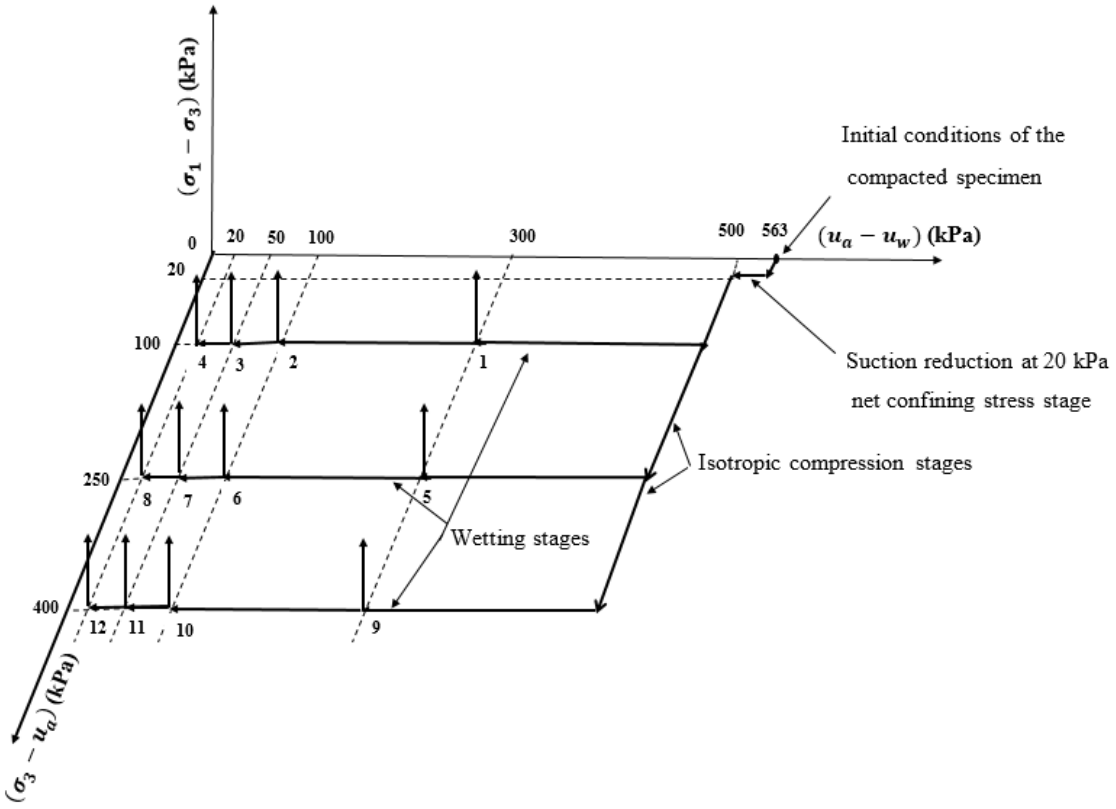

Figure 5.1 Stress and suction paths for the twelve specimens during wetting tests under isotropic stress conditions (Test type III)

5.3 Test results and discussion

5.3.1 Volumetric parameters (water, air and total volume) during wetting

Figure 5.2 presents the elapsed time versus the variation of water, air, and total volume change for the single specimen (Test type II) and the multiple specimens (Test type III) during the wetting processes at the net confining stress of 100 kPa. This figure was presented to compare the variation of the volumetric parameters of a single and multiple specimen at constant net confining stress during the wetting process. Figure 5.3 shows the elapsed time versus the variation of water, air, and total volume change for the twelve specimens (Test type III) during wetting processes at various net confining stresses (100, 250 and 400 kPa). Figure 5.3 was presented to study the effects of various net confining stresses on the volumetric parameters of multiple specimens during the wetting process. It appears from the test results that the time required to attain suction equilibrium

varied from 5 to 10 days. Oliveira and Marinho (2008) stated that the suction equilibration time during drying or wetting SWCCs tests depends upon the difference between the initial and target suction value.

The experimental results in Figures 5.2 and 5.3 indicated that wetting process results in an increase in the water volume of the specimens, as the volume of air in the pore space decreases due to pore collapse. Studies in the past have shown that any type of soil compacted at dry-of-optimum conditions may develop a collapsible fabric or metastable structure (Tadepalli and Fredlund 1991; Lawton et al. 1992; Houston et al. 1993). Fredlund and Rahardjo (1994) and Almahbobi et al. (2018) stated that the meta-stable structure of collapsible soils is associated with the cementation provided by the fine-grained soil fractions at the inter-particle contacts of coarse fractions in the soils. The cementation at the inter-particle contacts weakens with a decrease in soil suction. The collapse in collapsible soils is due primarily to a decrease in the shear strength at interparticle level.

It can be seen from Figure 5.2 that at constant confining stress (100 kPa) and at the same suction values (300, 100 and 50 kPa) the single specimen generally shows larger water, air, and total volume changes as compared to these values result from the multiple specimens at the end of wetting stages. Figure 5.3 shows that at equilibrium for each value of suction (300, 100, 50 and 20 kPa), with an increase in the confining stress the total volume change increased, and the water volume changes decreased. Further, at each applied value of confining stress, the amount of water, air and total volume changes during the wetting process were found to be greater when the suctions were reduced to the lower values.

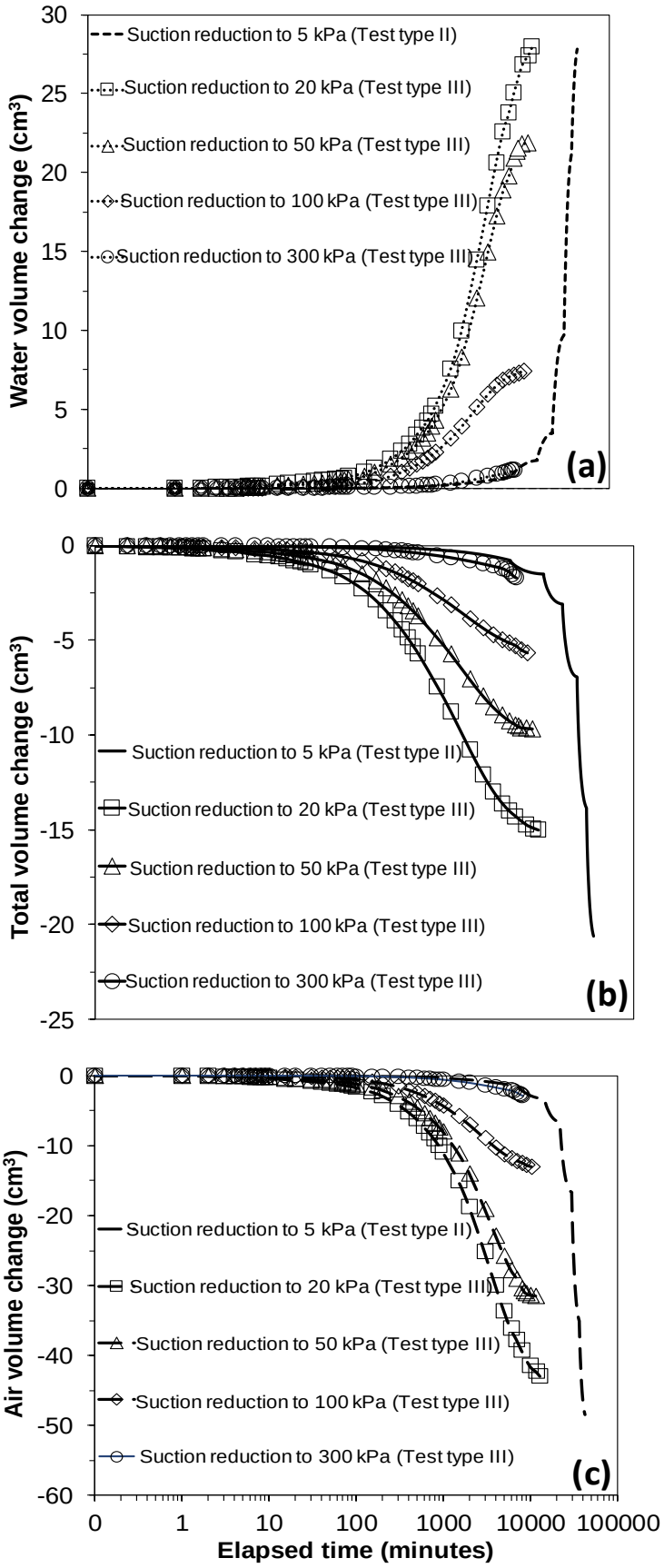

Figure 5.2 (a) Water, (b) total, and (c) air-volume change versus elapsed time for single and multiple specimens during wetting processes at confining stress of 100 kPa

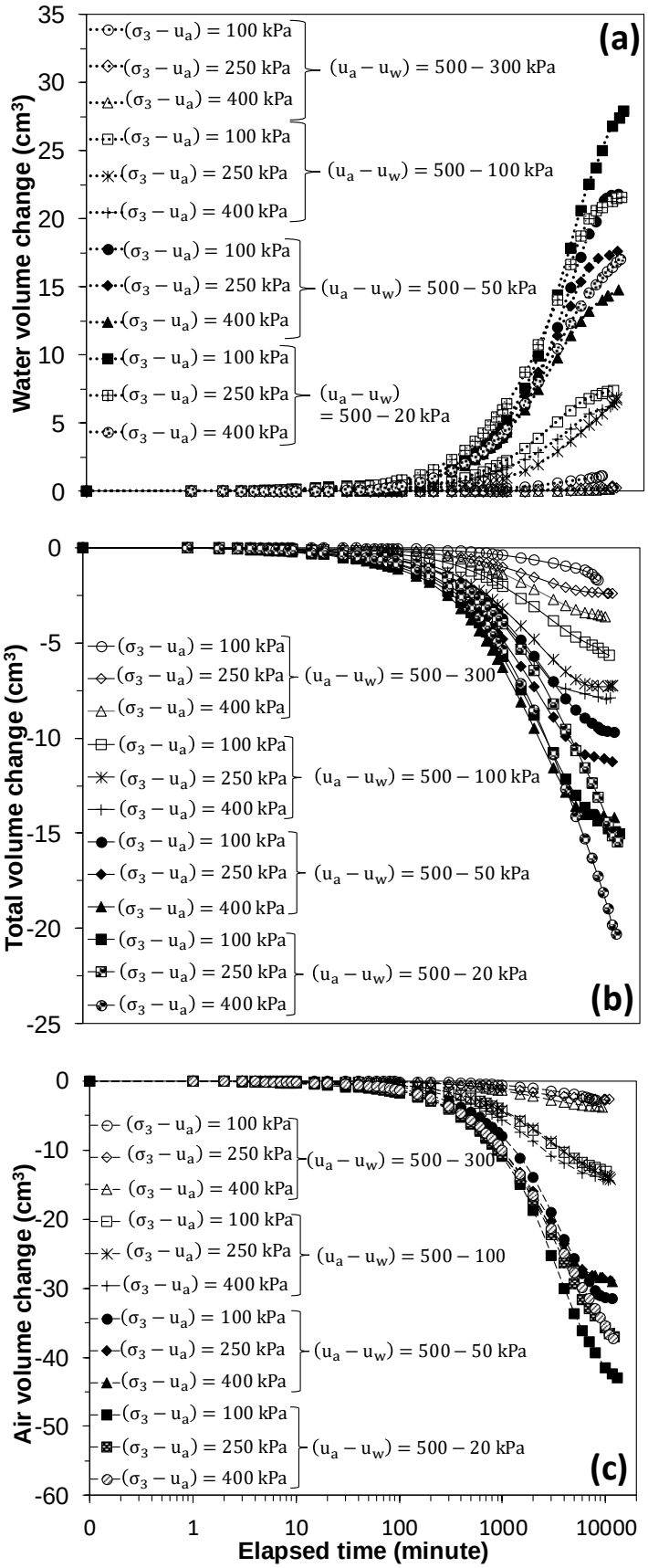

Figure 5.3 (a) Water, (b) total, and (c) air-volume change versus elapsed time for twelve specimens during wetting processes at confining stresses of 100, 250 and 400 kPa

5.3.2 Calculation of volume-mass soil properties

The mechanical behaviour of compacted soil is strongly dependent upon the volume-mass soil properties, namely, the void ratio, the water content, and the degree of saturation (Fredlund and Morgenstern 1977). The state surfaces (i.e., water content, void ratio and degree of saturation versus stress state variable relationships) are the constitutive relationships required for the volume change behaviour of a collapsing soil (Pereira and Fredlund 2000). The water content (w), the void ratio (e) and the degree of saturation (S_r) of the specimens tested at the final of the wetting stages were calculated based on the volume change measurements (the water volume change (ΔV_w) inferred from specimen water-change measurements, and the total volume change (ΔV) inferred from specimen volume-change measurements).

The volumetric strain (ε_v) was calculated based on the change in the total volume of the specimen (ΔV) and the initial volume of the compacted specimen (V_0= 196 cm^3) and expressed as a percentage as follows:

$$\varepsilon_v(\%) = -\frac{\Delta V}{V_0} \tag{5.1}$$

5.3.3 Effects of confining stress and suction on volume change

Figures 5.4 and 5.5 show the suction versus volumetric strain and void ratio, respectively, for the single and the multiple specimens at confining stresses of 100, 250, and 400 kPa during the wetting processes. Figures 5.5 also presents the chilled-mirror dew-point potentiometer (WP4C) test results at different water content values (different suctions) and at a constant void ratio of 0.732.

The test results presented in Figure 5.4 show that at any applied suction (300, 100, and 50 kPa) and at constant net confining stress of 100 kPa, the volumetric strain obtained from Test series II (single specimen) was greater than that obtained from Test series III (multiple specimens). This noticeable difference in the volumetric strain during the step-wise wetting processes can be explained by the effect of the continuous and the quick softening of cementing bonds in a metastable soil structure of the single and the multiple

specimens, respectively. However, the findings of the current study do not support the previous research by Maswoswe (1985) who stated that the faster the wetting test, the greater the collapse of the specimens subjected at equal confining stresses.

It is also noted from Figure 5.4 that at any applied suction, the volumetric strain due to collapse was greater for the specimen with a higher applied net confining stress. This is attributed to the fact that as confining stress increases, caused more slippage between particles (Maswoswe 1985). Sun et al. (2007) stated that the volume changes due to a suction decrease mainly depends on the mean net stress and yield stress. At applied stress lower than the yield stress, the soil structure remains largely unchanged and collapse increases slightly with the mean net stress, then the maximum collapse occurs when the mean net stress equals the initial yielding stress (applied compaction pressure to prepare specimen).

It can be seen from Figures 5.5 that the specimens exhibited reductions in the void ratio due to the applied confining stresses at the constant suction of 500 kPa. Further, the test results showed that at any applied suction, the reductions in the void ratio during the wetting process was greater for the specimen with a higher applied confining stress.

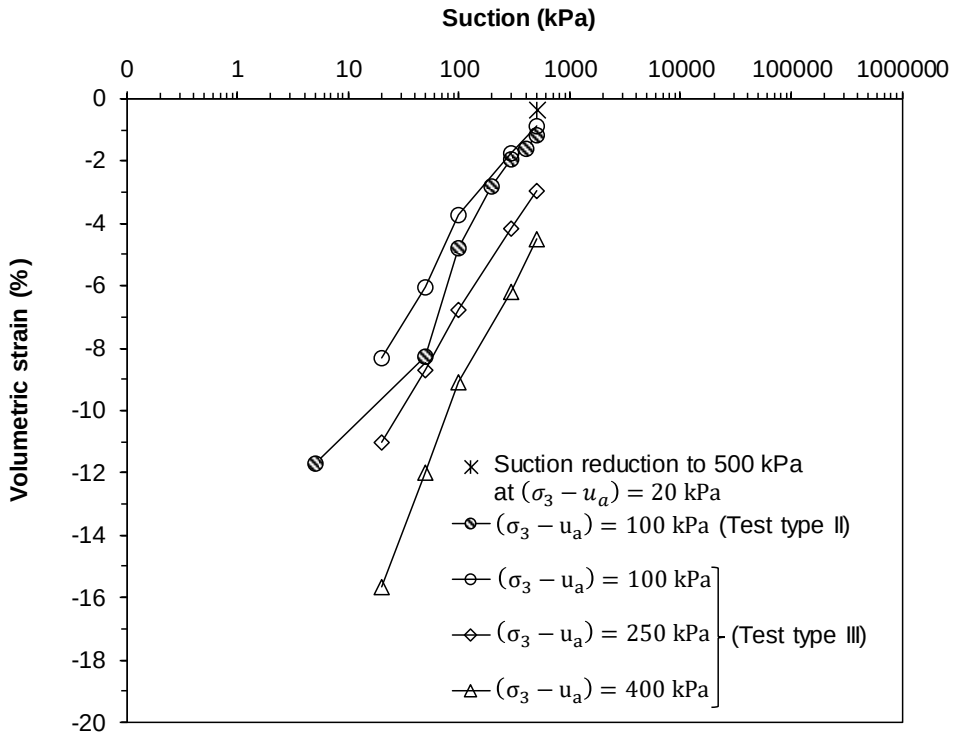

Figure 5.4 Variation in volumetric strain with suction for single and multiple specimens at various confining stresses during the wetting process

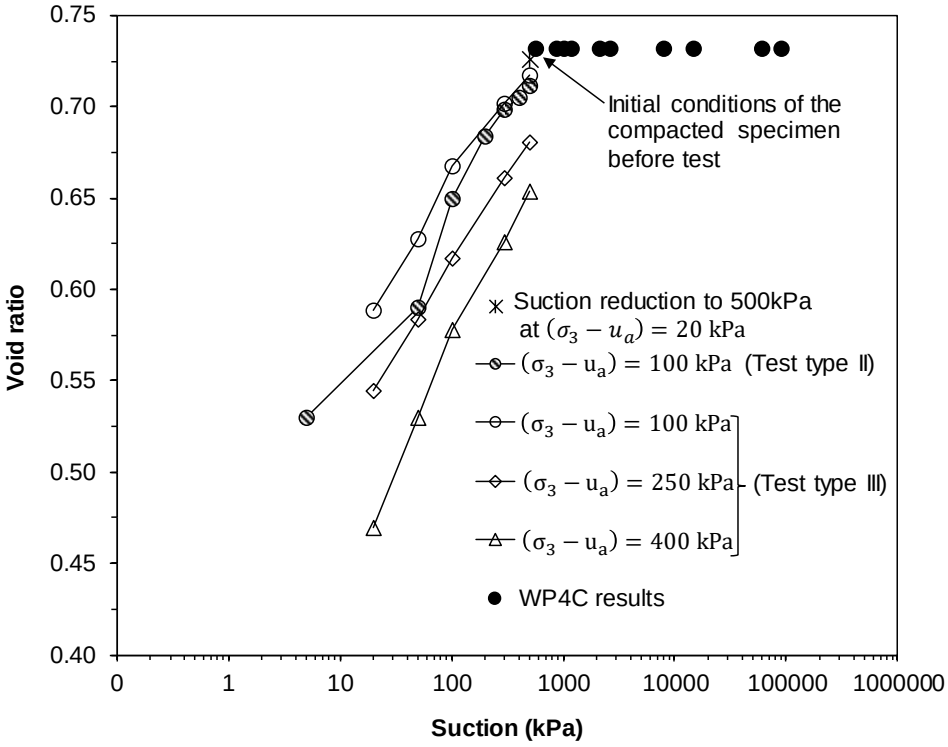

Figure 5.5 Variation in void ratio with suction for single and multiple specimens at various confining stresses during the wetting process

5.3.4 Water content and degree of saturation SWCCs

The test results for the water absorption of the soil specimens (Tests type II and III) are shown in Figures 5.6 and 5.7 in terms of water content. The water content value (the ratio of the mass of water to the mass of soil solids as a percentage) was determined based on the water volume change measurements. Figures 5.8 and 5.9 show the test results for the water absorption in terms of the degree of saturation. The degree of saturation value (the ratio of the volume of water to the volume of soil voids as a percentage) was calculated based on the volume change measurements (water and total volume change). The test results for the water absorption in terms of the effective degree of saturation (An effective degree of saturation is defined as the volume of the freely available water partially filling the soil macroporosity (Alonso et al. 2010), i.e. the water available between the AEV and the residual value) are shown in Figure 5.10 and 5.11. The effective degree of saturation value was calculated based on the volume change measurements and with the residual degree of saturation (S_{res}) as 6% from Equation 5.2. The WP4C results are presented in Figures 5.6 to 5.11 to establish the SWCCs for a large range of suction. Fredlund and Rahardjo (1993a) stated that in order to measure a wide range of suction, a combination of two or more techniques might be used. The data points in Figures 5.6 to 5.11 represent the actual experimental test results, whereas the lines represent the best-fit curves based on van Genuchten (1980) model in Figures 5.6, 5.8 and 5.10 and Fredlund & Xing (1994) model in Figures 5.7, 5.9 and 5.11. Table 5.1 and 5.2 present the w and S_r results for test series II and III. The SWCC models and model parameters are presented in the next section.

$$S_e = \frac{S_r - S_{res}}{1 - S_{res}} \tag{5.2}$$

A slight difference in the water content, the degree of saturation and the effective degree of saturation values between the single specimen (Test type II) and the multiple specimens (Test type III) at the applied net confining stress of 100 kPa and at the same suction value can be noted in Figures 5.6 to 5.11 and tables 5.1 and 5.2. These differences might be attributed as mentioned before to the effect of the continuous and the quick

softening of interparticle bonding in a metastable soil structure during the wetting process of the single and the multiple specimens, respectively.

The test results presented in Figures 5.6 and 5.7 and tables 5.1 and 5.2 showed that, at any applied suction, the magnitude of the water content was greater for the specimen subjected under lower applied net confining stress. For example, the magnitudes of the water contents at the suction of 20 kPa were found to be 19.6, 17.5 and 16.1% at net confining stress of 100, 250 and 400 kPa, respectively. This can be attributed to the greater volume of the specimen's voids subjected under low net confining stress during wetting as compared to the specimen was saturated under high confining stress. Similar findings were reported by other researchers (e.g., Vanapalli et al. 1996; Ng and Pang 2000; Oh and Lu 2014). Additionally, the test results indicated that the variations of the water content due to the applied net confining stress at higher suction were found to be not very significant, whereas, the effect of the net confining stress on the specimens' water content at lower suctions were found to be significant.

The results presented in Figures 5.8 to 5.11 and tables 5.1 and 5.2 showed that the variations of the degree and effective degree of saturation values with the net confining stress at each value of suction were not significant. For the matric suction range, the maximum difference in the degree and effective degree of saturation due to the applied confining stresses were found to be about 6% and 0.06, respectively.

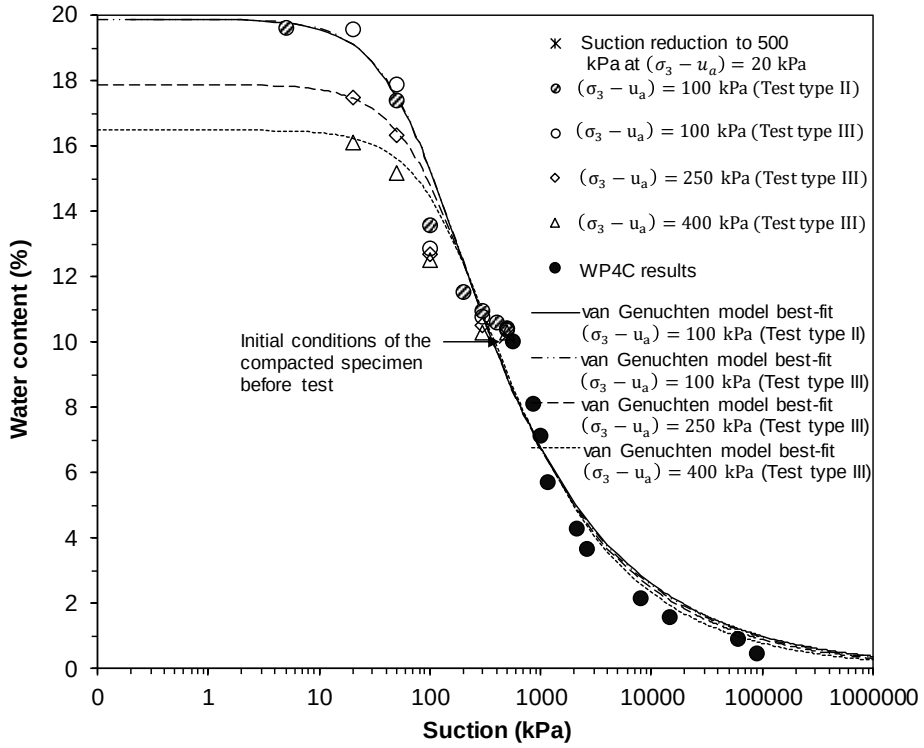

Figure 5.6 Suction-water content SWCCs at various confining stresses during the wetting process (Best fit by van Genuchten model)

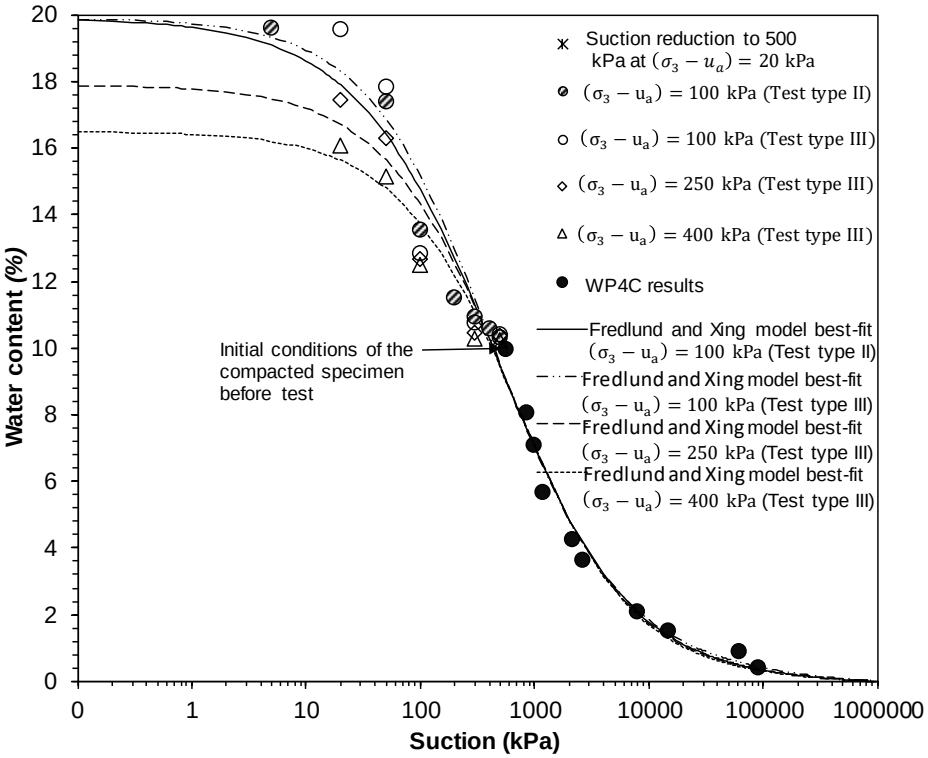

Figure 5.7 Suction-water content SWCCs at various confining stresses during the wetting process (Best fit by Fredlund and Xing model)

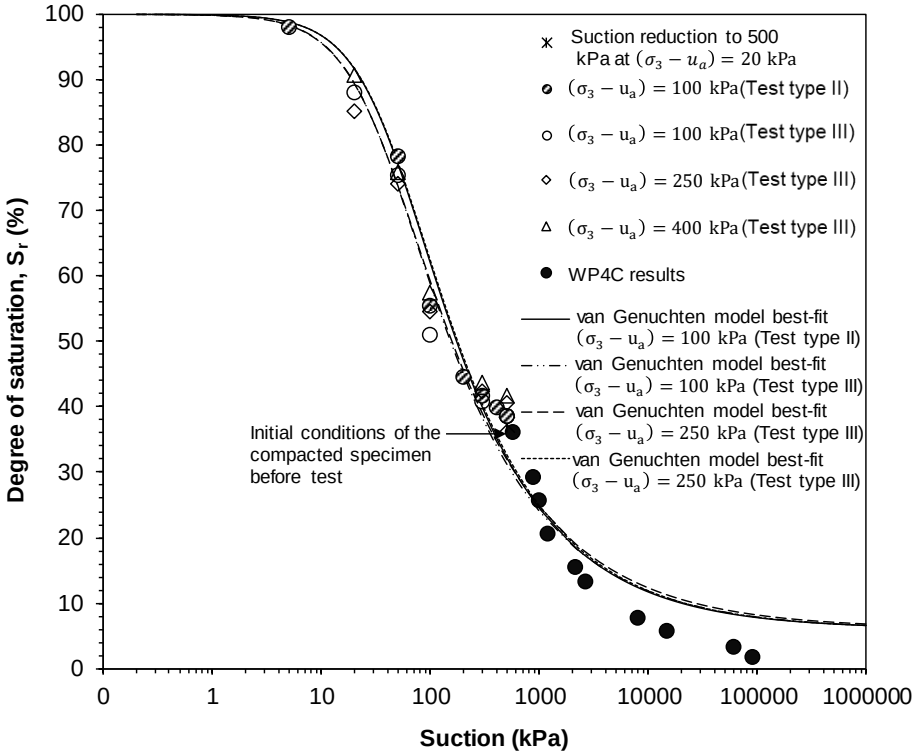

Figure 5.8 Suction-degree of saturation SWCCs at various confining stresses during the wetting process (Best fit by van Genuchten model)

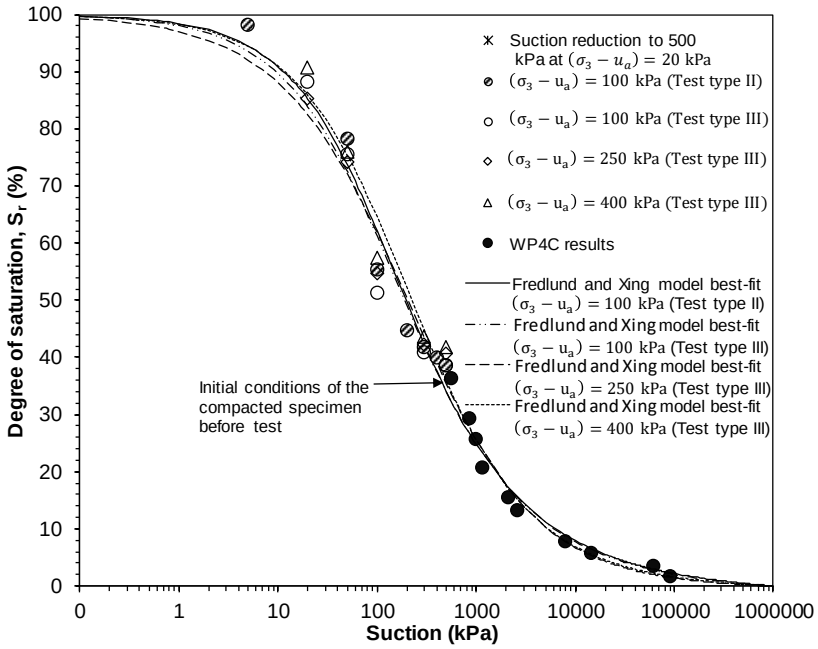

Figure 5.9 Suction-degree of saturation SWCCs at various confining stresses during the wetting process (Best fit by Fredlund and Xing model)

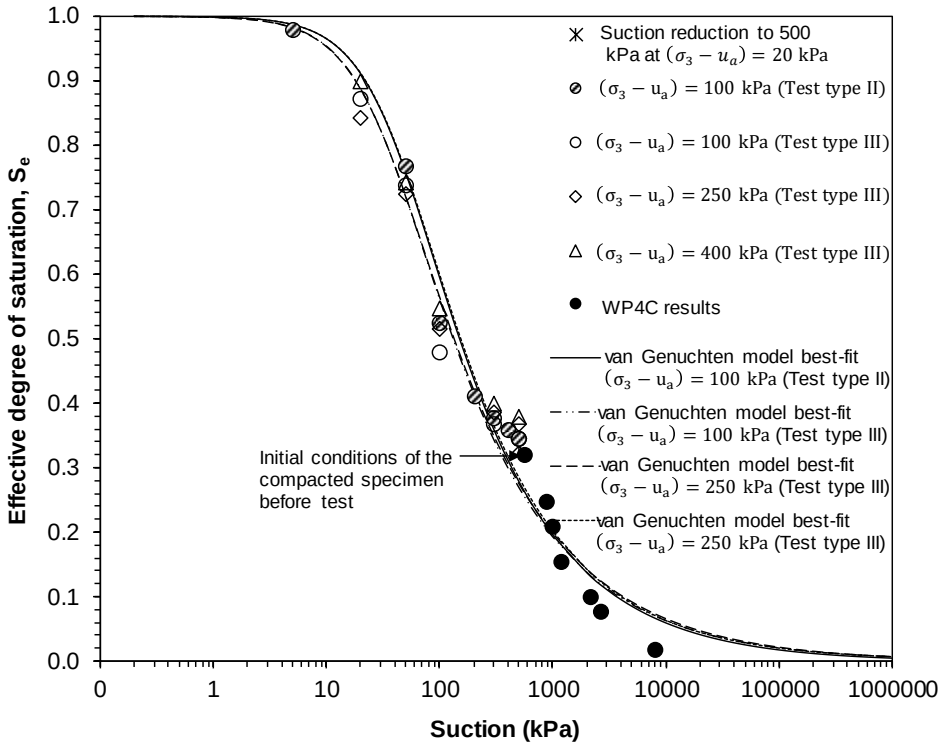

Figure 5.10 Suction-effective degree of saturation SWCCs at various confining stresses during the wetting process (Best fit by van Genuchten model)

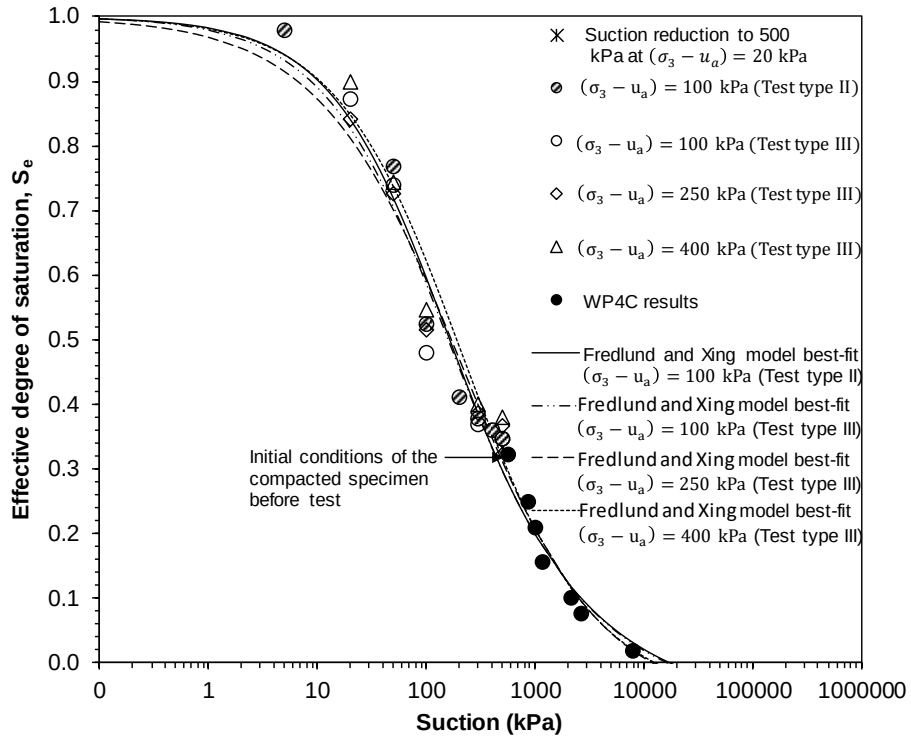

Figure 5.11 Suction-effective degree of saturation SWCCs at various confining stresses during the wetting process (Best fit by Fredlund and Xing model)

5.3.5 SWCC models and model parameters

The SWCCs in terms of water content, the degree of saturation and effective degree of saturation at various net confining stresses shown in Figures 5.6 to 5.11 were best fitted by van Genuchten (1980) and Fredlund and Xing (1994) equations. To obtain a closer fit to the experimental data, the model parameters were determined using the least squares method. A non-linear regression analysis was performed using the "solver" add-in in Microsoft Excel. The best-fit parameters were obtained by minimizing the objective function with respect to the sum of the squared residuals. The best-fit parameters for each model resulted in the minimums the sum of the squared residuals value.

The equations for SWCC in terms of water content (w), the degree of saturation (S_r) and effective degree of saturation (S_e) based on van Genuchten (1980) model can be expressed as follows:

$$w = \frac{w_s}{\{1+[\alpha(u_a-u_w)]^n\}^{(1-1/n)}} \tag{5.3}$$

$$S_r = S_{res} + \frac{(1-S_{res})}{\{1+[\alpha(u_a-u_w)]^n\}^{(1-1/n)}} \tag{5.4}$$

$$S_e = \left\{\frac{1}{1+[\alpha(u_a-u_w)]^n}\right\}^{(1-1/n)} \tag{5.5}$$

where w_s is the saturated soil water content, α is a fitting parameter primarily related to the inverse of air-entry value and typically varies between 0 and 0.5 kPa^{-1} (Lu and Likos 2004), and n is a dimensionless parameter reflecting the pore size distribution of a soil, and its value typically falls in the range of 1.1–8.5 (Lu and Likos 2004).

Based on the assumption that the shape of SWCC is dependent on the pore-size distribution of soil, Fredlund and Xing (1994) proposed the best-fit equations for SWCC as applicable to the full suction range (Equations 5.6 to 5.8). Equations 5.6, 5.7 and 5.8

can be used to best-fit SWCCs in terms of w, S_r and S_e and further determine the air expulsion value (AExV) and residual degree of saturation (S_{res}).

$$w = \left[1 - \frac{\ln\left(1+\frac{(u_a-u_w)}{(u_a-u_w)_{res}}\right)}{\ln\left(1+\frac{10^6}{(u_a-u_w)_{res}}\right)}\right] * \frac{w_s}{\left\{\ln\left[e+\left(\frac{(u_a-u_w)}{a}\right)^n\right]\right\}^m} \tag{5.6}$$

$$S_r = \left[1 - \frac{\ln\left(1+\frac{(u_a-u_w)}{(u_a-u_w)_{res}}\right)}{\ln\left(1+\frac{10^6}{(u_a-u_w)_{res}}\right)}\right] * \frac{1}{\left\{\ln\left[e+\left(\frac{(u_a-u_w)}{a}\right)^n\right]\right\}^m} \tag{5.7}$$

$$S_e = \left\{\left[1 - \frac{\ln\left(1+\frac{(u_a-u_w)}{(u_a-u_w)_{res}}\right)}{\ln\left(1+\frac{10^6}{(u_a-u_w)_{res}}\right)}\right] * \frac{1}{\left\{\ln\left[e+\left(\frac{(u_a-u_w)}{a}\right)^n\right]\right\}^m}\right\} - S_{res}\Big/(1 - S_{res}) \tag{5.8}$$

where $(u_a - u_w)_{res}$ is soil suction at residual conditions that is generally be in the range of 1500 to 3000 kPa (Fredlund and Xing 1994; Vanapalli et al. 1996), e is the natural number (2.71828), while a, n and m are the curve fitting parameters, are estimated from the experimental data. a is suction related to the inflection point on the curve and is somewhat greater than the air-entry value; n is a fitting parameter that control the slope at the inflection point in the SWCC; m is soil parameter related to the residual water content or residual degree of saturation.

The common practice for determining the residual suction and the residual degree of saturation is by the graphical method (Fredlund and Xing, 1994, Vanapalli et al., 1998). Figure 5.12 illustrated the residual state condition that was identified at the intersection point of the two straight lines, a tangent line is drawn at the inflection point of the SWCC, and another line is approximated at high soil suction values (Vanapalli et al. 1998). As a result, the residual suction and the residual degree of saturation which adopted in this study were found to be about 2500 kPa and 6%, respectively.

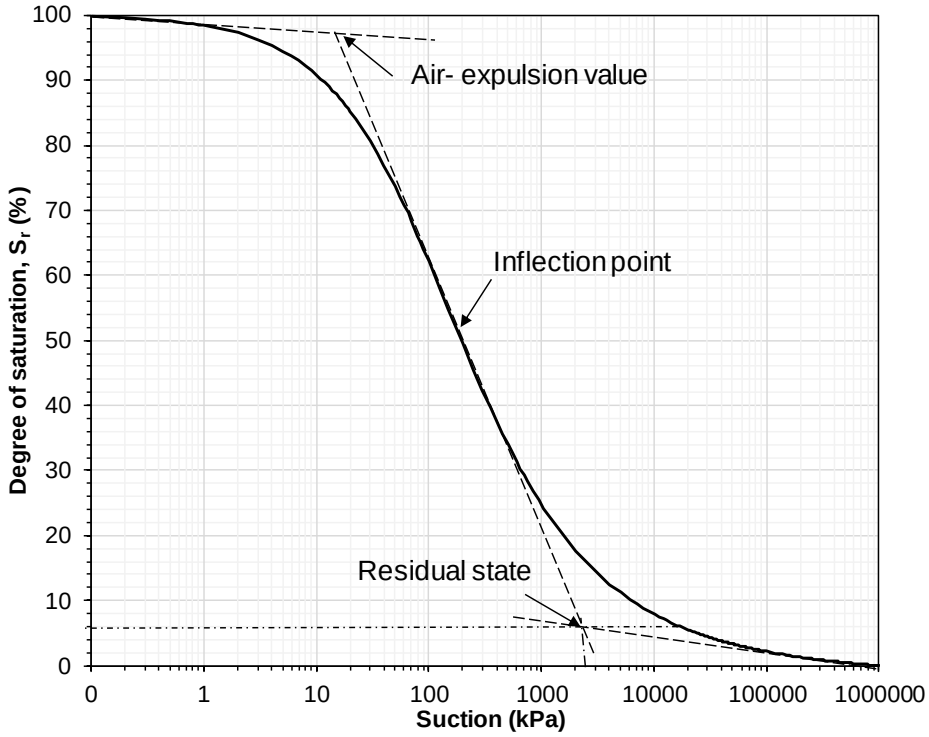

Figure 5.12 Illustration of the residual state condition

The SWCCs (in terms of water content, degree of saturation and effective degree of saturation) fitting parameters with the correlation coefficient (R^2) obtained from the two fitting procedures (van Genuchten (1980) and Fredlund and Xing (1994)) for the two wetting tests (Test types II and III) are presented in Tables 5.3. Table 5.4 presents the air expulsion values (AExV) for the SWCCs determined from the three different procedures (van Genuchten (1980), Fredlund and Xing (1994) and the graphical method). The AExV values determined from van Genuchten (1980) is equal to the inverse of the α fitting parameter. The AExV that determined by Fredlund and Xing (1994) was approximately equal to a fitting parameter. The graphical procedures suggested by Vanapalli et al. (1998) were also followed for estimating the air expulsion value from SWCCs. This value was obtained by extending the constant slope portion of the SWCCs to intersect the line on the portion of the curve for suction at the saturated.

All the suction-water content (SWCCs) data points represent actual experimental test results were best fitted using van Genuchten equation (1980) (Equation 5.3) and Fredlund and Xing (1994) equation (Equation 5.6), and the fitting results are presented in Figures 5.6 and 5.7, respectively, and Tables 5.3 and 5.4. It can be noted from the test

results that both the two fitting equations proper compatibility with experimental results with correction factors were found to be 0.999. The test results also show that as the soil underwent the wetting process from the initial matric suction (563 kPa) of the compacted specimen, with a decrease in the net confining stress the SWCC shifted slightly in an upward direction at higher suctions (500, 300 and 100 kPa), whereas the SWCC shifted significantly in an upward direction at lower suctions (50 and 20 kPa). Further, due to the inclusion of WP4C test results, the SWCCs tend to converge at the very higher suction range. The results in Table 5.3 showed that there is a slight decrease in the α value as the confining stress increase. The value of α was found to be equal to 0.013 kPa^{-1} for the single and multiple specimens at confining stress of 100, whereas the α values were found to be 0.009 and 0.006 kPa^{-1} at confining stress of 250 and 400 kPa, respectively. As a result, the air expulsion value (AExV) increases slightly from 77 kPa at confining of 100 kPa to 158 kPa at confining stress of 400 kPa (see Table 5.4). In all cases, the values of n were found to be approximately the same (was found to be about 1.4) and remained less than 2.0. The test results also showed that generally the higher values of Fredlund and Xing fitting parameter (a), and it was greater for the SWCC at a higher applied confining stress. Similarly, the values of n were found to be approximately the same (was found to be about 0.7) and remained less than 2.0. Table 5.4 also shows that the air expulsion values which were derived from SWCCs in terms of water content by graphical method were found to be ranged from 32 to 80 kPa and generally increased as the confining stress increased.

The suction-degree of saturation (SWCCs) data points were also best fitted using van Genuchten (1980) and Fredlund and Xing (1994) equations (Equations 5.4 and 5.7), and the fitting results are presented in Figures 5.8 and 5.9, respectively and Table 5.3 and 5.4. The SWCCs in terms of the effective degree of saturation was best fitted using van Genuchten (1980) and Fredlund and Xing (1994) equations (Equations 5.5 and 5.8), respectively, and the fitting results are presented in Figures 5.10 and 5.11 and Table 5.3 and 5.4. The best-fit parameters (α and n) which determined from the suction – effective degree of saturation relationship using Equation 5.5 were used to calculate the SSCC based on the method proposed by Lu et al. (2010). The concept of the SSCC express the influence of the degree of saturation on the effective stress of unsaturated soil (Jiang et al. 2017). The effective degree of saturation (S_e) influence the form of the proposed shear strength equation by Lu et al. (2010).

The results presented in Figures 5.8 to 5.11 showed that the two types of SWCCs (in terms of degree of saturation and in term of effective degree of saturation) follow a similar pattern, both SWCCs revealed *S*-shaped curves with smooth transitions over the entire range of suctions and all are congruent or be very close to one another in the inflection point portion of the curves. However, at low suctions the van Genuchten equation leads to better agreement with experimental results, whereas, the measured data were slightly underestimated in the high range of matric suction, but overall, they were well represented by the fitted with correction factors was found to be approximately 0.998. Fredlund & Xing (1994) equation provided more reliable closeness of fit with experimental data sets and more flexibility, particularly at the residual zone and at the inflection point of the wetting part of the SWCC in terms of degree of saturation. The correction factors were found to be more than 0.999 (see Table 5.3). In general, the test results show that the Fredlund and Xing model closer agreement with the measured data than the van Genuchten model. This assessment was also confirmed by many researchers such as Leong and Rahardjo (1997), Sillers et al. (2001) and Fredlund et al. (2012). It can be seen from Figures 5.8 to 5.11 that SWCC shifted very slightly to the right with an increase in the confining stress. Oh and Lu (2014) have found that confining stress affects only the SWCC in terms of water content and does not affect SWCC in terms of effective degree of saturation. The results in Table 5.3 showed that the effects of the confining stress on the α and n (van Genuchten fitting parameters) were not significant. In all cases, the value of α lies between 0.023 and 0.029 kPa^{-1}. As a result, the air expulsion value (AExV) were derived from the α parameter lies between 34 and 43 kPa. Further, the test results indicated that the quite difficult to define clear trends between air expulsion value and the confining stress when Fredlund and Xing's approach was adopted to best-fit SWCCs in terms of degree and effective degree of saturation.

The graphical procedures suggested by Vanapalli et al. (1998) were also followed for estimating the air expulsion value from SWCCs in terms of degree and an effective degree of saturation. The air expulsion values were found to be approximately similar (ranged from 17 to 20 kPa) and decreased very slightly as the confining stress decreased. Oh and Lu (2014) have shown that on the contrary to the drying process, in the case of the wetting curves, the air expulsion values remained similar and may be slightly increased as the confining stress increased. They also stated that this finding is attributed to the confining stress has less effect on smaller pores. Therefore the air-expulsion pressure which is largely controlled by smaller pores is much less affected by the

confining stress. In general, it is more reasonable to infer that the effects of the net confining stress on SWCCs (in terms of degree and an effective degree of saturation) parameters might be not significant. However, the findings of the current study do not support the other previous research results (Vanapalli et al. 1996; Ng and Pang 2000; Miller 2002; Pham et al. 2003; Lee et al. 2005; Thu et al. 2007; Nuth and Laloui 2008; Kim et al. 2010; Oh and Lu 2014; Tavakoli et al. 2014) that there is a general tendency for the soil specimens subjected to a higher stress to possess larger air entry values; this is probably caused by the presence of a smaller average pore size distribution in the soil specimen under the higher applied load (Ng and Pang 2000).

Table 5.3 Parameters of the van Genuchten and Fredlund and Xing models for SWCCs under various confining stresses

Relation type	Test type	Confining stress (kPa)	van Genuchten fitting parameters			Fredlund and Xing fitting parameters			
			α 1/kPa	n	R^2	a kPa	n	m	R^2
w–s	II	100	0.013	1.417	0.999	378	0.691	2.276	0.999
	III	100	0.013	1.423	0.999	288	0.788	1.908	0.999
	III	250	0.009	1.441	0.999	453	0.774	2.102	0.999
	III	400	0.006	1.472	0.999	576	0.797	2.126	0.999
s-S_r and s-S_e	II	100	0.023	1.516	0.998	94	0.804	1.659	0.999
	III	100	0.029	1.490	0.998	98	0.757	1.759	0.999
	III	250	0.029	1.479	0.998	176	0.648	2.322	0.999
	III	400	0.023	1.509	0.998	153	0.743	2.021	0.999

Table 5.4 Air expulsion values (AExV) under various confining stresses

Relation type	Test type	Confining stress (kPa)	Air expulsion value (kPa)		
			Graphical method	Van Genuchten (1980)	Fredlund and Xing (1994)
w–*s*	II	100	32	77	378
	III	100	32	78	288
	III	250	56	112	453
	III	400	80	158	576
s-S_r and *s*-S_e	II	100	19	43	94
	III	100	17	34	98
	III	250	17	34	176
	III	400	20	43	153

5.4 Concluding remarks

This chapter presented the test results of wetting tests on statically compacted specimens (dry unit weight = 15 kN/m^3, water content = 10%). The wetting tests were carried out under isotropic stress conditions. During the wetting process, the changes in the volume of water and the total volume of the specimens were monitored. The test results from the wetting tests in conjunction with the chilled-mirror dew-point potentiameter test results enabled establishing the SWCCs for a large range of suction at various confining stresses. The test results were fitted with two SWCCs models (van Genuchten 1980 and Fredlund & Xing 1994). The impact of confining stress on the volumetric strain and SWCCs were studied. The following points emerged from the study:

i. At constant confining stress and at the same suction values, the single specimen in the step-wise suction reduction test generally shows larger water, air, and specimen-volume changes at the end of wetting stages as compared to the values result from the multiple specimens. This primarily due to the effect of the continuous softening of the bonding between the interparticle during the several wetting stages of the single specimen, and the effect of the quick softening of the interparticle bonding during wetting processes of the multiple specimens.
ii. The impact of confining stress on the volumetric strain was distinct; the volumetric strain became more negative as the applied confining stress increased. The tests results agree well with the findings reported in the literature.
iii. At low suctions the van Genuchten (1980) equation leads to better agreement with experimental results, whereas, the Fredlund & Xing (1994) equation provided more reliable closeness of fit with experimental data sets at high suctions. This assessment was confirmed by several researchers such as Leong and Rahardjo (1997), Sillers et al. (2001), Fredlund et al. (2012) and Jiang et al. (2017).
iv. The wetting suction-water content SWCCs were affected the applied confining stress. The SWCC shifted to the up with a decrease in the confining stress. Similar findings were reported by other researchers (e.g., Vanapalli et al. 1996; Ng and Pang 2000; Oh and Lu 2014). However, the effects of the confining stress on the SWCCs in terms of the degree and effective degree of saturation was found to be not significant. This finding is consistent with those of Oh and Lu (2014) who have found that under wetting

conditions, even though the SWCCs were different under different confining stresses, a unique SWCCs could be defined if the degree of saturation was used.

v. The van Genuchten fitting parameter (α) and Fredlund & Xing fitting parameter (a) derived from suction-water content relationship effect by confining stress changes and that effects cause the air expulsion value generally increased as the confining stress increased. However, the effects of the confining stress on the fitting parameters (α) and (a) which inferred from suction-degree of saturation and suction-effective degree of saturation relationships were not significant, and the air expulsion values remained similar and may be very slightly increased as the confining stress increased. Further, in all relationships, the values of the fitting parameter (n) were found to be approximately the same and remained less than 2.0.

CHAPTER 6

Effects of suction on the shear strength behaviour during wetting

6.1 Introduction

The saturated and unsaturated shear strength of soil defined as the maximum internal resistance per unit area the soil is capable of sustaining under external or internal stress loading (Fredlund and Rahardjo 1993a; Lu and Likos 2004). Shear strength can be related to the stress state variables, the net normal stress ($\sigma - u_a$) and the matric suction ($u_a - u_w$) (Fredlund et al. 2012). There are three main approaches as described previously in chapter two to evaluate the stress state in unsaturated soil; the single stress-state variable approach proposed by Bishop (1959), the two stress-state variable approach proposed by Fredlund and Morgenstern (1977), and the true effective stress concept introduced by Lu and Likos (2006). Referring to these approaches, different failure criteria have been formulated to describe the shear strength behaviour of unsaturated soil (Bishop et al. 1960; Fredlund et al. 1978; Fredlund et al. 1996; Vanapalli et al. 1996; Rassam and Williams 1999; Rassam and Cook 2002; Khalili et al. 2004; Tarantino 2007; Sheng et al. 2011).

A number of general observations can be made based on various shear strength studies that have been undertaken by several researchers (i.e., Escario and Sáez 1986; Fredlund and Rahardjo 1993; Vanapalli et al. 1996; Cunningham et al. 2003; Lu and Likos 2004; Lee et al. 2005; Zhan and Ng 2006; Fredlund et al. 2012):

i. Under the same matric suction, a linear failure envelope for the shear strength with respect to confining stress is obtained, and the higher confining stress results in higher shear strength (Donald 1956; Fredlund and Rahardjo 1993a; Fredlund et al. 2012).
ii. Under the same confining stress, the higher matric suctions result in higher shear strength. The shear strength of all soil types increases in response to the effective angle of internal friction ($\emptyset'$) for matric suctions up to the air-entry value of the soil. There

is curvature in the shear strength envelope once the air-entry value is exceeded. The shear strength increases most rapidly in the low-matric-suction range and then gradually flattens (or even decreases) at high suctions (Ho and Fredlund 1982a; Fredlund et al. 1987; Escario and Sáez 1986; Thu 2006; Houston et al. 2008; Fredlund et al. 2012). A comparison of the SWCCs and the shear strength envelopes showed that there was a correlation between the air-entry value for each soil and the point at which the shear strength envelope became nonlinear (Donald 1956; Vanapalli et al. 1996; Fredlund et al. 2012).

The effects of a decrease in matric suction on the shear strength of collapsible soils can be studied by carrying out unsaturated triaxial tests (Lawton et al. 1991; Sun et al. 2007; Jiang et al. 2012; Houston et al. 2008; Haeri et al. 2014; Almahbobi et al. 2018; McCartney 2018). Studies covering the step-wise wetting under various confining stresses and their impact on the shear strength are expected to provide a thorough understanding of the macroscopic behaviour of collapsible soils.

The objectives of this chapter were; (i) to explore the impact of confining stress and suction on the shear behaviour of the compacted collapsing soil specimens during the wetting process, (ii) to study the effects of suctions on the Mohr circles and the drained failure envelopes and (iii) to study the effects of suctions on the saturated and unsaturated shear strength parameters such as c, $\emptyset'$ and $\emptyset^b$.

This chapter is presented in several sections. The experimental program of triaxial tests (Test type I and III; section 3.5.5.2) are recalled in section 6.2. Section 6.3 presents the test results and discussion. The results involving the three conventional CD triaxial tests were conducted on saturated soil specimens at several effective confining stresses, and the twelve unsaturated CD triaxial shear strength tests at several matric suction and net confining stresses are presented and discussed. The concluding remarks are presented in section 6.4.

6.2 Experimental program

Saturated and unsaturated triaxial shear strength tests were carried out on compacted soil specimens that were prepared by statically compacting soil-water mixture at an initial water content of 10% and a dry unit weight of 15 kN/m^3 (see Table 3.5 in chapter 3). The diameter and height of the specimens were 50 and 100 mm, respectively.

The triaxial tests were conducted using two separate GDS automated triaxial devices, such as a conventional triaxial device and an unsaturated triaxial device (HKUST-type) (see section 3.5.5.3 and 3.5.5.4).

Three consolidated drained tests were carried out on compacted-saturated specimens at effective confining stresses of 100, 250 and 400 kPa (Test type I; section 3.5.5.2) to evaluate the effective shear strength parameters, c' and $\emptyset'$, and to compare the behaviour of saturated specimens with that of unsaturated specimens. In the consolidated drained unsaturated triaxial tests (Test type III; section 3.5.5.2), twelve compacted specimens were used under various magnitudes of applied suction (20, 50, 100 and 300 kPa), and net confining stresses (100, 250 and 400 kPa) (see chapter 5, Table 5.2 and Figure 5.1). The saturated and unsaturated specimens were sheared by increasing the deviatoric stress at a displacement rate of 0.0015 mm/min. The shearing stage was terminated at an axial strain of 25% in all cases.

6.3 Test results and discussion

6.3.1 Saturated shear strength behaviour and parameters

During the isotropic consolidation and drained shearing stage in the saturated test, the flow of water from the specimen which is equal to the reduction of the specimen's volume was measured. As a result, the water contents, void ratios and volumetric strains of the specimens subjected under the three different confining stresses (100, 250 and 400 kPa) have been calculated based on the water (total) volume changes.

Table 6.1 presented the state of the saturated triaxial specimens at the end of consolidation and shearing stages. After saturation and consolidation of the initially unsaturated triaxial specimen, the measured volumetric strain (based on the water volume change) at the isotropic confining stresses of 100 kPa was found to be 11.6% (see Table 6.1). For specimen compacted and wetted in oedometer with an initial water content of 10% and the dry unit weight of 15 kN/m^3 and the vertical inundation stress of 100 kPa, the collapse strains of 10.8% was recorded. The test results indicated that the one-dimensional wetting test shows similar volumetric strain value to that observed in isotropic consolidation stage at the same initial water content, dry unit weight and applied stress during wetting with a difference not exceed 0.6%. Similar findings were reported by (Chiu 2001).

Figure 6.1 shows the results of volume changes with time under the three effective confining stresses of 100, 250 and 400 kPa during the consolidation stages. The results indicate that most of the specimens' volume change had reached a relatively constant value after a period of less than five hours. The maximum specimens' volume changes due to 100, 250 and 400 kPa confining stress were found to be about 9.6, 14.7 and 16.2 cm^3, respectively.

Table 6.1 State of the saturated triaxial specimens after consolidation and shearing stages

Confining stress $(\sigma_3 - u_w)$ (kPa)	After consolidation			After shearing			
	Water content, w (%)	Void ratio, e	Maximum volumetric strain, $-\varepsilon_v$ (%)	Maximum deviator stress $(\sigma_1 - \sigma_3)$ (kPa)	Water content, w (%)	Void ratio, e	Maximum volumetric strain, $-\varepsilon_v$ (%)
100	19.9	0.529	11.6	172	18.4	0.487	2.7
250	17.9	0.476	14.8	436	15.8	0.420	3.8
400	16.5	0.438	17.0	660	13.5	0.358	5.5

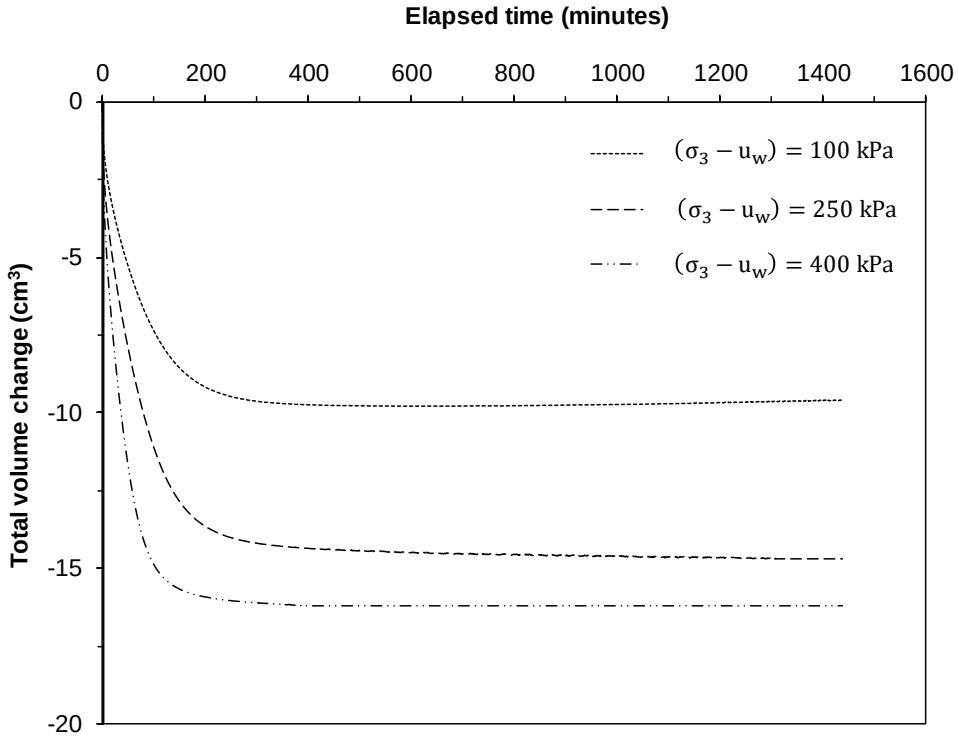

Figure 6.1 Volume change of saturated specimens during consolidation

Figures 6.2a and b show the axial strain versus deviator stress and the axial strain versus volumetric strain, respectively. It can be seen clearly from the test results that the deviator stresses increase monotonically without pronounced clear peak observed, and the stress-strain curves show ductile behaviour without obvious evidence of strain softening (The strain softening means that the peak deviator stress is obvious from the curves of deviator stress against axial strain). The exhibition of ductile behaviour is commonly observed in normally consolidated specimens (Head 1998). The stress-strain curve for soil specimen consolidated to an effective stress of 400 kPa was found to rise to a peak at an axial strain of 15% and then slightly decreases, whereas the deviator stresses for the specimens under effective confining stress of 100, and 250 kPa were found to increase linearly at an axial strain of less than 13% and then remained nearly constant. It also appears from the test results that the magnitude of maximum deviator stress (436 kPa) determined at confining stress of 250 kPa was found to be greater by more than two times the value (172 kPa) noted for the specimen subjected to confining stress of 100 kPa, whereas at confining stress of 400 kPa, the maximum deviator stress (660 kPa) was found to be approximately fourth times higher than the maximum deviator stress value at effective confining stress of 100 kPa.

The contractive volumetric strain was recorded for all the three tests, and the maximum volumetric strains were found to be 2.7, 3.8 and 5.5% during shearing at effective confining stresses of 100, 250 and 400 kPa, respectively. Herkal et al. (1995) and Chaney et al. (1996) stated that higher stresses caused a greater reduction of the pore spaces during shearing. An explanation in terms of soil structure is that more closely packed particles result in reduced inter-connections between pore spaces. Close particle packing gives specimens more resistance to external stress (Fredlund and Rahardjo 1993a).

The test results showed that the critical states were reached for all tests at an axial strain of around 25%. Additionally, bulging failures were observed for all the specimens at the end of triaxial tests.

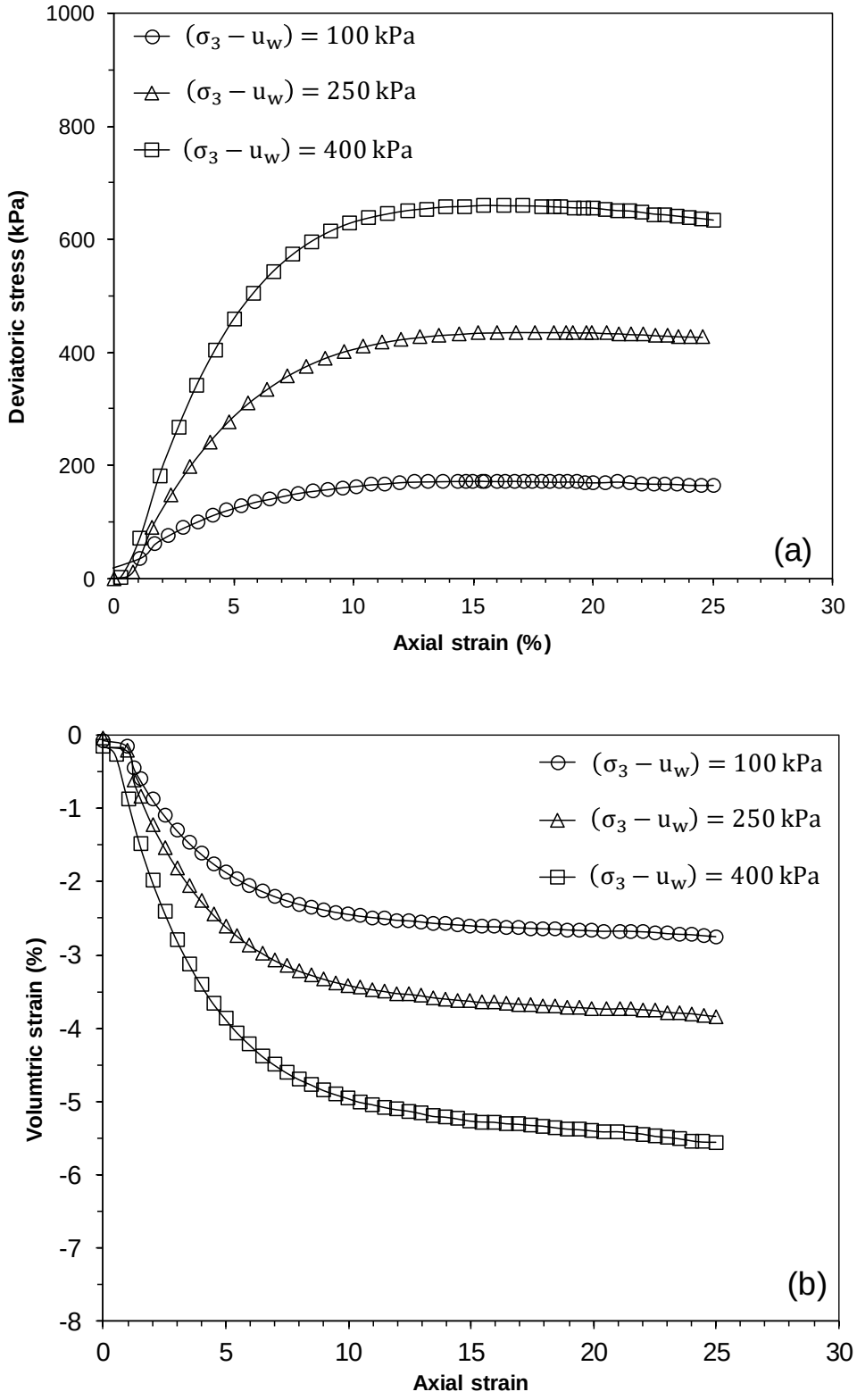

Figure 6.2 Results of the CD triaxial compression tests for saturated specimens (a) axial strain versus deviator stress and (b) axial strain versus volumetric strain

Figure 6.3 presents the Mohr circles and the failure envelope for the saturated shear strength tests. The peak deviatoric stress values (see Figure 6.2a) were considered for establishing the Mohr circles and the Mohr-Coulomb failure envelope, which was constructed with a straight line drawn through all the points of tangency of the Mohr circles. The interception of the failure envelope and shear stress axis is the effective cohesion (c′), and the slope of the failure envelope is the effective frictional angle (∅′). c′ and ∅′ were found to be about 5 kPa and 26.66^0, respectively. These effective shear strength parameters will be used to calculate the suction stress of the soil that was established from the shear strength test results. The values of suction stresses will be presented later in Chapter 7.

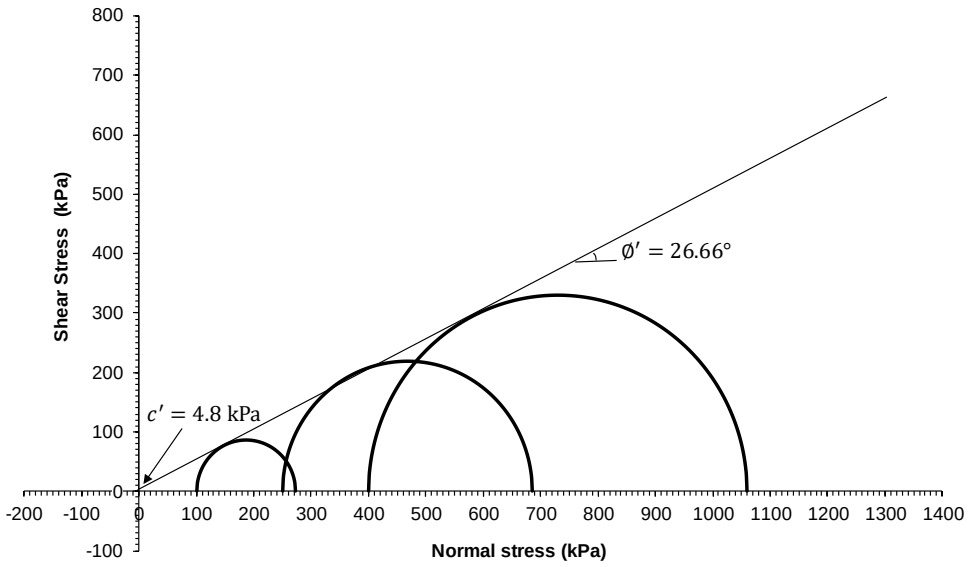

Figure 6.3 Mohr-Coulomb failure envelope for saturated soil under various effective confining stresses

6.3.2 Effects of suction on the unsaturated shear strength and volume change behaviour during shearing

Table 6.2 presented the states of the unsaturated triaxial specimens at the end of the shearing stages. It can be seen from this table that the unsaturated triaxial tests were divided into four groups, namely Groups 1, 2, 3 and 4. Each group consists of three tests. The aim of divided the test results to these groups was to investigate the shear behaviour at a suction of 20, 50, 100 and 300 kPa at each applied net confining stresses (100, 250 and 400 kPa).

Table 6.2 States of the unsaturated triaxial specimens after shearing

Group no.	$(\sigma_3 - u_a)$ (kPa)	$(u_a - u_w)$ (kPa)	$(\sigma_1 - \sigma_3)$ (kPa)	w (%)	e	S_r (%)	$-\varepsilon_v$ (%)
1	100	20	208	18.19	0.538	89.6	3.2
	250	20	474	15.21	0.480	83.9	4.2
	400	20	710	13.05	0.397	87.1	5.0
2	100	50	252	18.26	0.578	83.8	3.1
	250	50	504	17.17	0.507	89.7	4.8
	400	50	758	16.25	0.450	95.6	5.2
3	100	100	308	13.12	0.625	55.7	2.6
	250	100	554	13.10	0.541	64.2	4.7
	400	100	836	13.00	0.478	72.2	6.4
4	100	300	380	10.94	0.668	43.4	2.0
	250	300	644	10.80	0.590	48.5	4.3
	400	300	910	10.72	0.512	55.5	7.0

Figure 6.4a shows the axial strain versus deviatoric stress for the twelve specimens tested in the unsaturated triaxial device. The test results for the saturated specimens that were tested in a conventional triaxial device are also included in Figure 6.4a. The strength of the unsaturated specimens was found to be greater than the strength of a saturated specimen at the same confining stress. For example, at net confining stresses of 100 kPa, the maximum deviator stress for unsaturated specimens with the suction of 20, 50, 100 and 300 kPa were found to be about 1.2, 1.5, 1.8 and 2.2 times greater than that of the saturated specimen at the same confining stress. For the specimens under both net confining stress of 250 and 400 kPa, the maximum deviator stress for unsaturated specimens with the suction of 20, 50, 100 and 300 kPa were found to be around 1.1, 1.2, 1.3 and 1.5 times greater than that of the saturated specimen at the same confining stress. Fredlund and Rahardjo (1993) stated that during the drying process, a contractile skin begins to form around the points of contacts between particles. The capillary action arising from suction at the contractile skin increases the normal forces at the inter-particle contacts. These additional normal forces may enhance the friction and the apparent cohesion at the inter-particle contacts. As a result, the unsaturated soil exhibits higher strength than the saturated one. The results show agreement with the studies presented by Hillel et al. (1998), Lee et al. (2005) and Goh (2012) where matric suction plays an important role in contributing additional strength to the soil.

Figure 6.4b shows the axial strain versus volumetric strain. The test results show that the contractive behaviour was observed for the all curves during drained shearing stages (The sign of volumetric change is negative when specimen under contraction), and the final value of volumetric strain generally increase with an increase in the confining stresses. For more description, when the unsaturated soil specimen was subjected to a drained shearing in a triaxial apparatus, the increase in deviator stress resulted in an increase in both net mean and shear stress. The increase in net mean stress leads to a compression of the larger voids while the increase in shear stress tends to cause slippage at the contact points and leads to the collapse of the fabric arrangement of voids. As results, both these two kinds of effect result in the substantial contraction of the unsaturated specimens (Liangtong 2003). The results are consistent with the experimental data published by Cui and Delage (1996). However, it seems to be contrary to the test results obtained by Ng and Chiu (2001) in which they stated that the overall volumetric contraction decreases with an increase in net confining stress.

The variation of the maximum value of the volumetric strain with the applied suction under a low confining stress (100 kPa) was found to be close and approximately in the range of 2–3.2% with the lowest value was found to be at suction of 300 kPa, whereas the greater magnitude of volumetric deformation was found at low suction value (20 kPa). In other words, at confining stress of 100 kPa as matric suction increases the unsaturated specimens show less contractive strain. This behaviour is consistent with the experimental data published by Satija (1978), Leroueil et al. (1995), Cui and Delage (1996), Liangtong (2003) and Garakani et al. (2015). Approximately similar volumetric strain behaviour was recorded during shearing at confining stress of 250 kPa. However, the specimens under a higher net confining pressure (400 kPa) were different in the volume change behaviour during shearing. The maximum value of volumetric strain tends to increase with the value of applied suction. In other words, the larger the applied suction (300 kPa), the larger the contractive strain (about 7%) was recorded. This behaviour appears to be consistent with experimental data published by Ng and Chiu (2001), Liangtong (2003), Goh (2012) and Haeri et al. (2017).

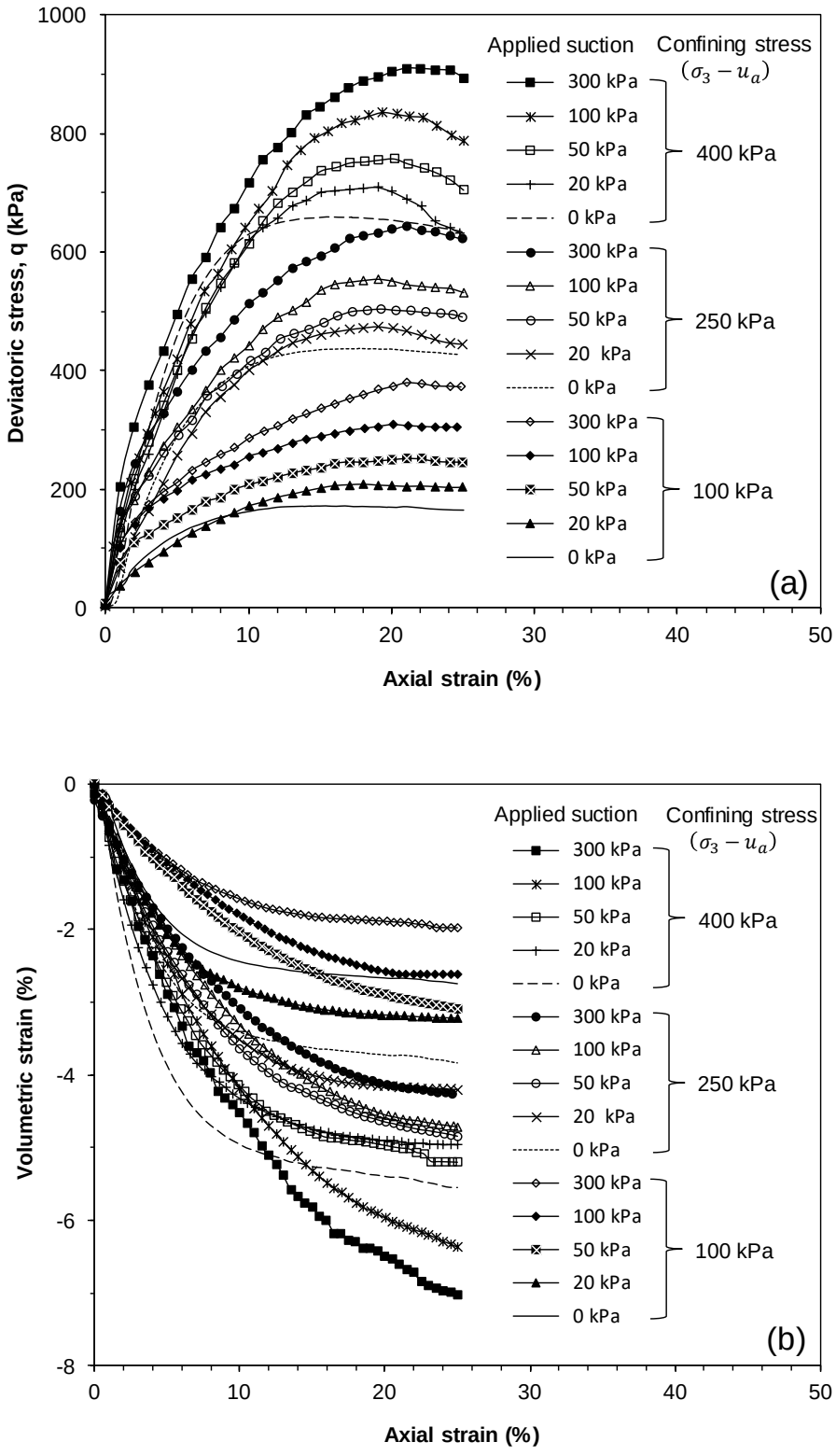

Figure 6.4 Results of the CD triaxial compression tests for saturated and unsaturated specimens (a) axial strain versus deviator stress and (b) axial strain versus volumetric strain

Figure 6.5 shows failure envelopes on the shear strength versus suction plane. These results clearly show that the shear strength decreased with a decrease in matric suction as the soil underwent the wetting process. Figure 6.5 also indicates that the variations of the maximum shear stress with suction at each confining stress value remained between 125 to 56 kPa, and the magnitude of variation generally increased with an increase in the applied confining stress. Additionally, the shapes of the shear stress versus suction plots at all confining stresses were found to be similar.

As before in fully saturated specimens, most of the unsaturated specimens were observed to fail by barreling without a formation of a clear failure plane. However, some specimens which were sheared under high net confining stress and suction exhibit a distinct failure plane. Figures 6.6a and b show an actual photograph of the soil specimens failed by barreling without a formation of a clear failure plane at the suction of 20 kPa and net confining stress of 100 kPa and a clear failure plane at the suction of 300 kPa and net confining stress of 400 kPa, respectively.

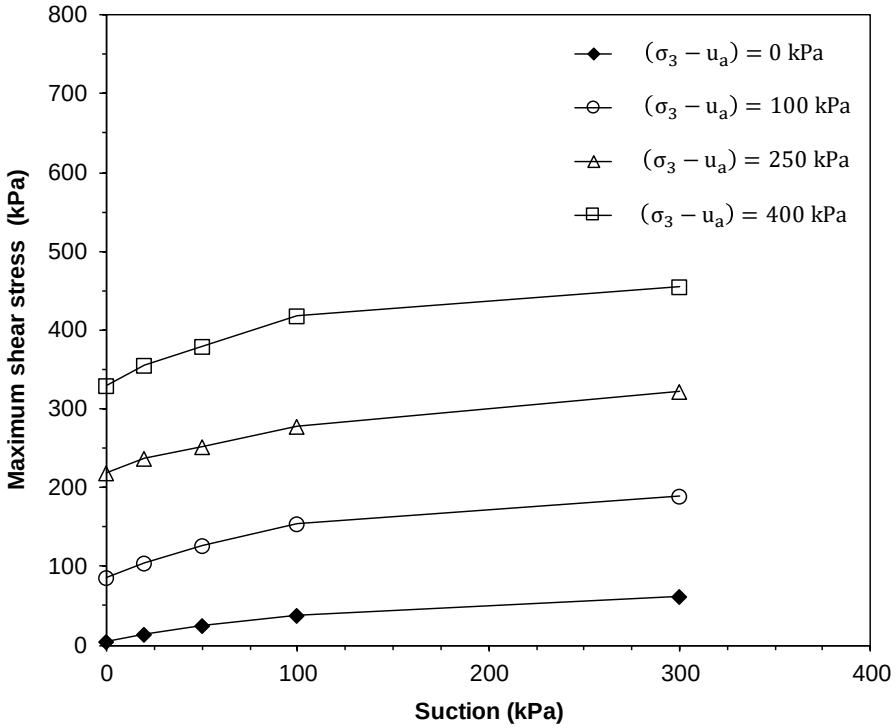

Figure 6.5 Failure envelopes on the shear strength versus suction plane

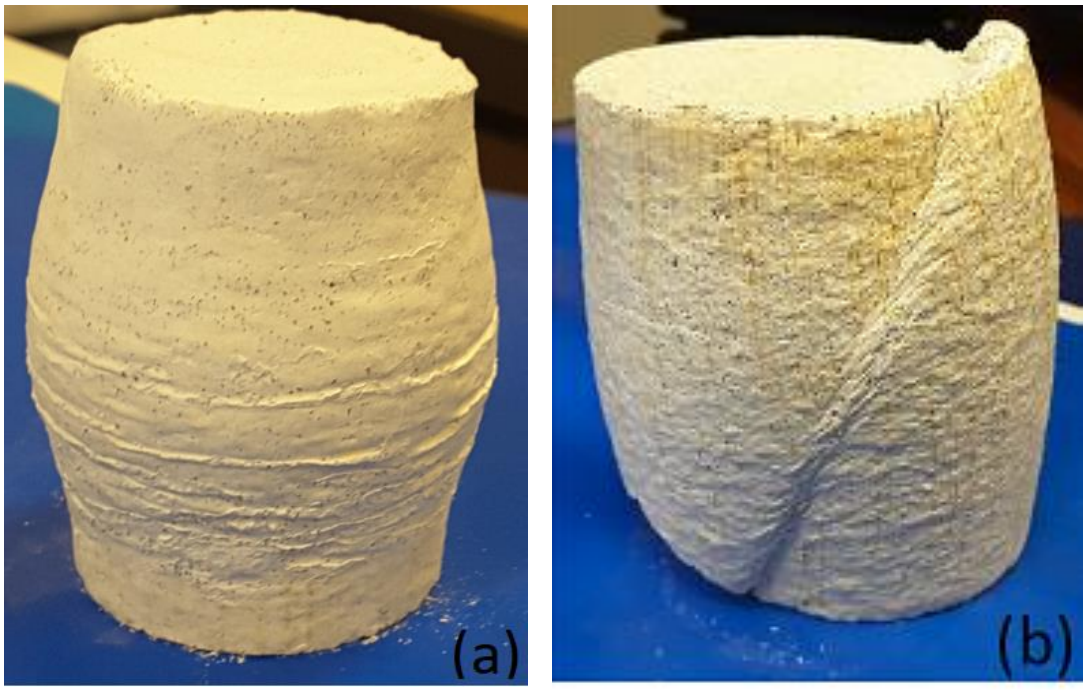

Figure 6.6 Photograph of the failed specimens under CD triaxial shearing (a) barreling failure, and (b) with failure plane

Figure 6.7 presents the Mohr circles and the failure envelopes for the saturated and unsaturated shear strength tests. The peak deviatoric stress values (see Figure 6.4a) were considered for establishing the Mohr circles. The failure envelopes shown in Figure 6.7 provided the values of slope angle ($\emptyset'$), and the cohesion intercept (c) corresponding to various applied suctions. It is clearly seen from the test results that with an increase in the applied suction, the failure envelopes for unsaturated soil specimens were shifted in an upward direction.

Table 6.3 presents the friction angles ($\emptyset'$) and the cohesion intercepts (c) for different suction values. Figure 6.8 shows the impact of suctions on the friction angle ($\emptyset'$). Both Table 6.3 and Figure 6.8 show that the friction angle increases slightly with an increase in the matric suction. It may be reasonable that the wetting may reduce the angle of shearing resistance. Escario and Sáez (1986) and Gan and Fredlund (1996) have stated that as $\emptyset'$ is a strength parameter related to the frictional characteristic of the interparticle contacts, which is an intrinsic property of the soil, it may be independent of the stress state variable, such as suction. However, other researchers have shown that $\emptyset'$ is a function of the suction by considering a wider range of suctions and the experimental evidence indicates that $\emptyset'$ increase only slightly with increasing suction (Maatouk et al. (1995); Wheeler and Sivakumar (1995b); Khalili and Khabbaz 1998; Alawaji 2001; Cunningham et al. 2003; Lee et al. 2005; Futai and Almeida 2005; Zhan and Ng 2006; Oh et al. 2008; Shen et al.;2009; Wang et al. 2014; Haer and Garakani 2016).

Table 6.3 shows that the cohesion values remained between 61 and 4.8 kPa for a matric suction range of 300 to 0 kPa. These results also show that the cohesion decreased with a decrease in matric suction as the soil underwent the wetting process. The decrease in the cohesion during the wetting process can be explained as follows: The total cohesion in an unsaturated soil consists of two components. The first component is the effective cohesion of the soil in saturated condition (c'), and the other component is due to the contribution of suction, which is equal to (u_a - u_w) tan $\emptyset^b$ (Fredlund and Rahardjo 1993a). Hence, when an unsaturated soil becomes saturated, the total cohesion approaches the original cohesion value (c') since the contribution of suction disappears (Oh et al. 2008). Similar findings have been reported by several researchers (e.g., Micheals 1959; Lu and Likos 2004; Futai and Almeida 2005; Murray and Sivakumar 2010; Fredlund et al. 2012). They stated that for any soil the apparent cohesion parameter (c) increases with increasing suction.

Figure 6.9 shows the impact of suction on the cohesion intercept. It can be seen that cohesion decreased non-linearly (Fredlund et al. 2012) with a decrease in suction during the wetting process. At smaller applied matric suctions (≈ AExV), the values of cohesion intercept followed a line with a slope approximately equal to tan $\emptyset'$. Sivakumar (1993) and Fredlund et al. (2012) stated that the air-entry value provides an indication of the point where the shear strength versus matric suction starts to exhibit nonlinear shear strength behaviour.

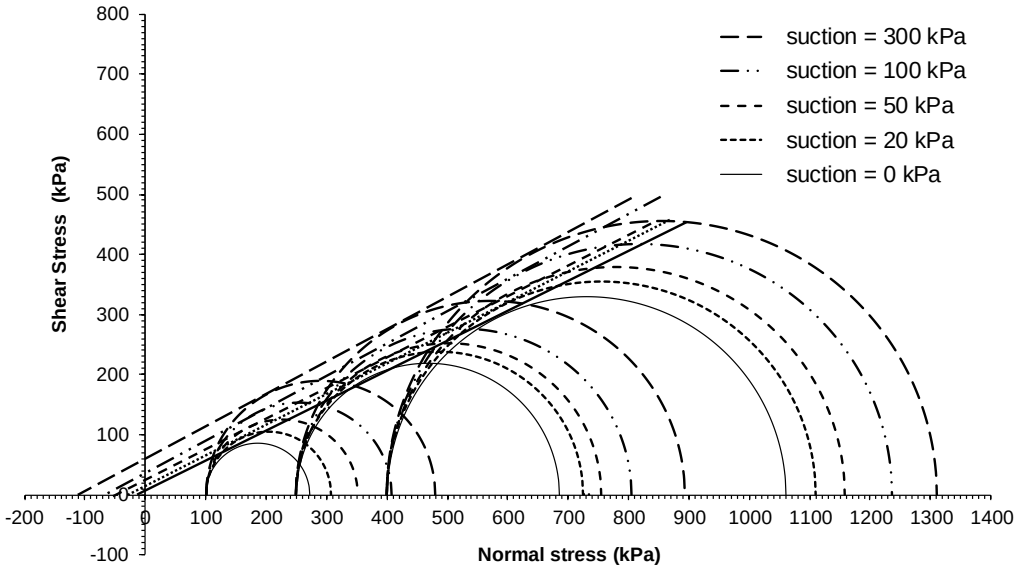

Figure 6.7 Mohr-Coulomb failure envelopes

Table 6.3 Variation of $\emptyset'$ and *c* with applied suctions

	Suction, $(u_a - u_w)$ (kPa)				
Parameter	300	100	50	20	0
$\emptyset'$ ($^\circ$)	28.0	27.9	27.2	27.1	26.7
c (kPa)	61.0	37.8	25.3	13.9	4.8

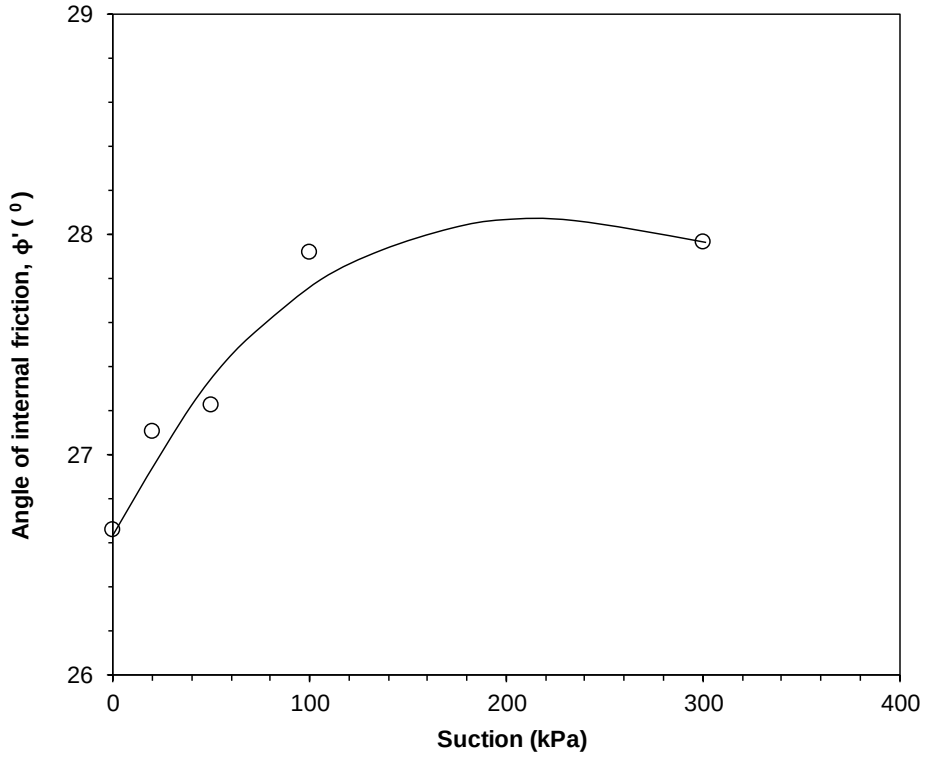

Figure 6.8 Impact of applied suction on the angle of internal friction

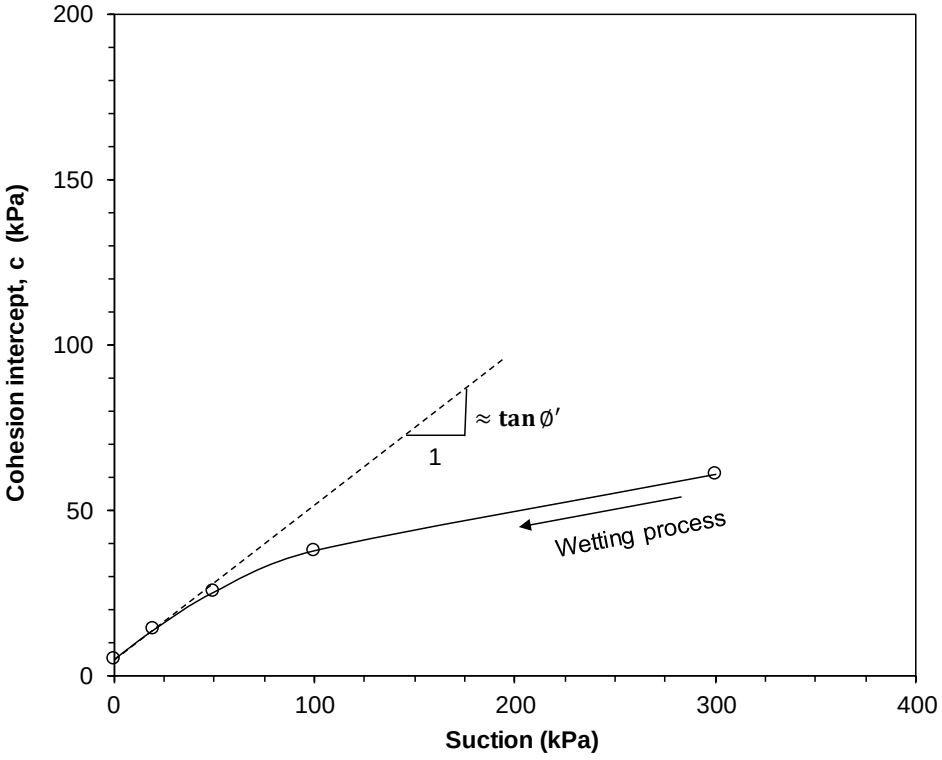

Figure 6.9 Impact of applied suction on cohesion intercept

The value of the angle of shearing resistance with respect to matric suction ($\emptyset^b$) can be calculated from the cohesion versus suction curve and its relationship to suction is shown in Figure 6.10. It can be seen from this figure that $\emptyset^b$ increased nonlinearly with a decrease in suction as the soil underwent the wetting process to attain a maximum value at saturation. The value of $\emptyset^b$ at saturation (about 24.4^0) was found to be a little lesser than $\emptyset'$ angle (26.7^0). These results related to the nonlinearity behavior of $\emptyset^b$ with suction for the tested soil are consistent with those of studies on other types of unsaturated soils such as Satija (1978), Fredlund et al. (1978), Escario and Sáez (1986), Fredlund et al. (1987), Gan et al. (1988), Vanapalli et al. (1996), Rassam and Williams (1999), Vanapalli and Fredlund (2000), Lee et al. (2005), Monroy 2005, Thu et al. (2006), Oh et al. (2008), Goh et al. (2010), Eyob (2011), Nyunt (2012) and Fredlund et al. (2012), who reported that the value of $\emptyset^b$ decreased with increasing suction. These previous authors also reported that $\emptyset^b$ was equal to $\emptyset'$ when suction was zero.

The variation in the $\emptyset^b$ angle with respect to suction can be understood better by considering the pore-volume when the pore water act. At a low value of suction (less than the air entry value), the soil specimen remains saturated, and the entire pore volume is filled water. Therefore, the effects of pore water pressure and total normal stress on the shear strength are characterized by the effective friction angle. For that reason, an increase in suction produces the same increase in shear strength as an increase in net normal stress which leads to being $\emptyset^b$ close to $\emptyset'$ and intercepts cohesion values increase according to tan $\emptyset'$, indicating that suction increments are equivalent to effective normal stress increments as in saturated soil. However, when the air entry value (AEV) is reached, air displaces water in the pores. As the soil becomes unsaturated the cross-sectional area through which the water phase acts are decreased, and the unsaturated soil illustrated by the suction $(u_a - u_w)$ and net stress $(\sigma - u_a)$ variables. In this case, an increase in net confining stress is more effective in increasing the shear strength of the soil than the increase in suction, resulting in a decrease in $\emptyset^b$ with suction (Fredlund et al. 1987; Fredlund and Rahardjo 1993a).

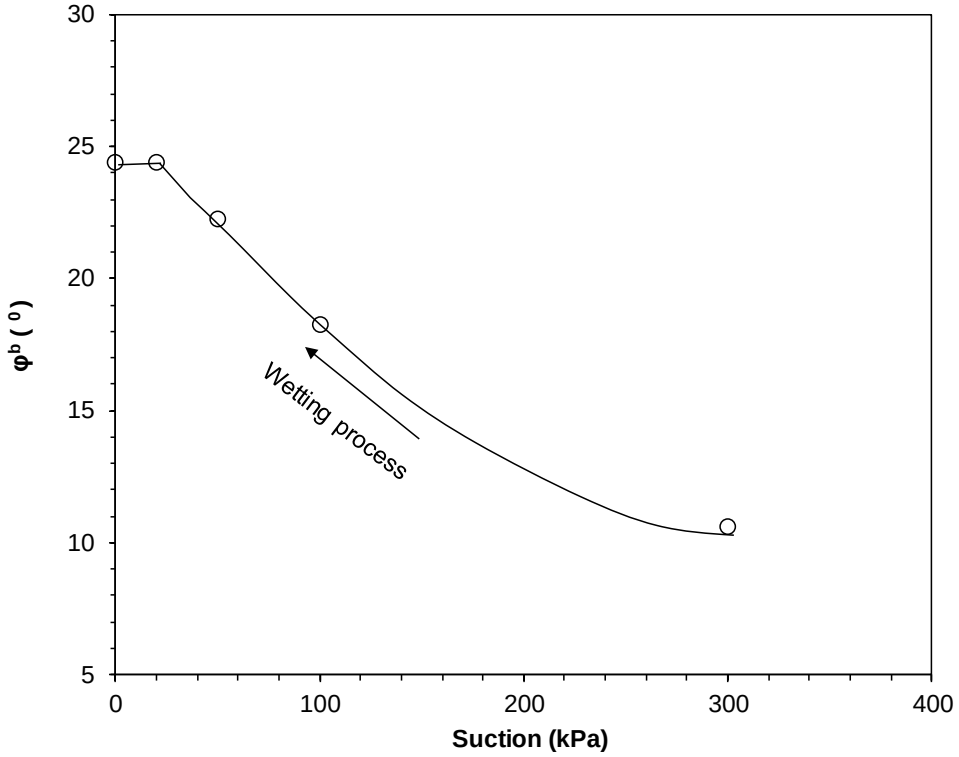

Figure 6.10 Impact of applied suction on the $\emptyset^b$ angle

6.3.3 Effects of confining stress and suction on the shape of the stress-strain curves

Figure 6.4a shows that for the considered range of suction, a rapid rise in deviatoric stress over a short axial strain range was quickly followed by a fairly wide range of constant rate of change in the deviatoric stress with the axial strain. These transition stages indicate the progressive mobilization of the shear strength of the specimens. It is noticed that maximum deviatoric stress is reached at an axial strain varied between 16 to 18%. It appears from the test results that at the same confining stress, the impact of the decrease in the soil suction was found to have a minor influence on the shape of the stress-strain curves. The above results are consistent with the studies by Oh et al. (2008) and Eyob (2011). They stated that an increase in matric suction did not affect the general shape of the stress-strain relationships.

6.3.4 Effects of confining stress and suction on the final water content and degree of saturation

As illustrated in Table 6.2 an increase in the final water content value was observed of all specimens shearing at the suction of 50, 100 and 300. A possibility of such a cause can be explained as follows: the increase in shear stress during triaxial shearing produced a shear effect on the fabric of the large collapsible soil aggregates. The shearing lead to the contract of the unsaturated aggregate and hence air pressure increased. Therefore, to keep suction constant, the resultant water pressure deficiency would lead to a flow of water into the specimen during drained shearing (Ng and Chiu 2001; Liangtong 2003). As a result, an increase in water content in the specimens under suctions of 50, 100 and 300 kPa was noted. However, an interesting observation in this study at relatively low suction (20 kPa) in which the soil voids are almost filled with water, by raising the axial stress during shear the specimen loses water. As a result, a decrease in the specimens' water content was observed. A decrease in water content was observed because of the contractive volume change which similar to the behaviour of the fully saturated specimen (suction = 0 kPa) during shearing. It can, therefore, be argued that as suction values close to the air entry value (such as suction of 20 kPa), the soil will be in a saturated state and the mechanics of saturated soils apply. Based on the test results shown in Table 6.2, it can also be noted that the magnitude of an increase in the final value of the specimens' water content during shearing decreases with the increases of net confining stress.

During shearing at different confining stresses, the test results in Table 6.2 shows that the final degree of saturation increased for suction of 50, 100 and 300 kPa, whereas it is value decreased at the suction of 20 kPa. Also, the results show that at each value of suction with increasing the confining stress from 100 to 400 kPa, the final degree of saturation was found to be greater and the variation in the measured values was found to be in the range of about 5 to 8%. This may suggest that at constant suction the greater reduction in the void ratio at higher applied confining stress during shearing stage exerts a more significant effect on the final measured degree of saturation than the effect of water content.

Figures 6.11a, b and c show a comparison between the change in the specific volume (v=1+e) and the change in specific water volume (v_w=1+ wGs) during shearing tests at net confining stresses of 100, 250 and 400 kPa, respectively. As shown in these

figures that the change in specific volume appears to be significantly greater than the change in specific water volume of the unsaturated specimens at suction greater than 20 kPa. This may suggest that the application of external deviator stress exerts a more significant effect on the soil skeleton than on the water phase as the application of net confining stress during the wetting stage. However, at the suction of 20 kPa, the change in specific volume was found to be slightly greater, approximately equal and slightly lesser as compared with the change in specific water volume at net confining stresses of 100, 250 and 400 kPa, respectively. For the saturation shearing tests (suction = 0 kPa), the variation in the specific volume change is equal to the change in the specific water volume. Additionally, it can be seen clearly from Figure 6.11a, b and c that the magnitudes of the change in the specific volume and in the specific water volume were found to increase with an increase in the net confining stress for the considered range of suction (o to 300 kPa). Further, at suction greater than 20 kPa, the difference between specific volume change and specific water volume change values were also found to increase with an increase in the net confining stress.

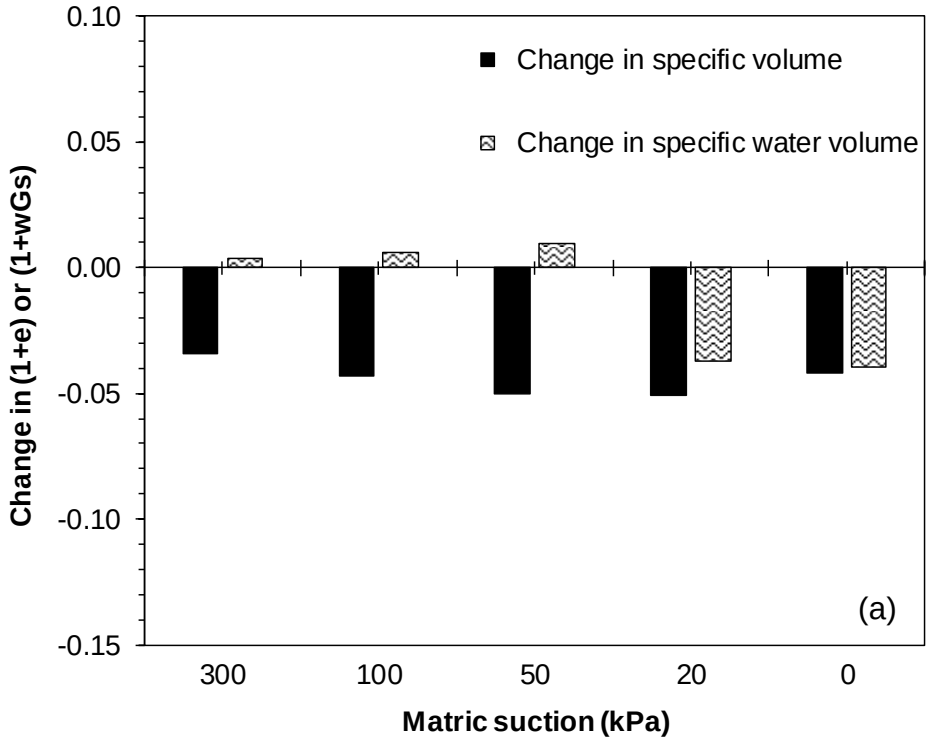
0.10
0.05
0.00
-0.05
-0.10
-0.15
Change in (1+e) or (1+wGs)
Change in specific volume
Change in specific water volume
(a)
300
100
50
20
0
Matric suction (kPa)

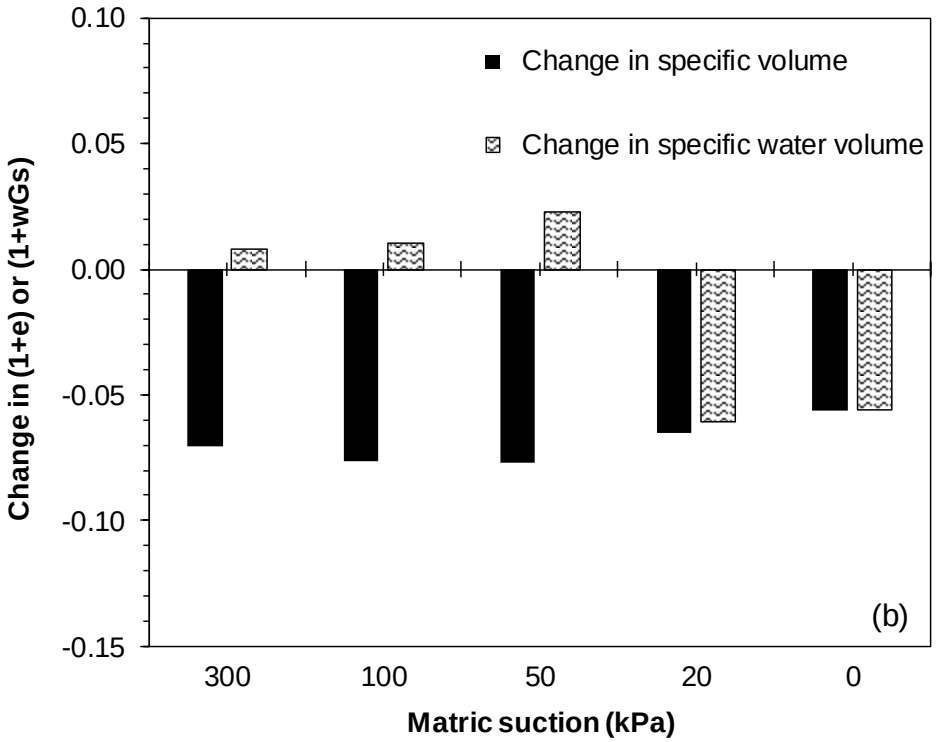
0.10
0.05
0.00
-0.05
-0.10
-0.15
Change in (1+e) or (1+wGs)
Change in specific volume
Change in specific water volume
(b)
300
100
50
20
0
Matric suction (kPa)

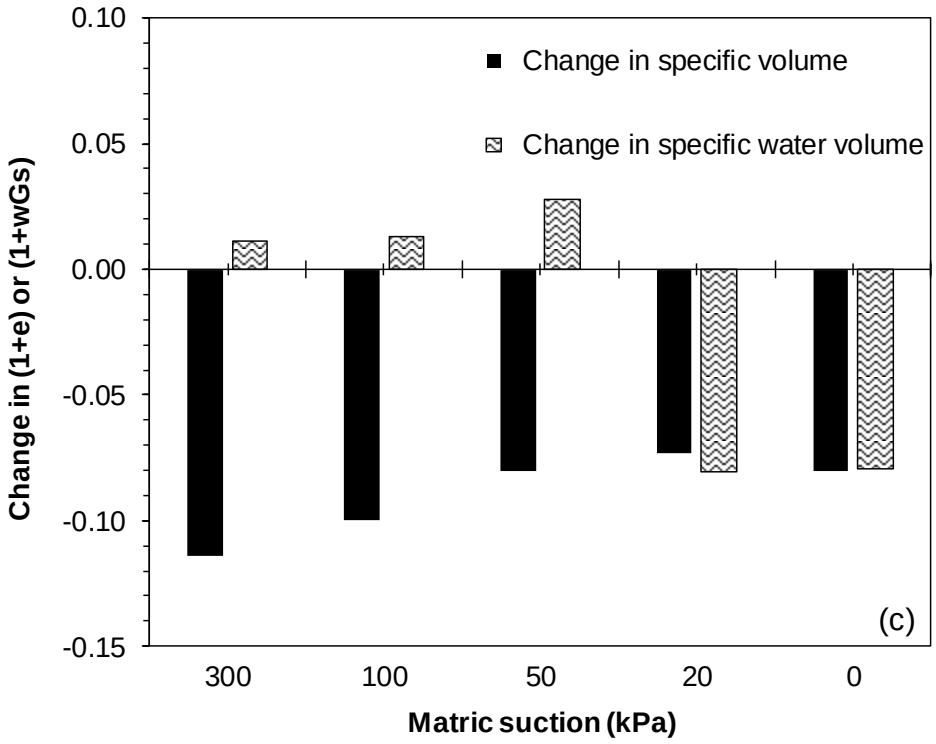

Figure 6.11 Comparison of the change in specific volume and specific water volume during shearing tests conducted at different suctions: (a) $(\sigma_3 - u_a) = 100$ kPa, (b) $(\sigma_3 - u_a) = 250$ kPa and, (c) $(\sigma_3 - u_a) = 400$ kPa

6.4 Concluding remarks

In this chapter, the results of saturated and unsaturated triaxial shear strength tests were carried out on statically compacting soil-water mixture at an initial water content of 10%, and a dry unit weight of 15 kN/m^3 was presented. The effective shear strength parameters were determined from the saturated tests under three confining stresses (100, 250 and 400 kPa). The suction-controlled triaxial shear strength tests were carried out under various magnitudes of applied suction (300, 100, 50, 20 kPa) and net confining stress (100, 250, and 400 kPa). The main features of soil behaviour during shearing (including shear strength, volume change, water content and degree of saturation) were determined and discussed. Effects of suction on the shear strength parameters were presented. The following points emerged from the test results.

i. The peak shear stress increased with an increase in the confining stress and decreased with a decrease in matric suction as the soil underwent the wetting process. Similar findings were reported by other researchers such as Escario and Sáez (1986), Vanapalli et al. (1996), Hillel et al. (1998), Cunningham et al. (2003), Lee et al. (2005), Zhan and Ng (2006), Eyob (2011) and Goh (2012).
ii. The soil exhibited a contraction behaviour and the amount of contraction increases with the applied net confining stress. Further, at lower net stress, the larger the applied suction, the less volumetric contraction were observed. However, at higher net confining stress stresses value, the maximum volumetric strain tends to increase with the applied suctions.
iii. At a constant value of net confining stress, the impact of the decrease in the soil suction during the wetting process was found to have a minor influence on the shape of the stress-strain curves.
iv. The friction angle ($\emptyset'$) slightly decreases, whereas the cohesion value (c) decreases significantly and non-linearly with a decrease in suction as the soil underwent the wetting process. This indicates that the angle $\emptyset^b$ increased with a decrease in suction to attain a maximum value at saturation. Similar findings have been reported by several researchers (Lu and Likos 2004; Murray and Sivakumar 2010; Fredlund et al. 2012).
v. An increase in the final water content and final degree of saturation values were observed of all specimens shearing at the suction greater than air explosion value of SWCCs. However, all specimens show a decrease in these values when shearing at suction very close or less than AExV.

vi. During shearing tests of the unsaturated specimens, the change in specific volume appears to be greater than the change in specific water volume.

CHAPTER 7

Validation of suction stress approach

7.1 Introduction

An effective stress principle is one of the key aspects where the hydraulic properties may be linked with the stress state and the mechanical properties of soils (Loret and Khalili 2002; Khalili and Zargarbashi 2010; McCartney 2018). To date, an increasing number of laboratory tests have shown that macroscopic effects from soil–water interaction when dealing with shear strength related problems have been sufficiently described by effective stress framework (Fredlund et al. 2012).

Many engineering projects may not be able to justify the measurement of the unsaturated shear strength relationship. However, an estimation of the unsaturated soil shear strength envelope provides the engineer with a significantly improved ability to analyse practical problems (Fredlund et al. 2012). In most cases, the estimated shear strength equations and models are based on the saturated shear strength parameters (c' and $\emptyset'$) and the SWCC of the soil (e.g., Vanapalli et al. 1996; Fredlund et al. 1996; Oberg and Sällfors 1997; Khalili and Khabbaz 1998; Rassam and Cook 2002; Loret and Khalili 2002; Vilar 2006; Lu and Likos 2006; Houston et al. 2008; Aloso et al. 2010; Sedano and Vanapalli 2010; Rojas et al. 2015; Patil et al. 2016; Han and Vanapalli 2016; Patil et al. 2017; Han et al. 2017; Patil et al. 2018). Consequently, there is continuity between the shear strength equations for saturated and unsaturated soils (Lu and Likos 2004; Houston et al. 2008; Fredlund et al. 2012).

An approach for studying the behaviour of unsaturated soils and examining the influence of changes in mean net stress and matric suction on the stress-strain behaviour of unsaturated soils is the use of suction stress concept proposed by Lu and Likos (2006). The part of effective stress resulting from soil moisture or soil suction variation can be defined by the suction stress characteristic curve (SSCC) (Lu et al. 2010; Oh et al. 2012; Almahbobi et al. 2018). The most significant advancements of the effective stress with

the SSCC are its complete avoidance of the problems associated with Bishop's parameter χ and its ability to physically describe the effective stress change for all types of soils (Lu et al. 2010; Oh et al. 2013).

Studies in the past have provided some key validations of suction stress model of Lu et al. (2010) based on the shear strength and volume change behaviour of different types of soils (Oh et al. 2012; Baille et al. 2014; Oh et al. 2013; Pourzargar et al. 2014; Oh and Lu 2014; Kato et al. 2012; Lu et al. 2014; Alsherif and McCartney 2014; Baille et al. 2016; Maleksaeedi et al. 2017). These studies have provided some significant step forward to consider effective stress as the sum of net stress and suction stress. Oh et al. (2012) have shown that suction stress of residual soil based on water retention tests and that determined from the shear strength tests remained within tens of kilopascals. However, detailed studies of the suction stress characteristic curve (SSCC) of collapsible soils derived from both shear strength and volumetric variables under isotropic conditions and for a large range of suction and higher stress levels have not yet been fully examined and the validity of the effective stress principle by conducting suction stress concept is still a matter of intense discussion for this type of soil especially by using a modified triaxial apparatus.

The motivation for the use of suction stress approach for this particular soil is based on two major hypotheses: firstly, the collapse strain processes that occur during wetting in collapsible soils could not be predicted using the Bishop's effective stress approach because this approach was defined only in stress state with no reference to volume change (Jennings and Burland 1962). Secondly, the application of the effective stress parameter for collapsible soils was found to be challenging, and under changing suction and net stress conditions, there were some uncertainties in its uniqueness (Garakani et al. 2015). Therefore, interpret the collapsing phenomenon by suction stress approach need a new light.

The objectives of this chapter were; (*i*) to study the effects of step-wise suction reduction and the confining stress on the SSCCs of collapsible soil, (*ii*) to investigate the validity of the SSCCs of collapsible soils derived based on suction - degree of saturation SWCCs at various applied confining stresses and shear strength test data at several suctions and (*iii*) to study the validity of the effective stress principle of the statically compacted collapsible soil.

This chapter is presented in several sections. The methods used to establish the SSCC were described in section 7.2. Section 7.3 presents the test results and discussion. The results involving the impact of confining stress and suction on the SSCCs is studied. The inferred SWCC and SSCC based on the CD triaxial compression tests and the SWCCs are cross-compared and discussed. The uniqueness of the critical state line in the deviatoric stress–effective mean stress are investigated, and the application of the effective stress principle to volume change in collapsible soil is demonstrated. Bishop's effective stress approach is presented and discussed. The concluding remarks are presented in section 7.4.

7.2 Suction stress approach

Lu and Likos (2006) extended Bishop's effective stress by modifying the matric suction contribution to the effective stress (σ') as follows:

$$\sigma' = (\sigma - u_a) - \sigma^s \tag{7.1}$$

Later, Lu et al. (2010) established closed-form equations for suction stress, either as a function of suction ($u_a - u_w$) (Equation 7.2) or effective degree of saturation (S_e) (Equation 7.3).

$$\sigma^s = -(u_a - u_w)\left[\frac{1}{1+\{\alpha(u_a-u_w)\}^n}\right]^{1-1/n} \tag{7.2}$$

$$\sigma^s = -\frac{S_e}{\alpha}\left(S_e^{\frac{n}{1-n}} - 1\right)^{\frac{1}{n}} \tag{7.3}$$

The van Genuchten (1980) fitting parameters (α and n) that are required for establishing suction stress in terms of suction and effective degree of saturation using

Equations (7.2) and (7.3) can be determined from the suction – effective degree of saturation relationship using Equation 5.5.

Lu et al. (2010) stated that if $n \leq 2$, the suction stress decreases with an increase in suction, whereas if $n > 2$, the suction stress decreases and then increases with an increase in suction. Lu et al. (2010) noted that the air-entry parameter (α) controls the minimum value of suction stress, whereas the pore size distribution parameter (n) controls the effective degree of saturation corresponding to the minimum suction stress (Oh et al. 2012; Almahbobi et al. 2018).

From saturated and unsaturated shear strength test results, the SSCC can be established (Lu and Likos 2006; Lu et al. 2010). For triaxial tests, the mean total stress is defined as $p = (\sigma_1 + 2\sigma_3)/3$, and the mean effective stress is defined as $p' = (\sigma_1 + 2\sigma_3)/3 - u_a - \sigma^s$. Suction stress at a known suction value can be evaluated by projecting the unsaturated failure envelope linearly onto the (p - u_a) axis. By evaluating suction stress values at shear failure under different matric suctions, the SSCC can be quantified. The failure criterion can be defined by the effective stress in terms of mean effective stress (p') and deviatoric stress (q) as follows (Oh et al. 2012; Oh et al. 2013; Oh and Lu 2014):

$$q_f = d' + MP_f' \tag{7.4a}$$

or regarding suction stress, as follows

$$q_f = d' + M(p - u_a)_f - M\sigma^s \tag{7.4b}$$

in which, on ($p - u_a$) - q space, M is the slope of the failure envelopes, and d' is the intercept of the failure envelope corresponding to the saturated condition. The subscript f refers to the state of failure.

In triaxial tests, the saturated friction angle and cohesion can be derived from M and d as follows (Oh et al. 2012; Oh et al. 2013):

$$\emptyset' = sin^{-1}\{3M/(6+M)\} \quad (7.5)$$

$$c' = \frac{d}{M}\, tan\emptyset' \quad (7.6)$$

Suction stress (σ^s) as a function of matric suction can be calculated from the stress state at failure from Equation 7.4 (Oh and Lu 2014):

$$\sigma^s = \frac{d'+M(P-u_a)_f-q_f}{M} \quad (7.7)$$

7.3 Results and discussion

7.3.1 The effects of confining stress and suction on the SSCCs

The suction stress characteristic curves (SSCCs) in terms of suction and effective degree of saturation were established from the wetting water retention data (see chapter 5, Tables 5.1 and 5.2 and Figure 5.10) at various applied confining stresses and suctions are presented in section 7.3.1.1. Similarly, the SSCC and SWCC were established based on the shear strength test data (see chapter 6, section 6.3.1 and 6.3.2) are presented in section 7.3.1.2. The influence of volumetric strain on the shape of the SSCCs and the magnitudes of the minimum and maximum suction stresses were explored. The SSCCs established from the two sources were compared in section 7.3.2. The SWCCs determined from experimental water retention data and established based on the shear strength test data were also compared in section 7.3.2.

7.3.1.1 Water absorption behaviour and suction stress

The values of α and n that were obtained from SWCCs in terms of effective degree of saturation based on Equations 5.5 (see chapter 5, Table 5.3) were used to establish the SSCCs in terms of suction and effective degree of saturation based on Equations 7.2 and

7.3, respectively. The SSCCs in terms of suction and the effective degree of saturation at various net confining stresses (100, 250 and 400 kPa) are shown in Figures 7.1 and 7.2, respectively.

It can see from the test results in Figures 7.1 and 7.2 that the influence of confining stress on the SSCCs for the soil studied was found to be insignificant with a difference in the magnitude of the suction stress no more than 5 kPa in all cases. Oh and Lu (2014) experimentally examined the effect of confining stress (up to 200 kPa) on the SSCCs under both drying and wetting conditions through the silty sand soil. They stated that SSCCs are almost independent of the confining stress. The results presented in Figure 7.1 show that the magnitude of suction stress is about 100 kPa with an applied suction of 500 kPa. With a decrease in suction, suction stress increased (or became less negative). At smaller applied suctions, the values of suction stress followed the line, $- \sigma^s = (u_a - u_w)$. The shape of the SSCCs in terms of suction was found to be in accordance with the n value (Lu et al. 2010) that were less than 2.0 for all cases. The results presented in Figure 7.2 show that the magnitude of minimum suction stress is about 6500 kPa at a very dry state (effective degree of saturation of 0 kPa). With an increase in the effective degree of saturation as the collapsible soil underwent the wetting process, suction stress increased monotonically. Further, the SSCC was found to be shifted very slightly to an upward direction with increasing confining stress.

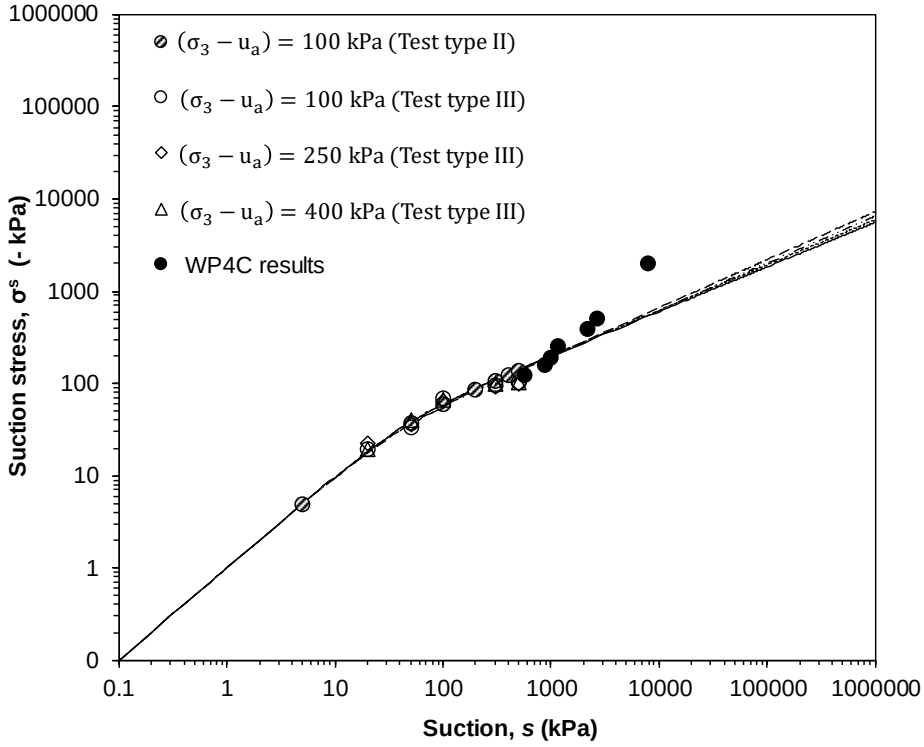

Figure 7.1 Suction stress characteristic curves in terms of suction at various confining stresses based on water absorption and volume change

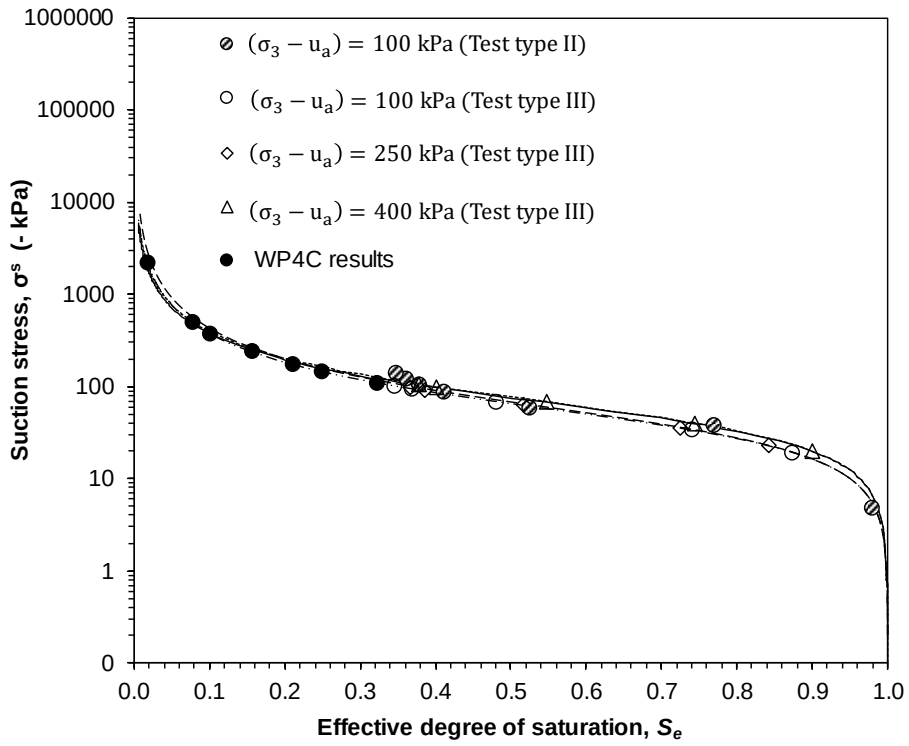

Figure 7.2 Suction stress characteristic curves in terms of effective degree of saturation at various confining stresses based on water absorption and volume change

7.3.1.2 Shear strength and suction stress

Figure 7.3 shows the failure envelopes for both saturated and unsaturated conditions of the soil in ($p - u_a$) - q space. The unsaturated failure envelopes were found to be all parallel and higher than the saturated failure envelope. The tests results agree well with the findings reported in the literature (i.e., Escario and Sáez 1986; Fredlund and Rahardjo 1993b; Vanapalli et al. 1996; Cunningham et al. 2003; Lee et al. 2005; Jotisankasa 2005; Zhan and Ng 2006; Hossain and Yin 2010). The variation of M with suction is also shown in Figure 7.3. The value of M was found to remain very similar for a matric suction range of 0 to 300 kPa.

The unsaturated shear strength data can be used to infer suction stress for each individual value of matric suction as illustrated in Figure 7.4. The suction stress values corresponding to various applied suctions (i.e., SSCC from shear strength tests) are plotted on the bottom left of Figure 7.4. The experimental data were best-fitted using Equation 7.2. The best-fit parameters α and n were found to be 0.018 1/kPa and 1.601, respectively.

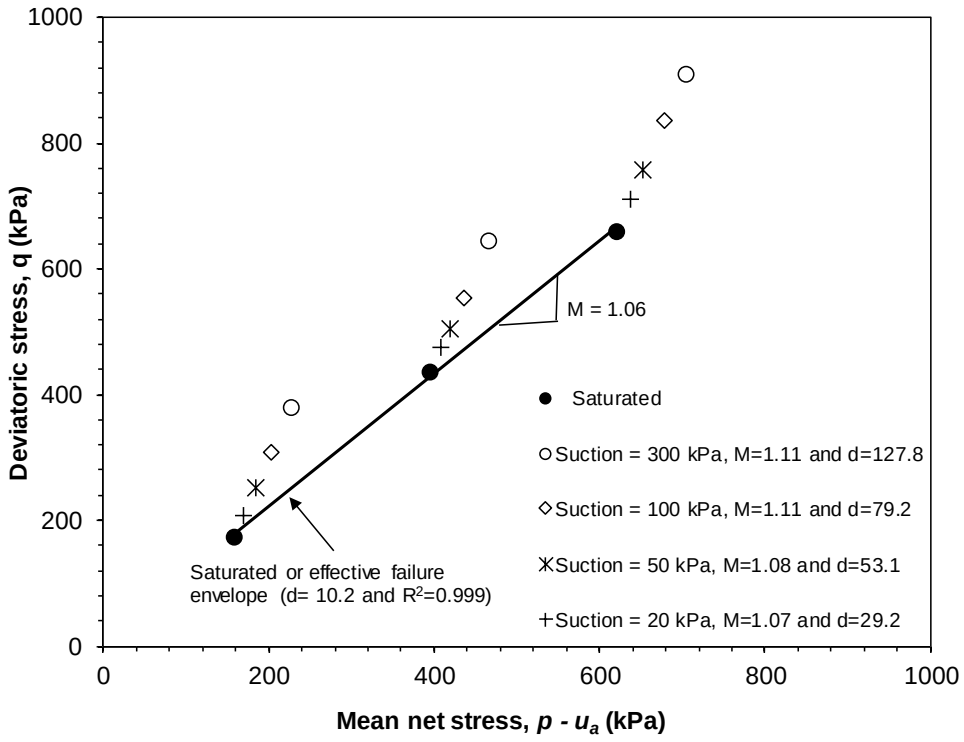

Figure 7.3 Failure criteria from the triaxial test results in the ($p - u_a$) - q space

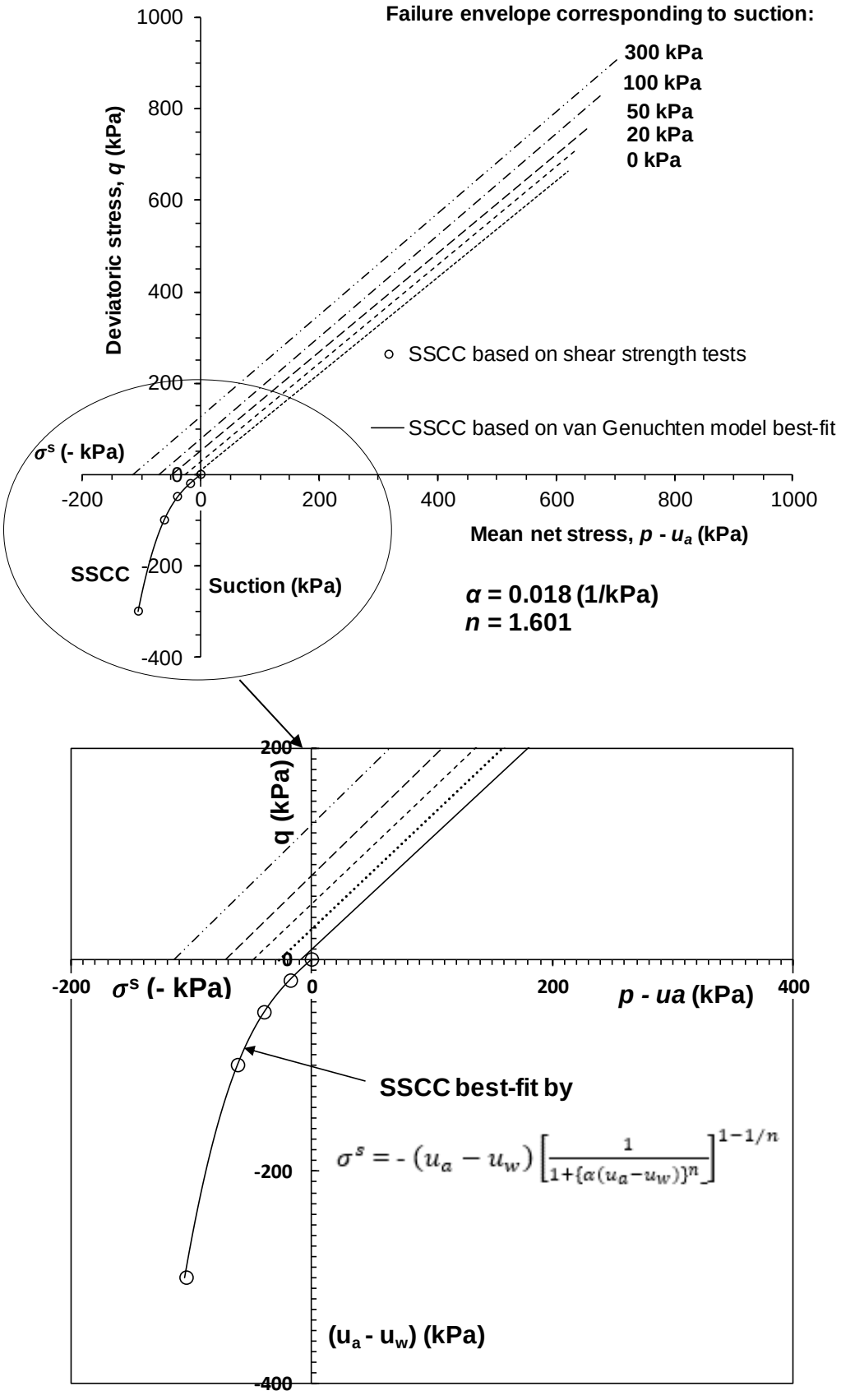

Figure 7.4 Suction stress characteristic curve from Mohr-Coulomb failure envelopes in (p - u_a) – q space

7.3.2 Validation of the intrinsic relationship between SSCC and SWCC

To study the interrelationship between SSCCs and SWCCs for the collapsible soil during the wetting process, two types of comparison were conducted: (*i*) the SSCCs that were established based on the SWCCs and based on the shear strength tests on saturated and unsaturated soil specimens were compared, and (*ii*) the measured SWCCs and SWCC inferred from the SSCC based on shear strength tests data were compared. A cross-examination between SWCC and SSCC determined from the two independent types of tests (wetting under isotropic stress conditions tests and shear strength tests) can be used to examine the intrinsic relationship between water absorption and shear strength of unsaturated collapsible soils.

Figure 7.5 presents the SSCCs that were established based on the SWCCs and the shear strength tests on saturated and unsaturated soil specimens of the statically compacted collapsible soil. The shapes of the SSCCs can be found to be similar from both approaches. At a suction of 500 kPa, a difference in the suction stress based on the SWCC at confining stress of 400 kPa and the SSCC from the shear strength tests was found to be about 12 kPa. At smaller suctions and at lesser confining stresses, the differences were lesser. This result is indicating the intrinsic relationship between SWCC and SSCC for collapsible soil. Studies in the past have provided some key validations of suction stress approach based on the shear strength and SWCC for nondeformable soils (Lu et al. 2010, Oh et al. 2012, Chen et al. 2013; Oh and Lu 2014, Oh and Lu 2014 and Lu et al. 2014). Lu et al. (2014) stated that the mathematical equation for the SWCC is intrinsically related to the mathematical equation for the SSCC by examining the shear-strength and soil-water retention test results reported in the literature for six soils ranged in texture from sandy to silty to clayey, suggesting that the SWCCs and the SSCCs are consistent. Oh and Lu (2014) examined the SSCCs under both drying and wetting conditions through silty sand. They found that the SSCC inferred from the shear strength tests was similar to that from the SWCC measurement under the respective wetting. Under drying conditions, such uniqueness is not as clear as that of the wetting branch. The results of this study differ from Haeri et al. (2017) test results. They compare the measured suction stress values from triaxial shear strength tests and those calculated using Lu et al.'s (2010)

approach for loessial soil specimens. Based on their results, the proposed framework by Lu et al. (2010) underestimates the suction stress for reconstituted specimens.

The fitting parameters (α and *n*) inferred from SSCC based on shear-strength test results (see section 7.3.1.2) were used to calculate SWCC of a collapsible soil for a large range of suction. Figure 7.6 shows the measured SWCCs based on water retention data and SWCCs calculated by using the triaxial test results. The SWCC based on the shear strength tests and the SWCCs were found to be very similar with a difference in the magnitude of the degree of saturation of less than about 4%. This result is reconfirming the intrinsic relationship between SWCC and SSCC. Oh et al. (2012) have found that the SWCC inferred from the triaxial shear-strength tests can predict the soil-water retention data very well for various residual soils under different remoulding conditions. Lu et al. (2014) have found similar results when examined the shear strength and soil-water retention test results reported in the literature for six soils that ranged in texture from sandy to silty to clayey.

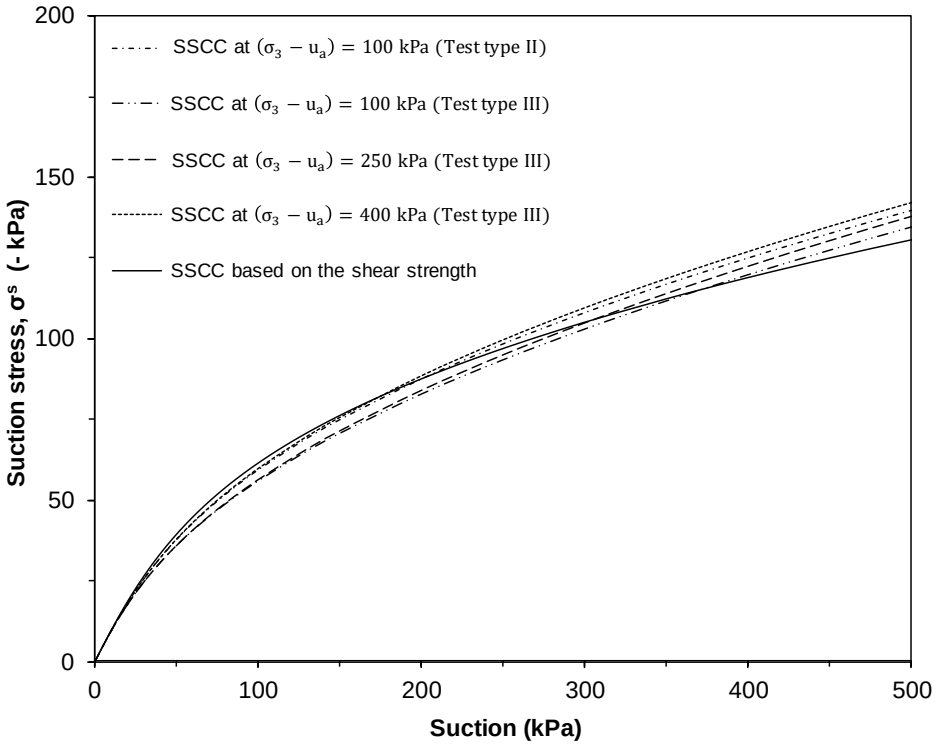

Figure 7.5 Suction stress characteristic curves (SSCCs) in terms of suction from SWCCs and shear strength tests

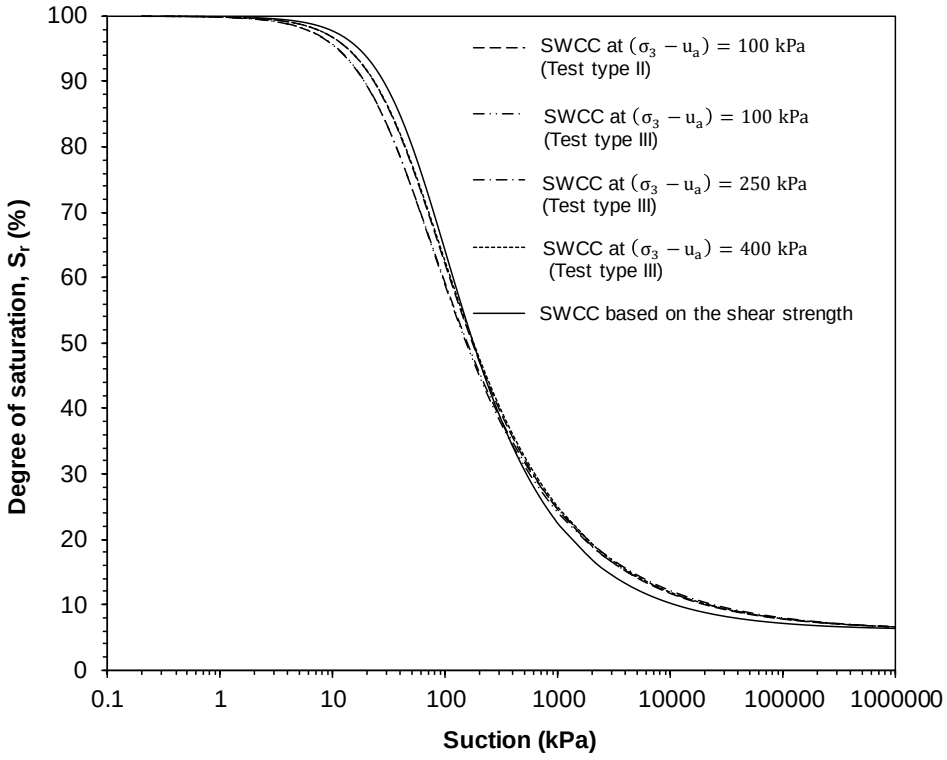

Figure 7.6 Soil water characteristic curves (SWCCs) in terms of degree of saturation from measured data and shear strength tests

7.3.3 Effects of the suction stress on the effective stress

The impact of suction stress approach on the effective stress was investigated by several researchers for several types of soils (Karube et al. 1997; Kato et al. 2001; Khalili et al. 2004; Lu and Likos 2006; Chae et al. 2010; Kim et al. 2010; Oh and Lu 2014; Pourzargar et al. 2014; Haeri et al. 2015; Nuth and Laloui 2008). However, the impact of the effective stress based on the suction stresses model of Lu et al. (2010) on the volumetric strain of collapsible soils has not been fully explored yet.

The uniqueness of the critical state line in the deviatoric stress and effective mean stress plane was explored in the past by many researchers (Geiser 1999; Wheeler and Sivakumar 1995; Cui and Delage 1996; Maatouk et al. 1995; Khalili et al. 2004; Oh et al. 2012). Oh et al. (2012) evaluated the SSCC for Korean residual soils and found that the failure criteria were defined uniquely for all saturations with the effective stress, confirming that the SSCC-based effective stress concept is valid for the failure behaviour of residual soils. However, the literature is limited in this aspect for the collapsible soils. Therefore, such uniqueness still needs to explore for the collapsible soils based on suction stress approach during the wetting process especially by using triaxial compression tests.

Figure 7.7 shows the volumetric strain – effective stress results based on the suction stress that, in turn, were established from the SWCCs under various applied net confining stresses (100, 250 and 400 kPa) (see section 7.3.1.1). The effective stress was calculated based on Equation 7.1. The volumetric strain is the measured values at various confining stresses during the wetting process have been presented in Figure 5.4. The results clearly showed that the trend of SSCC during the wetting process was reflected in the effective stress behaviour. The results presented in Figure 7.7 show that the magnitude of effective stress was about 230 kPa at the minimum volumetric strain value. Further, at any applied net confining stress, the magnitude of volumetric strain increases with a decrease in the effective stress as the collapsible soil underwent the wetting process. The effective stress, for example, corresponding to the maximum volumetric strain value of the single specimen (Test type II) at the suction of 5 kPa was found to be 100 kPa. The volume decreases in the specimen tested in this study while the effective stress decreases at the same time (see Figure 7.7) is attributed to the collapse of the open pore structure in collapsible soils which is due primarily to a decrease in the shear strength at interparticle level is observed to be much higher than the amount of elastic rebound due to the effective

stress decrease. Barden et al. (1973) and Fredlund and Gan (1994) conducted laboratory tests on collapsible soil. They explained that the phenomenon of the collapse was a conflict of the principle of effective stress, as wetting cause increase in pore pressures, as a result, decrease the effective stress and hence is expected to cause swell rather than collapse. However, more detailed consideration of the mechanism indicated the collapse of dry collapsible soil is due to the loss in the normal stress between soil particles leading to local shear failure as a result of a reduction of suction from wetting, and hence is appropriate with the principle of effective stress. Baille et al. (2014) have found that a decrease in suction stress due to a decrease in suction from a very dry state of the clays would increase the effective stress, which in turn cause compression of Spergau kaolin and NX illite, whereas a decrease in suction causing an increase of suction stress aids in decreasing the effective stress, which in turn causes swelling of bentonite.

Volumetric strain during the wetting process versus effective stress based on the suction stress at different suction values was presented in Figure 7.8. It is noticed that at each value of suction an increase in the absolute value of volumetric strain as the effective stress increases due to an increase in net confining stress.

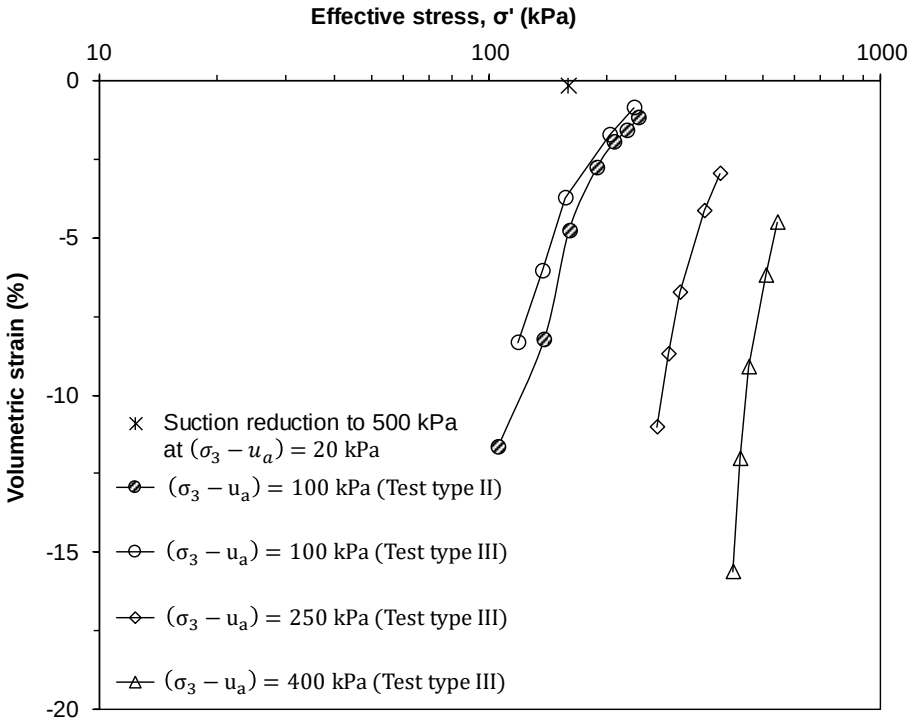

Figure 7.7 Volumetric strain versus mean effective stress at various confining stresses during the wetting process

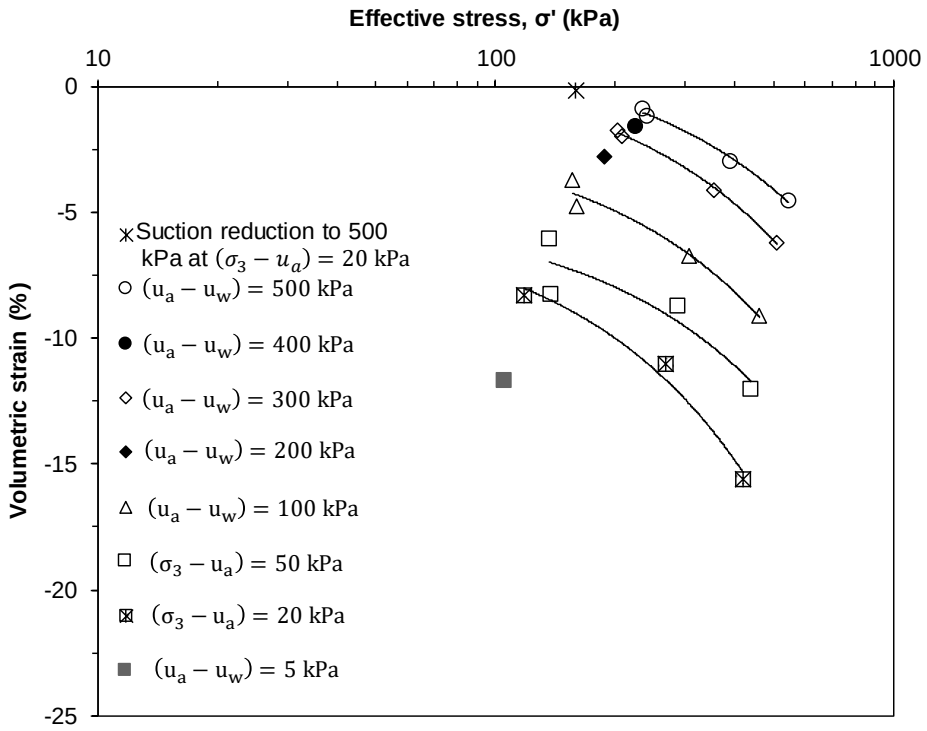

Figure 7.8 Volumetric strain versus effective stress at different suction values during the wetting process

Figure 7.9 presents the test results in terms of the maximum deviatoric stress (see chapter 6, Figure 6.4a and 6.7) versus the mean effective stress (p') based on the suction stress that was derived from triaxial test results at different values of suction. Figure 7.9a shows the best-fit saturated and unsaturated shear strength data in the q-p' plane. The test results indicate that the best-fit unsaturated shear strength data (M = 1.10, d'= 6.06 kPa and R^2 = 0.998) was found to be very similar to the saturated best-fit data (M =1.06, d'= 10.16 kPa and R^2 = 0.999). Figure 7.9b shows the saturated critical-state line (CSL) through the origin with unsaturated shear strength data at different suction values (300, 100, 50, 20 and 0 kPa) in the q-p' plane. As is shown, most data points plot for the range of the suction values tested were found to be close to the critical state line, defined using the saturated test data, confirming the uniqueness of the CSL for both saturated and unsaturated states in the effective stress approach based on suction stress concept for the collapsing soil specimens. Fredlund et al. (1987) and Alonso et al. (1990) stated that the deviator stress applied to the specimens during shear destroys the initial soil fabric of the tested specimens, producing an ultimate soil structure which is very similar in all specimens, independent of the applied state of stress and stress paths (Wheeler and Sivakumar 1995; Khalili et al. 2004).

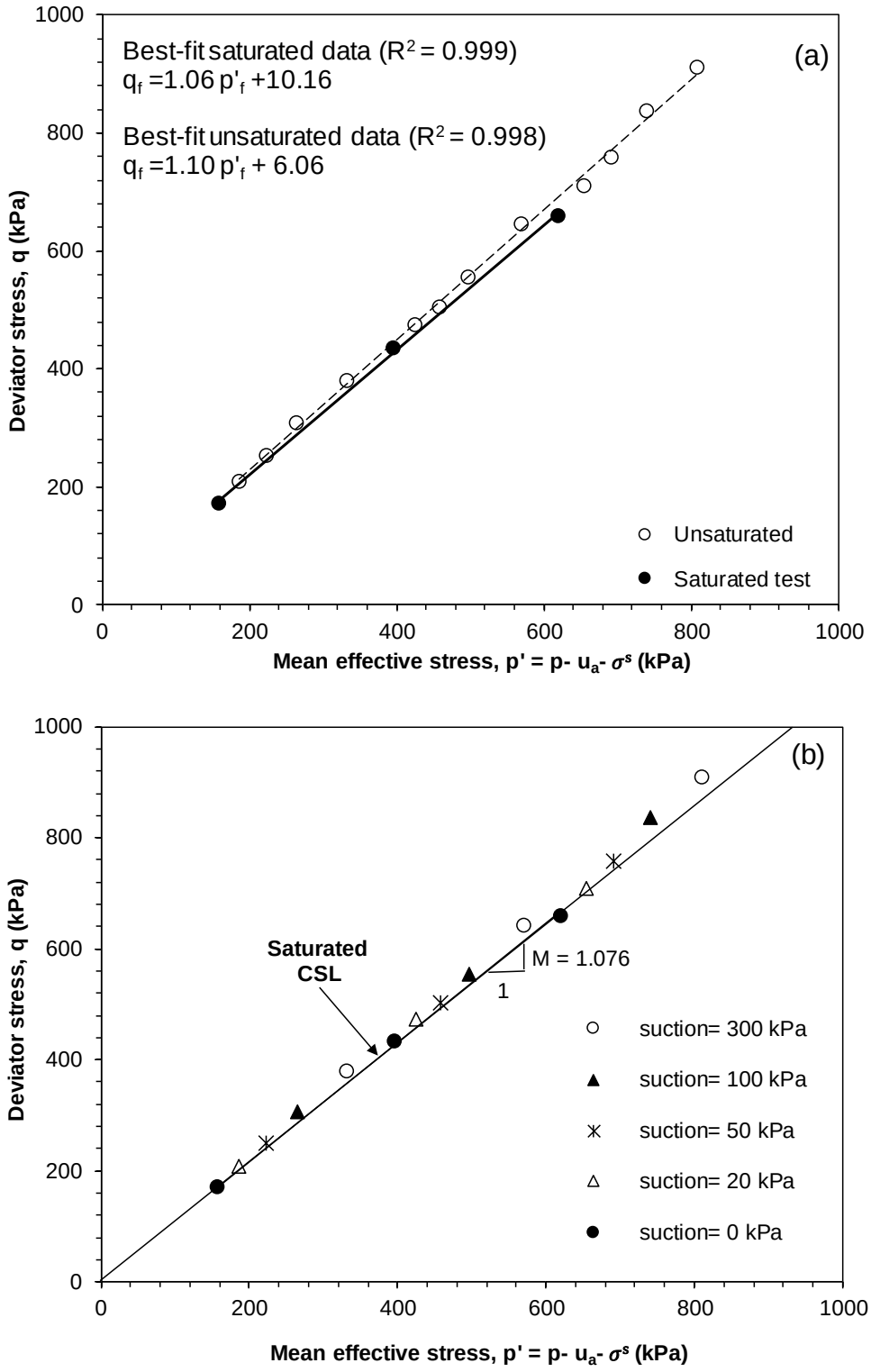

Figure 7.9 Peak deviator stress versus the mean effective stress (p') defined as net mean stress (= (σ_1 + 2σ_3)/3-u_a) plus suction stress (σ^s) derived from shear strength (a) unsaturated and saturated best-fit shear strength data (b) CSL

For the effective stress principle to be valid, it must be applicable to both the volume change as well as the shear strength data (Khalili et al. 2004). The specific volume of the collapsible soil specimens during CD shearing tests at different suctions and net confining stress are plotted in Figure 7.10 as a function of the corresponding mean effective stress based on the suction stress values. In this figure, there is a clear trend of decreasing in specific volume as the mean effective stress decrease during the triaxial shearing process.

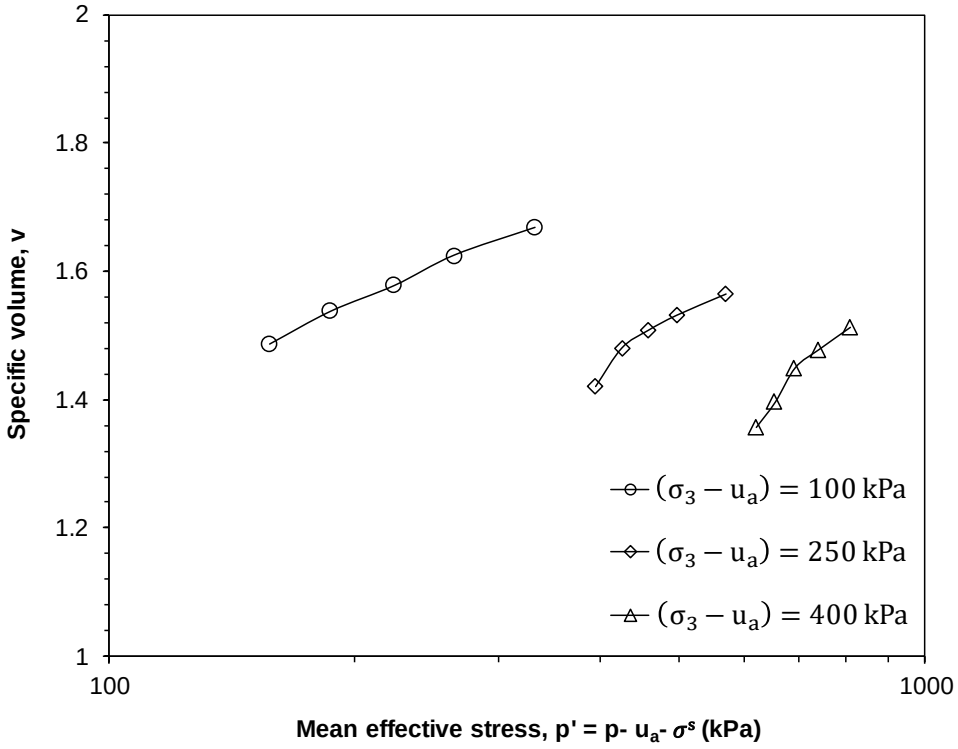

Figure 7.10 Specific volume versus mean effective stress from shearing tests

7.3.4 The applicability of effective stress-based on the SSCC for collapsible soil

Studies in the past stated that the suction stress approach (Lu and Likos 2004, 2006; Lu et al. 2010) has been shown to better conjugate the effective stress in describing the shear strength behaviour of unsaturated soils for the entire range of degree of saturation and the findings of Lu et al. (2010) study will help to the elimination of the need for any new shear strength criterion for unsaturated soil (Lu et al. 2010; Oh et al. 2012). Kim et al. (2010) proposed suction stress-soil water retention curve method to

evaluate effects of suction on the shear strength of unsaturated soils under low confining pressure using developed direct shear testing equipment for compacted weathered granite soils. They have been found that the stress states at the peak shear strength point are on the same failure line for the saturated state when the suction stress is treated as a component of confining stress. It is also noted that the estimated unsaturated shear strengths using the suction stress-soil water retention curve method agree well with the measured values from laboratory testing. Kim et al. (2013) also reported that the unsaturated shear strength could be estimated by means of the concept of the suction stress.

Figure 7.11 shows the measured peak deviator stresses data determined from saturated and unsaturated shear strength tests and those calculated based on suction stresses verse suction. It can be seen from this figure that the measured and calculated deviator stresses were found to be very similar. This good agreement indicates that the suction stress approach is reliable for estimating unsaturated shear strength for collapsible soil under the triaxial condition for a large range of suction and higher stress level.

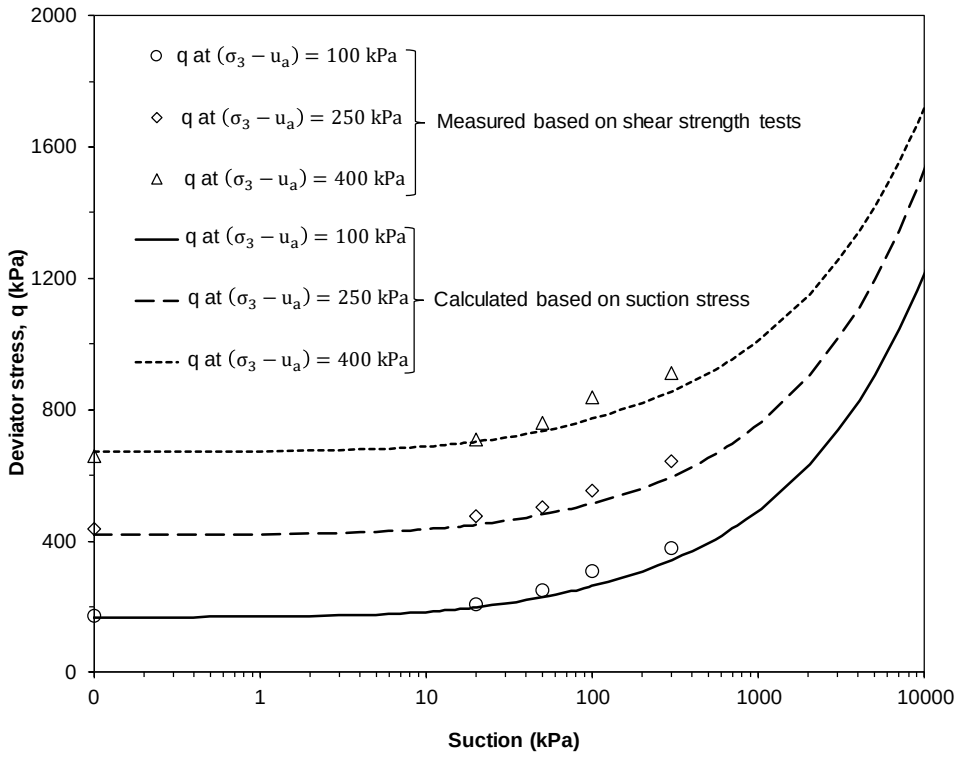

Figure 7.11 Measured (shear strength tests) and calculated (based on suction stress) peak deviator stresses verse suction

7.3.5 Effects of Bishop's parameter on the effective stress

Determination of the Bishop effective stress parameter is essential in order to evaluate effective stress in unsaturated soil (Lu and Likos 2004). Many attempts have been made in the past to quantify Bishop's effective stress parameter (χ) theoretically and experimentally (Khalili and Khabbaz 1998; Nuth and Laloui 2008; Pourzargar et al. 2014; Heibrock et al. 2018). However, many of these relationships were developed based on shear strength data under the drying process. Indeed, there is currently very limited information on the variation of effective stress parameter (χ) along the wetting path. Curvature in the shear strength envelope results in nonlinearity of the χ parameter. As a result, there were various χ values corresponding to different matric suction values for envelopes which are curved with respect to matric suction (Fredlund et al. 2012). This section describes some of the most citation approaches have been included in literature to define Bishop's effective stress parameter (χ) for the soil studied. It can be noticed that these approaches are mathematically the same but physically are different. Based on these approaches' different values of the χ parameter were determined and presented in Table 7.1.

i. The shear strength computed using Fredlund et al. (1978) shear strength equation (Equation 2.7) can be made to be equal to the shear strength given by Bishop et al. (1960) equation (Equation 2.8) (Lu and Likos 2004). Then it is possible to illustrate the relationship between $\tan \emptyset^b$ and χ (Delage 2002; Ng and Menzies 2007; Fredlund et al. 2012) as follows:

$$(u_a - u_w) \tan \emptyset^b = \chi (u_a - u_w) \tan \emptyset' \quad (7.8a)$$

$$\chi = \frac{\tan \emptyset^b}{\tan \emptyset'} \quad (7.8b)$$

where $\emptyset^b$ and $\emptyset'$ were determined from shear strength test results (see chapter 6, section 6.3.1 and 6.3.2).

ii. Khalili and Khabbaz (1998), based on experimental results from 13 different soils, proposed the following expression of Bishop's χ parameter to describe the shear strength of unsaturated soils (Delage 2002; Lu and Likos 2004; Tavakoli et al. 2014):

$$\chi = \left\{\frac{(u_a - u_w)_f}{(u_a - u_w)_b}\right\}^{-0.55} \tag{7.9}$$

where $(u_a - u_w)_f$ = matric suction in the specimens at failure conditions, $(u_a - u_w)_b$= the air- expulsion value that was determined from SWCC during the wetting process (see chapter 5, Table 5.4). An average value of 39 kPa for the air- expulsion value was adopted for the purposes of this investigation.

iii. Some studies have proposed using an effective degree of saturation (S_e) as the parameter χ (Vanapalli and Fredlund 2000; Romero and Vaunat 2000; Tombolato and Tarantino 2005; Sawangsuriya et al. 2008; Alonso et al. 2010; Lu et al. 2010). The value of χ then defined as follow:

$$\chi = S_e = \frac{S_r - S_{res}}{1 - S_{res}} = \left\{\frac{1}{1 + [\alpha(u_a - u_w)]^n}\right\}^{1-1/n} \tag{7.10}$$

iv. From triaxial testing, the M-C criterion can be written as (Lu and Likos 2004):

$$(\sigma_1 - u_a)_f = (\sigma_3 - u_a)_f \, tan^2\left(\frac{\pi}{4} + \frac{\emptyset'}{2}\right) + 2c_1' \, tan\left(\frac{\pi}{4} + \frac{\emptyset'}{2}\right) \tag{7.11a}$$

$$c_1' = c' + \chi(u_a - u_w) \, tan \, \emptyset' \tag{7.11b}$$

Rearranging Equation 7.11 leads to χ values at a given matric suctions can be measured experimentally based on shear strength tests data (see chapter 6, section 6.3.1 and 6.3.2) as follows:

$$\chi = \frac{(\sigma_1 - u_a) - (\sigma_3 - u_a)\tan^2\left(\frac{\pi}{4}+\frac{\emptyset'}{2}\right) - 2c'\tan\left(\frac{\pi}{4}+\frac{\emptyset'}{2}\right)}{(u_a - u_w)\left[\tan^2\left(\frac{\pi}{4}+\frac{\emptyset'}{2}\right) - 1\right]} \tag{7.12}$$

Figure 7.12 shows the variation of the single stress state variable (χ) that were determined based on the methods adopted (i to iv) with suction. The χ values were found to be nearly identical.

Table 7.1 Bishop's effective stress variable values (χ)

Suction (kPa)	χ parameter			
	i	ii	iii	iv
300	0.37	0.33	0.35	0.35
100	0.66	0.60	0.62	0.62
50	0.82	0.87	0.79	0.80
20	0.90	1.00	0.93	0.89

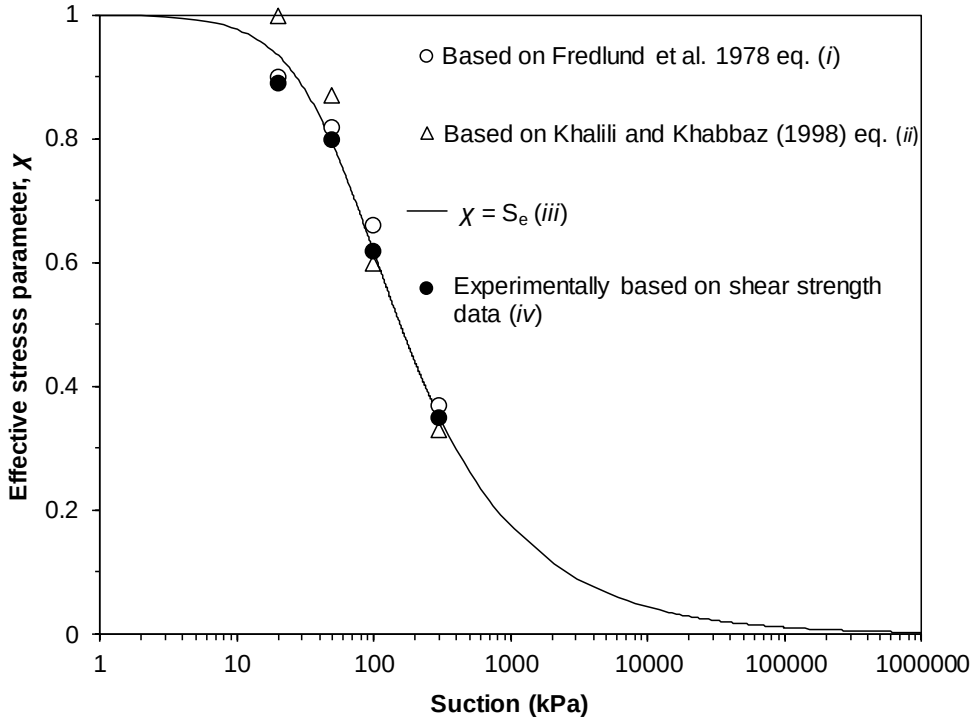

Figure 7.12 Variation of the single stress state variable (χ) with suction

Figure 7.13 presents the critical state line (CSL) in the deviatoric stress–effective mean stress based on the Bishop's effective stress parameter that was obtained based on Khalili and Khabbaz (1998) equation (Equation 7.9) at various values of suction for saturated as well as unsaturated soils. The results show that the unsaturated data points were found to be almost close to the saturated critical state line.

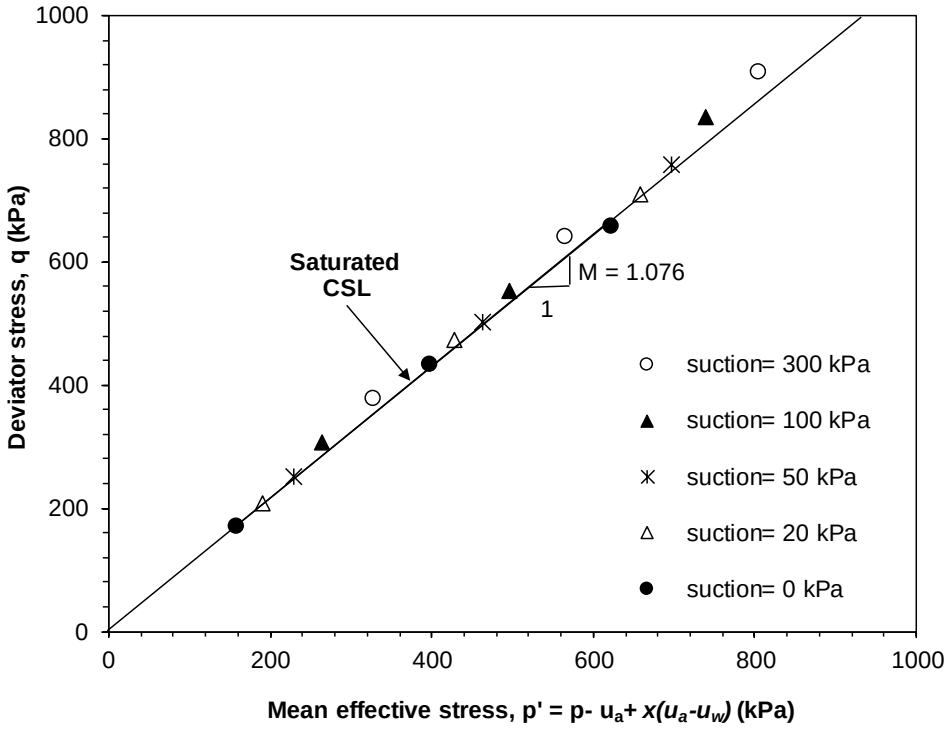

Figure 7.13 Peak deviator stress versus the mean effective stress (p') defined as net mean stress (= (σ_1 + 2σ_3)/3-u_a) plus χ (u_a-u_w) (where χ derived from Khalili and Khabbaz (1998) eq.)

Equation 7.12 was used to calculate the peak deviator stress ($\sigma_1 - \sigma_3$) for a large range of suction based on the effective stress parameter χ that was obtained from Khalili and Khabbaz (1998) equation (Equation 7.9) (Bishop and Blight 1963; Sivakumar 1993; Khalili et al. 2004; Lu and Likos 2004). Figure 7.14 shows the measured and the calculated (based on χ the parameter) deviator stresses versus suction. These results show that the measured strength from the triaxial compression tests for the collapsed specimens were matched well with these established based on Bishop's effective stress parameter (χ).

Figure 7.15 compares the calculated deviator stress values based on χ parameter on the y-axis with the values of deviator stress measured experimentally from the triaxial compression tests at various net confining stresses and suctions (on the x-axis). As presented in this figure, the calculated values tend to be similar to the measured data at low suction and slightly different at high suction. Oh et al. (2012) stated that the interparticle physicochemical force could not be captured accurately by using Bishop's effective stress when suction is high.

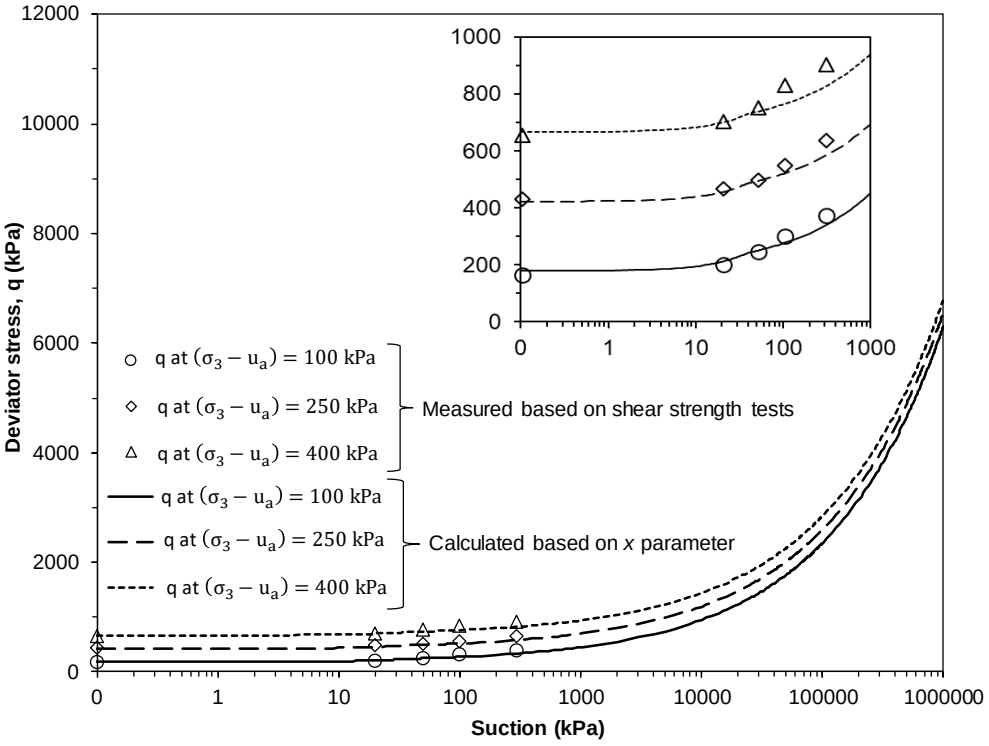

Figure 7.14 Measured and calculated deviator stress (based on effective stress parameter χ from Khalili and Khabbaz (1998)) at various net confining stresses versus suction

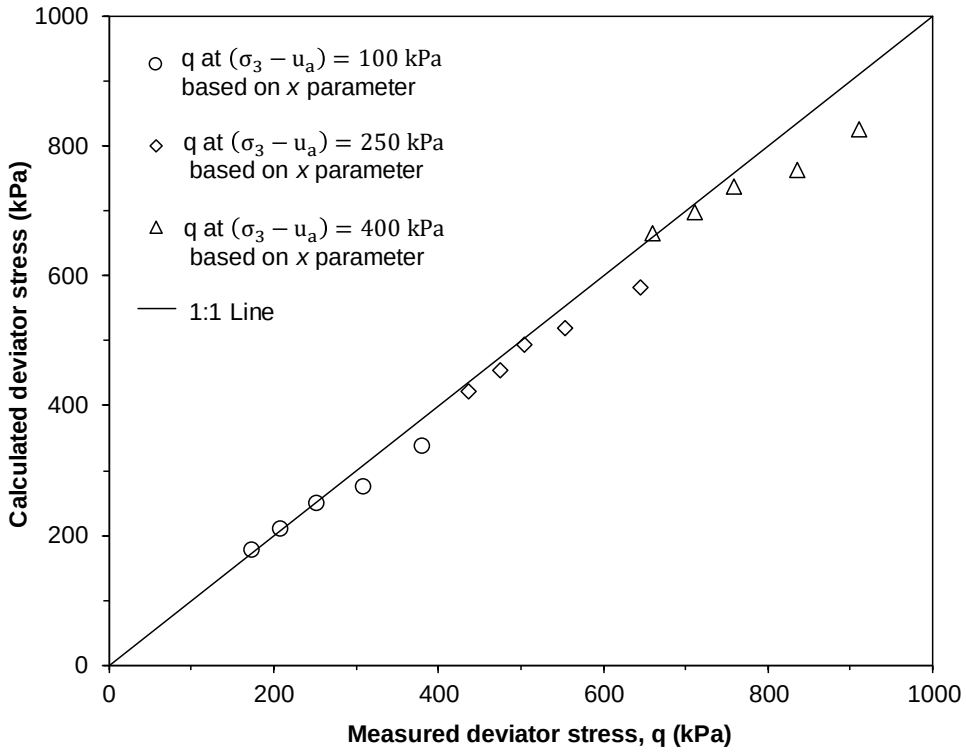

Figure 7.15 Measured deviator stress values versus calculated deviator stress (based on effective stress parameter χ from Khalili and Khabbaz (1998)

7.4 Concluding remark

Based on the suction stress approach the suction stress characteristic curves (SSCCs) of the soil studied were established from the SWCCs and from the shear strength test results. The impact of confining stress and suction on the SSCCs of the soil was studied. The uniqueness of the SSCC deduced independently from both the SWCCs and the shear strength test results were investigated. The SWCC was established from shear strength test results during the wetting process and compared with the experimental water retention data. The uniqueness of the critical state line in the deviatoric stress–effective mean stress based on suction stress for saturated as well as unsaturated soils were investigated, and the application of the effective stress principle based on suction stress to volume change in collapsible soil was demonstrated. The variations of the χ parameter derived from different approaches were studied. This chapter also provides comparisons between the measured and calculated value of unsaturated shear strength based on suction stress approach and based on Bishop's effective stress approach. The following points emerged from the test results.

i. The confining stresses did not have an impact on the suction stress characteristic curves (SSCC) for the collapsed specimens.
ii. The SSCCs established from the SWCCs accord well with that inferred from the triaxial compression tests. Further, the measured SWCCs and that established based on the SSCC which derived from shear strength test results were found to be similar. These findings emphasized the strong linkage between SWCC and SSCC for collapsible soils that underwent a wetting process.
iii. A decrease in suction as the collapsible soil underwent the wetting process causing an increase of suction stress aids in decreasing the effective stress, which in turn reduced the volume of the collapsible soil.
iv. The effective stress-based on the SSCCs describes the same unique failure criterion as that for the saturated failure criterion for collapsible soil that underwent a wetting process.
v. The experimental shear strength data and those calculated using Lu et al.'s (2010) suction stress approach corresponded fairly well. However, the calculated shear strength based on the χ parameter was found to be similar to experimental data at low suctions but tend to become dissimilar as the suction increased.

CHAPTER 8

Conclusions and recommended further research

8.1 Conclusions

Studies indicate that any unsaturated soil may undergo collapse under specific conditions. Collapsible soils are known to withstand relatively high stresses at unsaturated state. Upon exposure to a saturation front at a constant surcharge, the volume change of such soils generally occurs within a short time period. The aim of this thesis was to study the volume change and shear strength behaviour of unsaturated collapsible soil during the wetting process (decrease in matric suction) when subjected to various confining stresses and to interpret the collapsing phenomenon by suction stress approach.

A laboratory program was designed to investigate the hydraulic and mechanical behaviour of statically compacted unsaturated collapsible soil. The soil used in this investigation was a prepared soil. A mixture of M400 silt (40%), Leighton Buzzard sand (40%) and 20% Speswhite kaolin was considered for preparing the soil. The percentages of various particle-size fractions in the soil are similar to that found in many aeolian soil deposits, such as loess, loessic deposits and loess-derived sediments. The basic properties of the soil were determined following the standard laboratory procedures prior to carrying out the main tests.

Static compaction curves of the soil were established by statically compacting soil-water mixtures. The impact of compaction mould size (oedometer and triaxial moulds) and initial water content on the static compaction curves were studied, both in terms of applied pressure and applied energy. A series of double and single oedometer tests were conducted to investigate the effects of initial water content, initial dry unit weight, compaction pressure and overburden pressure on the collapse strain of the selected soil.

The wetting tests were carried out on the statically compacted specimens (dry unit weight = 15 kN/m^3, water content = 10%) by using the unsaturated triaxial device

(HKUST-type). One test was carried out to investigate the volume change behaviour of a single specimen during step-wise wetting at net confining stress of 100 kPa, and various suctions (500, 400, 300, 200, 100, 50 and 5 kPa), and the other tests were carried out to investigate the volume change and shear strength behaviour of twelve multiple specimens during step-wise wetting and unsaturated consolidated drained shearing tests under various magnitudes of applied matric suction (300, 100, 50, and 20 kPa), and net confining stress (100, 250, and 400 kPa). Further, saturated consolidated drained shearing tests were also carried out on three specimens at confining stresses of 100, 250 and 400 kPa.

The initial suction of the compacted soil specimens and the water retention behaviour of the soil at high suctions were determined by using a chilled-mirror dew-point potentiameter (WP4C). The test results from the wetting tests in conjunction with the chilled-mirror dew-point potentiameter test results enabled establishing the SWCCs for a large range of suction at various confining stresses. The test results were fitted with two SWCCs models (van Genuchten 1980 and Fredlund & Xing 1994). The impact of confining stress on the volumetric strain and SWCCs were studied.

The relationship between suction and suction stress (i.e., suction stress characteristic curves, SSCCs) were established from the wetting water retention data at various applied confining stresses and suctions. Similarly, the SSCC was established based on the shear strength test data. The impact of confining stress on the SSCCs of the soil was studied. The inferred SSCC and SWCC based on the triaxial compression tests and the SWCCs are cross-compared and discussed. The uniqueness of the critical state line in the deviatoric stress – effective mean stress plane for saturated as well as unsaturated soils under varying stress state conditions was investigated, and the application of the effective stress principle to the volume change of collapsible soil under varying stress state conditions was also investigated. The measured shear strength values were compared with the calculated values using suction stress approach and Bishop's effective stress approach.

Based on the findings reported in this thesis, the following conclusions were drawn.

1. At the same Proctor curve energy, the shape of static compaction curves was different from the dynamic one as the static compaction curves presented no wet side of optimum in contrast to the Proctor curve. The tests results agree well with some findings reported in the literature. The static compaction energy contribution to the soil varies with the specimen mould size. At the same compaction water content and Proctor energy, as compared to the dry unit weight based on standard Proctor, the dry unit weight produces based on statically compacted specimens using oedometer compaction mould was found to be much higher, whereas it was relatively lower for statically compacted specimens using triaxial mould.

2. During wetting tests, the magnitude of collapse strain increases with an increase in the applied stress and the maximum collapse results in stress equal to the compaction pressure (yield stress). The test results agree well with the findings reported in the literature. At the same initial water content, dry unit weight and applied stress during wetting, the collapse strains determined based on one-dimensional wetting test and isotropic consolidation were found to be very similar with a difference in the magnitude of collapse strain of less than about 1%.

3. The impact of confining stress on the volumetric strain and SWCC of the soil was distinct. Collapse strain increased as the applied confining stress increased. The suction - water content SWCCs were affected the applied confining stress; however, the differences in the SWCCs in terms of the degree of saturation were found to be insignificant. The SWCC best-fit model parameters followed similar trends. The test results complement well the findings reported in the literature. Some differences in the test results were noted when single, and multiple specimens were tested at an applied confining stress of 100 kPa. The difference in the test results can be attributed to the effect of continuous and the quick softening of interparticle bonding in a metastable soil structure during the wetting process of the single and the multiple specimens, respectively.

4. During shearing tests, the peak shear stress increased with an increase in the confining stress. With a decrease in suction as the soil underwent the wetting process, the peak shear stress decreased, the angle of friction ($\emptyset'$) slightly decreased, the cohesion value decreased non-linearly and the angle $\emptyset^b$ increased to attain a maximum value at

saturation. The trend reported in the literature on other soils and at various stresses in triaxial stress environment are similar.

5. The impact of applied confining stress on the suction stress characteristic curve (SSCC) was found to be insignificant as that occurred in case of suction - degree of saturation SWCCs.

6. The agreements between the SSCCs derived based on suction - degree of saturation SWCCs and the shear strength test data at several suctions (based on the effective shear strength parameters) were found to be very good indicating that a strong linkage exists between water absorption and shear strength of unsaturated collapsible soils.

7. The practical benefit of the research can be expanded on implications, such as estimating $\emptyset^b$ and a single effective stress parameter (χ) based on suction stress concept.

8.2 Recommended further research

1. Further testing is recommended to investigate the collapse behaviour of compacted soils with further initial conditions select along static compaction curves.

2. Additional testing using different types of naturally occurring collapsible soils with chemical bonding is recommended to check if the research findings can be generalized.

3. More supplementary tests may be needed on this collapsible soil to measure the drained shear strength failure envelope for wider ranges of net mean stress and high suction magnitudes.

4. Future experimental work should also study the effect of thermal and hydraulic hysteresis on the volume change, water retention characteristics and stress-strain behaviour of compacted collapsible soil.

5. Propose a fully coupled effective stress constitutive model hydraulic and mechanical model need. Stress–strain relations. Then, comparison of the numerical and experimental results.

Reference

Abbeche, K., Hammoud, F. and Ayadat, T. 2007. Influence of relative density and clay fraction on soils collapse. In: *Experimental Unsaturated Soil Mechanics*. Berlin, Heidelberg: Springer Berlin Heidelberg, pp. 3–9.

Adams, B. a and Wulfsohn, D. 1997. Variation of the critical-state boundaries of an agricultural soil. *European Journal of Soil Science* 48(4), pp. 739–748.

Agus, S.S. and Schanz, T. 2005. Comparison of Four Methods for Measuring Total Suction. *Vadose Zone Journal* 4(4), p. 1087.

Al-badran, Y.M.H. 2011. Volumetric yielding behaviour of unsaturated fine-grained soils.

Al-obaidi, Q.A.J. 2014. Hydro-mechanical behaviour of collapsible soils. Ruhr-Universität Bochum Schriftenreihe.

Al-Saoudi, N., Al-Khafaji, A.N. and Al-Mosawi, M. 2013. Challenging problems of gypseous soils in Iraq. *Proceedings of the 18th International Conference on Soil Mechanics and Geotechnical Engineering*, pp. 479–482.

Alan W Bishop 1962. The measurement of soil properties in the triaxial test. , pp. 1–148.

Alawaji, H.A. 2001. Shear induced collapse settlement of arid soils. *Geotechnical and Geological Engineering* 19(1), pp. 1–19.

Almahbobi, S., Tripathy, S. and Cleall, P.J. 2018. Effects of confining stress and suction on volume change and shear strength behaviour of a collapsible soil. In: *The 7th International Conference on Unsaturated Soils*. Hong Kong, p. 6.

Alonso, E.E., Gens, A. and Josa, A. 1990. A constitutive model for partially saturated soils. *Geotechnique* 40(3), pp. 405–430.

Alonso, E.E., Pereira, J.-M., Vaunat, J. and Olivella, S. 2010. A microstructurally based effective stress for unsaturated soils. *Géotechnique* 60(12), pp. 913–925.

Alsherif, N.A. and McCartney, J.S. 2014. Effective Stress in Unsaturated Silt at Low Degrees of Saturation. *Vadose Zone Journal*.

Alwail, T.A., Ho, C.L. and Fragaszy, R.J. 1994. Collapse mechanism of compacted clayey and silty sands. In: *Vertical and Horizontal Deformations of Foundations and Embankments*. ASCE, pp. 1435–1446.

Assallay, A.M., Rogers, C.D.F. and Smalley, I.J. 1997. Formation and collapse of metastable particle packings and open structures in loess deposits. *Engineering Geology* 48(1–2), pp. 101–115.

Assallay, A.M. 1998. Structure and hydrocollapse behaviour of loess.

ASTM D4546-14 2014. Standard test methods for one-dimensional swell or collapse of soils. *ASTM Standards*, pp. 1–10.

ASTM D4943−08 2010. Standard Test Method for Shrinkage Factors of Soils by the Wax Method. *ASTM Standards*, pp. 1–5.

ASTM D5333-03 2012. Standard test method for measurement of collapse potential of soils. *ASTM Standards*.

ASTM D6836-16 2016. Standard test methods for determination of the soil water chararcteristic curve for desorption using a hanging column , pressure extractor , chilled mirror hygrometer , and / or Centrifuge 1. *ASTM Standards*, p. 20.

Aversa, S. and Nicotera, M.V. 2002. A Triaxial and oedometer apparatus for testing unsaturated soils. *Geotechnical Testing Journal* 25(1), pp. 3–15.

Baille, W., Tripathy, S. and Schanz, T. 2014. Baille. *Vadose Zone Journal* 13(5), p. 10.

Barden, L., Madedor, A.O. and Sides, G.R. 1969. Volume change characteristics of unsaturated clay. *Journal of Soil Mechanics & Foundations Div*.

Barden, L., McGown, A. and Collins, K. 1973. The collapse mechanism in partly saturated soil. *Engineering Geology* 7(1), pp. 49–60.

Basma, A.A. and Tuncer, E.R. 1992. Evaluation and control of collapsible soils. *Journal of Geotechnical Engineering* 118(10), pp. 1491–1504.

Benchouk, A., Abou-Bekr, N. and Taibi, S. 2013. Potential Collapse for a Clay Soil. *International Journal of Emerging Technology and Advanced Engineering* 3(10), pp. 43–47.

Bennett, C. 2014. An experimental study on the hydraulic conductivity of compacted bentonites in geoenvironmental applications. Cardiff University.

Bishop, A.W. 1959. The principle of effective stress. *Teknisk ukeblad* 39, pp. 859–863.

Bishop, A.W., Alpan, I. and Blight, G.E. 1960. Factors controlling the shear strenth of partly saturated cohesive soil. In: *ASCE Res. Conf. Shear Strength of Loheslve Soil. Univ. of Colordo, Boulder P*.

Bishop, A.W. and Blight, G.E. 1963. Some aspects of effective stress in saturated and partly saturated soils. *Géotechnique* 13(3), pp. 177–197.

Bishop, A.W. and Wesley, L.D. 1975. A hydraulic triaxial apparatus for controlled stress path testing. *Géotechnique* 25(4), pp. 657–670.

Bishop, A.W.T. and Donald, I.B. 1961a. Experimental study of partly saturated soil in the triaxial apparatus. In: *Proceedings of the 5th International Conference on Soil Mechanics and Foundation Engineering*. Paris, France: Paris, Dunod, pp. 13–21.

Bishop, A.W.T. and Donald, I.B. 1961b. The experimental study of partly saturated soil in the triaxial apparatus. In: *5th International Conference on Soil Mechanics and Foundation Engineering*. pp. 13–21.

Booth, A. 1976. Compaction and preparation of soil specimens for oedometer testing. In: *Soil specimen preparation for laboratory testing*. ASTM International, pp. 216–228.

Booth, A.R. 1975. The factors influencing collapse settlement in compacted soils. In: *Proc, Sixth Regional Conf. for Africa on Soil Mechanics and Foundation Engineerin*. Durban, pp. 57–63.

Booth, A.R. 1977. Collapse Settlement of compacted soils. *CSIR Research Report 324*, pp. 1–40.

Boso, M. 2005. Shear strength behaviour of a reconstituted partially saturated clayey silt.

Brooks, R. and Corey, A. 1964. Hydraulic properties of porous media. *Hydrology Papers, Colorado State University* 3(March), p. 37 pp.

BS 1377-2 1990. Soils for civil engineering purposes. *British Standard Institution* 3(1).

BS 1377-4 1990. Soils for civil engineering purposes. *British Standard Institution* 3(1).

BS 1377-6 1990. Soils for civil engineering purposes. *British Standard Institution* 3(1).

BS 1377-8 1990. Soils for civil engineering purposes. *British Standard Institution* 3(1).

Bulut, R. and Leong, E.C. 2008. Indirect measurement of suction. *Geotechnical and Geological Engineering* 26(6), pp. 633–644.

Burland, J., Chapman, T., Skinner, H.D. and Brown, M. 2012. *ICE manual of geotechnical engineering volume 2: Geotechnical design, construction and verification*.

Burland, J.B. 1965. Correspondence. *Geotechnique* 15(2), pp. 211–214.

Caicedo, B., Murillo, C., Hoyos, L., Colmenares, J.E. and Berdugo, I.R. 2013. *Advances in unsaturated soils*. Caicedo, B. et al. eds.

Campbell, G.S., Smith, D.M. and Teare, B.L. 2007. Application of a Dew Point Method to Obtain the Soil Water Characteristic. In: *Proceedings of the Second International Conference on Mechanics of Unsaturated Soils*. Weimar, Germany, pp. 71–77.

Cerato, A.B., Miller, G.A. and Hajjat, J.A. 2009. Influence of clod-size and structure on wetting-induced volume change of compacted soil. *Journal of Geotechnical & Geoenvironmental Engineering* 135(11), pp. 1620–1628.

Chae, J., Kim, B., Park, S. wan and Kato, S. 2010. Effect of suction on unconfined compressive strength in partly saturated soils. *KSCE Journal of Civil Engineering* 14(3), pp. 281–290.

Chiu, C.F. 2001. Behavior of unsaturated loosely compacted weathered materials. Hong Kong University.

Coleman, J.D. 1962. Stress-strain relations for partly saturated soil. *Géotechnique* 12(4), pp. 348–350.

Cui, Y.-J., Terpereau, J.-M., Marcial, D., Delage, P., Antoine, P., Marchadier, G. and Ye, W.-M. 2004. A geological and geotechnical characterisation of the loess of Northern France. In: *Advances in geotechnical engineering: The Skempton conference: Proceedings of a three day conference on advances in geotechnical engineering, organised by the Institution of Civil Engineers and held at the Royal Geographical Society, London, UK, on 29–31* . Thomas Telford Publishing, pp. 417–428.

Cui, Y.J. and Delage, P. 1996. Yielding and plastic behaviour of an unsaturated compacted silt. *Géotechnique* 46(2), pp. 291–311.

Cunningham, M.R., Ridley, A.M., Dineen, K. and Burland, J.B. 2003. The mechanical behaviour of a reconstituted unsaturated silty clay. *Géotechnique* 53(2), pp. 183–194.

Decagon Device, I. 2013. *WP4C Dew Point PotentiaMeter. Operator's Manual*.

Delage, P. 2002. Experimental unsaturated soil mechanics. In: *Proc. 3rd Int. Conf. on Unsaturated Soils, UNSAT'2002*. Brazil, pp. 973–996.

Delage, P., Cui, Y.J. and Antoine, P. 2005. Geotechnical problems related with loess deposits in Northern France. In: *Proceedings of International Conference on Problematic Soils*. pp. 517–540.

Delage, P., Romero, E. and Tarantino, A. 2008. Recent developments in the techniques of controlling and measuring suction in unsaturated soils. In: Toll, D. G. et al. ed. *1st European Conference on Unsaturated Soils, E-UNSAT 2008*. Durham, UK., pp. 33–52.

Derbyshire, E. and Mellors, T.W. 1988. Geological and geotechnical characteristics of some loess and loessic soils from China and Britain: A comparison. *Engineering Geology* 25(2–4), pp. 135–175.

Donald, I.B. 1956. Shear strength measurements in unsaturated non-cohesive soils with negative pore pressures. In: *Proceedings of the 2nd Australia–New Zealand*

Conference on Soil Mechanics and Foundation Engineering, Christchurch, New Zealand. Technical Publications Ltd., Wellington, New Zealand. pp. 200–204.

Doris, M., Hafez, M.A. and Nurbaya, S. 2011. Static laboratory compaction method. *Electronic Journal of Geotechnical Engineering* 16, pp. 1583–1593.

Drnevich, V., Lutenegger, A. and Saber, R. 1988. Determination of collapse potential of soils. *Geotechnical Testing Journal* 11(3), p. 173.

Dudley, J.H. 1970. Review of collapsing soils. *Journal of Soil Mechanics & Foundations Div* 97(SM1), pp. 925–947.

Elgabu, H.M. 2013. Critical evaluation of some suction measurement techniques.

Escario, V. 1989. Strength and deformation of partly saturated soils. In: *In Proceedings of the 12^ International Conference on Soil Mechanics and Foundation Engineering*. Rio de Janerio, pp. 43–46.

Escario, V. and Saez, J. 1973. Measurement of the properties of swelling and collapsing soils under controlled suction. In: *Proc. 3rd Int. Conf. Expansive Soils, Haifa*. pp. 195–200.

Escario, V. and Sáez, J. 1986. The shear strength of partly saturated soils. *Géotechnique* 36(3), pp. 453–456.

Estabragh, A.R. and Javadi, A.A. 2008. Critical state for overconsolidated unsaturated silty soil. *Canadian Geotechnical Journal* 45(3), pp. 408–420.

Estabragh, A.R. and Javadi, A.A. 2014. Roscoe and hvorslev surfaces for unsaturated silty soil. *International Journal of Geomechanics* 14(2), pp. 230–238.

Eyob, T. 2011. Unsaturated shear strength characteristics and stress-strain behaviour of silty soils of Hawassa.

Fai, C.C. 2001. Behaviour of unsaturated loosely compacted weathered materials. Hong Kong.

Fazeli, A., Habibagahi, G. and Ghahramani, A. 2009. Shear strength characteristics of shiraz unsaturated silty clay. *Iranian Journal of Science & Technology* 33(B4), pp. 327–341.

Feda, J. 1988. Collapse of loess upon wetting. *Engineering Geology* 25(2–4), pp. 263–269.

Foss, I. 1973. Red soil from Kenya as a foundation material. In: *Proc., 8th ICSMFE*. pp. 73–80.

Fredlund, D., Stone, J., Stianson, J. and Sedgwick, A. 2011. Determination of water storage and permeability functions for oil sands tailings. In: *Proceedings Tailings and Mine Waste*.

Fredlund, D.G., Morgenstern, N.R. and Widger, R. 1978. The shear strength of unsaturated soils. *Canadian Geotechnical Journal* 15, pp. 313–321.

Fredlund, D.G., Rahardjo, H. and Gan, J.K.M. 1987. Non-linearity of strength envelope for unsaturated soils. In: *Proceedings, 6th International Conference of Expansive Soils*. pp. 49–54.

Fredlund, D.G. 1989. Negative pore-water pressures in slope stability. In: *Simposio Suramericano de Deslizamiento, Paipa, Columbia*. pp. 1–31.

Fredlund, D.G., Vanapalli, S.K., Xing, A. and Pufahl, D.E. 1995. Predicting the shear strength function for unsaturated soils using the soil-water characteristic curve. In: pp. 63–70.

Fredlund, D.G., Xing, A., Fredlund, M.D. and Barbour, S.L. 1996. The relationship of the unsaturated soil shear to the soil-water characteristic curve. *Canadian Geotechnical Journal* 33(3), pp. 440–448.

Fredlund, D.G. 2006. Unsaturated soil mechanics in engineering practice. *Journal of geotechnical and geoenvironmental engineering* 132(3), pp. 1090–2413.

Fredlund, D.G., Sheng, D. and Zhao, J. 2011. Estimation of soil suction from the soil-water characteristic curve. *Canadian Geotechnical Journal* 48(2), pp. 186–198.

Fredlund, D.G., Rahardjo, H. and Fredlund, M.D. 2012. *Unsaturated soil mechanics in engineering practice*.

Fredlund, D.G. and Gan, J.K.M. 1994. The collapse mechanism of a soil subjected to one-dimensional loading and wetting. In: *Genesis and properties of collapsible soils*. Springer Netherlands., pp. 173–205.

Fredlund, D.G. and Morgenstern, N.R. 1977. Stress state variables for unsaturated soils. *Journal of the Geotechnical Engineering Division* 5(103), p. 447--466.

Fredlund, D.G. and Rahardjo, H. 1993a. *Soil mechanics for unsaturated soils*. John Wiley & Sons.

Fredlund, D.G. and Rahardjo, H. 1993b. The role of unsaturated soil behaviour in geotechnical engineering practice. In: *11th Southeast Asian Geotechnical Conference*. pp. 4–8.

Fredlund, D.G. and Rahardjo, H. 1994. Unsaturated soil consolidation theory and laboratory experimental data. *The Emergence of Unsaturated Soil Mechanics*, pp. 450–456.

Fredlund, D.G. and Xing, A. 1994. Equations for the soil-water characteristic curve. *Canadian Geotechnical Journal* 31(6), pp. 1026–1026.

Futai, M.M. and Almeida, M.S.S. 2005. An experimental investigation of the mechanical behaviour of an unsaturated gneiss residual soil. *Géotechnique* 55(3), pp. 201–213.

Gallipoli, D., Gens, A., Sharma, R. and Vaunat, J. 2003. An elasto-plastic model for unsaturated soil incorporating the effects of suction and degree of saturation on mechanical behaviour. *Géotechnique* 53(1), pp. 123–136.

Gallipoli, D., Bruno, A.W., D'onza, F. and Mancuso, C. 2015. A bounding surface hysteretic water retention model for deformable soils. *Géotechnique* 65(10), pp. 793–804.

Gan, J.K.-M. and Fredlund, D.G. 1996. Shear strength characteristics of two saprolitic soils. *Canadian Geotechnical Journal* 33(4), pp. 595–609.

Gan, J.K.M., Fredlund, D.G. and Rahardjo, H. 1988. Determination of the shear strength parameters of an unsaturated soil using the direct shear test. *Canadian Geotechnical Journal* 25(3), pp. 500–510.

Gan, K. and Fredlund, D. 1988. Multistage direct shear testing of unsaturated soils. *Geotechnical Testing Journal* 11(2), p. 132.

Gao, Y. and Sun, D. 2017. Soil-water retention behavior of compacted soil with different densities over a wide suction range and its prediction. *Computers and Geotechnics* 91, pp. 17–26.

Garakani, A.A., Haeri, S.M., Khosravi, A. and Habibagahi, G. 2015. Hydro-mechanical behavior of undisturbed collapsible loessial soils under different stress state conditions. *Engineering Geology* 195, pp. 28–41.

Gau, F.L. and Olson, R.E. 1971. Uniformity of specimens of a compacted clay. *Journal of Materials* 6(4).

GDS Instruments Ltd 2014. *GDS unsaturated triaxial testing systems handbook*.

Gens, A., Alonso, E.E. and Lloret, A. 1995. Effect of structure on the volumetric behaviour of a compacted soil. In: *Proc. 1st Int. Conf. on Unsaturated Soil*. Paris, pp. 83–88.

van Genuchten, M.T. 1980. A Closed-form equation for predicting the hydraulic conductivity of unsaturated soils. *Soil Science Society of America Journal* 44(5), p. 892.

Georgiadis, K. 2003. Development, implementation and application of partially saturated soil models in finite element analysis. University of London.

Goh, S.G., Rahardjo, H. and Leong, E.C. 2010. Shear strength equations for unsaturated soil under drying and wetting. *Journal of Geotechnical and Geoenvironmental Engineering* 136(4), p. 2.

Goh, S.G. 2012. Hysteresis effects on mechanical behaviour of unsaturated soils.

Goh, S.G., Rahardjo, H. and Leong, E.C. 2014. Shear strength of unsaturated soils under multiple drying-wetting cycles. *Journal of Geotechnical and Geoenvironmental Engineering* 140(2), p. 06013001.

Grim, R.E. 1960. *Clay Mineralogy*. McGraw-Hill.

Habibagahi, G. and Mokhberi, M. 1998. A hyperbolic model for volume change behavior of collapsible soils. *Canadian Geotechnical Journal* 35(2), pp. 264–272.

Haeri, S., Khosravi, A. and Garakani, A.A. 2012. Variation of the volume change and water content of undisturbed loessial samples in controlled matric suction odometer tests. *4th International Conference on Problematic Soils, Wuhan, China*, pp. 1–8.

Haeri, S., Akbari, A., Khosravi, A. and Meehan, C.L. 2014. Assessing the hydro-mechanical behavior of collapsible soils using a modified triaxial test device. *Geotechnical Testing Journal* 37(2), p. 20130034.

Haeri, S., Khosravi, A., Ghaizadeh, S., Garakani, A.A. and Meehan, C.L. 2014. Characterization of the effect of disturbance on the hydro- mechanical behavior of a highly collapsible loessial soil. In: *Unsaturated Soils: Research & Applications*. pp. 261–266.

Haeri, S.M., Khosravi, A. and Ghazizadeh, S. 2015. The measurement of suction stress characteristic curve for a highly collapsible loessial soil. In: *IFCEE 2015*. Reston, VA: American Society of Civil Engineers, pp. 2482–2491.

Haeri, S.M., Khosravi, A., Garakani, A.A. and Ghazizadeh, S. 2017. Effect of soil structure and disturbance on hydromechanical behaviour of collapsible loessial soils. *International Journal of Geomechanics* 17(1), p. 04016021.

Haeri, S.M. and Garakani, A.A. 2016. Hardening behavior of a hydro collapsible loessial soil. *Japanese Geotechnical Society Special Publication* 2(4), pp. 253–257.

Hafez, M.A., Doris Asmani, M. and Nurbaya, S. 2010. Comparison between static and dynamic laboratory compaction methods. *Electronic Journal of Geotechnical Engineering* 15 O(1), pp. 1641–1650.

Han, Z., Vanapalli, S.K. and Zou, W. 2017. Integrated approaches for predicting soil-water characteristic curve and resilient modulus of compacted fine-grained subgrade soils. *Canadian Geotechnical Journal* 54(5), pp. 646–663.

Head, K.H. 1982. *Manual of Soil Laboratory Testing. Vol. 2, Permeability, Shear Strength, and Compression Tests*. Halsted Press, New York.

Head, K.H. 1995. *Manual of soil laboratory testing. volume 2. Permeability, shear strength and compressibility tests*.

Head, K.H. 1998. *Manual of Soil Laboratory Testing, Volume 3: Effective Stress Test*.

Heibrock, G., König, D., Datcheva, M., Pourzargar, A., Alabdullah, J. and Schanz, T. 2018. Prediction of effective stress in partially saturated sand kaolin mixtures. *Geomechanics for Energy and the Environment*.

Hilf, J.W. 1956. An investigation of pore-water pressure in compacted cohesive soils.

Hillel, D., Warrick, A.W., Baker, R.S. and Rosenzweig, C. 1998. *Environmental soil physics*. Academic Press.

Ho, Y.F. and Fredlund, D.G. 1982a. A Multistage triaxial test for unsaturated soils. *Geotechnical Testing Journal* 5(1), p. 18.

Ho, Y.F. and Fredlund, D.G. 1982b. Increase in strength due to suction for two Hong Kong soils. In: *Proceedings, ASCE Geotechnical Conference on Engineering and Construction in Tropical and Residual Soils*. pp. 263–295.

Ho, Y.F. and Fredlund, D.G. 1982c. Strain rates for unsaturated soil shear strength testing. In: *Proceedings of the Seventh Southeast Asian Geotechnical Conference , Hong Kong*. Southeast Asian Geotechnical Society, Bangkok, pp. 787–803.

Hossain, M.A. and Yin, J.-H. 2010. Shear strength and dilative characteristics of an unsaturated compacted completely decomposed granite soil. *Canadian Geotechnical Journal* 47(10), pp. 1112–1126.

Houston, S., Dye, H. and Singhal, S. 2008. Response of collapsible soils to various landscape and drainage conditions. In: *GeoCongress 2008*. Reston, VA: American Society of Civil Engineers, pp. 436–443.

Houston, S.L. 1995. Foundations and pavements on unsaturated soils-Part one: Collapsible soils. In: Alonso, E.E., P. Delage, P. eds, Balkema, Rotterdam, P. des P. et and Chaussees, pp. 1421–1439 eds. *proceedings of the first international conference on unsaturated soils, volume 3*. Paris.

Houston, S.L., Houston, W.N., Zapata, C.E. and Lawrence, C. 2001a. Geotechnical engineering practice for collapsible soils. In: *Unsaturated Soil Concepts and Their Application in Geotechnical Practice*. Dordrecht: Springer Netherlands, pp. 333–355.

Houston, S.L., Houston, W.N., Zapata, C.E. and Lawrence, C. 2001b. Geotechnical engineering practice for collasible soils. *Geotechnical and Geological Engineering* 19, pp. 333–355.

Houston, S.L., Perez-Garcia, N. and Houston, W.N. 2008. Shear strength and shear-induced volume change behavior of unsaturated soils from a triaxial test program. *Journal of Geotechnical and Geoenvironmental Engineering* 134(11), pp. 1619–1632.

Houston, W.N., Mahmoud, H.H. and Houston, S.L. 1993. Laboratory procedure for partial-wetting collapse determination. In: *Proceedings of the 1993 ASCE National Convention and Exposition*.

El Howayek, A., Huang, P.-T., Bisnett, R. and Santagata, M. 2011. *Identification and behavior of collapsible soils*.

Hoyos, L.R., Velosa, C.L. and Puppala, A.J. 2010. A novel suction-controlled ring shear testing apparatus for unsaturated soils. In: *Experimental and Applied Modeling of Unsaturated Soils*. pp. 32–39.

Hoyos, L.R., Velosa, C.L. and Puppala, A.J. 2011. A servo/suction-controlled ring shear apparatus for unsaturated soils: Development, performance, and preliminary results. *Geotechnical Testing Journal* 34(5), pp. 1–11.

Jefferson, I. and Ahmad, M. 2007. Formation of artificial collapsible Loess. In: *Problematic soils and rocks and In Sstu characterization*. Reston, VA: American Society of Civil Engineers, pp. 1–10.

Jennings, J.E. and Knight, K. 1957. The additional settlement of foundations due to collapse of sandy soils on wetting. In: *The 4th International Conference on Soil Mechanics and Foundation Engineering*. pp. 316–319.

Jennings, J.E. and Knight, K. 1975. *A guide to construction on or with materials exhibiting additional settlement due to" Collapse" of grain structure*.

Jennings, J.E.B. and Burland, J.B. 1962. Limitations to the use of effective stresses in partly saturated soils. *Géotechnique* 12(2), pp. 125–144.

Jiang, M., Hu, H. and Liu, F. 2012. Summary of collapsible behaviour of artificially structured loess in oedometer and triaxial wetting tests. *Canadian Geotechnical Journal* 49(10), pp. 1147–1157.

Jiang, Y., Chen, W., Wang, G., Sun, G. and Zhang, F. 2017. Influence of initial dry density and water content on the soil–water characteristic curve and suction stress of a reconstituted loess soil. *Bulletin of Engineering Geology and the Environment* 76(3), pp. 1085–1095.

Jotisankasa, A. 2005. Collapse behaviour of a compacted silty clay. Imperial College London.

Jotisankasa, A., Ridley, A. and Coop, M. 2007. Collapse behavior of compacted silty clay in suction-monitored oedometer apparatus. *Journal of Geotechnical and Geoenvironmental Engineering* 133(7), pp. 867–877.

Justo, J.., Delgado, A. and Ruiz, J. 1984. The influence of stress-path in the collapse-swelling of soils at the laboratory. In: *Fifth International Conference on Expansive Soils*. Barton, ACT: Institution of Engineers, Australia,: The Institution, pp. 67–71.

Karube, D., Kato, S., Hamada, K. and Honda, M. 1996. The relationship between the mechanical behavior and the state of pore water in unsaturated soil. *Geotechnical Engineering Journal, JSCE.* 535((III-34):), p. 83–92.

Karube, D., Honda, M., Kato, S. and Tsurugasaki, K. 1997. The relationship between shearing characteristics and the composition of pore-water in unsaturated soil. *Doboku Gakkai Ronbunshu* 1997(575), pp. 49–58.

Karube, D. and Kato, S. 1994. An ideal unsaturated soil and the Bishop's soil. In: *Proc. 13th ICSMFE*. pp. 43–46.

Kato, S., Yoshimura, Y., Kawai, K. and Sunden, W. 2001. Effects of suction on strength characteristics of unconfined compression test for a compacted silty clay. *Geotechnical Engineering Journal* 2001(687), pp. 201–218.

Kato, S., Kim, B.S. and Park, S.W. 2012. Applicability of suction stress for unsaturated shear strength. In: *5th Asia-Pacific Conference on Unsaturated Soils*. pp. 242–247.

Kato, S. and Kawal, K. 2000. Deformation characteristics of a compacted clay in collapse under isotropic and triaxial stress state. *Soils and Foundation* 40(5), pp. 75–90.

Khalili, N., Geiser, F. and Blight, G. 2004. Effective stress in unsaturated soils: Review with new evidence. *International Journal of Geomechanics* 4(2), pp. 115–126.

Khalili, N. and Khabbaz, M.H. 1998. A unique relationship for χ for the determination of the shear strength of unsaturated soils. *Géotechnique* 48(5), pp. 681–687.

Khalili, N. and Zargarbashi, S. 2010. Influence of hydraulic hysteresis on effective stress in unsaturated soils. *Géotechnique* 60(9), pp. 729–734.

Kim, B.-S., Shibuya, S., Park, S.-W. and Kato, S. 2010. Application of suction stress for estimating unsaturated shear strength of soils using direct shear testing under low confining pressure. *Canadian Geotechnical Journal* 47(9), pp. 955–970.

Kim, B.S., Shibuya, S., Park, S.W. and Kato, S. 2013. Suction stress and its application on unsaturated direct shear test under constant volume condition. *Engineering Geology* 155, pp. 10–18.

Kim, W.S. and Borden, R.H. 2011. Influence of soil type and stress state on predicting shear strength of unsaturated soils using the soil-water characteristic curve. *Canadian Geotechnical Journal* 48(11), pp. 1886–1900.

Knight, K. and Dehlen, G.L. 1963. The failure of a road constructed on a collapsing soil. In: *Proceedings of the 3rd Regional Conference.*

Knodel, P.C. 1992. *Characteristics and problems of collapsible soils*. US.

Laloui, L., Geiser, F., Vulliet, L., Li, X.L., Bolle, A. and Charlier, R. 1997. Characterisation of the mechanical behaviour of an unsaturated sandy silt. In: *XIV International Conference on Soil Mechanics and Foundation Engineering Hambourg97*. pp. 347–352.

Lawson, W.D., Kancharla, C. and Jayawickrama, P.W. 2011. Engineering properties of unstabilized compressed earth blocks. In: *Geo-Frontiers 2011: Advances in Geotechnical Engineering*. pp. 2679–2688.

Lawton, E. 1989. Collapse of compacted clayey sand. *Journal of Geotechnical ...* 115(9), pp. 1252–1267.

Lawton, E.C. 1986. Wetting-induced collapse in compacted soil. Washington State University, Pullman, Washington.

Lawton, E.C., Fragaszy, R.J. and Hardcastle, J.H. 1989. Collapse of compacted clayey sand. *Journal of Geotechnical Engineering* 115(9), pp. 1252–1267.

Lawton, E.C., Fragaszy, R.J. and Hardcastle, J.H. 1991. Stress ratio effects on collapse of compacted clayey sand. *Journal of Geotechnical Engineering* 117(5), pp. 714–730.

Lawton, E.C., Fragaszy, R.J. and Hetherington, M.D. 1992. Review of wetting-induced collapse in compacted soil. *Journal of Geotechnical Engineering* 118(9), pp. 1376–1394.

Lee, I., Sung, S.-G. and Cho, G.-C. 2005. Effect of stress state on the unsaturated shear strength of a weathered granite. *Canadian Geotechnical Journal* 42(2), pp. 624–631.

Leong, E.-C., Tripathy, S. and Rahardjo, H. 2003. Total suction measurement of unsaturated soils with a device using the chilled-mirror dew-point technique. *Géotechnique* 53(2), pp. 173–182.

Leong, E.C., Agus, S.S. and Rahardjo, H. 2004. Volume change measurement of soil specimen in triaxial test. *Geotechnical Testing Journal* 27(1), pp. 47–56.

Leong, E.C. and Rahardjo, H. 1997. Review of soil-water characteristic curve equations. *Journal of Geotechnical and Geoenvironmental Engineering* 123(12), p. 2.

Li, P., Vanapalli, S. and Li, T. 2016. Review of collapse triggering mechanism of collapsible soils due to wetting. *Journal of Rock Mechanics and Geotechnical Engineering* 8(2), pp. 256–274.

Liangtong, Z. 2003. Field and laboratory study of an unsaturated expansive soil associated with rain induced slop instability. The Hong Kong University of Science and Technology.

Lim, T.T. 1995. Shear strength characteristics and rainfall-induced matric suction changes in a residual soil slope. M. Eng. thesis, Nanyang Technological University, Singapore.

Lim, Y.Y. and Miller, G.A. 2004. Wetting-induced compression of compacted Oklahoma soils. *Journal of Geotechnical and Geoenvironmental Engineering* 130(10), pp. 1014–1023.

Lin, Z.G. and Wang, S.J. 1988. Collapsibility and deformation characteristics of deep-seated loess in China. *Engineering Geology* 25(2–4), pp. 271–282.

Loret, B. and Khalili, N. 2000. A three-phase model for unsaturated soils. *International Journal for Numerical and Analytical Methods in Geomechanics* 24(11), pp. 893–927.

Loret, B. and Khalili, N. 2002. An effective stress elastic-plastic model for unsaturated porous media. *Mechanics of Materials* 34(2), pp. 97–116.

Lu, N., Kim, T.-H., Sture, S. and Likos, W.J. 2009. Tensile Strength of Unsaturated Sand. *Journal of Engineering Mechanics* 135(12), pp. 1410–1419.

Lu, N., Godt, J.W. and Wu, D.T. 2010. A closed-form equation for effective stress in unsaturated soil. *Water Resources Research* 46(5), pp. 1–14.

Lu, N., Kaya, M. and Godt, J.W. 2014. Interrelations among the soil-water retention, hydraulic conductivity, and suction-stress characteristic curves. *Journal of Geotechnical and Geoenvironmental Engineering* 140(5), p. 04014007.

Lu, N. and Likos, J. 2004. *Unsaturated soil mechanics*.

Lu, N. and Likos, W.J. 2006. Suction stress characteristic curve for unsaturated soil. *Journal of Geotechnical and Geoenvironmental Engineering* 132(2), pp. 131–142.

Luckner, L., Van Genuchten, M.T. and Nielsen, D.R. 1989. A consistent set of parametric models for the two-phase flow of immiscible fluids in the subsurface. *Water Resources Research* 25(10), pp. 2187–2193.

Lynch, K., Sivakumar, V., Tripathy, S. and Hughes, D. 2018. Development of a laboratory technique for obtaining soil water retention curves under external loading in conjunction with high-capacity tensiometers. *Géotechnique* 18, pp. 1–26.

Ma, T., Wei, C., Wei, H. and Li, W. 2016. Hydraulic and mechanical behavior of unsaturated Silt: experimental and theoretical characterization. *International Journal of Geomechanics* 16(6), p. D4015007.

Maatouk, A., Leroueil, S. and La Rochelle, P. 1995. Yielding and critical state of a collapsible unsaturated silty soil. *Géotechnique* 45(3), pp. 465–477.

Maleki, M. and Bayat, M. 2012. Experimental evaluation of mechanical behavior of unsaturated silty sand under constant water content condition. *Engineering Geology* 141–142, pp. 45–56.

Maleksaeedi, E., Nuth, M., Sarlati, S. and Chekired, M. 2017. Experimental study of suction stress characteristic framework for granular materials using conventional direct shear test. *PanAm Unsaturated Soils 2017*, pp. 289–298.

Maswoswe, J.J. 1985. Stress path method for a compacted soil during collapse due to wetting. Imperial College London (University of London).

Mata, C., Romero, E. and Ledesma, A. 2002. Hydro-chemical effects on water retention in bentonite-sand mixtures. In: *Proceeding of the 3rd International Conference on Unsaturated soil.* pp. 283–288.

Matyas, E.L. and Radhakrishna, H.S. 1968. Volume change characteristics of partially saturated soils. *Géotechnique* 18(4), pp. 432–448.

McCartney, J.S. 2018. *General report : Geotechnical engineering problems in unsaturated soils*. Hong Kong.

McRae, J.L. 1991. Discussion of " Collapse of Compacted Clayey Sand " by Evert C. Lawton, Richard J. Fragaszy, and James H. Hardcastle (September, 1989, Vol. 115, No. 9). *Journal of Geotechnical Engineering* 117(11), pp. 1818–1820.

Medero, G.M., Schnaid, F., Gehling, W.Y.Y. and Gallipoli, D. 2005. Analysis of the mechanical response of an artificial collapsible soil. In: *Unsaturated Soils: Experimental Studies*. Berlin/Heidelberg: Springer-Verlag, pp. 135–145.

Medero, G.M., Schnaid, F. and Gehling, W.Y.Y. 2009. Oedometer behavior of an artificial cemented highly collapsible soil. *Geotech. Geoenviron. Eng.* 135(June), pp. 840–843.

Meilani, I., Rahardjo, H. and Leong, E.-C. 2005. Pore-water pressure and water volume change of an unsaturated soil under infiltration conditions. *Canadian Geotechnical Journal* 42(6), pp. 1509–1531.

Melinda, F., Rahardjo, H., Han, K.K. and Leong, E.C. 2004. Shear strength of compacted soil under infiltration condition. *Journal of Geotechnical and Geoenvironmental Engineering* 130(8), pp. 807–817.

Mesbah, A., Morel, J.C. and Olivier, M. 1999. Clayey soil behaviour under static compaction test. *Materials and Structures/Materiaux et Constructions* 32(223), pp. 687–694.

Micheals, A.S. 1959. Discussion to'Physico-chemical properties of soils: soil-water systems', by I. Th. Rosenqvist. *ASCE Proceedings, Journal of Soil Mechanics and Foundation Engineering Division* 85, pp. 91–102.

Miller, G., Muraleetharan, K. and Lim, Y. 2001. Wetting-induced settlement of compacted-fill embankments. *Transportation Research Record: Journal of the Transportation Research Board* (1755), pp. 111–118.

Miller, H. 2002. Modelling the collapse of metastable loess soils.

Mitchell, J.K. 1976. *Fundamentals of soil behavior*. 2 nd Editi. John Wiley and Sons ed. Inc., New York.

Mitchell, J.K. and Soga, K. 2005. *Fundamentals of soil behavior*. John Wiley & Sons.

Monroy, R. 2005. The influence of load and suction changes on the volumetric behaviour of compacted london clay.

Morgenstern, N.R. 1979. Properties of compacted soils. In: *Contribution to panel discussion, Session IV, Proc., 6th Panamerican Conf. on Soil Mechanics and Foundation Engineering*. pp. 349–354.

Mualem, Y. 1976. A New model for predicting the hydraulic conductivity of unsaturated porous media. *Water Resources Research* 12(3), pp. 513–522.

Murray, E.J. and Sivakumar, V. 2010. *Unsaturated soils : a fundamental interpretation of soil behaviour*. Wiley-Blackwell.

Ng, C.W.., Zhan, L.T. and Cui, Y.J. 2002. A new simple system for measuring volume changes in unsaturated soils. *Canadian Geotechnical Journal* 39(3), pp. 757–764.

Ng, C.W.. and Menzies, B. 2007. *Advanced unsaturated soil mechanics and engineering*. Taylor & Francis.

Ng, C.W.W., Chiu, A.C.F. and Rahardjo, H. 2000. Laboratory study of loosely compacted unsaturated volcanic fill in Hong Kong. In: *1st Asian Conference on Unsaturated Soils*. pp. 551–556.

Ng, C.W.W., Lai, C.H. and Chiu, C.F. 2012. A modified triaxial apparatus for measuring the stress path-dependent water retention curve. *Geotechnical Testing Journal* 35(3), pp. 490–495.

Ng, C.W.W., Sadeghi, H. and Jafarzadeh, F. 2017. Compression and shear strength characteristics of compacted loess at high suctions. *Canadian Geotechnical Journal* 54(5), pp. 690–699.

Ng, C.W.W. and Chiu, A.C.F. 2001. Behavior of a loosely compacted unsaturated volcanic soil. *Journal of Geotechnical and Geoenvironmental Engineering* 127(12), pp. 1027–1036.

Ng, C.W.W. and Chiu, A.C.F. 2003. Laboratory Study of Loose Saturated and Unsaturated Decomposed Granitic Soil. *Journal of Geotechnical and Geoenvironmental Engineering* 129(6), pp. 550–559.

Ng, C.W.W. and Pang, Y.W. 2000. Influence of stress state on soil-water characteristics and slope stability. *Journal of Geotechnical and Geoenvironmental Engineering* 126(2), pp. 157–166.

Nuth, M. and Laloui, L. 2008. Effective stress concept in unsaturated soils: Clarification and validation of a unified framework. *International Journal for Numerical and Analytical Methods in Geomechanics* 32(7), pp. 771–801.

Nyunt, T.T. 2012. Strength and stiffness characteristics of unsaturated.

Oh, S., Lu, N., Kim, Y.K., Lee, S.J. and Lee, S.R. 2012. Relationship between the soil-water characteristic curve and the suction stress characteristic curve: experimental evidence from residual soils. *Journal of Geotechnical and Geoenvironmental Engineering* 138(1), pp. 47–57.

Oh, S., Lu, N., Kim, T. and Lee, Y.H. 2013. Experimental validation of suction stress characteristic curve from nonfailure triaxial K0 consolidation tests. *Journal of Geotechnical and Geoenvironmental Engineering* 139(9), pp. 1490–1503.

Oh, S. and Lu, N. 2014. Uniqueness of the suction stress characteristic curve under different confining stress conditions. *Vadose Zone Journal* 13(5), pp. 1–10.

Oh, W.T., Garga, V.K. and Vanapalli, S.K. 2008. Shear strength characteristics of statically compacted kaolin. *Canadian Geotechnical Journal* 45(7), pp. 910–922.

Okochi, Y. and Tatsuoka, F. 1984. Some factors affecting K0 values of sand measured in triaxial cell. *Soils and Foundations* 24(3), pp. 52–68.

Okonta, F.N. 2012. Collapse settlement behaviour of remoulded and undisturbed weathered quartzite. *International Journal of the Physical Sciences* 7(32), pp. 5239–5247.

Oliveira, O.M. and Marinho, F.A.M. 2008. Suction equilibration time for a high capacity tensiometer. *Geotechnical Testing Journal* 31(1).

Olivier, M. and Mesbah, A. 1986. Le matériau terre: Essai de compactage statique pour la fabrication de briques de terre compressées. *Bull.liaison Labo P. et Ch* 146, pp. 37–43.

Oloo, S.Y. and Fredlund, D.G. 1996. A method for determination of φ b for statically compacted soils. *Canadian Geotechnical Journal* 33(2), pp. 272–280.

Pereira, J.H., Fredlund, D.G., Cardão Neto, M.P. and Gitirana, G. de F. 2005. Hydraulic behavior of collapsible compacted Gneiss soil. *Journal of Geotechnical and Geoenvironmental Engineering* 131(10), pp. 1264–1273.

Pereira, J.H. and Fredlund, D.G. 2000. Volume change behavior of collapsible compacted Gneiss soil. *Journal of Geotechnical and Geoenvironmental Engineering* 126(10), pp. 859–946.

Pham, H.Q., Fredlund, D.G. and Barbour, S.L. 2003. A practical hysteresis model for the soil–water characteristic curve for soils with negligible volume change. *Géotechnique* 53(2), pp. 293–298.

Pham, H.Q., Fredlund, D.G. and Barbour, S.L. 2005. A study of hysteresis models for soil-water characteristic curves. *Canadian Geotechnical Journal* 42(6), pp. 1548–1568.

Popescu, M.E. 1986. A comparison between the behaviour of swelling and of collapsing soils. *Engineering Geology* 23(2), pp. 145–163.

Pourzargar, A., König, D., Heibrock, G., Datcheva, M. and Schanz, T. 2014. Comparison of Measured and Predicted Suction Stress in Partially Saturated Compacted Mixtures of Sand and Clay. *Vadose Zone Journal* 13(5).

Rabbi, A.T.M.Z., Cameron, D.A. and Rahman, M.M. 2014a. Effect of initial partial saturation on collapse behavior of glacial sand with fines. In: *Geo-Congress 2014 Technical Papers*. Reston, VA: American Society of Civil Engineers, pp. 103–112.

Rabbi, A.T.M.Z., Cameron, D.A. and Rahman, M.M. 2014b. Role of matric suction on wetting-induced collapse settlement of silty sand. In: *Unsaturated Soils: Research & Applications*. pp. 129–135.

Rabbi, A.T.M.Z. and Cameron, D.A. 2014. Prediction of collapse potential for silty glacial. *Australian Geomechanics* 49, pp. 65–78.

Rahardjo, H., Lim, T.T., Chang, M.F. and Fredlund, D.G. 1995. Shear-strength characteristics of a residual soil. *Canadian Geotechnical Journal* 32(1), pp. 60–77.

Rahardjo, H., Heng, O.B. and Choon, L.E. 2004. Shear strength of a compacted residual soil from consolidated drained and constant water content triaxial tests. *Canadian Geotechnical Journal* 41(3), pp. 421–436.

Rahardjo, H. and Leong, E.C. 2006. Suction measurements. In: *Fourth International Conference on Unsaturated, UNSAT 2006*. pp. 81–104.

Rampino, C., Mancuso, C. and Vinale, F. 1999. Laboratory testing on an unsaturated soil: equipment, procedures, and first experimental results. *Canadian Geotechnical Journal* 36(1), pp. 1–12.

Rampino, C., Mancuso, C. and Vinale, F. 2000. Experimental behaviour and modelling of an unsaturated compacted soil. *Canadian Geotechnical Journal* 37(4), pp. 748–763.

Rao, S.M. and Revanasiddappa, K. 2000. Role of matric suction in collapse of compacted clay soil. *Journal of Geotechnical and Geoenvironmental Engineering* 126(1), pp. 85–90.

Rassam, D. and Cook, F. 2002. Predicting the shear strength envelope of unsaturated soils. *Geotechnical Testing Journal* 25(2), p. 215.

Rassam, D.W. and Williams, D.J. 1999. A relationship describing the shear strength of unsaturated soils. *Canadian Geotechnical Journal* 36(2), pp. 363–368.

Reddy, B.V.V. and Jagadish, K.S. 1993. The static compaction of soils. *Géotechnique* 43(2), pp. 337–341.

Rees, S. 2013. Part One: Introduction to the triaxial testing. *Published on the GDS website www.gdsinstruments.com* 1(Cd), pp. 1–4.

Reginatto, A.R. and Ferrero, J.C. 1973. Collapse potential of soils and soil-water chemistry. In: *Proceedings of the 8th International Conference on Soil Mechanics and Foundation Engineering*. Pergamon, pp. 177–183.

Rogers, C.D.F. 1995. Types and distribution of collapsible soils. In: *Genesis and properties of collapsible soils*. Springer, pp. 1–17.

Rollins, K.M. and Kim, J. 2010. Dynamic compaction of collapsible soils based on U.S. case histories. *Journal of Geotechnical and Geoenvironmental Engineering* 136(9), pp. 1178–1186.

Romero, E. 1999a. Chapter 5. , pp. 179–226.

Romero, E. 1999b. Characterisation and thermo-hydro-mechanical behaviour of unsaturated boom clay: an experimental study.

Romero, E. and Vaunat, J. 2000. Retention curves of deformable clays. In: *Experimental evidence and theoretical approaches in unsaturated soils*. CRC Press, pp. 99–114.

Saad, S., Mirzababaei, M., Mohamed, M., Miraftab, M. and Blanco, M. 2012. Uniformity of density of triaxial clay soil samples prepared by static compression. In: *5th European Geosynthetics Congress*.

Satija, B. Sen 1978. Shear behaviour of partially saturated soils.

Sawangsuriya, A., Edil, T.B. and Bosscher, P.J. 2008. Modulus−suction−moisture relationship for compacted soils. *Canadian Geotechnical Journal* 45(7), pp. 973–983.

Schanz, T. and Karim, H.H. 2018. Geotechnical characteristics of some Iraqi gypseous soils. In: Al-Attar, T. S. et al. eds. *MATEC Web of Conferences*. p. 01005.

Schnellmann, R., Rahardjo, H. and Schneider, H.R. 2013. Unsaturated shear strength of a silty sand. *Engineering Geology* 162, pp. 88–96.

Schnellmann, R. 2015. Uncertainties in the estimation of unsaturated shear strength from soil-water characteristic curve.

Shao, L., Zheng, G., Guo, X. and Liu, G. 2014. Principle of effective stress for unsaturated soils. In: *Unsaturated Soils: Research & Applications*. CRC Press, p. 239.

Sharma, R. 1998a. Mechanical behaviour of unsaturated highly expansive clays. University of Oxford.

Sharma, R. 1998b. Mechanical behaviour on unsaturated highly expansive clays. , p. 263.

Shen, C.N., Fang, X.W., Wang, H.W., Sun, S.G. and Guo, J.F. 2009. Research on effects of suction, water content and dry density on shear strength of remolded unsaturated soils. *Yantu Lixue/Rock and Soil Mechanics* 30(5), pp. 1347–1351.

Sheng, D., Zhou, A. and Fredlund, D.G. 2011. Shear strength criteria for unsaturated soils. *Geotechnical and Geological Engineering* 29(2), pp. 145–159.

Sibelco 2014. *Granulometric data and physical characteristics of M400 silt*.

Sillers, W.S., Fredlund, D.G. and Zakerzaheh, N. 2001. Mathematical attributes of some soil-water characteristic curve models. *Geotechnical and Geological Engineering* 19(3–4), pp. 243–283.

Singh, R.M. 2007. An experimental and numerical investigation of heat and mass movement in unsaturated clays Rao Martand Singh. Cardiff University Thesis.

Sivakumar, R., Sivakumar, V., Blatz, J. and Vimalan, J. 2006. Twin-cell stress path apparatus for testing unsaturated soils. *Geotechnical Testing Journal* 29(2), pp. 175–179.

Sivakumar, V. 1993. A critical state framework for unsaturated soil. University of Sheffield.

Sivakumar, V. and Wheeler, S.J. 2000. Influence of compaction procedure on the mechanical behaviour of an unsaturated compacted clay. Part 1: Wetting and isotropic compression. *Géotechnique* 50(4), pp. 359–368.

El Sohby, M.A. and Rabbaa, S.A. 1984. Deformational behaviour of unsaturated soils upon wetting. In: *Regional conference for Africa. 8*. pp. 129–137.

Song, Y.-S., Hwang, W.-K., Jung, S.-J. and Kim, T.-H. 2012. A comparative study of suction stress between sand and silt under unsaturated conditions. *Engineering Geology* 124(1), pp. 90–97.

Song, Y.S. 2014. Suction stress in unsaturated sand at different relative densities. *Engineering Geology* 176, pp. 1–10.

Sun, D., Sheng, D. and Xu, Y. 2007. Collapse behaviour of unsaturated compacted soil with different initial densities. *Canadian Geotechnical Journal* 44(6), pp. 673–686.

Sun, D., Zhang, J., Gao, Y. and Sheng, D. 2016. Influence of suction history on hydraulic and stress-strain behavior of unsaturated soils. *International Journal of Geomechanics* 16(6), p. D4015001.

Sun, D.A., Matsuoka, H. and Xu, Y.F. 2004. Collapse behavior of compacted clays in suction-controlled triaxial tests. *Geotechnical Testing Journal* 27(4), pp. 362–370.

Tadepalli, R., Rahardjo, H. and Fredlund, D. 1992. Measurements of matric suction and volume changes during inundation of collapsible soil. *Geotechnical Testing Journal* 15(2), p. 115.

Tadepalli, R. and Fredlund, D.G. 1991. The collapse behavior of a compacted soil during inundation. *Canadian Geotechnical Journal* 28(4), pp. 477–488.

Tarantino, A. 2007. A possible critical state framework for unsaturated compacted soils. *Géotechnique* 57(4), pp. 385–389.

Tarantino, A. 2009. A water retention model for deformable soils. *Géotechnique* 59(9), pp. 751–762.

Tarantino, A. and De Col, E. 2008. Compaction behaviour of clay. *Géotechnique* 58(3), pp. 199–213.

Tavakoli, M.H., Habibagahi, G. and Nikooee, E. 2014. Effect of confining stress on soil water retention curve and its impact on the shear strength of unsaturated soils. *Vadose Zone Journal* 0(0), p. 0.

Tekinsoy, M.A., Kayadelen, C., Keskin, M.S. and Söylemez, M. 2004. An equation for predicting shear strength envelope with respect to matric suction. *Computers and Geotechnics* 31(7), pp. 589–593.

Terzaghi, K. von 1936. The shearing resistance of saturated soils and the angle between the planes of shear. In: *Proceedings of the 1st international conference on soil mechanics and foundation engineering*. Harvard University Press Cambridge, MA, pp. 54–56.

Thu, T.M., Rahardjo, H. and Leong, E.-C. 2006. Shear strength and pore-water pressure characteristics during constant water content triaxial tests. *Journal of Geotechnical and Geoenvironmental Engineering* 132(3), pp. 411–419.

Thu, T.M., Rahardjo, H. and Leong, E.-C. 2007. Soil-water characteristic curve and consolidation behavior for a compacted silt. *Canadian Geotechnical Journal* 44(3), pp. 266–275.

Thyagaraj, T., Bhavani, P., Das, A.P. and Julina, M. 2016. Collapse Behaviour of Compacted Coal Ashes. *International Journal of Geosynthetics and Ground Engineering* 2(1), p. 6.

Toll, D.G. 1990. A framework for unsaturated soil behaviour. *Géotechnique* 40(1), pp. 31–44.

Toll, D.G. and Ong, B.H. 2003. Critical-state parameters for an unsaturated residual sandy clay. *Geotechnique* 53(1), pp. 93–103.

Tombolato, S. and Tarantino, A. 2005. Coupling of hydraulic and mechanical behaviour in unsaturated compacted clay. *Géotechnique* 55(4), pp. 307–317.

Tripathy, S., Leong, E. and Rahardjo, H. 2005. Suction of compacted residual soils. *Unsaturated Soils: Experimental Studies* 93, pp. 111–122.

Tripathy, S., Tadza, Y.M. and Thomas, H.R. 2014. Soil-water characteristic curves of clays. *Canadian geotechnical journal* 51(8), pp. 869–883.

Tripathy, S., Al-Khyat, S., Cleall, P.J., Baille, W. and Schanz, T. 2016. Soil suction measurement of unsaturated soils with a sensor using fixed-matrix porous ceramic discs. *Indian Geotechnical Journal* 46(3), pp. 252–260.

Tripathy, S. and Rees, S.W. 2013. Suction of some polyethylene glycols commonly used for unsaturated soil testing. *Geotechnical Testing Journal* 36(5), pp. 768–780.

Turnbull, W.J. 1950. Compaction and strength tests on soils. In: *Lambe, T. W. & Whitman, R. V. 1969. Soil mechanics*.

Vanapalli, S.K., Fredlund, D.G., Pufahl, D.E. and Clifton, A.W. 1996. Model for the prediction of shear strength with respect to soil suction. *Canadian Geotechnical Journal* 33(3), pp. 379–392.

Vanapalli, S.K., Sillers, W.S. and Fredlund, M.D. 1998. The meaning and relevance of residual state to unsaturated soils. In: *Proceedings of the 51st Canadian Geotechnical Conference*. pp. 4–7.

Vanapalli, S.K. and Fredlund, D.G. 2000. Comparison of different procedures to predict unsaturated soil shear strength. In: *Advances in Unsaturated Geotechnics*.

Viana da Fonseca, A., Rios, S. and Amaral, M.F. 2013. Structural anisotropy by static compaction. *Engineering Geology* 154, pp. 89–97.

Vogler, T.J., Lee, M.Y. and Grady, D.E. 2007. Static and dynamic compaction of ceramic powders. *International Journal of Solids and Structures* 44(2), pp. 636–658.

Walker, P.J. 2004. Strength and erosion characteristics of earth blocks and earth block masonry. *Journal of Materials in Civil Engineering* 16(5), pp. 497–506.

Wang, J.-J., Liu, M.-W., Zhang, H.-P., Wang, D.-Y. and Deng, W.-J. 2014. Effects of wetting on mechanical behavior and particle crushing of a mudstone particle mixture. In: *Proceedings of the 6th international conference on unsaturated soils, UNSAT*. pp. 233–238.

Wheeler, S.J. 1988. The undrained shear strength of soils containing large gas bubbles. *Géotechnique* 38(3), pp. 399–413.

Wheeler, S.J., Sh Arma{, R.S. and Uisson{, M.S.R.B. 2003. Coupling of hydraulic hysteresis and stress–strain behaviour in unsaturated soils. *Géotechnique* 53(1), pp. 41–54.

Wheeler, S.J. and Karube, D. 1996. *Constitutive modelling*.

Wheeler, S.J. and Sivakumar, V. 1995a. An elasto-plastic critical state framework for unsaturated soil. *Géotechnique* 45(1), pp. 35–53.

Wheeler, S.J. and Sivakumar, V. 1995b. An elasto-plastic critical state framework for unsaturated soil. *Géotechnique* 45(1), pp. 35–53.

White, N.F., Duke, H.R., Sunada, D.K. and Corey, A.T. 1970. Physics of desaturation in porous materials. *Journal of the Irrigation and Drainage Division* 96(2), pp. 165–191.

Whitman, R. V, Roberts, J.E. and Mao, S.-W. 1960. *One-dimensional compression compression and wave velocity tests*. Massachusetts inst of tech cambridge.

Witsman, G.R. and Lovell, C.W. 1979. *The effect of compacted prestress on compacted shale compressibility*.

Yang, H., Rahardjo, H., Leong, E.-C. and Fredlund, D.G. 2004. Factors affecting drying and wetting soil-water characteristic curves of sandy soils. *Canadian Geotechnical Journal* 41(5), pp. 908–920.

Yin, J.H. 2003. A double cell triaxial system for continuous measurement of volume changes of an unsaturated or saturated soil specimen in triaxial testing. *Geotechnical Testing Journal* 26(3), pp. 353–358.

Yong, R.N. and Townsend, F.C. 1980. Laboratory shear strength of soil. *American Society for Testing and Materials* 1, p. 720.

Zhai, Q. and Rahardjo, H. 2012. Determination of soil-water characteristic curve variables. *Computers and Geotechnics* 42, pp. 37–43.

Zhan, T.L. and Ng, C.W. 2006. Shear strength characteristics of an unsaturated expansive clay. *Canadian Geotechnical Journal* 43(7), pp. 751–763.

Zhang, J., Sun, D., Zhou, A. and Jiang, T. 2016. Hydromechanical behaviour of expansive soils with different suctions and suction histories. *Canadian Geotechnical Journal* 53(1), pp. 1–13.

Zhemchuzhnikov, A., Ghavami, K. and dal Toé Casagrande, M. 2016. Static compaction of soils with varying clay content. *Key Engineering Materials* 668, pp. 238–246.

Zorlu, K. and Kasapoglu, K.E. 2009. Determination of geomechanical properties and collapse potential of a caliche by in situ and laboratory tests. *Environmental Geology* 56(7), pp. 1449–1459.

Appendix A

Table A-1 Calibration of the HKUST-type triaxial apparatus transducers

Instrument	Resolution	Units
Axial load	0.34629	kN
Axial displacement	0.0049756	mm
Total volume change	33.827	m^3
Cell pressure	0.1019987	kPa
Pore air pressure	0.1008622	kPa
Pore water pressure	19.96407	kPa